2013 | Faculteit Wetenschappen

DOCTORAATSPROEFSCHRIFT

The pathosystem *Erwinia amylovora – Pyrus communis*: A multidisciplinary study of possible plant defence mechanisms with focus on the phenylpropanoid-flavonoid pathway

Proefschrift voorgelegd tot het behalen van de graad van doctor in de wetenschappen, biologie, te verdedigen door:

Kristof Vrancken

Promotor: prof. dr. Roland Valcke
Copromotor: prof. dr. ir. Wannes Keulemans

D/2013/2451/1

universiteit hasselt
KNOWLEDGE IN ACTION

"Nature does nothing without a purpose"

Αριστοτελης (384 BC – 322 BC)

"You mustn't be afraid to dream a little bigger"

Inception

"Ik zeg altijd: als ge in iets "geloof", ge "geloof" er echt in, dan "luk" het ook zo"

Guido Brepoels, trainer STVV

Woord vooraf

Voila, vijf jaar zijn omgevlogen zonder het goed en wel te beseffen. Uiteindelijk lijkt het een lange periode, maar plots breekt dan die dag aan waarop je dit boekje moet afhebben. Deze doctoraatsthesis is niet enkel een overzicht van 4-5 jaar hard werk, maar tevens vormt het ook voor mij een beginpunt van een volledig nieuwe en voorlopig nog onbekende wending in mijn leven.

Dit eindwerk is het resultaat van vele handen, groot en klein, en ik zou dan ook van de gelegenheid willen gebruik maken om een hele resem mensen te bedanken.

Allereerst zou ik mijn promoter, Professor Roland Valcke willen bedanken. Voor het bieden van deze kans, voor het voortdurend bijleren, voor de goede raad en daad, voor het vele verbeterwerk en het beantwoorden van mijn talrijke mails, voor de toffe momenten, voor de vele reizen en voor de leuke gesprekken die vaak nog leuker werden in het bijzijn van een schuimend pintje. Roland, bedankt voor alles !

Verder zou ik ook een dankwoordje willen richten aan mijn copromotor Prof. Wannes Keulemans. Zonder jouw boeiende lessen, je imposante kennis over de fruitteelt en je vertrouwen in mij tijdens mijn ingenieursthesis zou ik tijdens mijn bio-ingenieursjaren niet gebeten geweest zijn door het fruitteeltvirus. Wannes, een welgemeende dank je wel!

De volgende in het rijtje zijn Ir. Tom Deckers, Ir. Hilde Schoofs en Wim Verjans van pcfruit, omdat ze altijd voor mij klaar stonden, mij hielpen waar nodig en omdat ik er op ieder uur van de dag terecht kon voor een goede babbel. Ook de andere collega's van pcfruit verdienen natuurlijk een dikke pluim!

Off course, I have to say thanks to Prof. Treutter, who gave me the opportunity of doing a STSM at the University of Munich, who arranged me an appartment during my stay and who let me experience something totally new. Thank you very much!

Voorts zou ik Prof. Jean-Paul Noben willen bedanken voor het mij vakkundig assisteren bij de proteomics, voor het willen analyseren van de spots en het valideren van proteïnen. Natuurlijk gaat mijn dank ook uit naar Erik, Veronique en Annelies voor hun hulp tijdens mijn labomomenten op BIOMED.

Bedankt ook aan Dr. Ir. Tony Remans, voor de hulp met de RT-qPCR en het meermaals vragen hoe het nu met STVV gaat. Tony, bedankt!

Last but not least, I would like to thank the other jury members for being in my jury and for delivering me feedback for this doctoral thesis.

En op die manier belanden we dan weer bij de mensen van ons labo.

Greet, bedankt om gedurende die vijf jaar mijn labo-mama te zijn, mijn bestellingen te doen, mij te helpen waar nodig en de bureau te vullen met positieve energie, een glimlach of gewoon een goed gesprek. O zo simpele dingen, maar door mij o zo erg geapprecieerd.

Jan, bedankt om mij te helpen met het planten van mijn boompjes en de nooit slijtende woorden: "Hoe gaat het ermee?"

Mieke en Sofie, jullie waren al een tijdje bezig toen ik aan de UHasselt begon. Maar ondanks die vrij korte tijd dat we samen waren, heb ik toch veel bij jullie kunnen leren.

Karen, bedankt voor de leuke tijd en de vaak hilarische momenten in het proteomicslabo en daarbuiten. Bedankt om deel uit te maken van K3. Het werd stil toen jij vertrok.

Anne, het werd nog stiller toen jij naar Berlijn vertrok. Plots verloor ik mijn eilandgenootje waar ik mijn -al zeg ik het zelf- uitgebreide Wiki-kennis, goede anekdotes of vettige moppen aan verkocht kreeg. Vaak ging dit ook gepaard met een goede schaterlach (er was zelfs één moment bij dat ik dacht dat ik de 100 moest bellen). Uiteindelijk was jij de persoon waar ik misschien nog het meeste van geleerd heb. Anne, een dikke dank je wel. Ik wens je veel succes in het buitenland en hoop dat er je een grote carrière te wachten staat.

Gelukkig werd een groot deel van die stilte opnieuw opgevuld door Adrian, Inge en Michelle. Ik wens jullie veel succes toe met jullie onderzoek. Uiteindelijk komt het allemaal wel in orde, jullie zullen dat zelf wel ondervinden.

Brigitte, bedankt om tijdens de practica altijd alles mooi klaar te zetten en die afschuwelijke lever op tijd voor mijn neus weg te nemen.

Collega's -maar eigenlijk stuk voor stuk vrienden- van de dierkunde, het CMK en de groep van Tim (want die andere naam gebruikt toch geen kat), van doctoraatsstudent tot prof, door de jaren heen is de biologiegroep geëxpandeerd aan een snelheid waar zelfs het heelal niet kan aan tippen. Het is dan ook onbegonnen werk om hier iedereen bij naam te bedanken. Toch zou ik enkele mensen binnen de groep in het bijzonder willen bedanken. Natascha, bedankt voor het snijden van de coupes en het met de glimlach ondergaan van mijn talrijke plaagbuien. Ann en Carine, ook jullie bedankt voor jullie hulp bij bestellingen. Aan iedereen, bedankt voor een lach en een traan, voor de ettelijke momenten in het labo en het studentenrestaurant die me altijd bij zullen blijven, voor een helpende hand, hoe klein ook. Bedankt, het waren fijne jaren, jaren om nooit te vergeten.

Natuurlijk kan ik mijn vrienden ook niet vergeten, mannen en vrouwen van de Molen, door de jaren heen met elkaar verbonden geraakt door doodgewone dingen, maar uiteindelijk een vast geheel geworden. Paco,

Ducha, Frudolf, Mojo, Bissie, Gilbert, Spikke, Bokman, Futs, Fabio, Jeanjean, D, Mark, Jo, Yannick, Sanjam, Anneleen, Jolien, Joke, Pasquale en de vele aanhangsels, samen hebben we mooie dingen meegemaakt, ongetwijfeld zullen er nog vele volgen. Menig uur hebben we in de Molen gesleten, ons kindje dat we samen terug uit zijn as hebben doen herrijzen. Menig gesprek hebben we gevoerd, zelfs tot bij het krieken van de dag. Bedankt om bij jullie "thuis" te komen, interesse te tonen en om gewoon jullie te zijn. Bedankt !

Ook mijn klasgenootjes van de fytotechnie – we know everything of botany- zijn ondertussen onmisbaar geworden. Na de studies zijn onze wegen zich beginnen te scheiden, sommigen hebben hun doctoraat al afgelegd, anderen moeten dit nog doen. Uiteindelijk vinden we toch nog altijd wel een weekendje om die beruchte fytoweekendjes te organiseren. Ik wens ieder van jullie veel succes toe met jullie toekomst.

Aan al mijn vrienden en kennissen die ik niet expliciet genoemd heb, dank je wel !

Omdat ik anders naar mijn voeten ga krijgen, natuurlijk ook nog een dikke kus voor Kelly, die ik op de Uhasselt echt heb leren kennen. Voor de raad, voor de steun, de bemoedigende woorden. Soms zei een blik zelfs meer dan woorden. Bedankt!

Tot slot heb ik nog een woordje bewaard voor mijn ouders, zus en de rest van de familie, ook zij die er niet meer zijn. Bedankt voor de kansen die jullie mij gaven en nog steeds geven, jullie stonden altijd klaar voor mij. Bedankt om de persoon die ik nu ben.

Bedankt iedereen,

Kristof
10/02/2013

Summary

Fire blight, caused by the gram-negative bacterium *Erwinia amylovora*, is a devastating disease characterised by a rapid dissemination and a systemic distribution in *Rosaceae*, of which both apple and pear are important hosts. Due to the destructive character of the bacterium, the lack of effective control methods and the low adaptability grade of both apple and pear against environmental traits, fire blight is a disease which is difficult to control.
In this doctoral thesis, we used a multidisciplinary approach to clear the role of the phenylpropanoid-flavonoid pathway and possible other defence mechanisms involved in the pathosystem between *Erwinia amylovora* and *Pyrus communis*.

First, the role of leaf ontogenesis during a fire blight infection was investigated (chapter 3). We showed that fundamental differences were present between immature and mature leaf tissue, as disease symptoms occurred much faster in the immature leaves compared to the mature leaves and their transcripts of both antioxidative and phenylpropanoid-related genes were different. The higher levels of certain antioxidative-related transcripts and the resulting antioxidative endproducts in the mature leaves could have a function in lowering too high amounts of ROS during the first hours after infection and could partially explain the different infection rates that existed between these two type of leaves. Clear differences in antioxidative-related transcripts as a result of an infection were not found. Transcription patterns of two key genes anthocyanidin reductase (*ANR*) and chalcone synthase (*CHS*) related to the phenylpropanoid-flavonoid pathway showed differences between control, mock-inoculated and *E. amylovora* inoculated mature leaves, with the strongest reaction 48h after infection. The impact of *E. amylovora* was also visualised in histological sections, and confirmed by HPLC, as epicatechin –which is produced via ANR- augmented 72h after infection in *E. amylovora* inoculated leaf tissue. These results could indicate that induction of the phenylpropanoid-flavonoid pathway and epicatechin in particular could have a distinct function in protecting mature leaves against fire blight, as these metabolites then can act as an antioxidant, as a defence barrier strategy or as toxic compound against the bacteria. Compared to the mature

leaves, the role of the phenylpropanoid-flavonoid pathway in defence seemed to be not that pronounced in the immature leaves.

Second, we investigated possible cultivar dependent variations in immature pear leaves of the cultivars Conférence and Doyenné du Comice regarding their response to the fire blight pathogen *Erwinia amylovora* (chapter 4) and with an emphasis on the phenylpropanoid-flavonoid pathway. Conférence and Doyenné reacted differently to an inoculation with fire blight. Although the phenylpropanoid-flavonoid pathway seemed to play a minor role in immature leaves of both cultivars, a clear difference between cultivars was noticed, as transcripts were immediately down-regulated in Doyenné, whereas transcripts in Conférence appeared to fluctuate more during the experiment. No induction of the investigated transcripts was observed in the leaf above and below the *E. amylovora* inoculated leaf. The high natural concentrations of epicatechin in the very susceptible cultivar Doyenné compared to moderately resistant cultivar Conférence could put forward that an induction of the phenylpropanoid-flavonoid pathway at the site of inoculation is more crucial than the natural occurance of certain secondary metabolites in the total leaf tissue. These induced metabolites can then act as an antioxidant, as a defence barrier strategy or as toxic compound against the bacteria. Based on our proteomic results, both cultivars seem to adapt their energy-related and photosynthetic processes. However, in Conférence, the increased amount of defence-related major allergen genes and lipoxygenases could suggest a better dealing of the built-up stress by *E. amylovora* compared to Doyenné.

Last but not least, we investigated the possible effect of the application of a heat shock in immature pear leaves of the cultivar Conférence regarding their response to the fire blight pathogen *Erwinia amylovora* (chapter 5). Based on our results of the phenylpropanoid-flavonoid pathway, it seemed that applying a heat shock as an added value to fight fire blight has a rather negative impact, as the relative expression values of some genes decreased. Furthermore, infection was not suppressed but remained more or less the same without the heat shock. Last, although not all spots were identified, less defence-related mechanisms were found after the heat shock, suggesting that the plant favors recovery from the heat shock instead of plant defence.

Samenvatting

Bacterievuur, veroorzaakt door de gramnegatieve bacterie *Erwinia amylovora*, wordt gekenmerkt door een snelle en systemische verspreiding in de plantenfamilie van de *Rosaceae*, tot welke ook appel en peer behoren. Door het destructieve karakter van de bacterie, het gebrek aan efficiënte bestrijdingsmiddelen en het gering aanpassingsvermogen van zowel appel en peer, wordt bacterievuur beschouwd als een ziekte die moeilijk te bestrijden is.
In deze doctoraatsthesis werd gebruikt gemaakt van tal van technieken om zowel de rol van de fenylpropanoid-flavonoid syntheseweg als die van andere verdedigingsmechanismen op te helderen tijdens de specifieke interactie tussen *E. amylovora* en peer.

Eerst werd er gekeken naar het belang van bladouderdom tijdens een infectie met *E. amylovora* (hoofdstuk 3). We konden aantonen dat er fundamentele verschillen bestaan tussen jonge en oude bladeren, zowel wat betreft de snelheid van infectie als de aanwezigheid van transcripts. Zo vertoonde het oudere weefsel hogere transcriptieniveaus van welbepaalde antioxidatieve genen. De eindproducten van deze genen zouden tijdens een succesvolle infectie de te hoge concentraties aan ROS gevoelig kunnen verminderen en zouden ook kunnen verklaren waarom ouder weefsel minder gevoeliger is dan het jongere weefsel. Duidelijke verschillen in transcriptieniveaus als gevolg van een infectie konden niet worden aangetoond.
Dit is in groot contrast met de fenylpropanoid-flavonoid syntheseweg, waar zowel de expressie van anthocyanidin reductase (*ANR*) en chalcone synthase (*CHS*) duidelijke verschillen vertoonde in onbehandeld, pseudo-geïnoculeerd en met *E. amylovora* geïnoculeerd weefsel, met de meest uitgesproken verschillen 48u na de inoculatie. Deze impact werd niet enkel gevisualiseerd in histologische coupes, maar werd ook teruggevonden na analyse met HPLC, waar de concentratie aan epicatechine -dat via ANR geproduceerd wordt- ook gevoelig verhoogt. Deze resultaten doen vermoeden dat een snelle inductie van de fenylpropanoid-flavonoid syntheseweg en epicatechine in het bijzonder essentieel zijn in het defensiemechanisme van oudere bladeren van peer tegen bacterievuur. Deze metabolieten zouden dan dienst kunnen doen als

antioxidant, als een soort van fysiologische barrière of als een toxisch element tegen de bacterie. Het belang van deze syntheseweg in het defensiemechanisme lijkt miniem te zijn in de immature weefsels.

Vervolgens werd er gekeken naar eventueel cultivargerelateerde verschillen voor immature blaadjes van zowel Conférence als Doyenné du Comice na een infectie met *E. amylovora* en met nadruk op de fenylpropanoid-flavonoid syntheseweg (hoofdstuk 4). Hoewel het belang van deze syntheseweg eerder miniem was in de immature weefsels, reageerden zowel Conférence en Doyenné verschillend op de inoculatie met bacterievuur. In Doyenné vertoonden de transcripts onmiddellijk een verlaagde regulatie, waar Conférence meer fluctuaties bezat. Er werd geen significante inductie van deze transcripts waargenomen in het blad boven en onder het geïnfecteerde blad.
Doyenné vertoonde hogere concentraties aan epicatechine dan Conférence, wat er opnieuw kan op wijzen dat een inductie van de fenylpropanoid-flavonoid syntheseweg t.h.v. de inoculatiewond belangrijker is dan het natuurlijk voorkomen van deze polyfenolen in de weefsels. Op die manier kunnen ze hun functie van antioxidant, van fysiologische barrière of van toxisch element vervullen. Op basis van onze proteoomstudies konden we opmaken dat beide cultivars zowel hun energie- als hun fotosynthese-gerelateerde processen aanpassen tengevolge van een infectie. Bovendien werd er in Conférence een verhoogde hoeveelheid allergenen en lipoxygenasen aangetoond, wat erop kan wijzen dat deze cultivar beter gewapend is tegen bacterievuur dan Doyenné.

Tot slot werd er nog onderzocht of het toepassen van een warmteschok voor een infectie positieve of negatieve gevolgen heeft op het defensiemechanisme van Conférence tegen bacterievuur (hoofdstuk 5). Op basis van onze resultaten ziet het er naar uit dat het effect eerder nadelig is omdat de fenylpropanoid-gerelateerde genen lagere expressieniveaus vertoonden na de warmteshock en de infectie zich even snel verspreidde in weefsel met en zonder warmteschock. Hoewel in de proteoomstudie niet alle spots geïdentificeerd konden worden, waren er beduidend minder significante proteïnespots aanwezig zijn die gerelateerd zijn aan specifieke verdedingsmechanismen tegen de bacterie, wat erop kan wijzen dat de plant meer focust op het herstellen van warmteschock-gerelateerde schade dan de necrose veroorzaakt door *E. amylovora*.

Table of Contents

Summary..... i
Samenvatting..... iii
Table of Contents v
List of Figures. ix
List of Tables..... xv
Abbreviations.. xix

Chapter 1: General introduction

1. The pathogen *Erwinia amylovora* 2
   1.1 Morphology and physiology 2
   1.2 Virulence and pathogenicity 3
   1.3 Fire blight history, symptoms and cycle 8
   1.4 Economic impact of fire blight 13
   1.5 Management of fire blight 14
   1.6 Fire blight forecasting models 16
2. Defence mechanisms of the plant 17
   2.1 First signaling mechanisms 17
   2.2 Further signalling of the plant in response to *E. amylovora* 19
      2.2.1 ROS and the generation of an oxidative burst 20
      2.2.2 Secondary metabolites 22
      2.2.3 Plant hormones 25
      2.2.4 Pathogenesis related (PR) proteins 26
      2.2.5 Phytoalexins 26
      2.2.6 Photosynthesis 27

Chapter 2: Objectives

Chapter 3: Influence of leaf age on defence mechanisms against *E. amylovora* in *Pyrus*

1. Introduction 40
   1.1 The phenylpropanoid-flavonoid pathway and stress-related genes 40
   1.2 Photosynthesis and CO_2 metabolism 41
2. Objective 44

3. Material & Methods 45
3.1 Experimental design 45
3.2 Histological study 46
3.2.1 Light microscopy 46
3.2.2 Fluorescence microscopy 47
3.2.3 Transmission electron microscopy 47
3.3 RT-qPCR 48
3.4 HPLC 51
3.5 Chlorophyll fluorescence measurements 52
3.6 Leaf gas exchange measurements 53
3.7 Statistical analyses 54
4. Results 55
4.1 Symptom development 55
4.2 Antioxidative related genes 56
4.3 Phenylpropanoid-flavonoid pathway 58
4.3.1 Microscopic analysis shows the presence of bacteria and an increased accumulation of lignin and phenolic compounds near the vascular system of the leaf 58
4.3.2 RT-qPCR demonstrates significant up-regulation of genes of the phenylpropanoid-flavonoid pathway in the mature leaves 60
4.3.3 Epicatechin is more abundant in *Ea*-inoculated mature leaves, whereas chlorogenic acid is more abundant in *Ea*-inoculated immature leaves 63
4.4 Chlorophyll Fluorescence and respiration 67
4.4.1 Plant Efficiency Analyser and Fluorescence Imaging System 67
4.4.2 Respiration measurements 68
5. Discussion 75
Chapter 4: Comparison Conférence and Doyenné
1. Introduction 82
2. Objective 85
3. Material and Methods 87
3.1 Experimental design 87
3.2 RT- qPCR 88

3.3 HPLC 88
3.4 Proteomics 89
3.4.1 Total extraction procedure 89
3.4.2 Protein clean-up and quantification 89
3.4.3 Iso-electric focusing 89
3.4.4 2-D gel electrophoresis 90
3.4.5 Silver staining 90
3.4.6 Spotpicking and protein digestion 91
3.4.7 Mass spectrometric analysis and protein identification 91
3.5 Chlorophyll fluorescence 92
3.6 Statistics 92
4. Results 93
4.1 Symptom development 93
4.2 Conférence and Doyenné appear to have different transcription profiles regarding the phenylpropanoid-flavonoid pathway 94
4.3 HPLC profiling mainly shows differences between between the cultivars but not between treatments 99
4.4 Chlorophyll fluorescence in both cultivars indicates the presence of stress as a response to fire blight 101
4.5 Proteomics demonstrates differentially expressed spots in both Conférence and Doyenné after *Ea*-inoculation 108
5. Discussion 115

Chapter 5: Influence of a heat shock on defence mechanisms against *E. amylovora* in *Pyrus*

1. Introduction 122
2. Objective 125
3. Material & methods 126
3.1 Experimental design 126
3.2 RT-qPCR 127
3.3 Proteomics 127
3.4 Chlorophyll fluorescence 128
3.5 Statistics 128
4. Results 129

4.1 Symtom development 129

4.2 RT-qPCR indicates a down-regulation of some phenylpropanoid-flavonoid related genes in heat shock treated plants 130

4.3 Chlorophyll fluorescence measurements indicate a negligible effect on photosynthesis after the heat shock 132

4.4 Proteomics demonstrates differentially expressed spots after a heat shock and inoculation with *E. amylovora* 135

5. Discussion 144

Chapter 6: General Conclusion and Future Perspectives

References

List of Publications and Presentations

List of Figures

Figure 1.1: *Erwinia amylovora*, bacterial cell with internal structures and a certain amount of peritrichous flagella (bar = 500nm) 2
Figure 1.2: The structure of amylovoran, with Gal, galactose; Glc A, glucuronic acid; Pyr, pyruvate with keto-group; α and β, sugar linkages; D, sugar configuration; p, pyranoside; n, level of polymerisation (Nimtz *et al.*, 1996) 4
Figure 1.3: (A) The structure of a Type III Secretion System to inject bacterial effector proteins into the host cell. The needle complex consists of outer and inner rings with a neck in between. The cup is believed to be the entry point for substrates and the exit point for bacterial proteins (Schraidt and Marlovits, 2011). 6
(B) Model describing the role of Type III Secretion Systems in bacterial interactions with plants. The T3SS system (TTS) of plant pathogenic bacteria is associated with the Hrp pilus, which presumably spans the plant cell wall and serves as a conduit for secreted proteins. Among the secreted proteins are harpins (yellow) that presumably act at the plant cell surface by interacting with plant membranes and effector proteins (dark green) that act inside the cell (Buttner and Bonas, 2003). 6
Figure 1.4: The pathogenicity island of *E. amylovora* strain Ea321, which comprises a *hrp/hrc* region, a Hrc effectors and elicitors (HEE) region, a Hrp-associated enzymes (HAE) region and an island transfer (IT) region (Oh and Beer, 2005). 7
Figure 1.5: Symptoms of fire blight. A; Infected Conférence shoot with small yellow-coloured ooze drops on the side; B: Infected Kanzi blossom cluster ; C: Doyenné shoot with the extensive presence of red-coloured ooze drops; D: Infected Kanzi fruit with internal breakdown; E: Root stock blight with the typical flame structure. Pictures are own copyright except for E (Ministry of Agriculture, British Columbia, www.agf.gov.bc.ca) 10
Figure 1.6: The disease cycle of fire blight (Cornell University; www.nysipm.cornell.edu) 11
Figure 1.7: A zigzag model illustrates the quantitative output of the plant immune system. In phase 1, plants detect microbial- or pathogen-associated molecular patterns (MAMPs/PAMPs) via Pattern Recognition Receptors (PRRs) to trigger PAMP-Triggered Immunity (PTI). In phase 2, successful pathogens deliver effectors that interfere with PTI, or otherwise enable pathogen nutrition and dispersal, resulting in an Effector-Triggered Susceptibility (ETS). In phase 3, if an effector is recognized by an NB-LRR protein, Effector-Triggered Immunity (ETI) will be activated. ETI is an amplified version of PTI that often passes a threshold for induction of a hypersensitive respons (HR). In phase 4, pathogens that have gained new effectors are able to suppress ETI (Jones and Dangl, 2006). 18

Figure 1.8: Infection by *E. amylovora* causing the effector-related proteins DspA/E, Eop1, Eop3 and Eop4 to be secreted in the plant tissue, together with helper proteins and T3SS-related proteins. The result is an increase in ROS and different mechanisms to be triggered. 20
Figure 1.9: Antioxidative imbalance caused by *E. amylovora*, causing the amount of ROS to be increased and the antioxidative pool to be affected..... 22
Figure 1.10: Biosynthesis of the main constitutive flavonoids, phenols and polyphenols in pear (*Pyrus communis*). Enzyme abbreviations: phenylalanine ammonium lyase (PAL), chalcone synthase (CHS), chalcone isomerase (CHI), flavanon 3β hydroxylase (FHT), flavonoid-3'-hydroxylase (F3'H), flavonol synthase (FLS), flavonoid O-glucosyltransferase (FGT), dihydroflavonol-4-reductase (DFR), leucoanthocyanidin reductase 1 (LAR1), anthocyanidin synthase (ANS) and anthocyanidin reductase (ANR). Broken arrows indicate more than one biosynthetic step (Treutter, 2010). 23
Figure 1.11: Structure of a chloroplast, with inner and outer membrane, stroma, thylakoids and grana (Horton *et al.*, 2006). 28
Figure 1.12: Chemical structure of chlorophyll a, chlorophyll b and carotenoids and the absorption spectra of these molecules (cfb.unh.edu) 28
Figure 1.13: Overview of the carbon fixing cycle (Z-cycle) in plants (www.bio.ic.ac.uk) 29
Figure 1.14: Modified model of the possible fate of light energy once absorbed by PS II. Light energy absorbed by chlorophyll molecules in a leaf can undergo three different processes: it can be used to drive the photosynthetic energy conversion, and excess energy can be dissipated as heat or it can be reemitted as light (chlorophyll fluorescence). 31
Figure 1.15: The typical transient of OJIP curve that is created after illumination of a dark-adapted plant sample. On the X-coordinate, time is expressed in ms, the Y-coordinate shows the relative fluorescence intensity. .. 32
Figure 1.16: The quenching phase, where fluorescence is lowered to a basal level after a continuous actinic illumination. 33
Figure 3.1: Experimental design with the different treatments (left) and the sampling of the mature and immature leaves (right) 45
Figure 3.2: The HPLC equipment with a sample injector (Gilson Modell 231, Gilson Abimed, Ratingen, Germany) of two pumps (Kontron 422, Kontron, Eching, Germany) and a diode array detector (Bio Tek Kontron 540+, Kontron, Eching, Germany). 51
Figure 3.3: The Plant Efficiency Analyser developed by Hansatech Instruments. The PEA consists of a sensor with LEDs (black cylinder) and a control unit. Leaf clips cover up the parts that need to be measured. 53
Figure 3.4: The LCA4 equipment with broad leaf chamber unit (front) and control unit (back). 54
Figure 3.5: DAB-staining to show the presence of ROS (brown colour) at the cutting edge and the small veins in a *Ea*-inoculated immature leaf (A) and only

at the cutting edge in a mock-inoculated immature leaf (B), 48h after inoculation (bar=500µm, Stereoscopic Zoom Microscope Nikon SMZ800)..... 56
Figure 3.6: Relative expression values of Cu/Zn superoxide dismutase *CSD2* (A), Fe superoxide dismutase *FSD1* (B) and catalase *CAT1* (C) for different treatments (Untreated immature leaves, Mock-inoculated immature leaves, *Ea*-inoculated immature leaves, Untreated mature leaves, Mock-inoculated mature leaves and *Ea*-inoculated mature leaves), x hours after inoculation. Values are mean ± SE of 7 biological independent replicates. Gene expression data were expressed relatively to the reference genes and to the values of untreated immature leaves 3hours after inoculation (= relative expression value of 1) following the $2^{-\Delta Ct}$ method divided by the geometric mean of the reference genes..... 57
Figure 3.7: A and B: Electron micrographs of an *Ea*-inoculated immature (A) and an *Ea*-inoculated mature (B) leaf to show the occurrence of *E. amylovora* in the leaf tissue, 72h after inoculation (bars 5 (A) and 10 (B) µm, Philips EM 208 transmission electron microscope). Arrows indicate the presence of bacteria; C and D: Safranin-astra blue staining of an *Ea*-inoculated immature leaf (C) and an *Ea*-inoculated mature leaf (D), 72h after inoculation. Lignified and cutinized cell walls, stain bright red, cellulose cell walls and cytoplasm stain blue (bars 10 µm, Polyvar Reichert-Jung interference microscope); E and F: Naturstoff reagent A staining on an *Ea*-inoculated immature (E) and an *Ea*-inoculated mature (F) leaf, 72h after inoculation. The yellow fluorescence is consistent with the autofluorescence of phenolic compounds due to the NA-staining. In F, a bright yellow colour is clearly visible near the vascular system (bars 10µm, Fluorescence Microscope Nikon Eclips 80i). 59
Figure 3.8: Relative expression values of anthocyanidin reductase *ANR* (A), dihydroflavonol-4-reductase *DFR* (B) and flavonol synthase *FLS* (C) for different treatments (Untreated immature leaves, Mock-inoculated immature leaves, *Ea*-inoculated immature leaves, Untreated mature leaves, Mock-inoculated mature leaves and *Ea*-inoculated mature leaves), x hours after inoculation. Values are mean ± SE of 7 biological independent replicates. Gene expression data were expressed relatively to the reference genes and to the values of untreated immature leaves 3hours after inoculation (= relative expression value of 1) following the $2^{-\Delta Ct}$ method divided by the geometric mean of the reference genes..... 61
Figure 3.9: Total concentration (mg g^{-1} DW) of flavonols (A) and simple phenolics (B) for the different treatments (Untreated immature leaves, Mock-inoculated immature leaves, *Ea*-inoculated immature leaves, Untreated mature leaves, Mock-inoculated mature leaves and *Ea*-inoculated mature leaves), 48h and 72h after inoculation. Values are mean ± SE of 8 biological independent replicates..... 63
Figure 3.10: Total concentration of the hydroxycinnamic acids cis-neochlorogenic acid (A; µg g^{-1} DW), trans-neochlorogenic acid (B; µg g^{-1} DW), chlorogenic acid (C; mg g^{-1} DW) and cis-ferulic acid (D; µg g^{-1} DW) for the

different treatments (Untreated immature leaves, Mock-inoculated immature leaves, *Ea*-inoculated immature leaves, Untreated mature leaves, Mock-inoculated mature leaves and *Ea*-inoculated mature leaves), 48h and 72h after inoculation. Values are mean ± SE of 8 biological independent replicates..... 64
Figure 3.11: Concentration (µg g^{-1} DW) of the flavan-3-ols procyanidin B2 (A), catechin (B) and epicatechin (C) for the different treatments (Untreated immature leaves, Mock-inoculated immature leaves, *Ea*-inoculated immature leaves, Untreated mature leaves, Mock-inoculated mature leaves and *Ea*-inoculated mature leaves), 48h and 72h after inoculation. Values are mean ± SE of 8 biological independent replicates. 66
Figure 3.12: OJIP transient curves of mock-inoculated and *Ea*-inoculated immature leaves, 72h after inoculation. 72
Figure 3.13: Normalised FvF curves of mock-inoculated and *Ea*-inoculated immature leaves, 72h after inoculation. 72
Figure 3.14: OJIP transient curves of mock-inoculated and *Ea*-inoculated mature leaves, 72h after inoculation. 73
Figure 3.15: Normalised FvF curves of mock-inoculated and *Ea*-inoculated mature leaves, 72h after inoculation. 73
Figure 4.1: Experimental design with the different treatments (left) and the sampling of the 3rd , 4th and 5th leaf in Conférence and Doyenné (right)..... 87
Figure 4.2: The HPE-FlatTop Tower (SERVA)..... 90
Figure 4.3: Total concentration (mg g^{-1} DW) of flavonols (A) and simple phenolics (B) for the different treatments (mock-inoculated Conférence leaves, *Ea*-inoculated Conférence leaves, mock-inoculated Doyenné leaves and *Ea*-inoculated Doyenné leaves), 72hours and 4days after inoculation. Values are mean ± SE of 4 biological independent replicates. 99
Figure 4.4: Total concentration of the hydroxycinnamic acids cis-neochlorogenic acid (A; µg g^{-1} DW), trans-neochlorogenic acid (B; µg g^{-1} DW), chlorogenic acid (C; mg g^{-1} DW) and cis-ferulic acid (D; µg g^{-1} DW) for the different treatments (mock-inoculated Conférence leaves, *Ea*-inoculated Conférence leaves, mock-inoculated Doyenné leaves and *Ea*-inoculated Doyenné leaves), 72hours and 4days after inoculation. Values are mean ± SE of 4 biological independent replicates..... 100
Figure 4.5: Total concentration (µg g^{-1} DW) of the flavan-3-ols procyanidin B2 (A), procyanidin B5 (B), catechin (C) and epicatechin (D) for the different treatments (mock-inoculated Conférence leaves, *Ea*-inoculated Conférence leaves, mock-inoculated Doyenné leaves and *Ea*-inoculated Doyenné leaves), 72hours and 4days after inoculation. Values are mean ± SE of 4 biological independent replicates. 101
Figure 4.6: OJIP transient curves of leaf 4 (mock-inoculated), leaf 5 (with mock-inoculated leaf 4), leaf 4 (*Ea*-inoculated) and leaf 5 (with *Ea*-inoculated leaf 4) in Conférence, before inoculation (A), 4days after inoculation (B) and 8days after inoculation (C)..... 103

Figure 4.7: Normalised FvF curves of leaf 4 (mock-inoculated), leaf 5 (with mock-inoculated leaf 4), leaf 4 (*Ea*-inoculated) and leaf 5 (with *Ea*-inoculated leaf 4) in Conférence, before inoculation (A), 4days after inoculation (B) and 8days after inoculation (C). 104
Figure 4.8: OJIP transient curves of leaf 4 (mock-inoculated), leaf 5 (with mock-inoculated leaf 4), leaf 4 (*Ea*-inoculated) and leaf 5 (with *Ea*-inoculated leaf 4) in Doyenné, before inoculation (A), 4days after inoculation (B) and 8days after inoculation (C). 105
Figure 4.9: Normalised FvF curves of leaf 4 (mock-inoculated), leaf 5 (with mock-inoculated leaf 4), leaf 4 (*Ea*-inoculated) and leaf 5 (with *Ea*-inoculated leaf 4) in Doyenné, before inoculation (A), 4days after inoculation (B) and 8days after inoculation (C). 106
Figure 4.10: Spider plot of the trapping probability Φ_{P0} of leaf 4 (mock-inoculated), leaf 5 (with mock-inoculated leaf 4), leaf 4 (*Ea*-inoculated) and leaf 5 (with *Ea*-inoculated leaf 4) in Conférence and Doyenné, before inoculation and x days after inoculation. 107
Figure 4.11: Comparison between mock-inoculated and Ea-inoculated leaves leads to 55 differently expressed spots in Conférence (top) and 69 differently expressed spots in Doyenne (bottom), 72h after inoculation. 109
Figure 4.12: The hypothetical distribution of epicatechin (red) after inoculation with *E. amylovora* by scissors (black). It could be that epicatechin is more effective against fire blight when these molecules are present at the site of inoculation (right figure). 117
Figure 5.1: Experimental design with the different treatments (left) and the sampling of the heat shock in Conférence (right) 127
Figure 5.2: OJIP transient curves of mock-inoculated leaves without heat shock, mock-inoculated leaves with 15min heat shock, *Ea*-inoculated leaves without heat shock and *Ea*-inoculated leaves with 15min heat shock, before inoculation (A) and 72h after inoculation (B). 133
Figure 5.3: Normalised FvF curves of mock-inoculated leaves without heat shock, mock-inoculated leaves with 15min heat shock, Ea-inoculated leaves without heat shock and Ea-inoculated leaves with 15min heat shock,, before inoculation (A) and 72h after inoculation (B). 134
Figure 5.4: Differently expressed spots in Conférence without a heat shock (top; 70 spots) and with a heat shock (bottom; 97 spots), 72h after inoculation. 137

List of Tables

Table 3.1: Primer sequences of the used reference genes and genes of interest. 50
Table 3.2: Shoot infection values expressed as TH3 values, measured 6 and 8 days after inoculation, p<0.001 (Tukey) 55
Table 3.3: Percentage of the necrosis into the shoot, measured 6 and 8 days after inoculation, p<0.001 (Tukey) 55
Table 3.4: Heat map representation of the relative expression values for all investigated genes for the different treatments, x hours after inoculation. Each cell represents a relative expression value according to the colour scale at the bottom. Values in the cells are mean ± SE of 7 biological independent replicates. Gene expression data were expressed relatively to the reference genes and to the values of untreated immature leaves 3hours after inoculation (= relative expression value of 1) following the $2^{-\Delta Ct}$ method divided by the geometric mean of the reference genes. Mean values are followed by a letter. If values have the same letter, they do not differ significantly. Statistics are performed by a 2-way anova. Enzyme abbreviations, see text 61
Table 3.5: Explanation of the technical date of the OJIP curves and the selected JIP-test parameters 69
Table 3.6: The measured and calculated fluorescence PEA parameters for mock-inoculated immature leaves, *Ea*-inoculated immature leaves, mock-inoculated mature leaves and *Ea*-inoculated mature leaves, 24h after inoculation. Values are mean ± SE of 6 biological independent replicates. Bold numbers indicate a significant difference (α=0.05) compared to the corresponding mock-inoculated leaves. 70
Table 3.7: The measured and calculated fluorescence PEA parameters for mock-inoculated immature leaves, *Ea*-inoculated immature leaves, mock-inoculated mature leaves and *Ea*-inoculated mature leaves, 48h after inoculation. Values are mean ± SE of 6 biological independent replicates. Bold numbers indicate a significant difference (α=0.05) compared to the corresponding mock-inoculated leaves. 70
Table 3.8: The measured and calculated fluorescence PEA parameters for mock-inoculated immature leaves, *Ea*-inoculated immature leaves, mock-inoculated mature leaves and *Ea*-inoculated mature leaves, 72h after inoculation. Values are mean ± SE of 6 biological independent replicates. Bold numbers indicate a significant difference (α=0.05) compared to the corresponding mock-inoculated leaves. 71
Table 3.9: The measured and calculated gas exchange parameters for mock-inoculated immature leaves, *Ea*-inoculated immature leaves, mock-inoculated mature leaves and *Ea*-inoculated mature leaves, x hours after inoculation. Values are mean ± SE of 3 biological independent replicates. Bold numbers

indicate a (α=0.05) significant difference compared to the corresponding mock-inoculated leaves. 74
Table 4.1: Shoot infection values expressed as TH3 values, measured 7, 9 and 13 days after inoculation, p<0.001 (Tukey) 93
Table 4.2: Percentage of the necrosis in the shoot, measured 9 and 13 days after inoculation, p<0.001 (Tukey) 93
Table 4.3, 4.4 and 4.5: Heat map representation of the relative expression values for all investigated genes for the different treatments, x hours after inoculation for both Conférence (Conf) and Doyenné (Doy). Each cell represents a relative expression value according to the colour scale at the bottom. Values in the cell are mean ± SE of 10 biological independent replicates. Gene expression data were expressed relatively to the reference genes and to the values of mock-inoculated immature leaves 3hours after inoculation (= relative expression value of 1) following the $2^{-\Delta Ct}$ method divided by the geometric mean of the reference genes. Bold numbers indicate a significant difference (α=0.05) compared to the corresponding mock-inoculated leaves. Table 4.3 corresponds to leaf 3, table 4.4 corresponds to leaf 4 (= infected leaf) and table 4.5 corresponds to leaf 5. For enzyme abbreviations, see text. 95
Table 4.3 96
Table 4.4 97
Table 4.5 98
Table 4.6: Differentially expressed proteins in Conférence, 72h after inoculation. 110
Table 4.7: Differentially expressed proteins in Doyenné, 72h after inoculation. 112
Table 5.1: Shoot infection values expressed as TH3 values, measured 7 and 9 days after inoculation, p<0.001 (Tukey) 129
Table 5.2: Percentage of necrosis in the shoot, measured 7 and 9 days after inoculation, p<0.001 (Tukey) 129
Table 5.3: Heat map representation of the relative expression values for all investigated genes for the different treatments in Conférence (s h.s. = sine heat shock, c h.s. = cum heat shock), x hours after inoculation. Each cell represents a relative expression value according to the colour scale at the bottom. Values in the cell are mean ± SE of 8 biological independent replicates. Gene expression data were expressed relatively to the reference genes and to the values of mock-inoculated leaves without a heat shock, 3hours after inoculation (= relative expression value of 1) following the $2^{-\Delta Ct}$ method divided by the geometric mean of the reference genes. Mean values are followed by a letter. If values have the same letter, they do not differ significantly. Statistics are performed by a 2-way anova. For enzyme abbreviations, see text. 130
Table 5.4: Differentially expressed proteins in Conférence leaves without heat shock, 72h after inoculation. 138
Table 5.5: Differentially expressed proteins in Conférence leaves with 15min heat shock, 72h after inoculation. 140

Table 6.1: Summary table with the major trends of the conducted research 153

Abbreviations

Ams	Amylovoran synthesing
ANR	AnthocyanidiN Reductase
ANS	AnthocyanidiN Synthase
APX	Ascorbate PeroXidase
Avr	Avirulence
BIS	Billing's Integrated System
BRS	Billing's Revised System
CAT	Catalase
CFU	Colony Forming Units
CHI	Chalcone Isomerase
CHS	Chalcone Synthase
CS	Cross Section
CSD	Cu/Zn Superoxide Dismutase
DAB	3-3' diaminobenzidine
DFR	DihydroFlavonol-4-Reductase
Dsp	Disease specific
DW	Dry Weight
Ea	*Erwinia amylovora*
EPS	Exopolysaccharide
ESI	ElectroSpray Ionization
ETI	Effector-Triggered Immunity
ETS	Effector-Triggered Susceptibility
Fd	Ferredoxin

FGT	Flavonoid O-GlucosylTransferase
FHT	Flavanon 3β Hydroxylase
FIS	Fluorescence imaging System
FLS	FlavonoL Synthase
FSD	Fe Superoxide Dismutase
HAE	Hrp-Associated Enzymes
HEE	Hrc Effectors and Elicitors
HR	Hypersensitive Respons
Hrc	Hrp-conserved
Hrp	Hypersensitive response and pathogenicity
IEF	IsoElectric Focusing
IT	Island Transfer
JA	Jasmonic Acid
LAR1	LeucoAnthocyanidin Reductase 1
LHC	Light Harvesting Complex
Lhca	Light Harvesting Antenna Complex
LOX	LipOXygenase
MALDI	Matrix-Assisted Laser Desorption/Ionization
MAMP	Microbial-Associated Molecular Pattern
MS	Mass Spectrometry
MSD	Mn Superoxide Dismutase
NA	Naturstoff reagent A
NB-LRR	Nucleotide Binding-Leucine Rich Repeats
PAI	Pathogenicity Island
PAL	Phenylalanine Ammonium Lyase

PAMP	Pathogen-Associated Molecular Pattern
PBS	Phosphate Buffered Saline
PC	PlastoCyanin
PEA	Plant Efficiency Analyser
pI	Isoelectric point
PIPES	1,4-piperazinediethanesulfonic acid
PQ	Plastoquinone
PQH_2	Plastoquinol
PR	Pathogenesis-Related
PRR	Pattern Recognition Receptor
PS I	PhotoSystem I
PS II	PhotoSystem II
PTI	PAMP-Triggered Immunity
Q_A	Plastoquinone
Q_B	Plastoquinol
R	Resistance
RC	Reaction Center
RLK	Receptor-Like Kinase
RLP	Receptor-Like Protein
ROS	Reactive Oxygen Species
SA	Salicylic Acid
SAR	Systemic Acquired Resistance
SDS-PAGE	Sodium Dodecyl Sulphate-PolyAcrylamide Gel Electrophoresis
SOD	SuperOxide Dismutase
T3SS	Type III Secretion System

QS	Quorum Sensing
YPGA	Yeast Peptone Glucose Agar

Chapter 1:

General introduction

1. The pathogen *Erwinia amylovora*

1.1 Morphology and physiology

Erwinia amylovora Burrill Winslow *et al.* (1920), the causal agent of fire blight, is a rod-shaped gram-negative bacterium with an average length of 1-3µm and a width of 0.3-1.2µm. It is categorised into the family of *Enterobacteriaceae*, which harbours important pathogens, both plant-associated (*Dickeya*, *Pantoea*, *Enterobacter*,...) and animal/human-associated (*Escherichia*, *Yersinia*, *Salmonella*,...) species. The bacterium is equipped with 2-7 peritrichous flagella, which allow mobility of the organism (figure 1.1). The guanine-cytosine level of its DNA varies from 53.6 till 54.1 mol%.

E. amylovora is capable of growth between 3°C and 37°C. The optimal temperature of growth is situated between 24-27°C. Generation time during optimal conditions varies from 70-90 minutes (Billing, 1974). Nicotinic acid is obligatory for its growth (Starr and Mandel, 1950). Like all other *Enterobacteriaceae, E. amylovora* is not capable of reducing nitrate to nitrite. The colony-forming phenotype during growth depends strongly on the growth medium that was used and the cultivating conditions that were maintained. Colonies on a Yeast Peptone Glucose Agar (YPGA) growth medium at a temperature of 24°C are white, circular and mucoid.

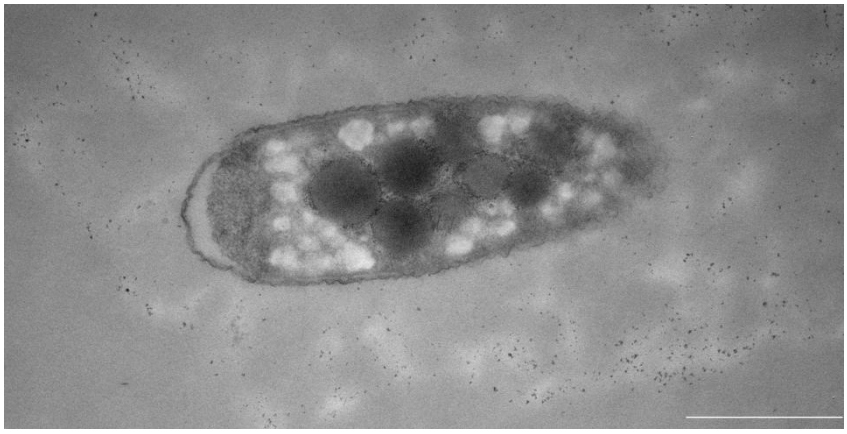

Figure 1.1: *Erwinia amylovora*, bacterial cell with internal structures and a certain amount of peritrichous flagella (bar = 500nm)

E. amylovora is a facultative anaerobic organism, which allows the bacteria to switch from an aerobic to an anaerobic metabolism depending on the environmental conditions to which the bacteria are exposed. During anaerobic conditions, fermentation is used for growth, whereas during aerobic conditions, they change to an aerobic respiration (van der Zwet & Keil, 1979;Paulin, 2000).
Contrary to the former "soft rot *Erwinias*", nowadays represented by the genera *Brenneria*, *Pectobacterium* and *Dickeya* (Hauben *et al.*, 1998), an important characteristic of *Erwinia amylovora* is a total inability to produce pectolytic, cellulolytic or xylolytic enzymes (Seemuller and Beer, 1976).

1.2 Virulence and pathogenicity

E. amylovora exists in an innumerable amount of strains with slight genetic variations. Throughout the different strains of *E. amylovora*, each strain has its own fitness, pathogenicity and virulence. Pathogenicity has been defined as the overall ability of a pathogen to infect a host and cause disease, whereas virulence is a quantitative measurement of the ability to cause disease (Shaner *et al.*, 1992).
Pathogenicity in *Erwinia amylovora* depends mainly on the production of EPS, which have been suggested to play a role in bypassing the plant defence system, in disturbing and obstructing the vascular system of the plant and in protecting the bacteria against water and nutrient loss during dry conditions (Denny, 1995; Ordax *et al.*, 2010).
One of these EPS is amylovoran, which is the main constituent of bacterial ooze. Amylovoran (figure 1.2) is a polymer of a pentasaccharide repeating unit that generally consists of four galactose residues and one glucuronic acid residue (Maes *et al.*, 2001; Nimtz *et al.*, 1996). The molecular size of amylovoran is influenced by several environmental conditions and cell metabolism related factors (Schollmeyer *et al.*, 2012). *E. amylovora* strains that do not have the capacity to produce amylovoran, are non-pathogenic and are unable to spread in plant vessels (Bellemann and Geider, 1992). Another EPS that is synthesized by *E. amylovora* is levan. Lack of levan synthesis can result in a slow development of symptoms in the host plant (Geier and Geider, 1993).

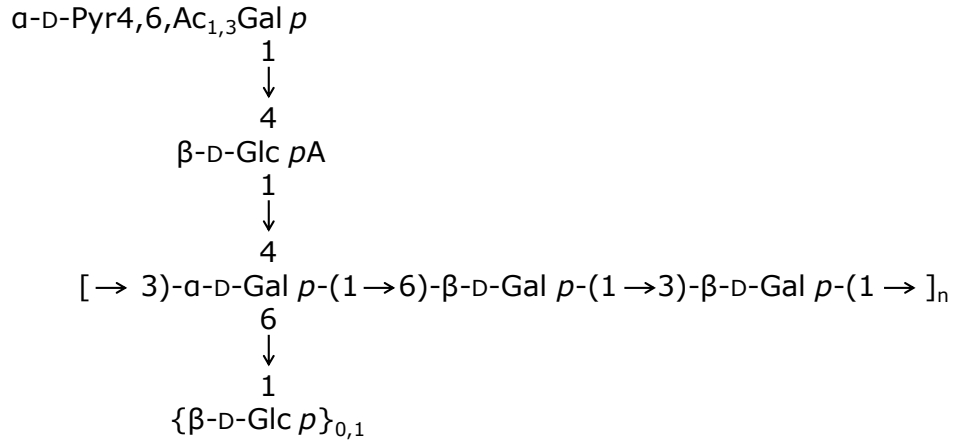

Figure 1.2: The structure of amylovoran, with Gal, galactose; Glc A, glucuronic acid; Pyr, pyruvate with keto-group; α and β, sugar linkages; D, sugar configuration; p, pyranoside; n, level of polymerisation (Nimtz *et al.*, 1996)

The *amylovoran synthesis* (*ams*) gene cluster involved in the biosynthesis of amylovoran leads to twelve *ams* encoded gene products (AmsA up to AmsL). AmsH, AmsL and AmsC are believed to be involved in oligosaccharide transport and assembly whereas AmsA possesses a tyrosine kinase activity. Both AmsG, AmsB, AmsD, AmsE, AmsJ and AmsK proteins appear to play part in annealing the different galactose, glucuronic acid and pyruvyl subunits to the lipid carrier in order to form an amylovoran unit. AmsF instead may process newly synthesized repeating units and/or their polymerization by adding them to an existing amylovoran chain. Finally, AmsI seems to have a distinct function in the recycling of the diphosphorylated lipid carrier after release of the synthesized repeating unit (Bugert and Geider, 1997; Eastgate, 2000; Langlotz *et al.*, 2011). Recently Koczan *et al.* (2009) discovered that EPS of *Erwinia amylovora* are also involved in biofilm formation. Biofilms are multicellular communities that attach to several surfaces (Koczan *et al.*, 2011). As a result of the complex network caused by exopolysaccharides, proteins and DNA, bacterial cells are able to adhere to surfaces and each other (Ramey *et al.*, 2004). Study in *Pseudomonas aeruginosa* reveals that the process of biofilm formation can be divided in five distinct phases including reversible attachment, irreversible attachment, maturation 1, maturation 2 and detachment of the dispersion phase (Sauer *et al.*, 2002). Biofilm infections appear to be very persistent and it is shown that

bacteria that are able to compose a biofilm can be up to 1000-fold more resistant to antibiotic treatment than their planctonic counterparts (Gander and Gilbert, 1997). Koczan *et al*. (2009) suggested that biofilm formation plays an important role in pathogenesis of *E. amylovora*. Their study showed that amylovoran is necessary for biofilm formation and that levan contributes to this biofilm formation. They also confirmed the results of Maes *et al.* (2001), in which was shown that the quantity of amylovoran produced by individual *E. amylovora* strains is correlated with the degree of virulence.

The mechanistic details behind biofilm formation remain largely unknown but it is suggested that they are formed in response to several environmental triggers (Davey and O'toole, 2000) and quorum sensing (QS) signals (Sauer *et al.*, 2002). Quorum sensing allows bacteria to communicate with each other by the secretion of signal molecules. Although research has shown that *Erwiniae* species produce two types of QS molecules namely N-acyl homoserine lactones and autoinducer-2 type signalling molecules (Barnard and Salmond, 2007; Molina *et al.*, 2005), Rezzonico and Duffy (2008) suggest a non-quorum sensing role for the autoinducer-2 *luxS* gene due to a lack of genomic evidence for autoinducer-2 receptors.

Another important factor in pathogenicity is confined by the action of the type III secretion system (T3SS) (figure 1.3). Gram-negative phytopathogenic bacteria such as *Erwinia amylovora* utilize this evolutionarily conserved secretion system to export and deliver effector proteins into the cytosol of host plant cells through a pilus-like structure, which forms the central core element of the T3SS. This needle complex is composed out of a large, cylindrically shaped macromolecular complex organised into a series of ring-like structures with inner rings, outer rings and a neck structure. It is embedded in the inner and outer membrane of the bacteria, while spanning the periplasmic membrane and extending into the extracellular environment with a needle filament (Alfano and Collmer, 2004; Block *et al.*, 2008; Buttner and Bonas, 2003; Buttner and Bonas, 2006; Buttner and He, 2009; Cornelis and Van Gijsegem, 2000; Galan and Wolf-Watz, 2006; Grant *et al.*, 2006; He *et al.*, 2004; Hueck, 1998; Jin *et al.*, 2001; Loquet *et al.*, 2012; Mccann and Guttman, 2008; Mudgett, 2005; Schraidt and Marlovits, 2011).

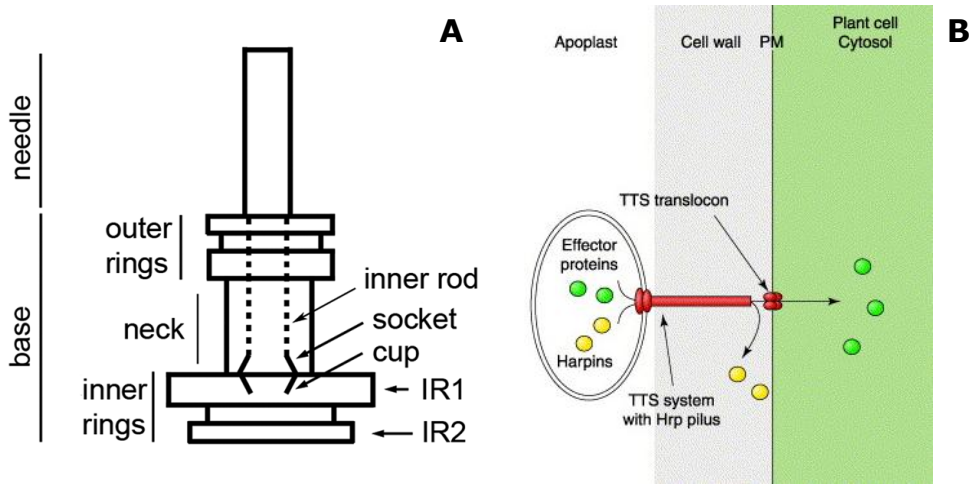

Figure 1.3: (A) The structure of a Type III Secretion System to inject bacterial effector proteins into the host cell. The needle complex consists of outer and inner rings with a neck in between. The cup is believed to be the entry point for substrates and the exit point for bacterial proteins (Schraidt and Marlovits, 2011).
(B) Model describing the role of Type III Secretion Systems in bacterial interactions with plants. The T3SS system (TTS) of plant pathogenic bacteria is associated with the Hrp pilus, which presumably spans the plant cell wall and serves as a conduit for secreted proteins. Among the secreted proteins are harpins (yellow) that presumably act at the plant cell surface by interacting with plant membranes and effector proteins (dark green) that act inside the cell (Buttner and Bonas, 2003).

The T3SS of plant pathogenic bacteria is mainly made out of Hrc proteins, encoded by *hrp*-conserved (*hrc*) genes among plant pathogenic bacteria, and Hrp proteins, encoded by hypersensitive response and pathogenicity (*hrp)* genes. In *E. amylovora*, *hrc* and *hrp* genes are clustered in a pathogenicity island (PAI) which contains four regions i.e. a *hrp*/*hrc* region, a Hrc effectors and elicitors (HEE) region, a Hrp-associated enzymes (HAE) region and an island transfer (IT) region (figure 1.4) (Oh and Beer, 2005). The key regulatory gene is *hrp*L, which encodes the extracytoplasmic function of σ-factor HrpL, which in turn recognizes conserved sequence motifs (*hrp* boxes) located in promoters of *hrp* secretion genes and of genes encoding secreted proteins (Mcnally *et al.*, 2012; Oh *et al.*, 2005; Pester *et al.*, 2012).

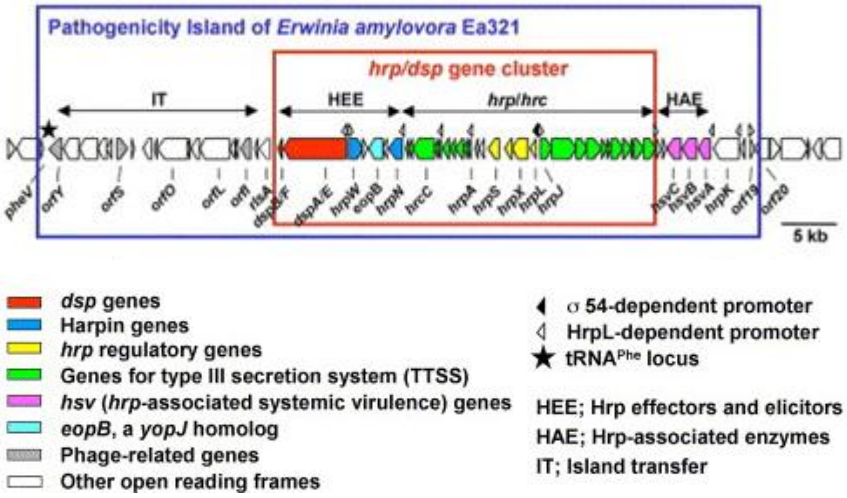

Figure 1.4: The pathogenicity island of *E. amylovora* strain Ea321, which comprises a *hrp/hrc* region, a Hrc effectors and elicitors (HEE) region, a Hrp-associated enzymes (HAE) region and an island transfer (IT) region (Oh and Beer, 2005).

Up till now, twelve proteins have been found that are secreted via this T3SS (Nissinen *et al.*, 2007).

Four of them (Eop1, Eop3, Eop4 and DspA/E) have clear similarity to known effectors. The 200kDa Disease Specific factor DspA/E for example, which is homologous to the type III effector AvrE discovered in soybean after inoculation with *Pseudomonas syringae* pv. *tomato*, is required for pathogenicity in several strains of *E. amylovora*. DspA/E interacts with the intracellular domains of host plant receptor kinases and preferredoxin (Boureau *et al.*, 2006; Meng *et al.*, 2006; Nissinen *et al.*, 2007; Oh *et al.*, 2007; Oh *et al.*, 2010; Triplett *et al.*, 2009). Efficient secretion of DspA/E requires a type III chaperone DspB/F, which is a small acidic protein that binds to its cognate secreted protein (Gaudriault *et al.*, 2002; Triplett *et al.*, 2010).

Five proteins belong to the helper protein class, namely Eop2, HrpK, HrpN, HrpW and HrpJ. Eop2 and HrpK have clear similarities to proteins in *P. syringae*, but their functions still remain elusive (Nissinen *et al.*, 2007). Both HrpN and HrpW are harpins. These proteins are glycine-rich, lack cysteine and are involved in inducing the hypersensitive response in non-host plants. Unlike HrpW, HrpN is required for full virulence in plants (Kim and Beer, 1998; Reboutier *et al.*, 2007;

Sinn *et al.*, 2008; Wei *et al.*, 1992) and plays an important role in the translocation of DspA/E (Bocsanczy *et al.*, 2008). HrpJ has been postulated to act as an essential extracellular chaperone to prevent aggregation of harpins in the apoplast, and thus facilitate translocation of effector proteins into the host cells (Nissinen *et al.*, 2007).

The three remaining proteins that are secreted via the T3SS are HrpA, TraF and FlgL. HrpA is an essential structural protein of the type III secretion pilus, TraF is involved in pilus formation and FlgL is similar to a flagellar hook-filament junction protein (Nissinen *et al.*, 2007).

Besides the synthesis of amylovoran and the mechanism of the T3SS and its associated proteins, the production of the siderophore desferrioxamine for the acquisition of iron molecules out of the host tissue (Dellagi *et al.*, 1998; Expert, 1999; Smits and Duffy, 2011) and the presence of other virulence factors such as metalloproteases (Zhang *et al.*, 1999), the presence of plasmids (Llop *et al.*, 2011; Llop *et al.*, 2012; Mcghee and Jones, 2000; Mohammadi, 2010), two component signal transduction systems (Wang *et al.*, 2009a; Zhao *et al.*, 2009) and histone-like proteins (Hildebrand *et al.*, 2006) are also important factors in pathogenesis.

Only recently the complete genome of *Erwinia amylovora* CFBP1430 was sequenced and annotated, revealing novel insights into the genome (Smits *et al.*, 2010), which will warrant evaluation of these systems in the virulence, host range and ecological behaviour of this pathogen on its host plants in the near future.

1.3 Fire blight history, symptoms and cycle

Fire blight, caused by *Erwinia amylovora*, was first discovered in 1780, in the neighbourhood of the Hudson River Valley, New York, from where it dispersed further throughout the rest of the United States. Mid 19th century, the disease was noticed in Canada. In 1919, it reached New-Zealand and in 1943, it was reported in Mexico. In 1957, fire blight arrived at the south-eastern coast of Great Britain, making this the first observation of *E. amylovora* in Europe. In 1972, fire blight was observed in Belgium in the surroundings of Adinkerke. It took the bacteria five years to spread out across the entire region of Flanders (Deckers, 1996). Nowadays, around 50 countries have reported the presence of

fire blight, of which Belarus is the last known new country where *E. amylovora* was observed (Lagonenko *et al.*, 2008).

Fire blight is considered as one of the most devastating diseases in the family of the *Rosaceae*. Besides to the economical important genera of pear (*Pyrus*) and apple (*Malus*), 129 species in 37 genera of *Rosaceae* have been reported to be susceptible to fire blight. Of these genera, six of them are fruit crops: *Cydonia*, *Eriobotrya*, *Fragaria*, *Mespilus*, *Prunus* and *Rubus*. The remaining genera are nearly all ornamental plants such as *Cotoneaster*, *Crataegus*, *Pyracantha* and *Sorbus*.

The name fire blight is descriptive for most of the true characteristics and easy diagnostics of the disease, namely a blackening of the twigs, flowers, leaves and fruits, as if they have been swept by fire. Infected shoots will first appear water soaked, next they will turn dark green and wilt, shrivel and finally turn brownish to black. Blighted twigs often form a shepherd's crook or cane-like bend, caused by a total collapse of the parenchyma cells. Infected leaves will not fall off, but remain attached to the infected twig. Blossom and fruit blight have the same symptoms as in the shoot or leaf (van der Zwet & Keil, 1979;Thomson, 2000; Van der Zwet *et al.*, 2012). The intensity of the blackening depends on the host. Apple and pear exhibit similar symptoms, although symptoms on pear are normally more pronounced. Regarding the primary plant part that is infected, the terms shoot blight, blossom blight, leaf blight, fruit blight, trunk blight and root(stock) blight are used (figure 1.5).

In all cases, sticky, amber-like ooze drops, composed out of viable bacteria in a polysaccharide matrix might be formed on the blighted plant parts. At low humidity, bacterial strands creating a fragile cobweb-like appearance can be observed. Without any doubt, the production of these wet or dry ooze drops is one of the most diagnostic symptoms of this disease.

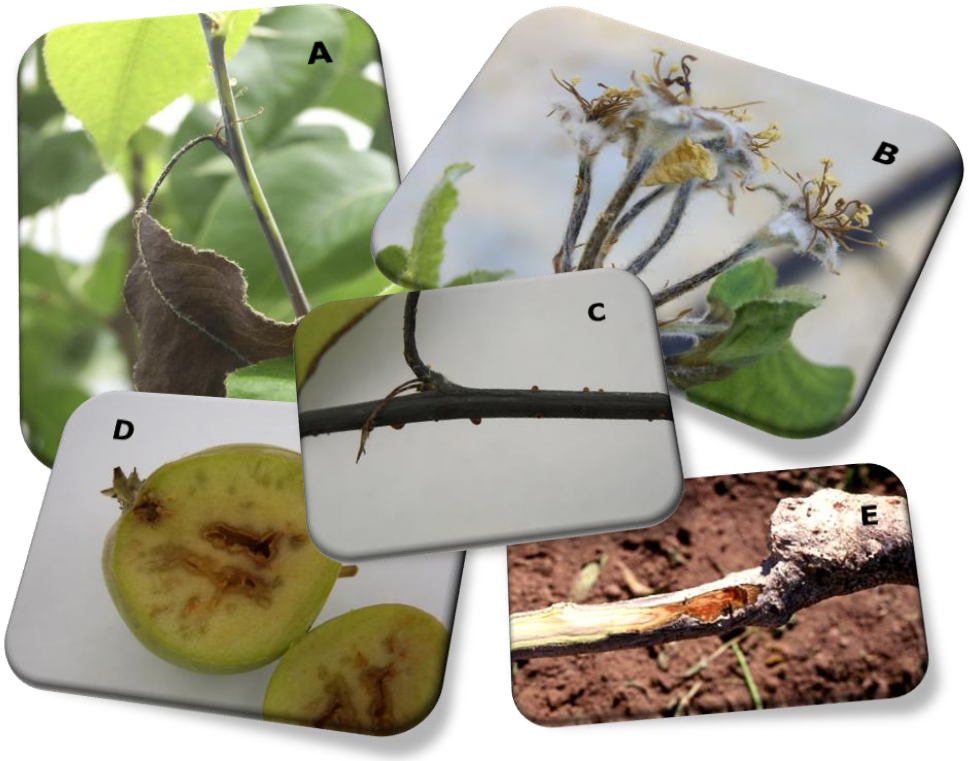

Figure 1.5: Symptoms of fire blight. A; Infected Conférence shoot with small yellow-coloured ooze drops on the side; B: Infected Kanzi blossom cluster ; C: Doyenné shoot with the extensive presence of red-coloured ooze drops; D: Infected Kanzi fruit with internal breakdown; E: Root stock blight with the typical flame structure. Pictures are own copyright except for E (Ministry of Agriculture, British Columbia, www.agf.gov.bc.ca)

Fire blight is a complex disease which passes its entire cycle in close association with the host plant (figure 1.6). A detailed description of this cycle can be found in van der Zwet & Keil (1979), Thomson (2000) and van der Zwet *et al.* (2012). Infection only takes place if the conditions are favourable and the inoculum density is high enough. For a successful infection, an amount of 10^6 Colony Forming Units (CFU) ml^{-1} is thought to be necessary, whereas in the blossoms already 10^3 CFU ml^{-1} is enough. Furthermore, a temperature above 18°C is needed with a relative humidity above 60%, with optima around 24°C and 95% humidity.

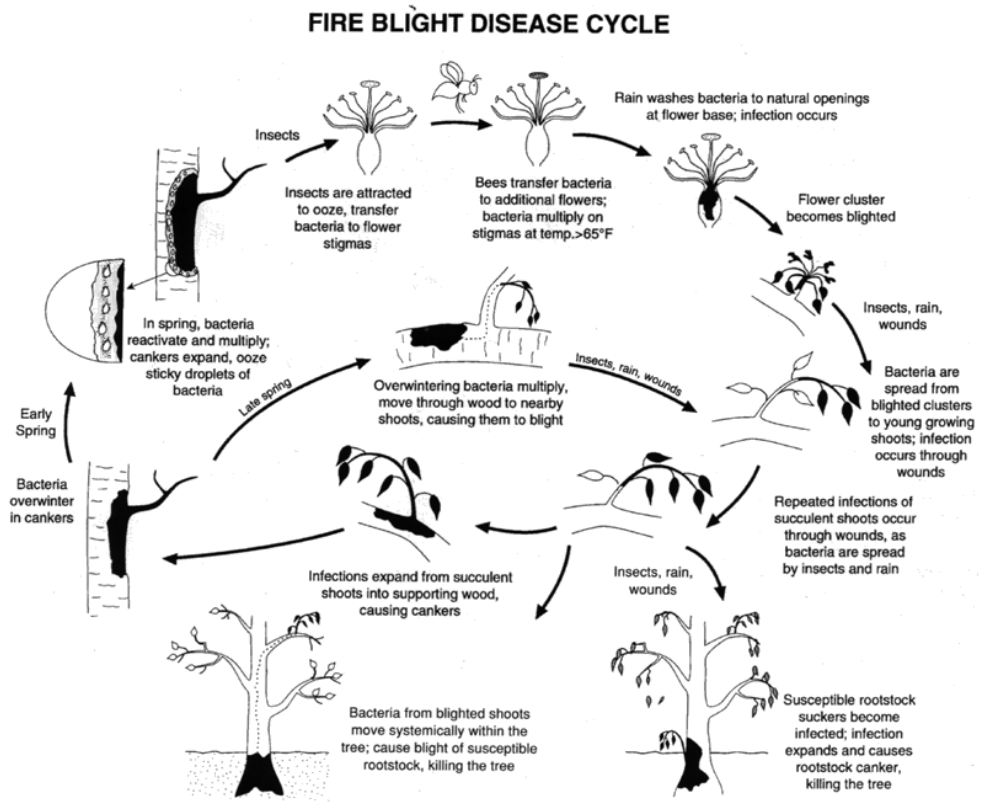

Figure 1.6: The disease cycle of fire blight (Cornell University; www.nysipm.cornell.edu)

The primary infection happens in spring during the blossom period, when temperatures start to increase and cankers are becoming active. Some of these cankers, the so-called holdover cankers, were infected the previous year and are a source of inoculum. This inoculum is situated in the demarcation line between the healthy and the diseased tissue. Often, this involves the production of ooze drops. However, ooze is not necessary for bacteria to be available. In some cases, viable bacteria have been isolated from non-oozing canker surfaces. Furthermore, it is also possible for *Erwinia amylovora* to reside as an epiphyte on plant tissue (Miller and Schroth, 1972; Thomson *et al.*, 1975).

The bacteria can be disseminated in different ways. Rain, the most common factor in *E. amylovora* dissemination, easily splashes the bacteria from ooze on cankers to flowers and leaves. Rain drops facilitate the movement, causing a

rise in humidity and a decrease of the internal amount of sugars inside the nectarthodes, making infection more successfully. Dry strands or ooze droplets can be dispersed by wind, even over long distances. Pollinating insects are important disseminators too, passing the bacteria on from flower to flower. Insects with piercing or sucking mouthparts like aphids or psyllas not only create wounds through which the bacteria can penetrate the tissue, they also are responsible for dissemination to other host plants. Migratory birds are responsible for the dispersal of the bacteria over longer distances. Contaminated pruning tools or non-disinfected propagation are the most important means of spread of the bacteria by man.

The bacteria enter through wounds (the so-called trauma blight) or through natural openings, such as nectarthodes, uncutinized stigmas, hydathodes, gland trichomes, lenticels and stomata. Once the bacteria have reached these natural or artificial entry points in the host, they will multiply and advance in the intercellular spaces. After a few days, the cells of the spongy parenchyma start to collapse as a result of plasmolysis, and in a next phase, discolorations and necrosis start to show. After killing off a blossom or a shoot, blight infection moves further into the host, reaching the main branches and the trunk. At this point, the infection, if walled off, produces a canker or penetrates further into the trunk and roots, leaving behind some sort of internal flame structure and finally resulting in the death of the tree.

Numerous studies have been done to elucidate the migration of *E. amylovora* in plant tissue. Often plants were inoculated by accidently damaging the vascular system, providing a path for movement in the xylem and phloem (Bogs *et al.*, 1998; Suhayda and Goodman, 1981). Nowadays, it is generally accepted that *E. amylovora* uses the intercellular spaces to migrate in the plant after a natural infection, but in some cases bacterial movement also takes place in the xylem (Bogs *et al.*, 1998). This advance might be seen as a simple consequence of the increased physical pressure in the intercellular space due to bacterial multiplication or absorption of water by the exopolysaccharides. Such pressure being exerted pushes the bacteria to move, seemingly in all directions, even outside the plant (ooze drops). The speed of migration in the host plant is estimated at about 15cm in 7h (Thomson, 2000).

Secondary infection occurs when secondary inoculum is available. Sources of secondary inoculum may be bacterial strands or ooze drops produced on leaves, shoots, fruit and larger branches upon primary infection. These bacteria can be dispersed again by rain, wind, insects, birds or man. The secondary infections are generally far more numerous and usually cause more injury to the trees. Secondary cycles may continue throughout the remainder of the growing season and may terminate as a canker, closing the lifecycle of *E. amylovora*.

1.4 Economic impact of fire blight

In 2011, the total surface area destined for the cultivation of fruit crops was more than 17000ha in Belgium, of which 7752ha apple trees and 8216ha pear trees. Most of this cultivation area is largely situated in the province of Limburg (Hesbaye) and to a much lower extent in Vlaams-Brabant. In 2011, about 228405 ton apples and 284827 ton pears were produced, emphasizing the importance of fruit production in Belgium (www.eurostat.be).

Erwinia amylovora has proven to be extremely difficult in properly managing the disease, due to its rapid spread in the host plant. That is the reason why the European Union considers fire blight as a quarantine disease and why it is included in the European Plant Protection Organisation (EPPO) list of A2 quarantine organisms. Hence, the Belgian Federal Agency for the Safety of the Food Chain (FASFC) does a profound control of protected areas around nurseries of possible *Erwinia amylovora* related host plants. If infection is noticed, then the diseased trees have to be removed and destroyed afterwards. Together with a total standstill in export, this may lead to severe economic losses.

Every year, fire blight infections are reported on apple and pear in Belgium, but also on the ornamental host plants. For instance, between 1981 and 1991, Belgium lost about 50% of the areal of the pear cultivar Durondeau due to fire blight.

For apple, there are less problems for the common cultivars Jonagold and Golden Delicious. However, some new apple cultivars are very susceptible to fire blight. Kanzi and Braeburn, for instance, are very sensitive for flower and shoot infections. The new apple cultivar Belgica is sensitive and has to face with massive flower infections when temperature rises during spring.

1.5 Management of fire blight

The control of fire blight is difficult, as most of the available techniques are not totally effective and rather have the ability to reduce or inactivate further spread of *Erwinia amylovora* instead of killing off the bacteria.

The chemical control is limited to two groups of compounds, namely copper(-derivatives) and antibiotics. Copper is a bacteriostatic compound that generally is applied during the dormant period and before budbreak to avoid phytotoxic effects on the leaves and russetting of the fruit skin (Geider, 1999; Loper *et al.*, 1991; Ordax *et al.*, 2006). Antibiotics such as streptomycin are considered to be the most effective control methods against fire blight, but inappropriate or abundant use can result in the development of several resistant bacterial strains. That is the reason why a lot of countries -including Belgium- prohibit the use of streptomycin in horticulture (Burr *et al.*, 1993; Loper *et al.*, 1991; McManus *et al.*, 2002; Schroth *et al.*, 1979).

Because of this lack in commercial, effective and non-phytotoxic compounds, the development of products capable of potentiating the plant's defence mechanisms have received a lot of attention over the last years and have become a booming business. Such products are for instance benzothiadiazole (Actigard®, Bion®, Blockade® or Boost®), prohexadione-Ca (Apogee® or Regalis®), phosetyl-Al (Aliette®), Laminarin (Vacciplant®) and harpin protein (Employ® or Harp-N-Tek®)

Benzothiadiazole or Acibenzolar-S-Methyl imitates the role of salicylic acid, resulting in the production of Pathogenesis Related (PR) proteins capable of degrading bacterial cell walls and inducing a systemic acquired resistance (Maxson-Stein *et al.*, 2002; Sparla *et al.*, 2004).

Prohexadione-Ca blocks a 2-oxoglutarate-dependent dioxygenase in the phenylpropanoid-flavonoid pathway. The consequence is that the luteoliflavan is formed together with the unstable and highly reactive flavan-4-ol luteoforol in pome fruits. Luteoliflavan shows phytoalexin-like properties against *E. amylovora* and other pathogens and it reduces shoot growth by inhibiting gibberellin biosynthesis (Bubab et al., 2003; Costa et al., 2001; Flachowsky et al., 2012; Halbwirth et al., 2003; Norelli and Miller, 2004; Roemmelt et al., 2003a; Spinelli et al., 2005b).

Fosetyl-Al or its metabolite phosphonic acid has, besides activating the defence mechanism of the plant in a systemic way, the ability to function as a bacteriostatic compound (Tsiantos et al., 2003).

Both laminarin, which is a linear β-1,3-glucan that is extracted and purified from the brown alga *Laminaria digitata*, and the commercially made available harpin protein are also sold as plant defence elicitors (Aziz et al., 2003; Klarzynski et al., 2000; Malnoy et al., 2005; Reboutier et al., 2007).

Control of fire blight using microbial antagonists has become a new angle of incidence as well. The last years, much research has been published using the bacteria *Pseudomonas fluorescens*, *Bacillus subtilis*, *Pantoea agglomerans, Pantoea vagans*, ... or the yeast *Aureobasidium pullulans* as antagonistic organisms (Broggini *et al.*, 2005; Cabrefiga *et al.*, 2007; Chen *et al.*, 2009; Giddens *et al.*, 2003; Kim *et al.*, 2012; Loncaric *et al.*, 2008; Ozaktan and Bora, 2004; Paternoster *et al.*, 2010; Pujol *et al.*, 2006; Pusey, 2002; Pusey *et al.*, 2011; Stockwell *et al.*, 2002; Stockwell *et al.*, 2011; Wilson and Lindow, 1993; Wright *et al.*, 2001). On one hand, their working mechanism is based on the production of antibiotics, which will kill off *E. amylovora*, and/or on the other hand on a fast multiplication, which gives these organisms the ability to compete with *E. amylovora* for space and available sugars. The use of bacterial viruses or bacteriophages is another alternative, as they are able to control the fire blight disease too (Gill *et al.*, 2003; Kim *et al.*, 2004; Nagy *et al.*, 2012). The effects of these antagonists in field trials are hopeful but remain precarious due to unstable population densities and/or the interdependence of environmental variables. Especially the timing of application and the maturity of the blossoms have a large influence on the efficacy of these antagonists against fire blight (Johnson *et al.*, 2000; Pusey, 1999; Pusey and Curry, 2004; Spinelli *et al.*, 2005a; Thomson and Gouk, 2003).

Of all the previous mentioned products and antagonists, only the use of Aliette® (phosetyl-Al 80%), Blossom Protect® (which is a combination of citric acid 42.7% and the antagonistic yeast *Aureobasidium pullulans* strain DSM 14940 & strain 19941) and Vacciplant® (45g/l Laminarin) is allowed in Belgium. Prohexadione-Ca (Regalis®) is allowed, but only for the removal of undesired shoots.

When a grower decides not to make use of chemical substances and/or antagonists, the only remaining remedial technique is a drastic pruning of the infected parts (at least 40cm away from the symptomatic shoots), which have to be burned afterwards. Pruning tools have to be disinfected properly by using dettol (chloroxylenol) for instance.

Breeding resistant cultivars is another option. It involves a combination of disease resistance together with the best characteristics of susceptible cultivars, but is very hard in practice due to strong heterozygosity, self-incompability and the long generation time of apple and pear (Flachowsky *et al.*, 2009; Flachowsky *et al.*, 2010; Le Roux *et al.*, 2012a; Norelli *et al.*, 2003).

1.6 Fire blight forecasting models

The first forecasting models were rather inaccurate as they were only based on temperature. Nowadays, these fire blight forecasting models integrate a lot of variables, varying from the physiological stage of the plant to the weather conditions, temperature and humidity. They combine the contemporary knowhow of the bacterial disease in an advanced computer model with an integrated trial and error method.

The most common forecasting models used are Billing's Integrated System (BIS), Billing's Revised System (BRS), Parefeu, the Cougarblight Model and the Maryblyt Model. BIS and BRS include the predicted generation time or potential doublings of the bacteria, the temperature and the rainfall. The Cougarblight and the MaryBlyt Model also integrate the presence and current flowering stadium of the blossoms. Parefeu is the French version of the MaryBlyt Model. One major disadvantage is that all these models can only be used during the regular blooming period, but not afterwards during a secondary bloom (Dewdney *et al.*, 2007; Jones, 1992; Lecomte *et al.*, 1998; Vanderzwet *et al.*, 1994).

These models have many times proven their efficacy and they give the growers a new possibility in their fight against *E. amylovora*. However, it is essential to carefully test these models, as introducing these systems in a new region, country or continent could lead to a misinterpretation of the data (Billing, 2007).

2. Defence mechanisms of the plant

In great contrast to the mammalian immune system composed of specialized and mobile defence cells such as lymphocytes, plants however have to rely on the ability of each cell to recognize a pathogen and possible signals emanating from the infection site. In that way, the plant can protect itself from the disease by using several defence mechanisms, which consist of physical barriers and the production of antimicrobial components, both in a preformed and an inducible manner.

Preformed defence mechanisms are present in the plant even before the pathogen comes into contact with the plant tissue. These include the amount and quality of wax, cellulose and other compounds that cover the epidermal cells but also chemical compounds that prevent the penetration of the pathogen.

Inducible defence responses are activated upon the recognition by plant cell receptors of elicitor molecules, either derived from invading microorganisms or from pathogen-induced degradation of plant tissue. This recognition event triggers a signal transduction cascade, leading to a range of defence responses (reactive oxygen species (ROS), plant hormones, secondary metabolites, …) and redeployment of cellular energy in a fast, efficient and multiresponse manner, which counteracts further pathogen ingress.

2.1 First signaling mechanisms

If fire blight infection occurs, *Rosaceaeous* plants have to rely on the ability of each cell to recognize a pathogen and the signals emanating from the infection site in order to protect themselves against the disease. There are intrinsically two levels of the plant immune system (figure 1.7) (Jones and Dangl, 2006; Robert-Seilaniantz *et al.*, 2007).

The first level is performed by the action of multiple transmembrane pattern recognition receptors (PRRs) belonging to either the receptor-like kinase (RLK) or receptor-like protein (RLP) families. PRRs bear structural similarities to animal Toll-like receptors (He *et al.*, 2007; McDowell and Simon, 2008; Segonzac and Zipfel, 2011) and respond to multiple cell-surface components of gram-negative bacteria, including lipopolysaccharide, a major constituent of the outer membrane (Dow *et al.*, 2000; Gerber *et al.*, 2004; Meyer *et al.*, 2001a; Newman

et al., 2002), and flagellin, the protein subunit of the flagellum (Asai *et al.*, 2002; Takeuchi *et al.*, 2003). In *Arabidopsis* plants for instance, a 22 amino acid synthetic peptide (flg22) corresponding to a highly conserved eubacterial flagellin amino terminus is sufficient for host receptor activation (Felix *et al.*, 1999). All previous mentioned microbial features, which are also called microbial- or pathogen-associated molecular patterns (MAMPs or PAMPs), are highly conserved across a wide range of microbes and are normally not present in the host (Chisholm *et al.*, 2006; Nurnberger *et al.*, 2004; Zipfel and Felix, 2005).

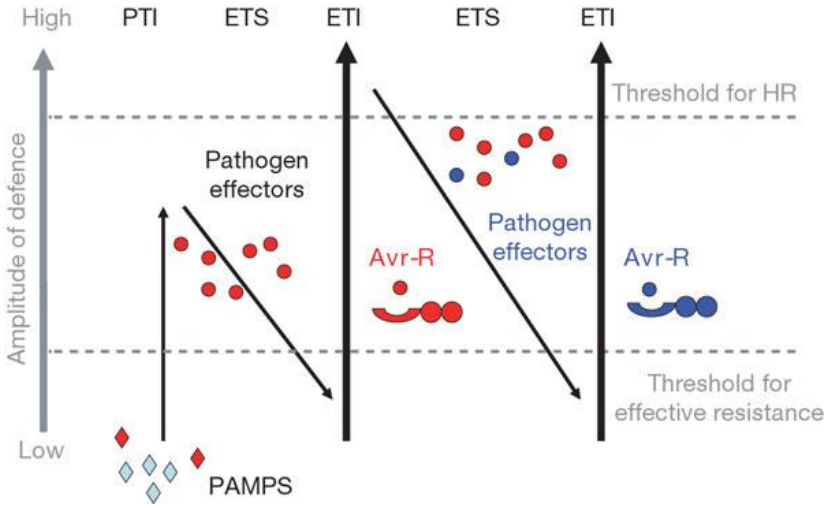

Figure 1.7: A zigzag model illustrates the quantitative output of the plant immune system. In phase 1, plants detect microbial- or pathogen-associated molecular patterns (MAMPs/PAMPs) via Pattern Recognition Receptors (PRRs) to trigger PAMP-Triggered Immunity (PTI). In phase 2, successful pathogens deliver effectors that interfere with PTI, or otherwise enable pathogen nutrition and dispersal, resulting in an Effector-Triggered Susceptibility (ETS). In phase 3, if an effector is recognized by an NB-LRR protein, Effector-Triggered Immunity (ETI) will be activated. ETI is an amplified version of PTI that often passes a threshold for induction of a hypersensitive respons (HR). In phase 4, pathogens that have gained new effectors are able to suppress ETI (Jones and Dangl, 2006).

The second level of the plant immune system acts largely inside the cell, using the polymorphic nucleotide binding-leucine rich repeats (NB-LRR) protein products encoded by plant-derived Resistance (R) genes to counter pathogen secreted effectors (Avirulence (Avr) proteins). Avr proteins are considered factors that contribute to host infection, although the biochemical function of

most Avr proteins remains unidentified. However, in those cases when Avr factors are recognized by resistant host plants through direct or indirect interaction with their complementary R gene-encoded protein counterparts, they act as specific elicitors of plant defence rather than as a virulence factor. When this genetic interaction takes place, a defence response is triggered and gene-for-gene resistance is established (Abramovitch and Martin, 2004; Belkhadir *et al.*, 2004; Bent and Mackey, 2007; Lahaye and Bonas, 2001; Mansfield, 2009; Martin *et al.*, 2003; McDowell and Simon, 2006; White *et al.*, 2000).
Contrary to other plant-bacteria interactions described by Kunkel *et al.* (1993), Ronald *et al.* (1992), Tai *et al.* (1999) and Tsiamis *et al.* (2000), up till now no related avirulence gene and the corresponding plant resistance gene have been reported in the pathosystem of *Erwinia amylovora*.

2.2 Further signalling of the plant in response to *E. amylovora*

When PAMPs are recognized by PRRs and/or pathogen secreted effectors by the R genes, a plant will respond by triggering a wide amount of signalling events and defence responses and a relocation of cellular energy, which may prevent the bacteria to move further into the host tissue. For instance, Sarowar *et al.* (2011) obtained a total of 3500 genes involved in metabolism, signal transduction, transport and stress responses, which were significantly modulated in fire blight infected blossoms of the apple cultivar "Gala". Peil *et al.* (2007) even have strong evidence for a major resistance gene in *Malus robusta* located on linkage group 3.
Over the last years, much research has been performed concerning these signalling pathways *in planta* and their different modes of protection, of which some of them are discussed here (figure 1.8).

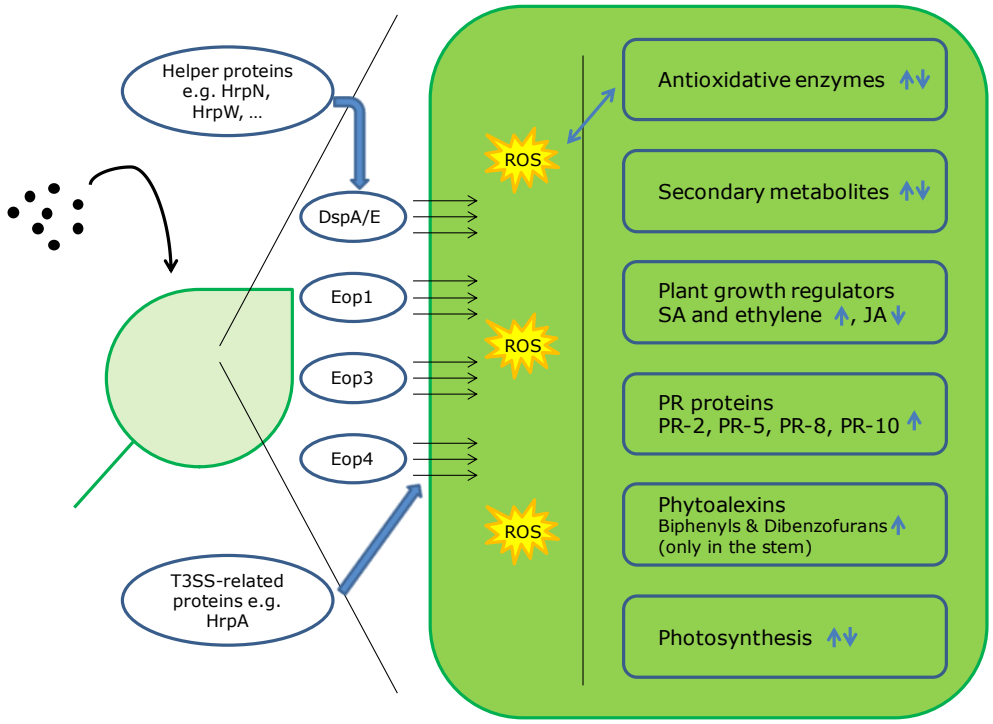

Figure 1.8: Infection by *E. amylovora* causing the effector-related proteins DspA/E, Eop1, Eop3 and Eop4 to be secreted in the plant tissue, together with helper proteins and T3SS-related proteins. The result is an increase in ROS and different mechanisms to be triggered.

2.2.1 ROS and the generation of an oxidative burst

Reactive oxygen species or ROS are normally only produced as side-products of some general pathways such as photosynthesis (Krieger-Liszkay, 2005). They are generated by various enzymatic activities of which the best studied are NADPH oxidases. However, during an incompatible reaction, an increased production of ROS and a hypersensitive response can be observed. In the case of the compatible interaction between *E. amylovora* and a host plant, *E. amylovora* is percepted by this host plant as an incompatible pathogen, which results in the generation of ROS by the plant. These bursts of ROS seem to be paradoxically necessary for a successful bacterial colonization (Venisse *et al.*, 2001). The oxidative burst is elicited by HrpN proteins in non-host plants (Baker *et al.*, 1993; Chang and Nick, 2012; Desikan *et al.*, 1998; Livaja *et al.*, 2008) and by both HrpN and DspA in host plants (Venisse *et al.*, 2003). Furthermore, it

is believed that the bacterial exopolysaccharide protects *E. amylovora* against the toxic effects of ROS since a non-capsular mutant of *E. amylovora* induced locally the same responses as the wild type but was unable to further colonize the host plant (Venisse *et al.*, 2001).

The first detectable oxidants among these ROS produced are the molecules hydrogen peroxide (H_2O_2) and superoxide anion radical ($O_2^{\cdot-}$) which are commonly released into the apoplast of primarily infected plant cells (Baker and Orlandi, 1995; Bolwell and Wojtaszek, 1997; Foyer and Noctor, 2005b; Torres *et al.*, 2006; Venisse *et al.*, 2001).

Hydrogen peroxide for instance could then fulfil a critical role in the expression of disease resistance. It could serve as a substrate for oxidative cross-linking of various plant cell wall components leading to the reinforcement of the cell structure, as a direct toxin against the pathogen and as a signal molecule for the induction of defence-related genes in the adjacent, still healthy tissues (Chamnongpol *et al.*, 1998; Dat *et al.*, 2000; Eyles *et al.*, 2010; Mittler *et al.*, 2011; Shetty *et al.*, 2008), which finally could result in cell collapse and necrosis (Navrot *et al.*, 2007).

As a response of this increase in ROS, the concomitant activity of some antioxidative enzymes and redox metabolites is often reported in pear and apple (Faize *et al.*, 1999; Sklodowska *et al.*, 2011; Venisse *et al.*, 2001; Venisse *et al.*, 2002; Venisse *et al.*, 2003; Viljevac *et al.*, 2009). Their expression is genetically controlled and regulated both by developmental and environmental stimuli, according to the necessity to carry out ROS detoxification to less neutral compounds in cells (Alscher *et al.*, 1997; Apel and Hirt, 2004; Arora *et al.*, 2002; Buchanan and Balmer, 2005; Foyer and Noctor, 2005a; Mittler *et al.*, 2004; Navrot *et al.*, 2007; Van Breusegem *et al.*, 2008). However, when the amount of ROS is too high – which is often the case after a fire blight infection - imbalances between the amount of oxidants and antioxidants can be developed *in planta*, finally resulting in cell death and necrosis (figure 1.9).

Widespread plant scavenging enzymes are superoxide dismutase (SOD) which catalyses the dismutation of $O_2^{\cdot-}$ to H_2O_2, catalase (CAT) which dismutates H_2O_2 to oxygen and water, and ascorbate peroxidase (APX) which reduces H_2O_2 to water by utilising ascorbate as specific electron donor. Often these scavenging enzymes occur in different isoenzymatic forms (Blokhina *et al.*, 2003).

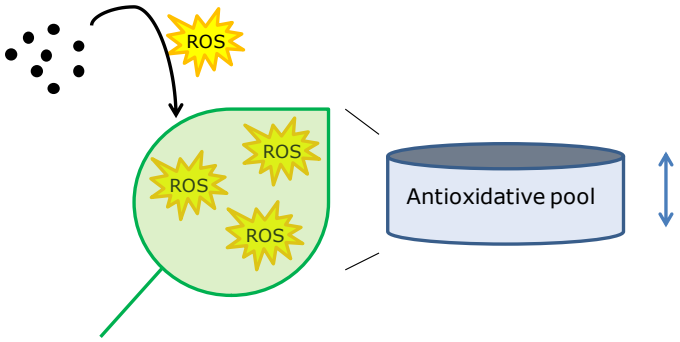

Figure 1.9: Antioxidative imbalance caused by *E. amylovora*, causing the amount of ROS to be increased and the antioxidative pool to be affected.

2.2.2 Secondary metabolites

The general phenylpropanoid metabolism generates an enormous array of secondary metabolites based on the few intermediates of the shikimate pathway as core units. The phenylpropanoid-flavonoid pathway is characterised by an enormous complexity, which is caused by a large amount of branches and branchpoints and a lot of endproducts. Hence, the pathway has the ability of producing a certain endproduct via different branches and by combining the function of large superfamilies of reductases, oxygenases, ligases and transferases. The overall result is an organ and developmentally specific pattern of metabolites, characteristic for each plant species. (figure 1.10).

The amino acid L-phenylalanine, the last step of the plant shikimate pathway, is the entry point to the biosynthesis of phenylpropanoids. Phenylalanine is then converted to cinnamic acid by phenylalanine ammonium lyase. In a further phase, p-coumaric acid and p-coumaroyl-CoA are formed by respectively cinnamate-4-hydroxylase and p-coumaroyl-CoA ligase. These initial three steps are mandatory and provide the basis for all subsequent branches and resulting metabolites. The production of p-coumaric acid probably represents the most important branchpoint within the central phenylpropanoid biosynthesis in plants. It is either the direct precursor for other compound such as flavonoids and lignins, or it is used for the production of methoxylated monolignols for example.

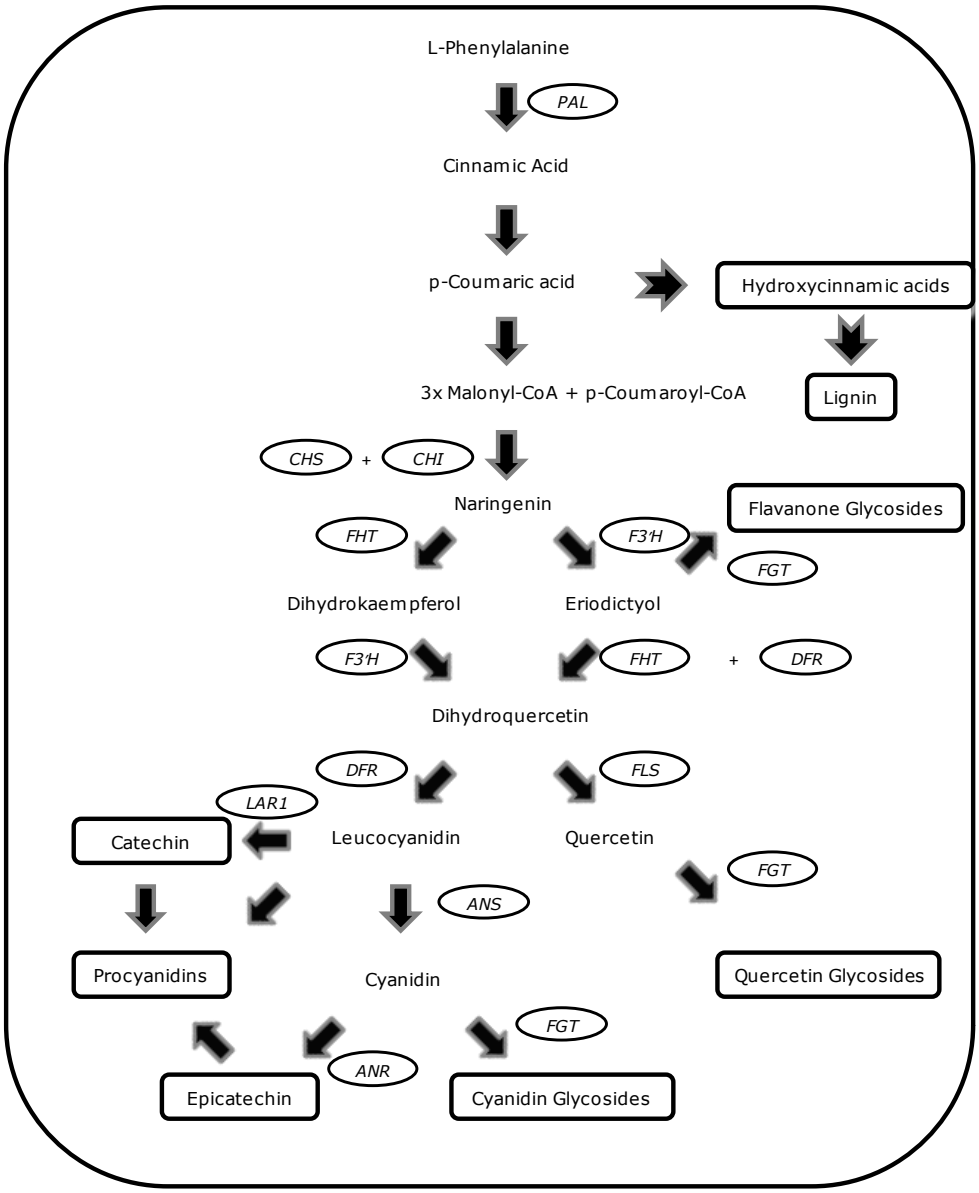

Figure 1.10: Biosynthesis of the main constitutive flavonoids, phenols and polyphenols in pear (*Pyrus communis*). Enzyme abbreviations: phenylalanine ammonium lyase (PAL), chalcone synthase (CHS), chalcone isomerase (CHI), flavanon 3β hydroxylase (FHT), flavonoid-3'-hydroxylase (F3'H), flavonol synthase (FLS), flavonoid O-glucosyltransferase (FGT), dihydroflavonol-4-reductase (DFR), leucoanthocyanidin reductase 1 (LAR1), anthocyanidin synthase (ANS) and anthocyanidin reductase (ANR). Broken arrows indicate more than one biosynthetic step (Treutter, 2010).

Phenylpropanoids contribute to all aspects of plant responses towards biotic and abiotic stimuli. Not only are they indicators of plant stress responses upon variation of light or mineral treatment, but they are also key mediators of plant resistance towards pests (Dixon *et al.*, 2005; Fischer *et al.*, 2007; Manetas, 2006; Pfeiffer *et al.*, 2006; Treutter, 2001; Treutter, 2010; Vogt, 2010; Winkel-Shirley, 2001).

Jensen *et al.* (2012) suggest that the expression of the phenylpropanoid pathway as a whole might be one of the many predictors of fire blight resistance. Burse *et al.* (2004) already showed that *E. amylovora* has the ability to protect itself against secondary metabolites in apple because of the internal efflux pump AcrAB, indicating the possible involvement of these metabolites in plant defence. Depending on the cultivar, the bacterial strain, the infection method and the time after inoculation, different results are reported throughout the literature regarding the phenylpropanoid-flavonoid pathway. For instance, both Venisse *et al.* (2002) and Milcevicova *et al.* (2010) found that most of the phenylpropanoid-flavonoid related enzymes investigated, were repressed in some apple cultivars after inoculation with a specific fire blight strain, whereas Sklodowska *et al.* (2011) and Pontais *et al.* (2008) demonstrated that the level of some hydroxycinnamate derivatives significantly augmented in both resistant and sensitive apple cultivars. Moreover, phloretin was found at a bacteriotoxic concentration in both genotypes, but *E. amylovora* exhibited the ability to stabilize this compound at sublethal levels (Pontais *et al.*, 2008). De Bernonville *et al.* (2011) hypothesised that the constitutive phenolic composition of two apple cultivars "Evereste" and "MM106" is not responsible for their contrasted differences in susceptibility to fire blight.

In pear, Gunen *et al.* (2005) reported a higher content of arbutin in resistant cultivars, while sensitive cultivars obtained a higher level of chlorogenic acid.

Although the real function of these secondary compounds in a fire blight – pome fruit interaction is still not clear, it is many times reported in literature that phenolic components have direct antioxidant properties which are even better than those of vitamins and ascorbic acid for instance (Agati and Tattini, 2010; Feucht *et al.*, 1996; Gould, 2004). Moreover, they share the ability to influence cell signalling by down-regulating pro-oxidant enzymes such as NADPH oxidases and lipoxygenases, by altering the phosphorylation state of target molecules or

by chelating transition metals that mask pro-oxidant actions of reactive nitrogen and oxygen species, both in plants (Treutter, 2005) and in human and mammalian tissue (Fraga and Oteiza, 2011; Williams *et al.*, 2004). However, because of a lack of convincing spatiotemporal correlations with the flavonoid oxidation products, the widely accepted antioxidant function of flavonoids in plants is still a matter of debate (Hernandez *et al.*, 2009). Furthermore, flavonoids are also described as having antibacterial, antitoxin, antiviral and/or antifungal activities (Ardi *et al.*, 1998; Friedman, 2007; Treutter, 2005) or to be involved in creating a structural defence, as research in other plant-pathogenic interactions revealed ultrastructural modifications with incorporated flavonoids, middle lamellae or callose-rich papillae to obstruct further progress of different pathogens (Dai *et al.*, 1996; Loureiro *et al.*, 2012; Nicaise *et al.*, 2009; Soylu, 2006). Probably, a combination of all these factors could affect the susceptibility for *E. amylovora*.

2.2.3 Plant hormones

Jasmonic acid (JA), salicylic acid (SA) and ethylene are three distinct plant hormones which also interfere during microbial attack. Both the SA and JA defence pathways are mutually antagonistic (Chisholm *et al.*, 2006; Robert-Seilaniantz *et al.*, 2007), which is also shown for the pathosystem *Erwinia amylovora-Malus*. Both de Bernonville *et al.* (2012) and Milcevicova *et al.* (2010) report a significant accumulation of total salicylic acid in different apple cultivars after infection with *E. amylovora*, of which de Bernonville *et al.* (2012) also demonstrate a down-regulation in jasmonic acid levels. Accordingly, treatment of these susceptible plants with methyl-jasmonate increases the resistance of these plants against *E. amylovora*, indicating that the down-regulation of the JA pathway is a critical step in the infection process.

Ethylene also seems to have a big part in the response of the plant after mechanical wounding and after a pathogen attack. The group of Spinelli *et al.* (2011) measured an ethylene production in both *E. amylovora*-inoculated and wounded apple plants, reaching a peak approximately five hours after inoculation. However, in wounded plants, this ethylene burst was much lower and faded away after six hours. Next to ethylene, the production of other volatiles such as 2,3-butanediole, isoprene-ozone and 3-hexenal were also

detected in the infected plants (Spinelli *et al.*, 2011). Whether this rise of ethylene and other volatiles is involved in a possible plant defence mechanism, is still not known for this pathosystem.

2.2.4 Pathogenesis related (PR) proteins

Pathogenesis related proteins of plants are divided in more than fifteen subfamilies and have been defined as host originating proteins with direct antimicrobial activity that are induced only in response to a pathogen attack or related event. Induction of PR proteins has been found in many plant species belonging to different families, suggesting a general role of these proteins in adaptation to biotic stress conditions. Not much scientific research has been published concerning PR-proteins in woody fruit perennials after infection with *E. amylovora*. Only a systemic up-regulation of the PR-5 (Bonasera *et al.*, 2006a; Venisse *et al.*, 2002), PR-2 (Bonasera *et al.*, 2006a; Heyens *et al.*, 2006), PR-8 (Bonasera *et al.*, 2006a) and PR-10 (Mayer *et al.*, 2011) family was reported in infected leaf tissues. The PR-1 gene family instead seems not to be involved (Bonasera *et al.*, 2006a; Pester *et al.*, 2012). Furthermore, overexpression of the MpNPR1 gene confers activation of PR-2, PR-5 and PR-8 in *Malus* x *domestica* (Malnoy *et al.*, 2007). Although some of these PR proteins exhibit potential *in vitro* antimicrobial activities and their accumulation in the plant is related to plant resistance responses, a direct functional role in defence could not be demonstrated for all (Sels et al., 2008; Van Loon and Van Strien, 1999).

2.2.5 Phytoalexins

Phytoalexins are low molecular mass secondary metabolites with antimicrobial activity, which are synthesized *de novo* after biotic and abiotic stress and occur in a wide variety of chemical structures and in different plant species. The biosynthesis of most phytoalexins, the regulatory networks involved in their induction by biotic and abiotic stress and the molecular mechanism behind their cytotoxicity remain largely unknown (Ahuja et al., 2012; Chizzali and Beerhues, 2012). In both *Malus* x *domestica* cv. Holsteiner Cox and *Pyrus commun*is cv. Conférence, the phytoalexin group of the biphenyls and dibenzofurans were detected in the transition between healthy and diseased zones of the stem after a fire blight infection. In leaves, no phytoalexins could be measured (Chizzali et

al., 2012a; Chizzali et al., 2012b; Huttner et al., 2010). Probably, both the outer membrane protein TolC and the AcrAB transport system in *E. amylovora* play important roles as protein complexes that are capable in offering resistance to phytoalexins (Al-Karablieh et al., 2009; Burse et al., 2004).

Remarkably, the flavan-4-ol luteoforol, which is the unstable and highly reactive precursor of luteoliflavan, is induced in pome fruits after treatment with the growth regulator prohexiadone-Ca and shows phytoalexin-like properties against *E. amylovora* and other pathogens (Flachowsky et al., 2012; Halbwirth et al., 2003; Spinelli et al., 2005b)

2.2.6 Photosynthesis

Oxygenic photosynthesis is a biological oxidation-reduction process, in which CO_2 acts as an electron acceptor and water serves as electron donor. H_2O is oxidised and the released electrons are transferred to oxygen and CO_2 causing the formation of a carbohydrate. The following molecular formula summarizes the photosynthetic reaction:

$$6\ CO_2 + 12\ H_2O \xrightarrow{hv} (CH_2O)_6 + 6\ O_2 + 6\ H_2O$$

In general, the light from the sun is captured and used to convert inorganic molecules into organic compounds.

The process of photosynthesis can be divided into both the light-dependent reactions and the light-independent reactions, which are respectively known as light reactions and the Calvin-Benson cycle or carbon reduction reactions.

These two reactions take place in specialised organelles called chloroplasts (figure 1.11). The chloroplasts contain an inner and outer envelope membrane which form the border between the chloroplast stroma and the cytoplasm. Two major parts can be distinguished in the membrane system: the grana and the stroma lamellae. Grana are closely packed stacks of short, disc-shaped lamellae or thylakoids. These stacks are interconnected by the stroma lamellae which form prolonged extensions into the stroma. This arrangement of the thylakoid membrane system creates a huge compartment inside the chloroplast called the thylakoid lumen. Thylakoids contain two important pigments which are key players in assimilating light energy, namely chlorophyll and the carotenoids.

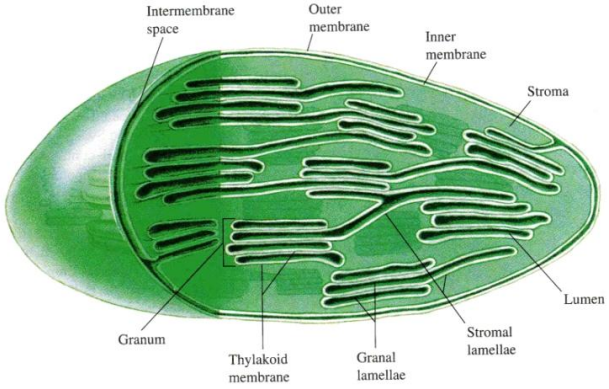

Figure 1.11: Structure of a chloroplast, with inner and outer membrane, stroma, thylakoids and grana (Horton *et al.*, 2006).

The carotenoids are usually red, orange or yellow coloured lipid-soluble pigments that consist of a polyene structure, whereas chlorophyll exists in two forms, chlorophyll a, which has a methyl-group on the porphyrin ring, and chlorophyll b, which has a formyl-group instead of the methyl-group (figure 1.12).

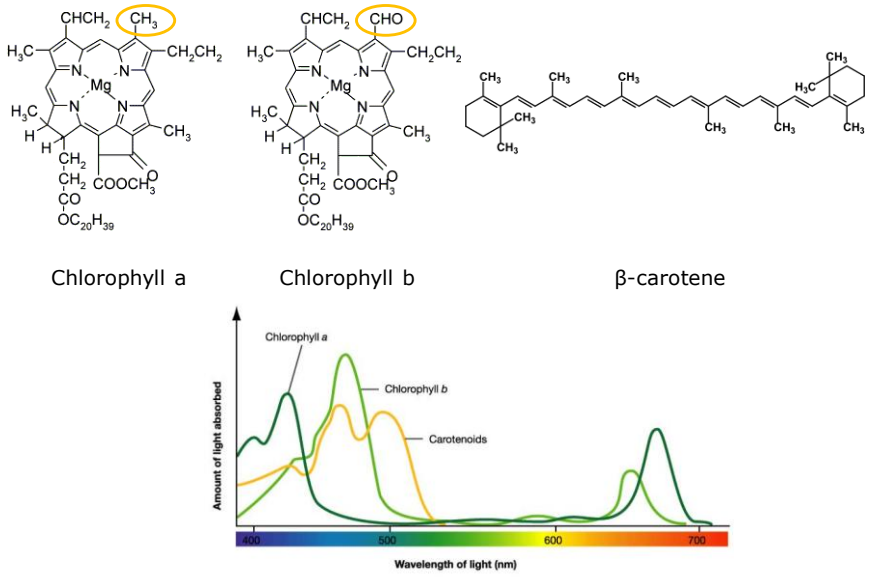

Figure 1.12: Chemical structure of chlorophyll a, chlorophyll b and carotenoids and the absorption spectra of these molecules (cfb.unh.edu)

Carotenoids and chlorophyll b cannot transfer sunlight energy directly to the photosynthetic pathway, but must pass their absorbed energy to chlorophyll a. For this reason, they are called accessory pigments.

In the thylakoid membranes, four protein complexes are involved in the light reactions of photosynthesis: photosystems (PS) I and II, which are light-sensitive complexes that catalyze the oxidation of H_2O and the reduction of $NADP^+$ (Barber, 2002; Brettel, 1997; Fromme *et al.*, 2001; Horton *et al.*, 2008; Iwata and Barber, 2004; Jensen *et al.*, 2003; Jensen *et al.*, 2007; Nelson and Ben-Shem, 2005; Shi and Schroder, 2004), the cytochrome b_6f complex, which mediates electron transport between PS II and PS I (Allen, 2004; Baniulis *et al.*, 2008; Dekker and Boekema, 2005), and the ATP-synthase, which produces ATP at the expense of the proton motive force formed by the light-driven electron-transfer reactions (figure 1.13) (Dekker and Boekema, 2005).

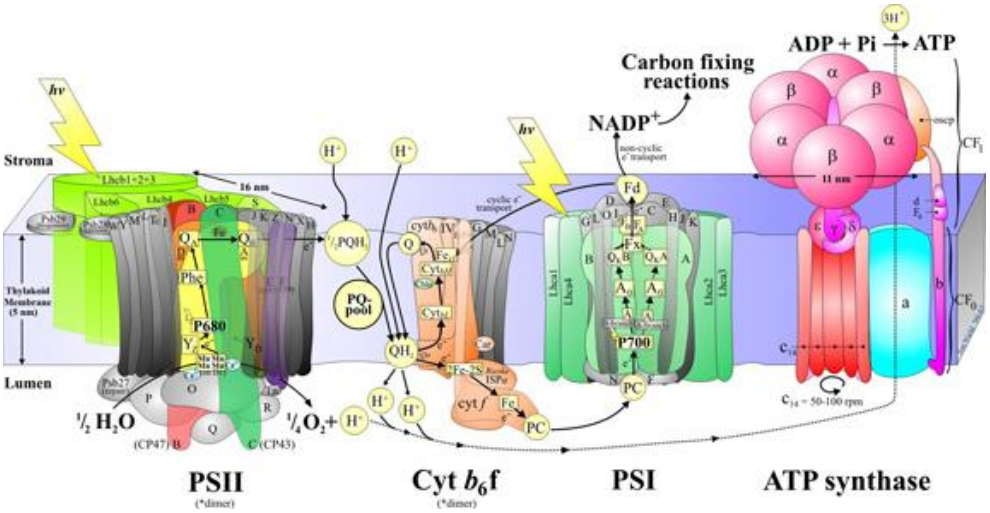

Figure 1.13: Overview of the carbon fixing cycle (Z-cycle) in plants (www.bio.ic.ac.uk)

PSII and its main light harvesting complex are limited to grana thylakoids, while PS I is only found in stroma-exposed thylakoids. This arrangement is important for the separation between the two photosystems and makes it possible to redistribute light harvesting according to the light conditions (Becker *et al.*, 2000; Berg *et al.*, 2002; Lodish *et al.*, 2008).

Absorption of light in photosystem II leads to the conversion of P680 into a strong reducing agent, P680*. Within a few picoseconds, P680* reduces a pheophytin molecule to form the radical pair state $P680^{\bullet+}Pheo^{\bullet-}$ and within a further few hundred picoseconds, a plastoquinone (PQ, Q_A) molecule bound to the D2 protein is reduced, resulting in plastoquinol (PQH2, Q_B). Q_B is bound to the D1 protein and can accept two electrons and two protons.

$$2\ PQ + 2\ H_2O \longrightarrow O_2 + 2\ PQH_2$$

The plastoquinol (PQH_2) produced by photosystem II contributes its electrons to continue the electron chain that terminates at photosystem I. These electrons are transferred, one at a time, to plastocyanin (PC), which is a copper protein in the thylakoid lumen.

$$PQH_2 + 2\ PC(Cu^{2+}) \longrightarrow PQ + 2\ PC(Cu^{+}) + 2\ H^{+}$$

This reaction is catalyzed by the cytochrome b_6f complex, creating the essential link between PS I and PS II.

The final stage of the light reactions is catalysed by PS I (Becker *et al.*, 2000; Berg *et al.*, 2002; Lodish *et al.*, 2008). In P700, a photo-induced charge separation takes place. This electron is then transferred down to a pathway via chlorophyll at site A_0 and quinone at site A_1 to a set of three Fe_4S_4 clusters F_X, F_A and F_B. From there, the electron is transferred to ferredoxin (Fd), a soluble protein containing a Fe_2S_2 cluster coordinated to four cysteine residues. The positive charge of $P700^+$ is neutralised by the transfer of an electron from reduced plastocyanin.

$$PC(Cu^{+}) + Fd_{ox} \longrightarrow PC(Cu^{2+}) + Fd_{red}$$

The reduced ferredoxin is then used to reduce $NADP^+$ into NADPH. This reaction is catalysed by the flavoprotein ferredoxin-$NADP^+$ reductase.

The proton motive force generated by the light reactions is converted into ATP by the ATP synthase of chloroplasts. ATP is essential in the development of CO_2 into sugars, also known as the light-independent Calvin-Benson cycle.

Photosynthetic processes in plants remain active only under a sufficiently long actinic irradiation (± 600 µmol m^{-2} s^{-1}) and sufficient supply of H_2O and CO_2 molecules. Once incident photons are absorbed by antenna pigments, the excitation energy is transferred via excitons to reaction centers of the photosystems II and I, as mentioned earlier. Therein, the energy drives primary

photochemical reactions that initiate the photosynthetic energy conversion. This photochemical pathway, involving a charge separation and electron transport via a set of carriers, is not the only way in which the excitation energy is consumed. Other two competitive pathways represent the thermal dissipation, a non-radiative de-excitation of excited states of pigment molecules to heat, and the chlorophyll fluorescence, the emission of photons by the radiative de-excitation of excited chlorophyll molecules (figure 1.14).

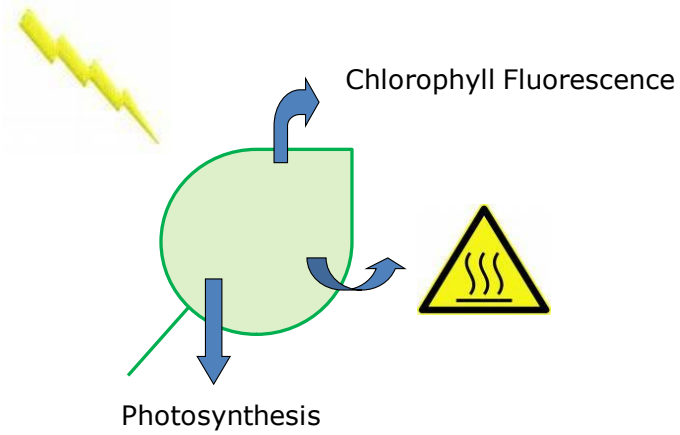

Figure 1.14: Modified model of the possible fate of light energy once absorbed by PS II. Light energy absorbed by chlorophyll molecules in a leaf can undergo three different processes: it can be used to drive the photosynthetic energy conversion, and excess energy can be dissipated as heat or it can be reemitted as light (chlorophyll fluorescence).

Most of the chlorophyll fluorescence is dissipated by chlorophyll a molecules of PS II (Goltsev *et al.*, 2009). This fluorescence has an emission peak at 685nm, with a smaller component at 730-740nm. However, significant absorption and reemission of fluorescence from underlying cells occurs, resulting in an increased emission at longer wavelengths.

When photosynthetic samples, kept in darkness, are illuminated afterwards, chlorophyll a fluorescence shows characteristic changes called fluorescence induction, fluorescence transient or simply the Kautsky effect, named after its German discoverer Hans Kautsky. The rapid fluorescence induction kinetic is also known as the OJIP-curve, where O is for origin, the first measured minimal level (figure 1.15). At phase O, the electron acceptor side of PS II is in oxidised state, the PS II reaction centers are open and the fluorescence intensity F_O is minimal. J and I are intermediate levels. The O to J rise, known as the photochemical

phase is very fast (approximately 2ms) and depends strongly on the intensity of the exciting light, whereas the J-I phase is much slower (30ms). The O-J transient reflects the primary photochemical reaction, which is the reduction of Q_A (reduction of PS II acceptor side). Once Q_A has been reduced, it is not able to accept another electron until it is reoxidised by passing the electron onto the subsequent electron carrier Q_B. The presence of such a closed reaction center in PS II results in a lowered efficiency of photosynthesis and a subsequent rise in fluorescence. The plateau at J has been attributed to the reoxidation of Q_A^- by Q_B. I is characterised by the closure of the remaining open PS II centers resulting in an accumulation of $Q_A^-Q_B^-$. In less than 1s, chlorophyll a fluorescence reaches the peak P, also called F_M or F_{max}, when the exciting light intensity is high and saturated. At this level, all Q_A molecules are completely reduced (i.e. all active PS II's are closed) (Cortleven and Valcke, 2012; Guo and Tan, 2011; Papageorgiou *et al.*, 2007; Papageorgiou and Govindjee, 2011; Rohacek and Bartak, 1999; Schansker *et al.*, 2011; Stirbet and Govindjee, 2011).

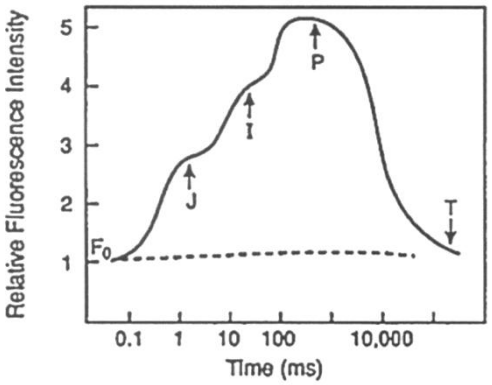

Figure 1.15: The typical transient of OJIP curve that is created after illumination of a dark-adapted plant sample. On the X-coordinate, time is expressed in ms, the Y-coordinate shows the relative fluorescence intensity.

After F_M is reached, the fluorescence level typically starts to fall over a time-scale of a few minutes, finally reaching a steady-state level (figure 1.16). This phenomenon, termed fluorescence quenching, is explained in two ways. First, there is an increase in the rate at which electrons are transported away from PS II. This is mainly due to the light-induced activation of enzymes involved in carbon metabolism and the opening of stomata. This kind of quenching is called

photochemical quenching. At the same time, there is an increase in the efficiency of energy conversion to heat, called non-photochemical quenching (Maxwell and Johnson, 2000). Although non-photochemical quenching is a single parameter, it is composed of at least three components: q_E, an energy-dependent component resulting from the generation of a transthylakoid pH gradient leading to energy dissipation in the antenna of PS II; q_T, the component that describes state transitions caused by the redistribution of light harvesting complexes between PS II and PS I; q_I, a photoinhibitory component. The non-photochemical quenching is dominated by q_E in unstressed leaves at moderate irradiances, but q_T and q_I become significant and even dominant at other times. q_T is important during low light conditions, whereas q_I plays a big part at high light and stress conditions (Muller *et al.*, 2001).

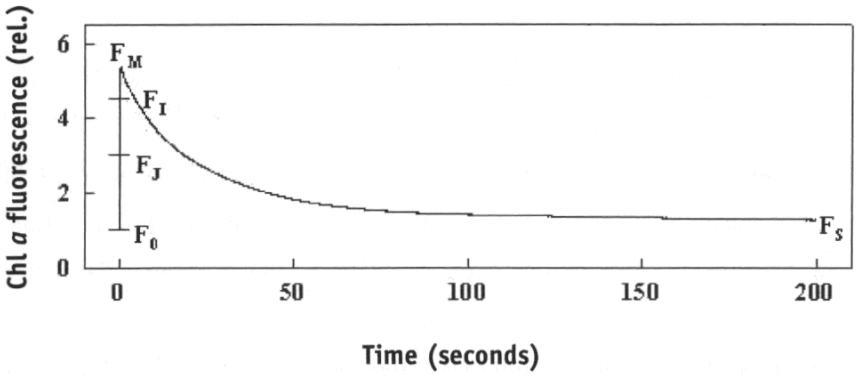

Figure 1.16: The quenching phase, where fluorescence is lowered to a basal level after a continuous actinic illumination.

The OJIP curve is a good tool for testing the physiological condition of the plant as the shape of this transient often changes when unfavourable environmental conditions are present. Strasser and co-workers developed a computational tool to analyze the OJIP fluorescence transient in terms of the various PS II reactions, which they called the JIP test (Strasser *et al.*, 1995). The JIP test allows the determination of several parameters, of which the maximum quantum efficiency of PS II primary photochemistry, termed the Genty-parameter or $\varphi_{P0} = (F_M-F_O)/F_M = F_V/F_M$ is one of the most common and important ones (Lazar and Jablonsky, 2009; Schansker *et al.*, 2006).

Measuring chlorophyll fluorescence has become a very useful technique in obtaining rapid qualitative and quantitative information on photosynthesis, and even pre-symptomatic diagnostics in the case of pathogens, phytotoxicity, ... are possible. Remarkable progress in the understanding and practical use of fluorescence was obtained by the urgent need of applied research for quantitative, non-invasive methods capable to assess photosynthesis in intact leaves.

Over the last decennia, numerous types of fluorimeters have been developed. Among them, the Plant Efficiency Analyser (PEA) developed by Hansatech (Norfolk, UK) is one of the systems that is used most. However, with this system, only a single point measurement is possible.

A Fluorescence Imaging System (FIS) that uses visible light to induce fluorescence, has the advantage that a large area of the sample can be analysed. The equipment has proven its efficacy in detecting photosynthetic changes as stated by Chaerle *et al.* (2004), Ciscato *et al.* (1999), Delalieux *et al.* (2009), Gielen *et al.* (2006) and Lotze *et al.* (2006).

Infection of apple by *E. amylovora* results in a decrease of photosynthetic activity, suggesting an inhibition of Photosytem I and/or II (Bonasera *et al.*, 2006b). Similarly, changes in the chlorophyll fluorescence of *E. amylovora*-challenged apple leaves are observed prior to the development of disease symptoms. Both Heyens and Valcke (2006) and Baldo *et al.* (2010) noticed an induction of some photosynthetic genes during the *Malus* - *E. amylovora* interaction. Research by Singh *et al.* (2010) suggested that *FIBRILLIN4,* which is associated with photosystem II, could also play a part in fire blight infections, as disease is more expressed in the knockdown mutant.

Chapter 2:

Objectives

In this work, a multidisciplinary study is performed to analyse possible defence mechanisms in *Pyrus communis* after inoculation with *Erwinia amylovora*. In all chapters, a special emphasis was put on the phenylpropanoid-flavonoid pathway, which is an important pathway in pear for fruit colouration, taste, UV protection, etc. but which also could be involved in defence mechanisms against pathogens.

In chapter 3, the main focus is put on the ontogenesis of a leaf. Because leaf age is considered to be a critical factor in the development of certain diseases, ontogenesis-related differences in both mature and immature leaves of two-year-old pear trees *Pyrus communis* cv. Conférence on Quince C rootstock after an inoculation with *Erwinia amylovora* strain SGB 225/12 were investigated.
The emphasis of this research was put on the transcription profiles of the phenylpropanoid-flavonoid pathway and some antioxidative related genes, because literature indicates that these two factors are important during both the ontogenesis of a leaf and during plant-pathogen interactions. Furthermore, both factors could be possible important causes for a difference in disease manifestation inside mature and immature leaf tissues. Research and conclusions were strengthened with HPLC, microscopy and photosynthesis-related research.
Used techniques: Inoculations and symptom assessment, microscopy, RT-qPCR, HPLC, chlorophyll fluorescence, gas exchange measurements

In chapter 4, the moderately susceptible cultivar Conférence and the highly susceptible cultivar Doyenné du Comice were compared. Because both cultivars differ in their susceptibility to fire blight, the involvement of the phenylpropanoid-flavonoid pathway towards these cultivar dependent differences was examined after the inoculation of immature leaves with the fire blight pathogen *Erwinia amylovora*. A proteomic approach was performed as well in order to receive vital information about the involvement of other proteins that are related to defence mechanisms in both cultivars Conférence and Doyenné after inoculation with *E. amylovora*.
Used techniques: Inoculations and symptom assessment, RT-qPCR, HPLC, chlorophyll fluorescence, proteomics

In chapter 5, the application of a heat shock was examined in order to know if the phenylpropanoid-flavonoid pathway is stimulated in the immature leaves of a heat shock-treated Conférence tree and if this has a positive effect on the plant's response to the fire blight pathogen *Erwinia amylovora*. A proteomic approach was performed as well in order to receive vital information about the involvement of other proteins that are related to defence mechanisms in heat shock and non-heat shock treated Conférence trees after inoculation with *E. amylovora*.

If heat shocks prove to be valuable against *E. amylovora*, fruit growers could use trailed heated air cannons as an extra alternative method to fight fire blight infections.

Used techniques: Inoculations and symptom assessment, RT- qPCR, chlorophyll fluorescence, proteomics.

Chapter 3:

Influence of leaf age on defence mechanisms against *E. amylovora* in *Pyrus*

1. Introduction

An interesting phenomenon in the pathogenetic cycle of *Erwinia amylovora* is a reduced capability or even a total incapability of infecting and spreading of the bacteria in the adult leaves of the host plant compared to the younger leaves, a phenomenon that is often found in other plant-pathogenic relations (Develey-Riviere and Galiana, 2007; Whalen, 2005), such as *Pseudomonas syringae* in *Arabidopsis thaliana (*Kus *et al., 2002), Ramularia collo-cygni* on barley (Schutzendubel *et al.*, 2008) and *Venturia inaequalis* on apple (Li and Xu, 2002). This reduced susceptibility is often associated with major transitions occurring during the plant's life cycle.

1.1 The phenylpropanoid-flavonoid pathway and stress-related genes

Leaf ageing is under nuclear control and is a genetically programmed change in various cellular processes including photosynthesis and involves the hydrolysis of macromolecules such as proteins, lipids, etc. It is governed by the developmental age of the plant and is induced or enhanced by environmental stresses such as drought, heat, salinity and others.

Generation of reactive oxygen species (ROS) is one of the earliest responses of plant cells during leaf ageing (Khanna-Chopra, 2012). To protect cells against this type of oxidative damage, scavenging enzymes will act in synergy to carry out ROS detoxification and in scavenging them to neutral or less neutral compounds.

Another important factor in the development of immature leaves into mature leaves is the phenylpropanoid-flavonoid pathway, as phenolic profiles shift in the same manner as the several other changes that take place in ageing internal and external leaf parts. For instance, in different apple cultivars, a shift in flavanol pools from monomeric to oligomeric structures in the leaves and fruit tissue (Mayr *et al.*, 1995) and a drop of flavonoid and hydroxycinnamic acid concentration in fruit tissue during growth were demonstrated (Renard *et al.*, 2007). In Abbé Fétel pears, a significant decrease of phenolic compounds in leaf tissue could be observed during ontogenesis (Andreotti *et al.*, 2006). In addition, in strawberry fruits, it is shown that developmental cues play a key

role in flavonoid metabolism and are predominant over genotype and environmental factors (Carbone *et al.*, 2009).

Secondary metabolites are not only affected by ontogenesis, they also contribute to defence mechanisms in plants, as a change in specific secondary metabolites is often observed during plant-pathogen interactions (Fischer *et al.*, 2007; Gayler *et al.*, 2004; Gosch *et al.*, 2003; Gunen *et al.*, 2005; Gutha *et al.*, 2010; Milcevicova *et al.*, 2010; Miranda *et al.*, 2007; Pfeiffer *et al.*, 2006; Treutter, 2005).

1.2 Photosynthesis and CO_2 metabolism

Light is a predominant factor in the control of plant growth, development and stress responses as the plant is equipped with sophisticated light-sensing mechanisms that are localised inside and outside of the chloroplast and the nucleus. In normal situations, dissipation of excessive excitation energy is achieved by both photochemical and non-photochemical quenching. Any environmental stress that limits the photosynthetic metabolism, either through effects on gas exchange or upon primary metabolism can cause a sudden rise of excessive excitation energy. Failure to dissipate or to avoid exposure to this excessive excitation energy could lead to photo-oxidative damage, often manifested by bleaching, bronzing or chlorosis of the leaves. Several common features characterize the responses of plants to both excessive excitation energy and infection by incompatible pathogens. Both are characterised by a rapid increase in the foliar concentrations of ROS, the depletion of antioxidant pools, the chlorosis and necrosis of leaves, local and systemic defence responses and finally induction of defence gene expression (Karpinski *et al.*, 2003).

Chlorophyll fluorescence imaging can provide a non-invasive tool to measure these heterogeneous changes in the photosynthetic metabolism when infected by pathogens. In infected leaves or isolated mesophyll cells challenged with elicitor preparations from pathogens, depression of photosynthetic electron transport and simultaneous increases in both non-photochemical and photochemical quenching have been observed. This could indicate that the leaves suffer a decline in light use efficiency to drive photosynthetic metabolism and an increase in excessive excitation energy (Bechtold *et al.*, 2005). This reduction in leaf photosynthesis can be equal, greater or lower than the level of

visual disease severity, depending on the type of pathogen and the host (Shtienberg, 1992).

The impact on photosynthesis in leaves has been investigated in a wide range of plant-viral (Chaerle *et al.*, 2007; Kyselakova *et al.*, 2011; Perez-Bueno *et al.*, 2006) and plant-fungal interactions (Alves *et al.*, 2011; Bassanezi *et al.*, 2002; Bauriegel *et al.*, 2010; Carretero *et al.*, 2011; Dinis *et al.*, 2011; Kuckenberg *et al.*, 2009; Meyer *et al.*, 2001b; Prokopova *et al.*, 2010; Swarbrick *et al.*, 2006). A nice overview of these specific plant-pathogen interactions is given by Rolfe and Scholes (2010) and also by Gorbe and Calatayud (2012).

Despite the economic impact of bacteria in horticulture and agriculture, relatively few chlorophyll fluorescence imaging studies investigating the interactions between plants and bacteria have been published. Bonfig *et al.* (2006) compared spatio-temporal changes in leaves of *Arabidopsis thaliana* infected by both a virulent and an avirulent strain of *Pseudomonas syringae*. They noticed that for each strain the maximum PS II quantum yield, the effective PS II quantum yield and the non-photochemical quenching were decreased, whereas the quantum yield of non-regulated energy dissipation was increased after infection. The same reduction in non-photochemical quenching was observed in *Phaseolus vulgaris* after infection with *Pseudomonas syringae* (Rodriguez-Moreno *et al.*, 2008). Berger *et al.* (2007) and Matous *et al.* (2006) used a combination of conventional and combinatorial chlorophyll fluorescence imaging to identify optimal protocols and parameters to visualise infection of *Arabidopsis* by *P. syringae*.

Being a non-destructive tool, chlorophyll fluorescence imaging can be combined with other methods, such as gas exchange. The use of gas exchange systems can obtain more insight into the CO_2 assimilation and release rates, transpiration rates, intercellular concentrations of CO_2 and stomatal conductance, which are all processes that are tightly connected to photosynthesis. Leaf transpiration occurs through stomata covering the leaf surface. They play an essential role in controlling both water losses by transpiration and CO_2 uptake for photosynthesis. Transpiration also enables plants to lower excessive temperatures, to change osmotic pressure of cells and to create mass flow of mineral nutrients and water from roots to shoots (Damour *et al.*, 2010). As stomatal aperture is sensitive to multiple environmental influences, measuring

gas exchange can be a valuable tool for detecting anomalies in the plant tissue. For instance, Cavalcanti *et al.* (2006) used a combination of chlorophyll fluorescence analysis and gas-exchange measurements for tomato plants pre-treated by plant activators and inoculated by *Xanthomonas vesicatoria*. They showed that the water use efficiency and carboxylation efficiency revealed the strongest contrasting differences between plants sprayed with tested activators and the control plants, whereas fluorescence parameters showed minor contrasts.

2. Objective

Because leaf age is considered to be a critical factor in the development of certain diseases, the role of ontogenesis in leaves of two-year-old pear trees *Pyrus communis* cv. Conférence on Quince C rootstock after an inoculation with *Erwinia amylovora* strain SGB 225/12 was investigated. Therefore, symptom analysis was performed and a distinction between immature and mature leaves was made. In this chapter, immature leaves pointed towards the second and third fully unfolded leaf starting from the apex, whereas mature leaves merely indicated the sixth and seventh fully unfolded leaf starting from the apex.

The emphasis of this research was put on the phenylpropanoid-flavonoid pathway and some antioxidative related genes, because literature indicates that both factors are important during the ontogenesis of a leaf and during plant-pathogen interactions. Furthermore, both factors could be possible important causes for a different disease manifestation inside leaf tissues. For the antioxidative related genes, there was opted for SOD, APX and CAT as these enzymes are very abundant in plants, they have a large consistency throughout living organisms and they are well-studied in the literature.

Therefore, mature and immature leaf samples were taken at specific time points after inoculation and the expression pattern of not necrotic tissue close to the infection site was analysed for diverse isoforms of SOD, APX and CAT by using quantitative reverse transcription PCR. Several genes coding for enzymes of the phenylpropanoid-flavonoid pathway were also studied with RT-qPCR, as well as the profiles of soluble phenolic compounds with HPLC. Spectrophotometry-based enzyme analyses were not performed, as the available protocols of other plant species showed very low mechanistic consistency for these pear leaves.

In addition, antioxidative and phenylpropanoid-related histological studies were performed in an attempt to detect possible structural differences in immature and mature tissue due to infection.

Last but not least, chlorophyll fluorescence measurements were executed by using PEA and FIS equipment in combination with CO_2 measurements to visualise the effect of the bacteria on the global photosynthesis and gas exchange in the plant and to detect possible differences in susceptibility between the mature and immature leaves based on photosynthesis.

3. Material & Methods

3.1 Experimental design

Two-year-old trees (*Pyrus communis*) of the moderately susceptible cultivar Conférence on Quince C rootstock were grown in 20l containers in a quarantine protected greenhouse (pcfruit, Kerkom, Belgium) with a controlled environment with a temperature of 22°C, a relative humidity of 60% and a minimal light intensity of 150 µmol $m^{-2}s^{-1}$. Trees were grown until they contained enough active growing shoots with an average length of 25cm and a minimum of eight leaves on each shoot. Next, each tree with corresponding shoots was subjected to only one of the following treatments: (a) Untreated immature leaves, (b) Mock-inoculated immature leaves, (c) *Ea*-inoculated immature leaves, (d) Untreated mature leaves, (e) Mock-inoculated mature leaves and (f) *Ea*-inoculated mature leaves. Eight biological repetitions were applied, as eight shoots were used per variant and sampling date (figure 3.1).

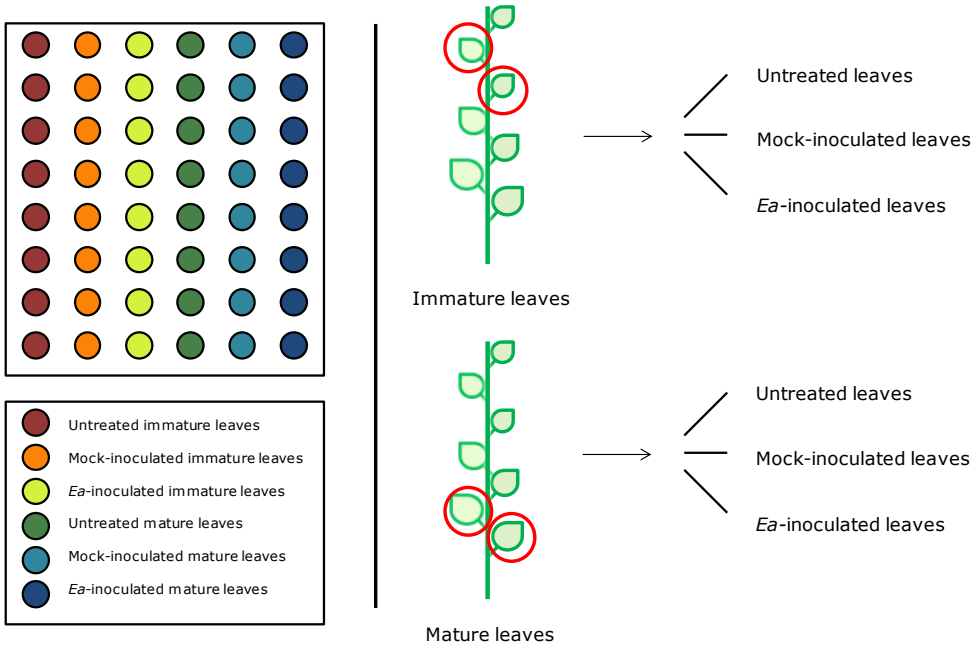

Figure 3.1: Experimental design with the different treatments (left) and the sampling of the mature and immature leaves (right)

A highly aggressive *E. amylovora* strain (BG16, isolated from *Malus sylvestris* (Bulgaria) with collection number SGB 225/12 (Maes *et al.*, 2001)) was

cultivated at a temperature of 25°C on Yeast Peptone Glucose Agar growth medium. After 24 hours, a suspension liquid of these bacteria was prepared in Phosphate Buffered Saline (PBS) at a density of 10^8 CFU ml^{-1} and used for inoculations.

For inoculation, both the second and third (immature leaves) or the sixth and seventh fully unfolded leaf (mature leaves) starting from the apex were cut perpendicular to the main vein with scissors dipped in the bacterial suspension liquid (figure 3.1). For mock-inoculated leaves, scissors were dipped in PBS. No cutting was performed for the control.

Total leaf samples of both the second and third (immature leaves) or both the sixth and seventh leaf were taken 6, 24, 30, 48 and 72h after inoculation. Leaf samples were immediately used for histological analysis or were stored at -80°C for further analysis with quantitative reverse transcription PCR or HPLC.

The progression of the shoot infection was measured 6 and 8 days after inoculation on minimum four shoots per tree. The susceptibility of the shoots was determined according to the percentage of necrosis into the shoot and a Townsend-Heuberger equation (TH3) using the following formulae:

% of necrosis in the shoot = length of visible shoot necrosis / total shoot length

$$\text{Infection value TH3} = \frac{(0 \times n_0) + (1 \times n_1) + (2 \times n_2) + (3 \times n_3)}{3 \times N} \times 100$$

with : n_0 = number of shoots in class 0 (no infection)

n_1 = number of shoots in class 1 (infection visible on the infected leaf)

n_2 = number of shoots in class 2 (necrosis on the leaf and the shoot)

n_3 = number of shoots in class 3 (necrosis + ooze)

N = total amount of shoots

3.2 Histological study

3.2.1 Light microscopy

Leaf samples taken directly at the inoculation site were fixed for 4 hours at 4°C in 2% glutaraldehyde and malachite green 0.1%, buffered in 0.05M sodium PIPES (1,4-piperazinediethanesulfonic acid; pH 7.5). After dehydration in graded ethanol series, the tissues were impregnated and embedded in paraffin. Sections

(8µm) were obtained using a Leica MS 2000R rotary microtome equipped with a steel knife. The sections were stained with safranin and astra blue and mounted on DePex. The tissues were examined using a Polyvar Reichert-Jung interference microscope and the images were digitalized with an Olympus C-5050 zoom digital camera.

A 3,3'-diaminobenzidine staining (DAB-staining) to show the presence of ROS (Thordal-Christensen et al., 1997) was also performed on the leaves 24h and 48h after infection. In the presence of peroxidase and DAB, H_2O_2 is visualised as a reddish brown discoloration.

3.2.2 Fluorescence microscopy

Histochemical localization of flavonoids on 8µm thick sections (see previous section light microscopy) was performed by the protocol proposed by Pina and Errea (2008). The sections were deparaffinized in xylene, rehydrated in ethanol series for 2min (100%, 70% and 40%), washed in distilled water, stained for 5min in 1% (w/v) Naturstoff reagent A (NA; diphenylboric acid 2-aminoethyl ester, Sigma) in ethanol, and then repeatedly washed with ethanol. NA-stained sections were examined under a Fluorescence Microscope Nikon Eclips 80i with a filter cube comprised of a 540/25nm excitation filter, a 605/55nm barrier filter and a 565 dichroic mirror. Fluorescence micrographs were taken with an Imaging Source DFK H1AF02 camera coupled to the microscope. The yellow fluorescence of the stained material was consistent with the autofluorescence of the polyphenolic compounds due to the NA-staining.

3.2.3 Transmission electron microscopy

Leaf parts taken directly at the inoculation site were fixed for 20 hours at 4°C using vacuum infiltration in 2% v/v glutaraldehyde and 0,01% w/v malachite green, buffered in 0.05M sodium PIPES (pH 7.5). Samples were rinsed 3 times for 30min in 0.05M sodium PIPES (pH 7.5) and postfixed in 2% w/v osmium tetroxide, buffered in 0.2M sodium cacodylate and twice in distilled water before staining in 2% w/v uranyl acetate overnight at 4°C. After dehydration, the fixed tissues were imbedded in Spurr's epoxy resin. Ultra thin sections (65nm) obtained using a Leica Ultracut UCT ultramicrotome, were mounted on 0.7% w/v formvar coated copper grids 50 mesh. The sections were contrasted with uranyl

acetate (4% w/v in 50% ethanol) followed by lead citrate (4% w/v solution) and examined in a Philips EM 208 transmission electron microscope operated at 80k. Images were digitalized with a MORADA 10/12 camera (Olympus, Germany).

3.3 RT-qPCR

Frozen and not necrotic leaf tissue adjacent to the infection site was grinded using two stainless steel beads in each sample and the Retsch Mixer Mill MM2000. Seven independent samples per treatment were used.

RNA was extracted using the protocol of Gasic *et al.* (2004), which is optimized for trees belonging to the family of *Rosaceae*. The concentration and purity of RNA was spectrophotometrically tested at a ratio of respectively 260/280nm and 260/230nm by a Nanodrop 1000 machine (Thermo Fischer Scientific Inc). RNA integrity was checked through denaturing gel electrophoresis.

All RNA samples were adjusted to an identical concentration (1µg/µl) and incubated in gDNA wipe-out buffer at 42°C for 2min to remove contaminating gDNA (QuantiTect reverse transcription kit, Qiagen). First strand cDNA synthesis was primed with a combination of oligo(dT)-primers and random hexamers according to the manufacturer's instructions using a QuantiTect reverse transcription kit (Qiagen). A ten-fold dilution of the cDNA was made using 1/10 diluted TE buffer (1mM Tris–HCl, 0.1mM EDTA, pH 8.0) and stored at −20°C.

RT-qPCR was performed with the ABI Prism Fast 7500 (Applied Biosystems), SYBR Green Chemistry.

Primers were designed and optimized by Primer3 (Whitehead Institute for Biomedical Research) starting from Ncbi database using orthologous (for the antioxidative related genes) or available gene sequences (for the phenylpropanoid-flavonoid related genes), were checked for similarities between biological sequences using BLAST (Ncbi) and were then verified for their quality, stability and efficacy using NetPrimer (Premier Biosoft). Specificity of the primers was checked after qPCR by verifying the occurrence of single peaks on the melting curve. The amplification efficiencies of all primer sets were investigated by a 2-fold serial dilution over 6 dilution points and were approved when they were greater than 80%. The transcription levels of the genes that code for phenylalanine ammonium lyase (*PAL*), chalcone synthase (*CHS*), flavanon 3β hydroxylase (*FHT*), flavonol synthase (*FLS*), flavonoid 7-O-

glucosyltransferase (*F7GT*), dihydroflavonol-4-reductase (*DFR*), leucoanthocyanidin reductase 1 (*LAR1*), anthocyanidin synthase (*ANS*) and finally anthocyanidin reductase (*ANR*) were investigated in case of the phenylpropanoid-flavonoid pathway (table 3.1; figure 1.10). For the antioxidative related genes, primers were designed and optimized by Primer3 (Whitehead Institute for Biomedical Research) starting from *Malus* Contigs, were checked for similarities between biological sequences using BLAST (Ncbi) and were verified for their quality, stability and efficacy using NetPrimer (Premier Biosoft). The transcription levels of Fe Superoxide Dismutase 1 (*FSD1*), Fe Superoxide Dismutase 2 (*FSD2*), Fe Superoxide Dismutase 3 (*FSD3*), Mn Superoxide dismutase 1 (*MSD1*), Cu/Zn Superoxide Dismutase 1 (*CSD1*), Cu/Zn Superoxide Dismutase 2 (*CSD2*), Cu/Zn Superoxide Dismutase 3 (*CSD3*), Ascorbate Peroxidase 1 (*APX1*), Ascorbate Peroxidase 3 (*APX3*), Ascorbate Peroxidase 4 (*APX4*), Ascorbate Peroxidase 5 (*APX5*), Catalase 1 (*CAT1*) and Catalase 3 (*CAT3*) were analysed (table 3.1). For Ascorbate Peroxidase 2 (*APX2*) and Catalase 2 (*CAT2*), no appropriate primers could be developed.

PCR amplifications were performed at universal cycling conditions (10min at 95°C, 40 cycles of 15s at 95°C and 60s at 60°C) in a total volume of 10µl, containing 2.5µl cDNA sample, 5µl SYBR Green Master Mix (Applied Biosystems), 1.2µl primers (10µM) and 1.3µl RNase-free H_2O.

Reference genes coding for a Clathrin adaptor complex subunit (*Clathrin*; Malus v4 Contig15159 derived from source file CN865508.1), an elongation factor *ef1-a* (CN941921 derived from source file DQ341381.1) and an elongation factor *ef4-a* (Malus v4 Contig5101 derived from source file AY347787.1) were used to normalise the data and were obtained by geNorm, an applet that analyses the most stable reference genes from our set of about ten tested candidate reference genes (Vandesompele *et al.*, 2002).

All samples were tested for the reference genes as well as for the genes of interest. Gene expression data were expressed relatively to the reference genes and to the values of untreated immature leaves 3hours after infection following the $2^{-\Delta Ct}$ method dived by the geometric mean of reference genes. In addition, an interrun calibration was implemented (three samples per plate).

Table 3.1: Primer sequences of the used reference genes and genes of interest.

Genes	Genbank Acc. Nr.	Left Primer (5'->3')	Right Primer (5'->3')
Phenylpropanoid-flavonoid pathway related genes			
PAL	DQ230992.2	*GCCACACCAAGCAACAAGA*	*CAATGTAGGATAGCGGGACAA*
CHS	AY786998.1	*CGAGAAAGGACTCAAAACAACC*	*AAACCCACGCTATGAAGCAC*
FHT	AY965342.1	*CAACGACTTCAGCAACGAAA*	*CGATGGCAAAGCAAAGAAC*
FLS	DQ230993.1	*TTACTGAGGCCAGCTCCAAC*	*ATTGTCCACCCACCCTTTCT*
F7GT	AY954922.1	*ATTGATTCCGTCCGCTTTCT*	*AACCCTTTTGCGATTTCCTC*
DFR	AY227730.1	*ACGACCTCTGCCTTTCTCAC*	*CTCAAACCCTATCTCCCTCAAC*
LAR1	DQ251190.1	*GACATCCGAGCAATCAACAA*	*CTTCCACCGCAAAATTAACC*
ANS	DQ230994.1	*AGGGAGGCTGGAGAAAGAAG*	*TGTTGTGGAGGATGAAGGTG*
ANR	DQ251189.1	*TCTGAAGTCGTGCGTGAAAG*	*AAGTGGGTGGCTTGACAGTAG*
Antioxidative related genes			
FSD1	Malus_v4_Contig16258	*GCCGTTAACCCCCTTATTTG*	*CTGCTTCCCATGATACGAGTT*
FSD2	Malus_v4_Contig18456	*AGAATATCACTGGGGGAAGCA*	*GCGCTGCCTGGTTGAAAG*
FSD3	Malus_v4_Contig5924	*GTCCTTCAGCAGATAGAAAAGG*	*AAGCCAAACCCAGCCAGA*
MSD1	Malus_v4_Contig8113	*CTTTGGTTCCATTGCTTGGT*	*CGGCTCAAGTGCTTTCTTTC*
CSD1	Malus_v4_Contig18911	*TGGTTAAGGGTGTTGCTGTTC*	*GGGCACCATGCTCTTTTC*
CSD2	Malus_v4_Contig18796	*CATATCCACAGGACCACATTTC*	*AAGTTCGTGTCCACCCTTTC*
CSD3	Malus_v4_Contig6927	*CAGATGGAGTTGCTGAGGTTT*	*ACTCTTGCTCCTGCGTTCC*
APX1	CN894028.1	*CCCCCATAACCTACAACC*	*GACCTGTGAGCTTCCTCCT*
APX2	Malus_v4_Contig22437	*GGCGGTAGAAAAATGCAAGA*	*CTCCAAAAGCCTAACCACGA*
APX3	Malus_v4_Contig8946	*TGGGTAGAGCACATCCAGAAA*	*TCAACATAGCGGCGGAAC*
APX4	Malus_v4_Contig23178	*GCTGTTATGTCTGCATTCTTGG*	*CGGCTGCGTTGGTATTTCT*
APX5	Malus_v4_Contig8946	*GTTCCCTTCCATCCTTCGTT*	*GTTTCGGCGTTGTATGTTCC*
CAT1	Malus_v4_Contig4354	*CCGTGATGCAATGAAAATCC*	*CATCGAATAGGAAGGCGAAC*
CAT3	Malus_v4_Contig3679	*TAATCACAGCCACGCTACCA*	*TTCAGTACCAAACGGCCAAC*
Reference genes			
Ef 1-a	CN941921	*AATCGCCTTTGTTCCCATC*	*GCACAGTTCCAATACCACCA*
Ef 4-a	Malus_v4_Contig5101	*ATCAGGCTCATCCCGTGT*	*AGCAACACCCTTCCTTCC*
Clathrin	Malus_v4_Contig15159	*CGCTCTCCATTCTCTTCCA*	*CCTTCCCGGTTACATCACA*

3.4 HPLC

Frozen leaf tissue was lyophilized and grinded with a mortar. The resulting powder was extracted with 100% methanol containing 0.1 mg ml^{-1} 6-methoxyflavone as an internal standard (500µl per 100mg of lyophilized powder), sonicated (30min, 4°C) and centrifugated for 10min at 10000g and 4°C. The HPLC equipment consisted of a sample injector (Gilson Modell 231, Gilson Abimed, Ratingen, Germany) of two pumps (Kontron 422, Kontron, Eching, Germany) and a diode array detector (Bio Tek Kontron 540+, Kontron, Eching, Germany). For post-column derivation, a Gynkotek pump (Modell 300C, Gynkotek, Germering, Germany) and the detector Kontron 432 (Kontron, Eching, Germany) were used (figure 3.2).

The phenolic compounds were separated on a column (250 x 4mm ID) prepacked with Hypersil ODS, 3µm particle size, following a stepwise gradient using mixtures of solvent A (formic acid, 5% in water) and solvent B (methanol, gradient grade) from 95:5 v/v with a flow rate of 0.5 ml min^{-1} (Treutter *et al.*, 1994). The gradient profile (%B in A) used was: 0-5 min, isocratic, 5% B; 5-15 min, 5-10% B; 15-30 min, isocratic, 10% B; 30-50 min, 10-15% B; 50-70 min, isocratic, 15% B; 70-85 min, 15-20% B; 85-95 min, isocratic, 20% B; 95-110 min, 20-25% B; 110-140 min, 25-30% B; 140-160 min, 30-40% B; 160-175 min, 40-50% B; 175-190 min, 50-90% B.

Figure 3.2: The HPLC equipment with a sample injector (Gilson Modell 231, Gilson Abimed, Ratingen, Germany) of two pumps (Kontron 422, Kontron, Eching, Germany) and a diode array detector (Bio Tek Kontron 540+, Kontron, Eching, Germany).

Peak identification was conducted by their UV absorbance spectra and by comparison with authentic standards (Mayr *et al.*, 1995; Mayr *et al.*, 1997; Roemmelt *et al.*, 2003b). Several compounds were completely identified, while other compounds were at least related to the respective phenolic classes. For quantification of simple phenolic compounds, the signals from detection at 280 nm were used. Hydroxycinnamic acids and flavonols were detected at 320 and 350nm respectively. Catechins and proanthocyanidins were estimated at 640nm after post-column derivatization with 4-dimethylaminocinnamic aldehyde (Treutter *et al.*, 1994). Eight independent samples per treatment were used. Analyses were performed at the lab of Prof. Treutter, Unit of Fruit Science, Technische Universität München, Germany.

3.5 Chlorophyll fluorescence measurements

The photosynthetic efficiency was analysed on mock-inoculated and *E. amylovora* inoculated mature and immature leaves. Per treatment, six trees were measured with the PEA. After thirty minutes dark adaptation, chlorophyll fluorescence induction curves were measured using a Plant Efficiency Analyzer (PEA, Hansatech Instruments, Ltd. King's Lynn Norfolk, UK) with a recording time of 1s and an excitation light intensity of 3000µmol photon $m^{-2}s^{-1}$. The fluorescent signal was recorded every 10µs for the first 2ms and every 1ms thereafter up to 1s (figure 3.3). Trees were measured 24h, 48h and 72h after inoculation. PEA-measurements were done on leaf tissue (±1cm^2) close to the inoculation wound.

The curves of the chlorophyll a fluorescence transient were analyzed using the JIP test (Biolyzer© software R.M. Rodrigues, The Bioenergetics Laboratory, University of Geneva, Geneva, Switzerland) and a selection of chlorophyll fluorescence parameters were calculated based on the energy flux theory of Strasser (Strasser *et al.*, 1995).

Next to PEA measurements, Fluorescence Imaging was also performed by a Fluorescence Imaging System developed in the laboratory of Molecular and Physical Plant Physiology at Hasselt University. The excitation unit contains six lamps (3x20W, 3x50W). A blue cut-off low pass glass filter (BG39) and an infrared filter are mounted in front of the lamps. The detection unit consists of a charge coupled device camera (PVCM 3405) equipped with a red cut off (650nm)

high pass filter. The system takes two 8-bit images: a L-image (corresponds to F_s) and H-image (corresponds to F_m) after illumination with respectively actinic (I= 300µmol $m^{-2}s^{-1}$) and saturating light (I=1200 µmol $m^{-2}s^{-1}$) intensities, without dark adaption of the plant material (leaves were light adapted in the presence of actinic light). Software for the recording, processing and correcting of the image has been developed by Ciscato and Valcke (1998).

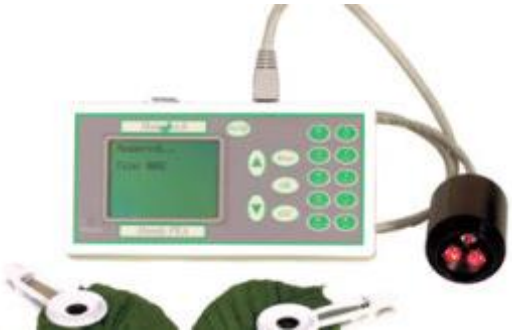

Figure 3.3: The Plant Efficiency Analyser developed by Hansatech Instruments. The PEA consists of a sensor with LEDs (black cylinder) and a control unit. Leaf clips cover up the parts that need to be measured.

3.6 Leaf gas exchange measurements

The primary functions of the infrared gas analyser (model LCA4, Analytical Development Co., Hoddesdon, UK) were to accurately measure the concentration of CO_2 and H_2O circulating through the leaf chamber, to control the flow rate of the gas, and if required, to modify the concentration of CO_2 and H_2O. These functions were performed by the IRGA Optical Bench, the Gas Control and the Gas Conditioning (figure 3.4).

The Optical Bench consists of two measurement cells in series to measure the difference in IR absorption arising from the respective levels of CO_2 and H_2O. The Gas Control times and selects the various gas flow paths and controls and monitors the flow rates through the system, whereas the GAS conditioning controls the levels of CO_2 and H_2O as set by the user.

The infrared gas analyzer, housed inside the broad leaf chamber of 6.25cm^2, provides accurate, fast, reliable and stable gas exchange performance. By housing the gas analyser directly in the leaf chamber head, response delays in gas exchange measurements are effectively eliminated. The proximity of the

chamber and the analyser also reduces the risk of gas hang-up or water vapour drop out in long lengths of gas tubing.

Various parameters inside the system were set as constant when working with broad type leaves. The boundary layer resistance to water vapour r_b was set to 0.8 $m \cdot s\ mol^{-1}$, the transmission factor of the total radiant energy H_{factor} was 0.168 and the transmission factor of the Photosynthetic Active Radiation T_{rw} was 0.88. A constant flow rate of 410 µmol s^{-1} was obtained throughout the experiment.

The rate of net CO_2 assimilation, the stomatal resistance, the transpiration and other parameters were measured on three trees per treatment. These trees were measured for five minutes and the first 2 minutes were discarded in order to calibrate the system more properly. Trees were measured before inoculation and 24h, 48h and 72h after inoculation.

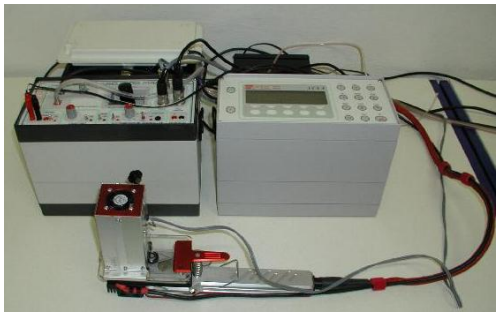

Figure 3.4: The LCA4 equipment with broad leaf chamber unit (front) and control unit (back).

3.7 Statistical analyses

For quantitative reverse transcription PCR data and HPLC, the different treatment means were subjected both to a 3-way ANOVA and a 2-way ANOVA (if that data were studied for just one time interval) with Tukey's pairwise comparisons and a log transformation to approximate normality. All data were tested for their equality of variances using a Levene's test and for their normal distribution using a Shapiro-Wilk test.

PEA data and respiration data were subjected to a pairwise comparison for their different parameters, using the untreated leaves for both mature and immature leaves as the control data.

Outliers were excluded based on a maximum normed residual test for all data. All statistical analyses were performed using the SAS 9.2 software.

4. Results

4.1 Symptom development

The development of the shoot infection in control, mock-inoculated and *Ea*-inoculated Conférence trees was measured 6 and 8 days after inoculation. Both the control and mock-inoculated leaves and shoots showed no visual signs of infection. *Ea*-inoculated leaves however did show disease symptoms. The TH3 values were higher when the inoculation was performed in the immature leaves compared to the mature ones (table 3.2). In case of the mature leaves, necrosis did not migrate into the shoot but remained present in the chlorenchym of the leaf. The progress of necrosis in the shoots was higher when inoculation was performed in the immature leaves. Eight days after inoculation, more than 50% of the shoot length was infected when the artificial inoculation was performed on the immature leaves (table 3.3).

Table 3.2: Shoot infection values expressed as TH3 values, measured 6 and 8 days after inoculation, p<0.001 (Tukey)

TH3 value	6DAI		8DAI	
Control / Mock inoculation immature leaf	0.00	a[1]	0.00	a
Control / Mock inoculation mature leaf	0.00	a	0.00	a
Ea-inoculation of an immature leaf (2nd and 3rd fully unfolded leaf in active growth)	67.61	c	90.14	c
Ea-inoculation of a mature leaf (6th and 7nd fully unfolded leaf in active growth)	33.33	b	33.33	b

[1]Means in a column followed by the same letter do not differ significantly

Table 3.3: Percentage of the necrosis into the shoot, measured 6 and 8 days after inoculation, p<0.001 (Tukey)

% of necrosis in the shoot	6DAI		8DAI	
Control / Mock inoculation immature leaf	0.00	a[1]	0.00	a
Control / Mock inoculation mature leaf	0.00	a	0.00	a
Ea-inoculation of an immature leaf (2nd and 3rd fully unfolded leaf in active growth)	16.41	b	51.89	b
Ea-inoculation of a mature leaf (6th and 7nd fully unfolded leaf in active growth)	0.00	a	0.00	a

[1]Means in a column followed by the same letter do not differ significantly

4.2 Antioxidative related genes

The presence of ROS was detected using a DAB-staining, by which H_2O_2 is visualised as a reddish brown discoloration. ROS is present near the wound where inoculation took place, both for mock-inoculated and *Ea*-inoculated leaves, and independent of leaf age. However, in the *Ea*-inoculated leaves, ROS were also present in the regions close to the wound, especially in the small veins near the wound (figure 3.5).

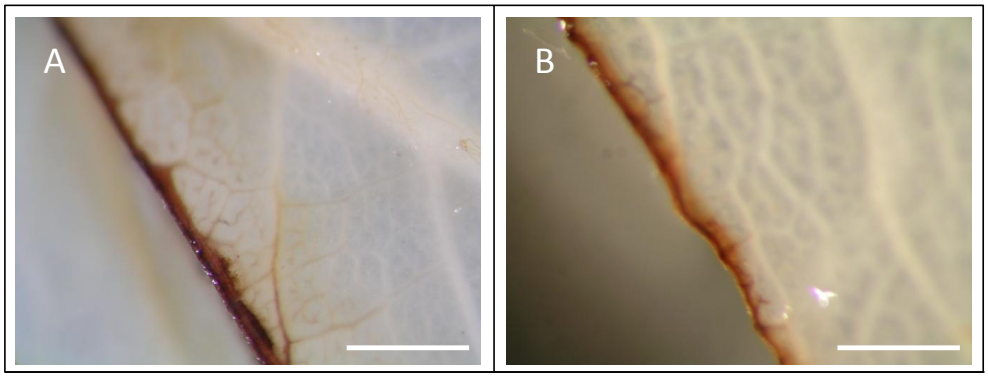

Figure 3.5: DAB-staining to show the presence of ROS (brown colour) at the cutting edge and the small veins in a *Ea*-inoculated immature leaf (A) and only at the cutting edge in a mock-inoculated immature leaf (B), 48h after inoculation (bar=500µm, Stereoscopic Zoom Microscope Nikon SMZ800).

The antioxidative related genes that were analysed with RT-qPCR showed different expression patterns. In broad terms, we could divide them into three main groups: genes with a normal expression pattern that remained more or less constant over time (*APX1*, *APX5* and *CSD1*; genes are not shown), genes with big fluctuations in relative expression between and within treatments and therefore no clear significant conclusions could be drawn (*APX3*, *CSD3*, *FSD3* and *MSD1*; genes are not shown) and finally genes with a large contrast in the expression pattern between immature and mature leaves (*APX4*, *CAT1*, *CAT3*, *CSD2*, *FSD1* and *FSD2*; see figure 3.6 for *CSD2*, *FSD1* and *CAT1*, the other three genes are not shown as they have similar transcript levels as one of the three previous mentioned genes). Both *CSD2* and *FSD1* seem to be inversely regulated. *CSD2* and *APX4* had much lower expression values in the mature leaves than in the immature leaves. They showed a clear and significant down-regulation in comparison with the untreated immature leaves (the relative expression values of *CSD2* and *APX4* for mature leaves fluctuated between 0.2

and 0.6, untreated immature leaves maintained more or less their expression value of 1). This was not the case for the genes *FSD1*, *FSD2*, *CAT1* and *CAT3*. These genes showed significantly higher expression levels in the mature leaves, independent of the treatment (control, mock, infection) that was applied ($p<0.001$). For the mature leaves, *CAT3* had approximately 3 times higher expression values in comparison with immature leaves, *CAT1* had 6 times higher values and *FSD1* and *FSD2* had 8 times higher values. Differences between control, mock-inoculated and *Ea*-inoculated leaves were not that distinct as the clear difference between immature and mature leaves.

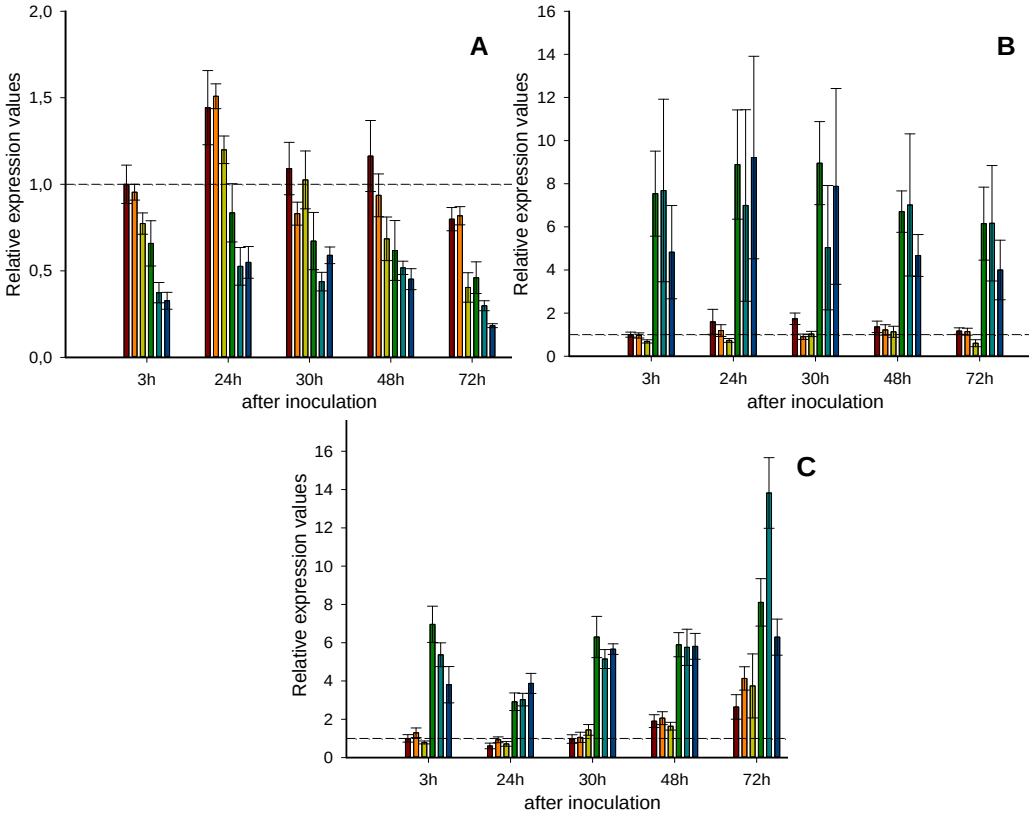

Figure 3.6: Relative expression values of Cu/Zn superoxide dismutase *CSD2* (A), Fe superoxide dismutase *FSD1* (B) and catalase *CAT1* (C) for different treatments (Untreated immature leaves (■), Mock-inoculated immature leaves (■), *Ea*-inoculated immature leaves (■), Untreated mature leaves (■), Mock-inoculated mature leaves (■) and *Ea*-inoculated mature leaves (■)), x hours after inoculation. Values are mean ± SE of 7 biological independent replicates. Gene expression data were expressed relatively to the reference genes and to the values of untreated immature leaves 3hours after inoculation (= relative expression value of 1) following the $2^{-\Delta Ct}$ method divided by the geometric mean of the reference genes.

For instance, *CSD2* had a significant lower expression value in the *Ea*-inoculated leaves 72h after infection, in both immature and mature leaves. This was also the case for *APX4*, which had significant differences 48 and 72h after inoculation. For the other genes, the differences were less clear. Furthermore, for *CAT1* and *CAT3*, a slight increase of the relative expression values in immature leaves independent of the treatment was observed, reaching the highest values 72h after inoculation.

4.3 Phenylpropanoid-flavonoid pathway

4.3.1 Microscopic analysis shows the presence of bacteria and an increased accumulation of lignin and phenolic compounds near the vascular system of the leaf

Transmission electron microscopy analysis of leaf sections taken in close proximity to the inoculation wound, showed the presence of bacteria in both mature and immature leaves, assuming a successful infection took place (figure 3.7; A and B). With this technique, distinct differences in cell ultrastructure between mature and immature leaf tissues, but not between mock and infected samples could be observed.

In safranin-astra blue combination staining, lignified and cutinized cell walls stained bright red due to their acidic properties, while cellulose cell walls and cytoplasm stained blue. These two distinct colours could be noticed 48 and 72 hours after inoculation with *E. amylovora*. In *Ea*-inoculated leaf tissue, both red and blue stained structures were visible, whereas in mock-inoculated leaves most of the cellular tissue only stained blue. The dense red colour was situated near the vascular system of the leaf, the light blue colour was distributed over the epidermis and the parenchyma cells (figure 3.7; C and D).

Fluorescence microscopy combined with the Naturstoff A reagent confirmed the results that the phenylpropanoid-flavonoid pathway is involved. When inoculation with *E. amylovora* was performed in mature leaves, a significant increase in flavonoids visible as a bright yellow colour was detected near the vascular tissue. This yellow colour was slightly decreased or even totally absent in the uninfected and mock-inoculated leaf tissues (figure 3.7; E and F). Immature leaves did not always respond to the NA reagent which, however is a significant difference compared to the mature leaves.

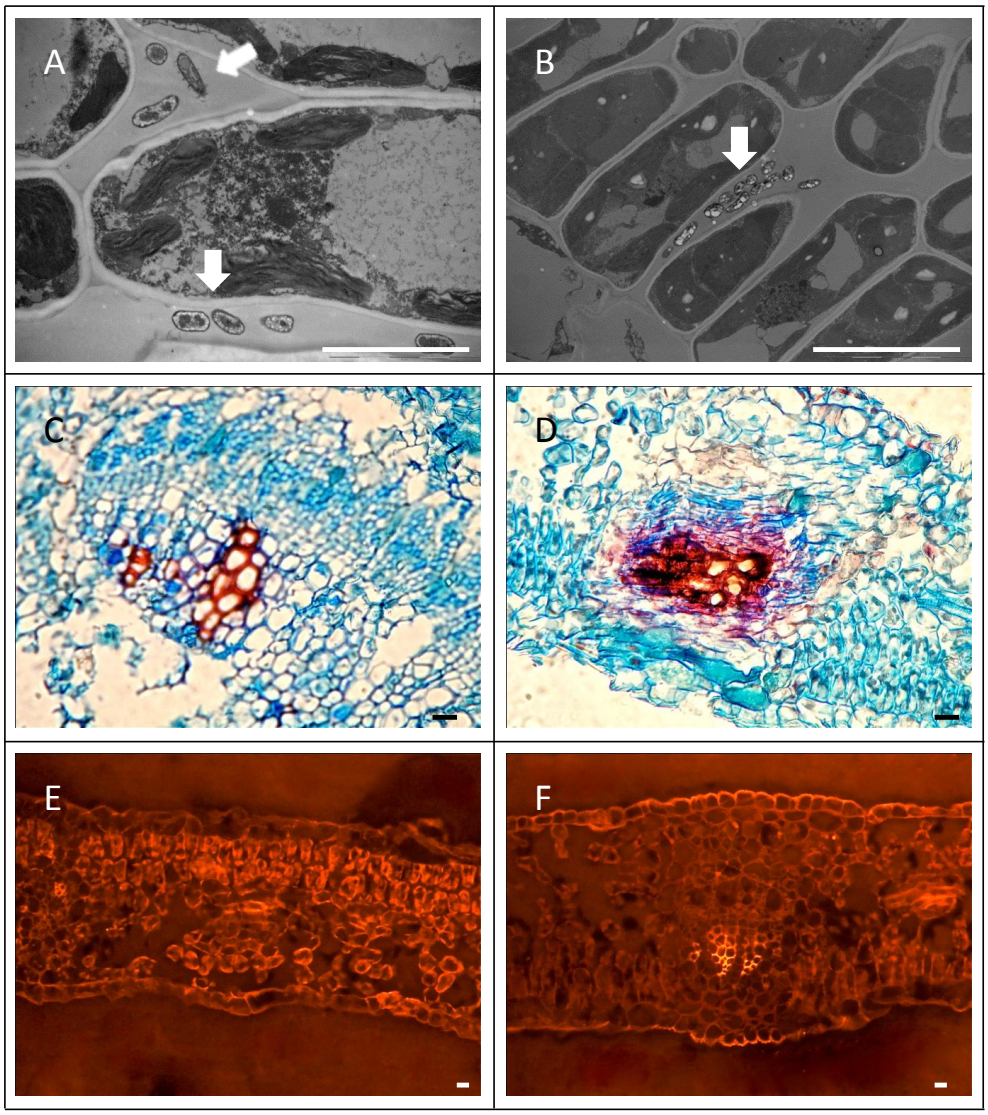

Figure 3.7: A and B: Electron micrographs of an *Ea*-inoculated immature (A) and an *Ea*-inoculated mature (B) leaf to show the occurrence of *E. amylovora* in the leaf tissue, 72h after inoculation (bars 5 (A) and 10 (B) µm, Philips EM 208 transmission electron microscope). Arrows indicate the presence of bacteria; C and D: Safranin-astra blue staining of an *Ea*-inoculated immature leaf (C) and an *Ea*-inoculated mature leaf (D), 72h after inoculation. Lignified and cutinized cell walls, stain bright red, cellulose cell walls and cytoplasm stain blue (bars 10 µm, Polyvar Reichert-Jung interference microscope); E and F: Naturstoff reagent A staining on an *Ea*-inoculated immature (E) and an *Ea*-inoculated mature (F) leaf, 72h after inoculation. The yellow fluorescence is consistent with the autofluorescence of phenolic compounds due to the NA-staining. In F, a bright yellow colour is clearly visible near the vascular system (bars 10µm, Fluorescence Microscope Nikon Eclips 80i).

4.3.2 RT-qPCR demonstrates significant up-regulation of genes of the phenylpropanoid-flavonoid pathway in the mature leaves

A heat map representation is an easy way in visualising differences for a large amount of data (table 3.4). With the heat map representation, it was clear that the phenylpropanoid-flavonoid related genes analysed with quantitative reverse transcription PCR showed different expression patterns. A significant up-regulation of *PAL*, *FHT*, *DFR*, *ANS*, *ANR* and to a much lower extent *CHS* and *LAR1* transcripts could be observed in the *Ea*-inoculated mature leaves for almost all measured time points. A large increase in the relative expression of these genes was noticed 48h after infection. This increased activity was the highest for *PAL* and *ANR*, where relative expression values of respectively 6.05 and 17.53 were measured. Compared to the untreated mature leaf, a seven-fold significant increased activity was measured in the *Ea*-inoculated mature leaves for *ANR* and *CHS*, whereas for *PAL*, *FHT*, *DFR*, *ANS* and *LAR1* only an approximately three to four-fold significant amplification was seen.

In comparison to the mock-inoculated mature leaves, the activity of all these genes in *Ea*-inoculated mature leaves was more or less doubled, but due to the relative large standard errors, no significant differences could be observed. Both *ANR* and *DFR* are respectively shown in figure 3.8 A and 3.8 B. After 72 hours, the relative expression of mature infected leaves decreased again and was more or less comparable to the values reached 30h after infection.

For these previously mentioned genes, the immature leaves exhibit hardly any differences, as relative expression values fluctuated around 1.00 - 2.00. However, 72hours after infection, the presence of low expression values in the infected immature leaves could be caused by an internal leaf plasmolysis as a result of a successful infection with *E. amylovora*.

In comparison to the *PAL*, *CHS*, *FHT*, *DFR*, *LAR1* and *ANS* transcripts, the transcript level of *F7GT* was not affected during the experiment, as expression values were around 3.00-4.00, independent of treatment and age.

Gene expression patterns of *FLS* transcripts were also clearly ontogenesis-associated. *FLS* transcripts were significantly ($p < 0.0001$) lower in the mature leaves compared to the immature leaves for all time intervals (figure 3.8 C). The relative expression value of *FLS* for mature leaves fluctuated between 0.05 and 0.34, immature leaves retained values of around 0.55-2.27. Between

treatments, no clear significant differences for *FLS* could be measured in immature or in mature leaves (except 72h after inoculation in mature leaves).

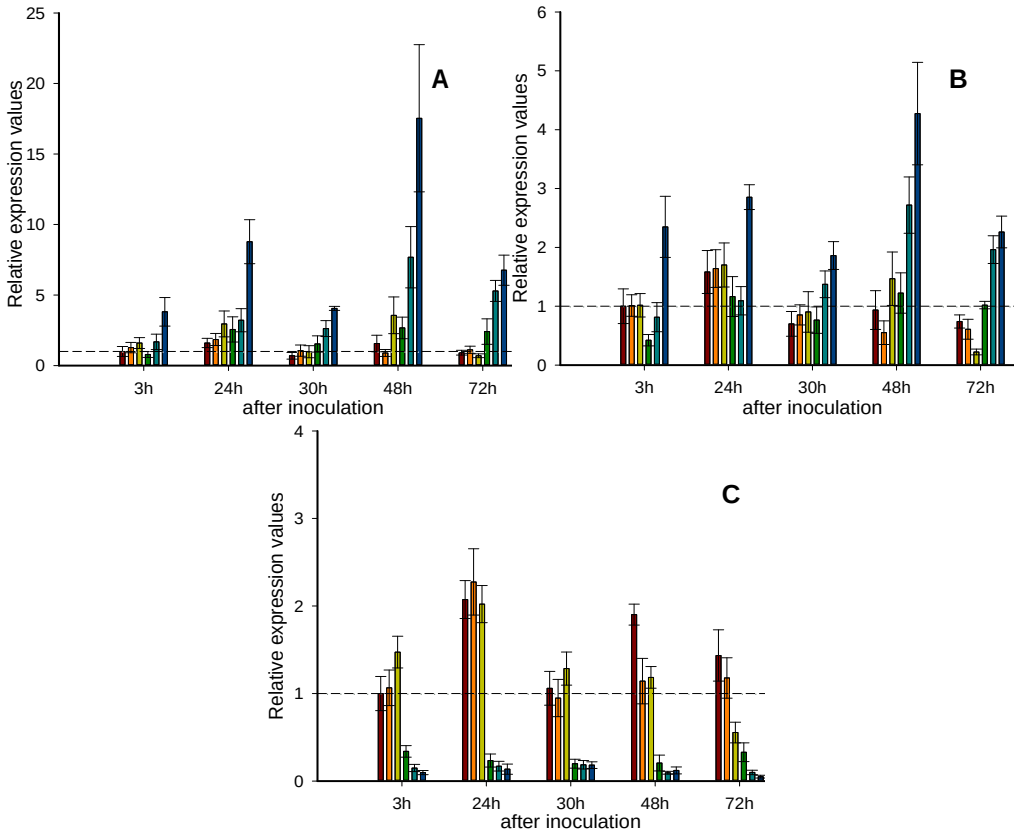

Figure 3.8: Relative expression values of anthocyanidin reductase *ANR* (A), dihydroflavonol-4-reductase *DFR* (B) and flavonol synthase *FLS* (C) for different treatments (Untreated immature leaves (■), Mock-inoculated immature leaves (■), *Ea*-inoculated immature leaves (■), Untreated mature leaves (■), Mock-inoculated mature leaves (■) and *Ea*-inoculated mature leaves (■)), x hours after inoculation. Values are mean ± SE of 7 biological independent replicates. Gene expression data were expressed relatively to the reference genes and to the values of untreated immature leaves 3hours after inoculation (= relative expression value of 1) following the $2^{-\Delta Ct}$ method divided by the geometric mean of the reference genes.

Table 3.4: Heat map representation of the relative expression values for all investigated genes for the different treatments, x hours after inoculation. Each cell represents a relative expression value according to the colour scale at the bottom. Values in the cells are mean ± SE of 7 biological independent replicates. Gene expression data were expressed relatively to the reference genes and to the values of untreated immature leaves 3hours after inoculation (= relative expression value of 1) following the $2^{-\Delta Ct}$ method divided by the geometric mean of the reference genes. Mean values are followed by a letter. If values have the same letter, they do not differ significantly. Statistics are performed by a 2-way anova. Enzyme abbreviations, see text.

Treatment\gene		*PAL*	*CHS*	*FHT*	*FLS*	*F7GT*	*DFR*	*LAR1*	*ANS*	*ANR*
3h	Untreated immat.	1.00±0.39 **a**	1.00±0.35 **b**	1.00±0.26 **ab**	1.00±0.20 **c**	1.00±0.10 **a**	1.00±0.30 **ab**	1.00±0.23 **ab**	1.00±0.35 **ab**	1.00±0.35 **a**
	Mock-inoc. immat.	1.67±0.34 **ac**	1.01±0.33 **b**	1.87±0.40 **bd**	1.07±0.20 **c**	2.05±0.12 **ab**	1.01±0.18 **ab**	0.79±0.07 **a**	0.93±0.18 **ab**	1.27±0.37 **ab**
	Ea-inoc. immat.	2.37±0.30 **bc**	1.51±0.37 **b**	2.03±0.29 **cd**	1.47±0.18 **c**	1.80±0.09 **ab**	1.02±0.20 **ab**	0.79±0.08 **a**	1.19±0.26 **b**	1.60±0.38 **ab**
	Untreated mat.	0.71±0.15 **a**	0.16±0.04 **a**	0.81±0.15 **a**	0.34±0.07 **b**	3.95±0.42 **c**	0.42±0.10 **a**	0.66±0.07 **a**	0.39±0.10 **a**	0.79±0.21 **a**
	Mock-inoc. mat.	1.28±0.26 **ab**	0.43±0.13 **ab**	1.41±0.29 **ac**	0.15±0.04 **ab**	3.26±0.64 **bc**	0.81±0.25 **a**	0.99±0.12 **ab**	0.67±0.15 **ab**	1.68±0.55 **ab**
	Ea-inoc. mat.	3.28±0.42 **c**	1.66±0.56 **b**	3.50±0.55 **d**	0.10±0.02 **a**	2.56±0.20 **bc**	2.35±0.52 **b**	1.47±0.19 **b**	1.66±0.33 **b**	3.81±1.01 **b**
24h	Untreated immat.	2.70±0.41 **a**	1.18±0.24 **ab**	1.91±0.30 **a**	2.07±0.22 **b**	2.35±0.53 **a**	1.58±0.37 **ab**	1.44±0.21 **a**	1.44±0.31 **a**	1.60±0.33 **a**
	Mock-inoc. immat.	3.82±0.74 **a**	1.91±0.51 **b**	2.54±0.50 **a**	2.27±0.38 **b**	3.99±0.29 **b**	1.64±0.32 **ab**	1.56±0.23 **a**	1.70±0.39 **a**	1.85±0.43 **a**
	Ea-inoc. immat.	3.69±1.09 **a**	1.64±0.49 **ab**	2.50±0.72 **a**	2.02±0.21 **b**	4.37±0.85 **b**	1.70±0.37 **ab**	1.05±0.22 **a**	1.61±0.35 **a**	2.96±0.92 **a**
	Untreated mat.	2.19±0.37 **a**	0.49±0.15 **a**	1.57±0.25 **a**	0.23±0.07 **a**	5.59±0.85 **b**	1.17±0.34 **a**	1.01±0.08 **a**	1.13±0.32 **a**	2.56±0.89 **a**
	Mock-inoc. mat.	2.40±0.46 **a**	0.44±0.09 **a**	1.49±0.31 **a**	0.17±0.06 **a**	4.07±0.29 **b**	1.09±0.24 **a**	0.86±0.10 **a**	1.22±0.23 **a**	3.21±0.82 **ab**
	Ea-inoc. mat.	3.59±0.73 **a**	1.39±0.24 **ab**	3.15±0.55 **a**	0.14±0.06 **a**	4.04±0.33 **b**	2.85±0.21 **b**	1.32±0.19 **a**	2.55±0.42 **a**	8.78±1.56 **b**
30h	Untreated immat.	1.40±0.38 **a**	0.58±0.24 **ab**	0.96±0.26 **a**	1.06±0.19 **b**	3.35±0.71 **a**	0.70±0.21 **a**	0.98±0.14 **a**	1.08±0.26 **ab**	0.69±0.24 **a**
	Mock-inoc. immat.	1.22±0.38 **a**	0.93±0.26 **ab**	1.22±0.32 **a**	0.95±0.21 **b**	3.34±0.59 **a**	0.85±0.17 **ab**	0.78±0.10 **a**	0.96±0.26 **ab**	1.06±0.40 **ab**
	Ea-inoc. immat.	1.09±0.39 **a**	0.94±0.35 **ab**	1.09±0.34 **a**	1.28±0.19 **b**	3.15±0.55 **a**	0.90±0.35 **ab**	0.80±0.14 **a**	1.09±0.44 **ab**	0.98±0.43 **ab**
	Untreated mat.	1.21±0.34 **a**	0.37±0.11 **a**	1.20±0.29 **a**	0.20±0.05 **a**	5.94±0.78 **a**	0.76±0.23 **ab**	0.63±0.06 **a**	0.71±0.25 **a**	1.53±0.57 **ab**
	Mock-inoc. mat.	1.98±0.37 **a**	0.75±0.18 **ab**	1.88±0.37 **ab**	0.19±0.05 **a**	3.07±0.43 **a**	1.37±0.23 **ab**	1.15±0.16 **a**	1.48±0.24 **ab**	2.62±0.57 **bc**
	Ea-inoc. mat.	2.74±0.32 **a**	1.46±0.36 **b**	3.16±0.33 **b**	0.18±0.04 **a**	4.30±0.43 **a**	1.86±0.24 **b**	1.14±0.08 **a**	2.19±0.26 **b**	4.05±0.14 **c**
48h	Untreated immat.	3.19±1.16 **a**	0.85±0.25 **ab**	1.66±0.55 **a**	1.90±0.12 **b**	2.74±0.32 **a**	0.94±0.33 **ab**	1.26±0.28 **ab**	0.82±0.28 **a**	1.56±0.59 **a**
	Mock-inoc. immat.	1.71±0.46 **a**	0.72±0.31 **a**	0.98±0.26 **a**	1.14±0.26 **b**	3.00±0.35 **a**	0.55±0.20 **a**	0.94±0.19 **a**	0.52±0.20 **a**	0.89±0.25 **a**
	Ea-inoc. immat.	3.08±0.83 **a**	1.43±0.43 **ab**	1.95±0.51 **ab**	1.18±0.12 **b**	3.11±0.35 **a**	1.47±0.45 **ab**	1.58±0.33 **ab**	1.86±0.43 **ab**	3.56±1.30 **ab**
	Untreated mat.	1.69±0.24 **a**	0.59±0.18 **a**	1.47±0.30 **a**	0.21±0.09 **a**	4.00±0.43 **a**	1.22±0.34 **ac**	0.89±0.06 **a**	0.78±0.21 **ab**	2.67±0.76 **ab**
	Mock-inoc. mat.	3.61±0.95 **a**	1.57±0.45 **ab**	2.92±0.70 **ab**	0.09±0.02 **a**	3.68±0.35 **a**	2.72±0.48 **bc**	1.02±0.15 **ab**	1.81±0.43 **ab**	7.68±2.17 **bc**
	Ea-inoc. mat.	6.05±1.93 **a**	4.20±1.52 **b**	6±1.49 **b**	0.12±0.04 **a**	3.58±0.17 **a**	4.27±0.87 **c**	2.06±0.29 **b**	3.28±0.92 **b**	17.53±5.22 **c**
72h	Untreated immat.	1.74±0.14 **ab**	0.48±0.10 **ab**	1.84±0.26 **bc**	1.43±0.29 **c**	3.22±0.43 **ab**	0.74±0.11 **b**	1.42±0.18 **b**	0.80±0.21 **ab**	0.91±0.17 **ab**
	Mock-inoc. immat.	1.51±0.35 **ab**	0.40±0.14 **ab**	1.31±0.27 **ab**	1.18±0.23 **c**	6.17±0.94 **c**	0.61±0.17 **b**	1.07±0.21 **b**	0.63±0.19 **ab**	1.12±0.25 **ab**
	Ea-inoc. immat.	0.82±0.11 **a**	0.25±0.06 **a**	0.67±0.10 **a**	0.55±0.12 **bc**	2.89±0.59 **a**	0.22±0.05 **a**	0.49±0.05 **a**	0.31±0.05 **a**	0.70±0.13 **a**
	Untreated mat.	2.69±0.34 **b**	0.29±0.04 **ab**	2.50±0.62 **bc**	0.33±0.11 **b**	6.82±0.58 **c**	1.02±0.06 **bc**	1.02±0.16 **b**	1.18±0.20 **b**	2.41±0.90 **b**
	Mock-inoc. mat.	2.84±0.83 **b**	1.06±0.20 **bc**	3.04±0.69 **bc**	0.10±0.03 **a**	4.99±0.40 **bc**	1.96±0.24 **c**	1.04±0.17 **b**	1.30±0.25 **b**	5.29±0.74 **c**
	Ea-inoc. mat.	2.63±0.45 **b**	2.22±0.39 **c**	4.14±0.61 **c**	0.05±0.02 **a**	2.35±0.12 **a**	2.26±0.27 **c**	1.04±0.10 **b**	1.43±0.23 **b**	6.76±1.07 **c**

4.3.3 Epicatechin is more abundant in Ea-inoculated mature leaves, whereas chlorogenic acid is more abundant in Ea-inoculated immature leaves

Phenolic profiling with HPLC was performed on immature and mature leaf samples 48h and 72h after the onset of all treatments (untreated, mock-inoculated and *Ea*-inoculated).

Regarding the total flavonol concentration (figure 3.9 A), immature leaf tissue revealed values of approximately 8 mg g^{-1} dry weight (DW) for both time points and were independent of the treatment. This was twice the concentration measured in mature leaf tissue, where values of about 4 mg g^{-1} DW were reached. Immature and mature leaves differed significantly in flavonol concentration ($p < 0.0001$).

The same significant difference could be found for the total amount of simple phenolic compounds (figure 3.9 B). A concentration of 10-12 mg g^{-1} DW of simple phenolics was measured for immature leaves, the mature leaves maintained values around 4-5 mg g^{-1} DW of simple phenolics. For flavonols and simple phenolics, no significant differences could be found between the treatments.

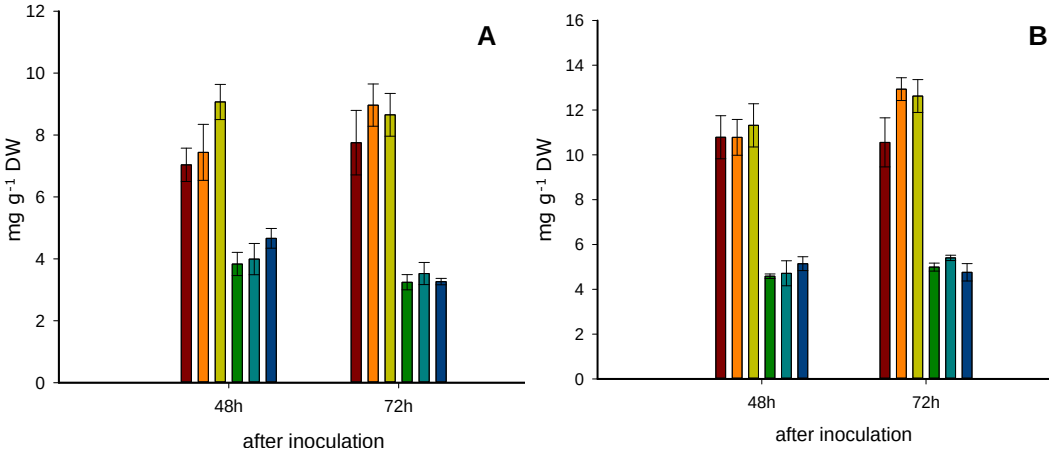

Figure 3.9: Total concentration (mg g^{-1} DW) of flavonols (A) and simple phenolics (B) for the different treatments (Untreated immature leaves (■), Mock-inoculated immature leaves (■), *Ea*-inoculated immature leaves (■), Untreated mature leaves (■), Mock-inoculated mature leaves (■) and *Ea*-inoculated mature leaves (■)), 48h and 72h after inoculation. Values are mean ± SE of 8 biological independent replicates.

Concerning the hydroxycinnamic acids, Cis- and trans-neochlorogenic acid (figure 3.10 A and 3.10 B) stayed more or less constant over time (values respectively around 220 µg g^{-1} DW and 620 µg g^{-1} DW).

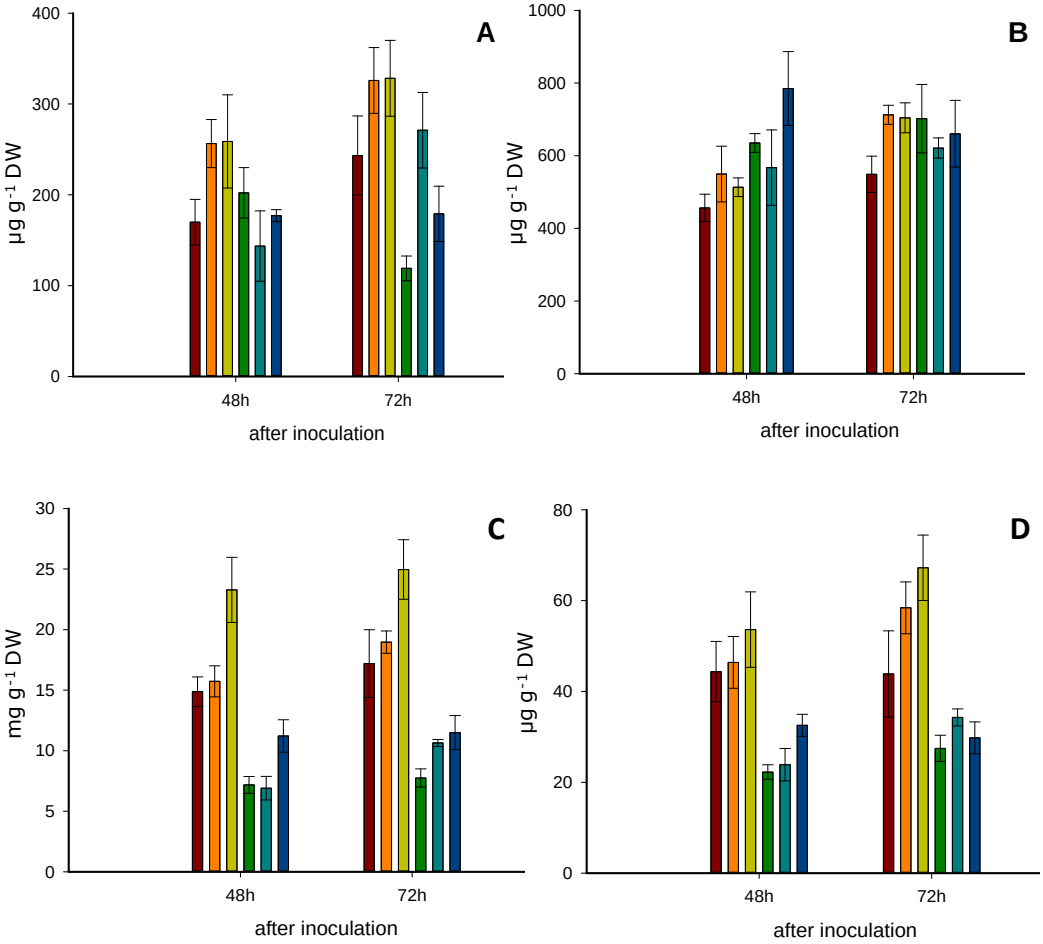

Figure 3.10: Total concentration of the hydroxycinnamic acids cis-neochlorogenic acid (A; µg g^{-1} DW), trans-neochlorogenic acid (B; µg g^{-1} DW), chlorogenic acid (C; mg g^{-1} DW) and cis-ferulic acid (D; µg g^{-1} DW) for the different treatments (Untreated immature leaves (■), Mock-inoculated immature leaves (■), *Ea*-inoculated immature leaves (■), Untreated mature leaves (■), Mock-inoculated mature leaves (■) and *Ea*-inoculated mature leaves (■)), 48h and 72h after inoculation. Values are mean ± SE of 8 biological independent replicates.

However, some significant differences could be found between the treatments in the immature leaves for chlorogenic acid (figure 3.10 C). Forty-eight hours after inoculation, *Ea*-inoculated immature leaves differed from untreated immature

leaves (p = 0.0101) and from mock-inoculated immature leaves (p = 0.0195). Mock-inoculated and untreated immature leaves (p = 0.9990) did not differ reciprocally. This observation was not significant 72 hours after inoculation. Cis-ferulic acid (figure 3.10 D) had the same tendency, but differences were less clear.

The flavan-3-ols, consisting of catechin, epicatechin and procyanidin B2, B5 and E-B5 expressed different profiles. Procyanidin B5 and E-B5 were present in too low concentrations or not detectable at all and therefore, no clear conclusions could be made. Contrary, procyanidin B2 and catechin (figure 3.11 A and 3.11 B) did show higher concentrations compared to B5 and E-B5 but remained more or less constant over time, with concentrations respectively ranging from 18-101 µg g^{-1} DW and 32-83 µg g^{-1} DW. Epicatechin however (figure 3.11 C) showed significant differences 72h after inoculation. Not much differences could be found in the immature leaves, but when considering only the mature leaves in a two-way ANOVA (treatment and leaf age), an approximately 1.5 x higher concentration of epicatechin could be measured in the *Ea*-inoculated mature leaves compared to mock-inoculated mature leaves ((p = 0.5522) and almost a 3x higher and significant concentration of epicatechin in the *Ea*-inoculated mature leaves than was present in the untreated mature leaves (p = 0.0002).

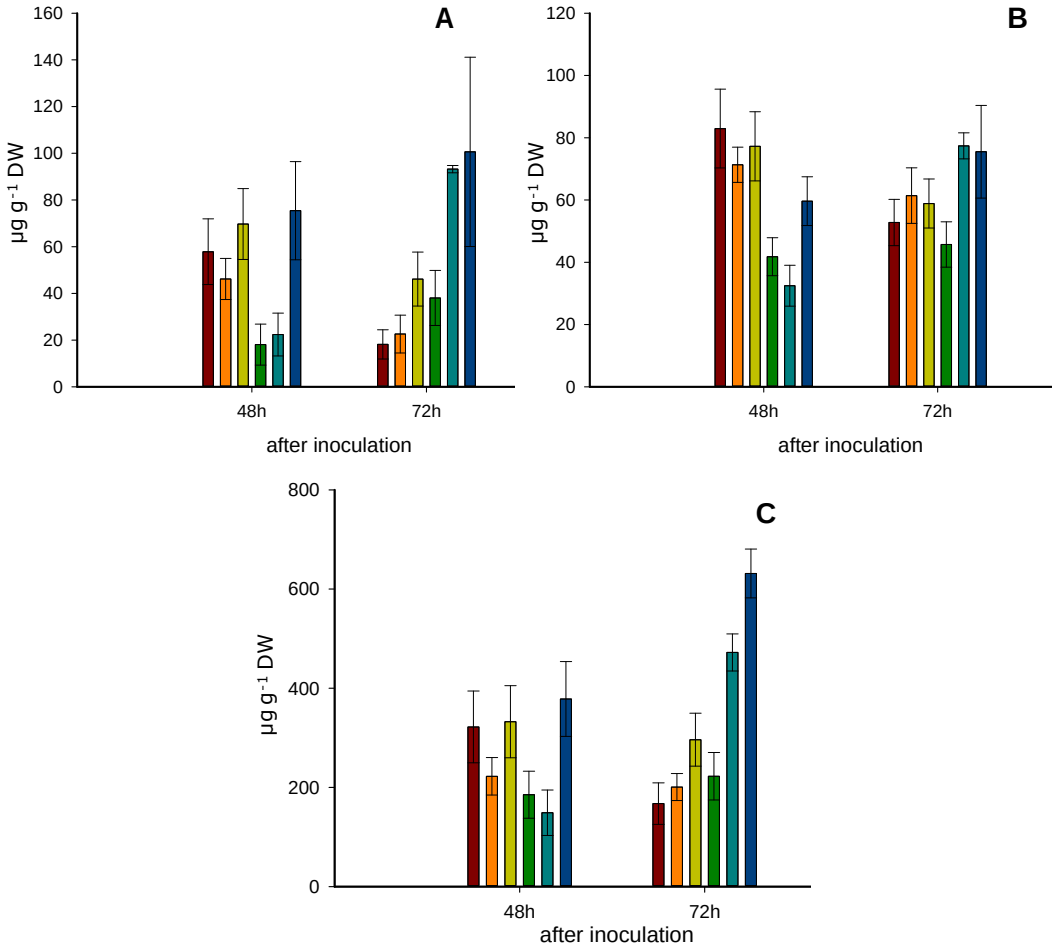

Figure 3.11: Concentration (µg g^{-1} DW) of the flavan-3-ols procyanidin B2 (A), catechin (B) and epicatechin (C) for the different treatments (Untreated immature leaves (■), Mock-inoculated immature leaves (■), *Ea*-inoculated immature leaves (■), Untreated mature leaves (■), Mock-inoculated mature leaves (■) and *Ea*-inoculated mature leaves (■)), 48h and 72h after inoculation. Values are mean ± SE of 8 biological independent replicates.

4.4 Chlorophyll Fluorescence and respiration

4.4.1 Plant Efficiency Analyser and Fluorescence Imaging System

In order to get a better view about the general aspects of photosynthesis after wounding and inoculating leaves and to detect possible differences in susceptibility between the mature and immature leaves based on photosynthesis, trees were measured with the PEA (table 3.5).

Twenty-four hours after inoculation (table 3.6), the effect of *Ea*-inoculating remained negligible in both the immature and mature leaves. Only the TR_0/RC and ET_0/RC parameters explaining the different photosynthetic fluxes inside the leaf tissue differed significantly from the mock-inoculated leaves.

Forty-eight hours after inoculation (table 3.7), *Ea*-inoculated leaves did not show differences at all, both for immature and mature leaves.

Seventy-two hours after inoculation (table 3.8), both the *Ea*-inoculated mature and immature leaves had a lowered trapping probability Ψ_0 of the excitons, a lower performance index PI_{abs} and a few lower photosynthetic fluxes compared to the mock-inoculated leaves, which could indicate that the effect of wounding in both treatments mainly disappeared after 72h and that photosynthesis was affected by the inoculation of *E. amylovora*. The quantum yield efficiency was not affected. In the *Ea*-inoculated immature leaves, both M_0, V_j and V_i increased. In the *Ea*-inoculated mature leaves V_i also increased, whereas sum k decreased, which is mainly caused by a significant reduction in the photochemical de-excitation constant k_P. These changes were clearly visible in the OJIP transient curve and the transient FvF, which depicts the same OJIP transient curve, with the big difference that the data have been normalised at 50µs (F_1) and F_M in order to visualise the variable fluorescence at point I and point J and the effects on F_0. In both the *Ea*-inoculated immature and mature leaves, a rise in fluorescence (figure 3.12 and 3.14) and a reduced electron transport (= higher FvF curve; figure 3.13 and 3.15) resulted in a lowered efficiency of photosynthesis and caused photosynthetic parameters to change.

Measurements with the FIS however could not reveal underlying imbalances in photosynthesis for the measured time points. Although the FIS has the major advantage of measuring the whole leaf, this poses also a disadvantage as the chance exists that small variations in the leaf remain undetected, which can be the case for our measurements as it is hypothesed that the largest fluorescence

is expected near the inoculation wound. For the following chapters, the results of the FIS measurements remained unsatisfactory as well, as results could not provide statistical significant differences between the different treatments. Therefore it was chosen not to mention these results in this thesis.

4.4.2 Respiration measurements

The rate of net CO_2 assimilation and H_20 fluxes, the stomatal resistance, the transpiration and other parameters were measured using a LCA-4 (table 3.9). The photosynthetic and transpiration rate seemed not be affected *in planta.* Only the substomatal CO_2 in *Ea*-inoculated mature leaves was higher compared to the mock-inoculated mature leaves, both 24 and 48h after inoculation.

Table 3.5: Explanation of the technical date of the OJIP curves and the selected JIP-test parameters

Technical fluorescence parameters	
$F_0=F_{30\mu s}$	Fluorescence intensity at 30µs
$F_1=F_{50\mu s}$	Fluorescence intensity at 50µs
$F_2=F_{100\mu s}$	Fluorescence intensity at 100µs
$F_3=F_{300\mu s}$	Fluorescence intensity at 300µs
$F_4=F_J= F_{2ms}$	Fluorescence intensity at 2ms, J-step
$F_5=F_I= F_{30ms}$	Fluorescence intensity at 30ms, I-step
$F_M=F_P$	Maximal fluorescence intensity
$M_0=(\Delta V/\Delta T)_0=4(F_{300\mu s}-F_0)/(F_M-F_0)$	Slope of the normalised curve at the origin of the fluorescence rise; measure of the rate of the primary photochemistry
$V_j=(F_J-F_0)/(F_M-F_0)$	Relative variable fluorescence at 2ms
$V_i=(F_I-F_0)/(F_M-F_0)$	Relative variable fluorescence at 30ms
Quantum Efficiency or flux ratios	
$\Phi_{P0}= TR_0/ABS=(1-(F_0/F_M)$	Quantum yield efficiency; expresses the probability that an absorbed photon will be trapped by the PS II reaction centre
$\Psi_0= ET_0/TR_0=(1-V_j)$	Expresses the probability that an exciton trapped by the PS II reaction center enters the electron transport chain
De-excitation constants	
Sum $k= k_n+k_p$	Sum k_n+k_p
$k_n=(ABS/CS)k_f(1/F_M)$	Non-photochemical de-excitation constant
$k_p=(ABS/CS)k_f[(1/F_0)Area/(F_M-F_0)/(1/F_M)]$	Photochemical de-excitation constant (k_f=fluorescence emission factor)
Specific fluxes or specific activities	
Per Q_a-reducing PS II reaction center	
$ABS/RC=M_0(1-V_j)(1/\Phi_{P0})$	Effective antenna size of an active reaction center RC; expresses the total numbers of photons absorbed by chlorophyll molecules of all RC divided by the total number of active RCs
$TR_0/RC=M_0(1-V_j)$	Maximal trapping rate of PS II; describes the maximal rate by which an exciton is trapped by the RC
$ET_0/RC=M_0(1-V_j)\Psi_0$	Electron transport in an active RC
$DI_0/RC= (ABS/RC)-(TR_0/RC)$	Effective dissipation in an active RC
Density of reaction centers	
RC/CS_m	Density of RCs per CS
Per excited cross section CS at $t=t_{Fm}$	
$TR_0/CS_m= \Phi_{P0}(ABS/CS)$	Energy flux per CS
$ET_0/CS_m= \Phi_{E0}(ABS/CS)$	Electron transport flux per CS
$DI_o/CS_m=(ABS/CS)-(TR_0/CS_m)$	Energy dissipation flux per CS
Performance index	
$PI_{abs}=(RC/ABS)(\Phi_{P0}/1-\Phi_{P0})(\Psi_0/1-\Psi_0)$	Performance index on absorption basis

Table 3.6: The measured and calculated fluorescence PEA parameters for mock-inoculated immature leaves, *Ea*-inoculated immature leaves, mock-inoculated mature leaves and *Ea*-inoculated mature leaves, 24h after inoculation. Values are mean ± SE of 6 biological independent replicates. Bold numbers indicate a significant difference (α=0.05) compared to the corresponding mock-inoculated leaves.

24h after inoculation	Mock-inoculated immat. leaves	*Ea*-inoculated immat. leaves	Mock-inoculated mat. leaves	*Ea*-inoculated mat. leaves
M_0	0.71 ± 0.03	0.67 ± 0.04	0.42 ± 0.02	0.42 ± 0.02
V_j	0.46 ± 0.01	0.47 ± 0.01	0.35 ± 0.01	0.38 ± 0.01
V_i	0.75 ± 0.01	**0.78 ± 0.01**	0.71 ± 0.01	0.73 ± 0.01
Φ_{P0}	0.79 ± 0.01	0.80 ± 0.01	0.82 ± 0.01	0.82 ± 0.01
Ψ_0	0.54 ± 0.01	0.53 ± 0.01	0.65 ± 0.01	0.62 ± 0.01
Sum k	1.72 ± 0.02	1.68 ± 0.02	1.73 ± 0.04	1.69 ± 0.02
k_n	0.35 ± 0.01	0.34 ± 0.01	0.31 ± 0.01	0.31 ± 0.01
k_p	1.37 ± 0.03	1.34 ± 0.02	1.42 ± 0.04	1.38 ± 0.01
ABS/RC	1.95 ± 0.04	1.76 ± 0.07	1.46 ± 0.04	1.37 ± 0.05
TR_0/RC	1.55 ± 0.03	**1.41 ± 0.05**	1.20 ± 0.03	1.12 ± 0.03
ET_0/RC	0.84 ± 0.01	**0.74 ± 0.01**	0.78 ± 0.02	**0.70 ± 0.01**
DI_0/RC	0.40 ± 0.01	0.35 ± 0.02	0.26 ± 0.01	0.25 ± 0.02
RC/CS_m	1458 ± 52	1703 ± 96	2251 ± 55	2437 ± 173
TR_0/CS_m	2247 ± 43	2376 ± 59	2705 ± 57	2700 ± 129
ET_0/CS_m	1219 ± 43	1256 ± 61	1759 ± 43	1690 ± 96
DI_o/CS_m	582 ± 10	595 ± 6	580 ± 14	593 ± 6
PI_{abs}	23.9 ± 1.9	26.1 ± 2.8	60.3 ± 4.1	57.0 ± 6.1

Table 3.7: The measured and calculated fluorescence PEA parameters for mock-inoculated immature leaves, *Ea*-inoculated immature leaves, mock-inoculated mature leaves and *Ea*-inoculated mature leaves, 48h after inoculation. Values are mean ± SE of 6 biological independent replicates. Bold numbers indicate a significant difference (α=0.05) compared to the corresponding mock-inoculated leaves.

48h after inoculation	Mock-inoculated immat. leaves	*Ea*-inoculated immat. leaves	Mock-inoculated mat. leaves	*Ea*-inoculated mat. leaves
M_0	0.70 ± 0.06	0.69 ± 0.05	0.41 ± 0.03	0.43 ± 0.05
V_j	0.46 ± 0.02	0.48 ± 0.01	0.37 ± 0.01	0.40 ± 0.03
V_i	0.77 ± 0.02	0.77 ± 0.01	0.72 ± 0.02	0.76 ± 0.02
Φ_{P0}	0.81 ± 0.01	0.80 ± 0.01	0.83 ± 0.01	0.82 ± 0.01
Ψ_0	0.54 ± 0.01	0.52 ± 0.01	0.63 ± 0.01	0.60 ± 0.03
Sum k	1.77 ± 0.02	1.80 ± 0.04	1.76 ± 0.06	1.74 ± 0.04
k_n	0.34 ± 0.01	0.37 ± 0.01	0.30 ± 0.01	0.31 ± 0.02
k_p	1.43 ± 0.02	1.43 ± 0.03	1.46 ± 0.05	1.43 ± 0.03
ABS/RC	1.88 ± 0.14	1.82 ± 0.09	1.33 ± 0.06	1.30 ± 0.05

TR_0/RC	1.52 ± 0.11	1.44 ± 0.06	1.10 ± 0.05	1.06 ± 0.03
ET_0/RC	0.82 ± 0.05	0.75 ± 0.01	0.69 ± 0.02	0.63 ± 0.03
DI_0/RC	0.36 ± 0.03	0.38 ± 0.03	0.23 ± 0.01	0.23 ± 0.02
RC/CS_m	1599 ± 130	1533 ± 118	2536 ± 86	2549 ± 201
TR_0/CS_m	2362 ± 38	2179 ± 91	2773 ± 61	2692 ± 187
ET_0/CS_m	1282 ± 51	1148 ± 76	1751 ± 37	1631 ± 167
DI_o/CS_m	565 ± 8	558 ± 12	571 ± 18	576 ± 13
PI_{abs}	27.9 ± 3.9	24.9 ± 3.4	64.7 ± 5.7	59.0 ± 9.4

Table 3.8: The measured and calculated fluorescence PEA parameters for mock-inoculated immature leaves, *Ea*-inoculated immature leaves, mock-inoculated mature leaves and *Ea*-inoculated mature leaves, 72h after inoculation. Values are mean ± SE of 6 biological independent replicates. Bold numbers indicate a significant difference (α=0.05) compared to the corresponding mock-inoculated leaves.

72h after inoculation	Mock-inoculated immat. leaves	*Ea*-inoculated immat. leaves	Mock-inoculated mat. leaves	*Ea*-inoculated mat. leaves
M_0	0.62 ± 0.02	**0.73 ± 0.03**	0.34 ± 0.02	0.41 ± 0.04
V_j	0.41 ± 0.01	**0.49 ± 0.01**	0.30 ± 0.01	0.36 ± 0.02
V_i	0.74 ± 0.01	**0.79 ± 0.01**	0.67 ± 0.02	**0.77 ± 0.02**
Φ_{P0}	0.80 ± 0.01	0.79 ± 0.01	0.83 ± 0.01	0.81 ± 0.01
Ψ_0	0.59 ± 0.01	**0.51 ± 0.01**	0.70 ± 0.01	**0.64 ± 0.02**
Sum k	1.69 ± 0.03	1.65 ± 0.03	1.77 ± 0.04	**1.61 ± 0.06**
k_n	0.34 ± 0.01	0.34 ± 0.01	0.31 ± 0.01	0.31 ± 0.01
k_p	1.35 ± 0.03	1.31 ± 0.03	1.46 ± 0.03	**1.30 ± 0.05**
ABS/RC	1.91 ± 0.06	1.85 ± 0.05	1.36 ± 0.04	1.40 ± 0.07
TR_0/RC	1.52 ± 0.04	1.47 ± 0.04	1.12 ± 0.03	1.13 ± 0.05
ET_0/RC	0.90 ± 0.03	**0.74 ± 0.01**	0.78 ± 0.02	0.72 ± 0.04
DI_0/RC	0.38 ± 0.02	0.39 ± 0.02	0.24 ± 0.01	0.27 ± 0.02
RC/CS_m	1551 ± 68	1594 ± 85	2402 ± 98	2371 ± 113
TR_0/CS_m	2347 ± 59	2323 ± 70	2674 ± 68	2647 ± 57
ET_0/CS_m	1392 ± 40	**1180 ± 62**	1863 ± 66	1691 ± 69
DI_o/CS_m	592 ± 12	608 ± 12	566 ± 14	**626 ± 2**
PI_{abs}	30.6 ± 1.4	**21.7 ± 2.1**	80.9 ± 5.1	**56.9 ± 6.9**

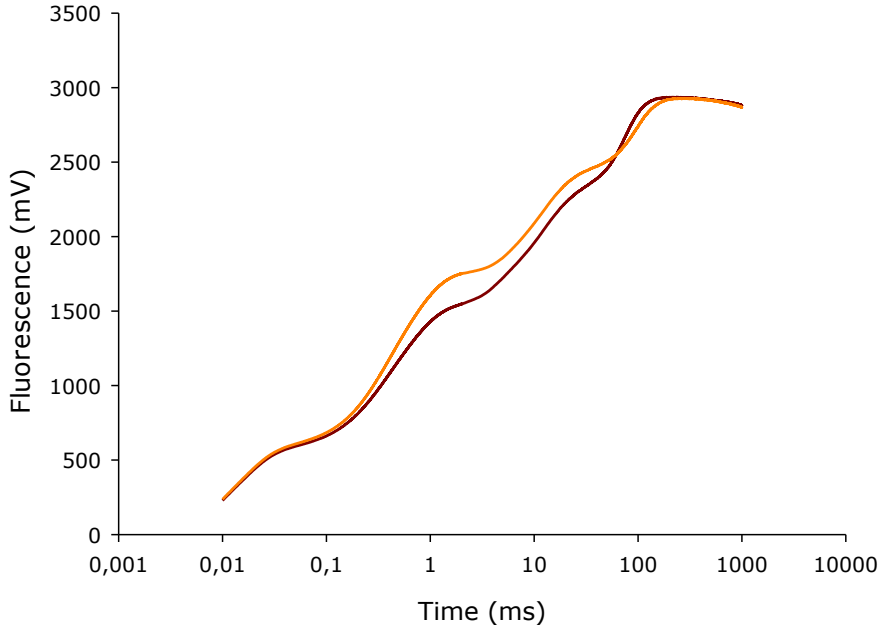

Figure 3.12: OJIP transient curves of mock-inoculated ( ) and *Ea*-inoculated ( ) immature leaves, 72h after inoculation.

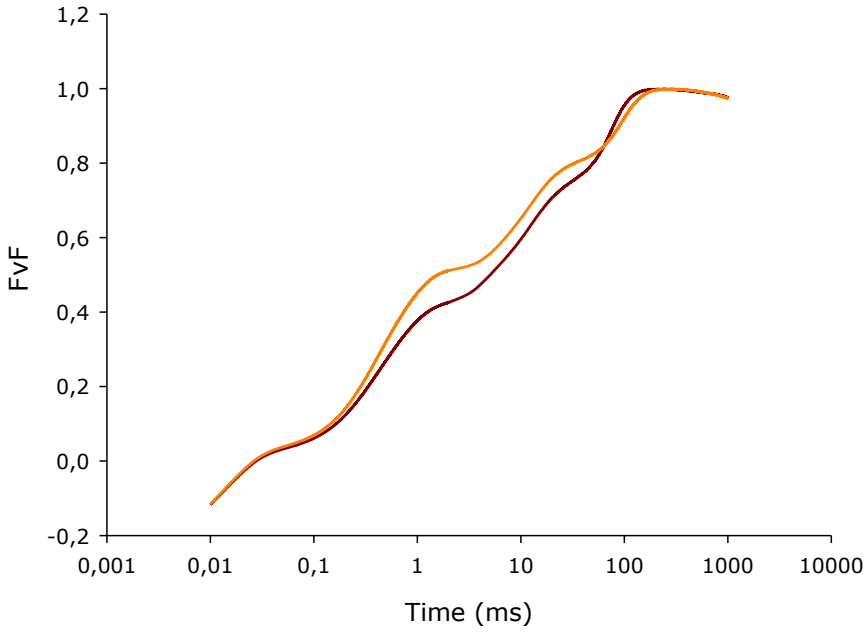

Figure 3.13: Normalised FvF curves of mock-inoculated ( ) and *Ea*-inoculated ( ) immature leaves , 72h after inoculation.

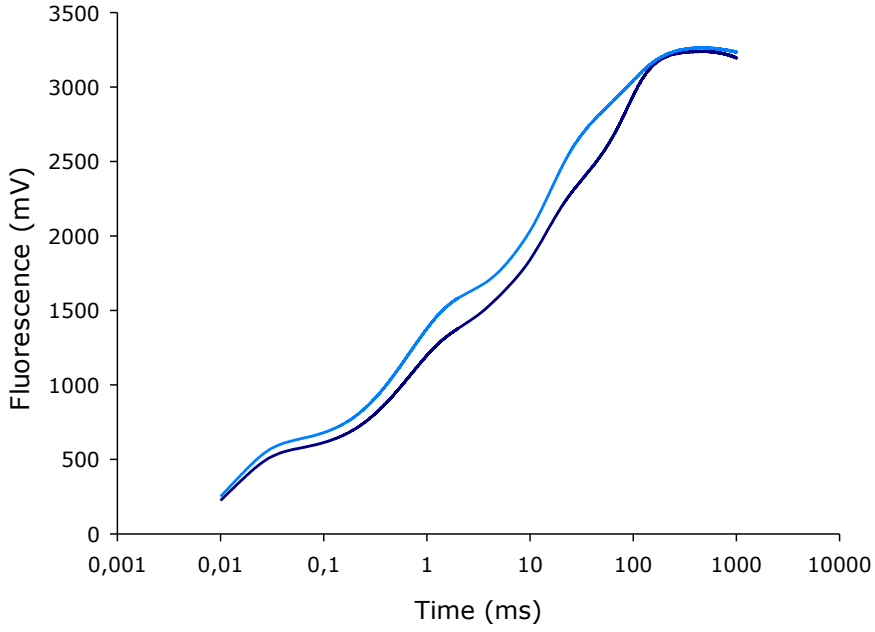

Figure 3.14: OJIP transient curves of mock-inoculated (■) and *Ea*-inoculated (■) mature leaves, 72h after inoculation.

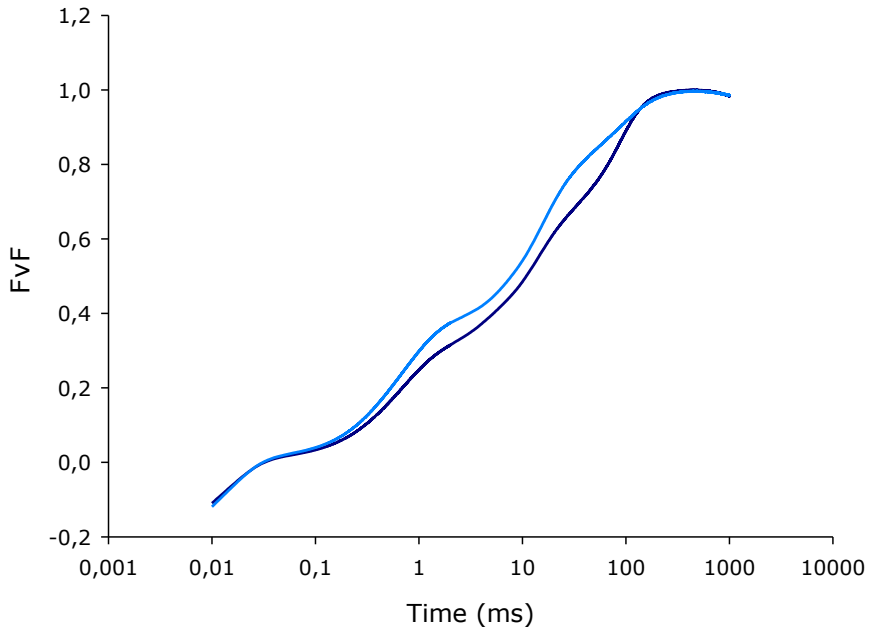

Figure 3.15: Normalised FvF curves of mock-inoculated (■) and *Ea*-inoculated (■) mature leaves, 72h after inoculation.

Table 3.9: The measured and calculated gas exchange parameters for mock-inoculated immature leaves, *Ea*-inoculated immature leaves, mock-inoculated mature leaves and *Ea*-inoculated mature leaves, x hours after inoculation. Values are mean ± SE of 3 biological independent replicates. Bold numbers indicate a (α=0.05) significant difference compared to the corresponding mock-inoculated leaves.

Gas Exchange Parameters							
After inoculation		Photosynthetic rate ($\mu mol\ CO_2\ m^{-2}\ s^{-1}$)	Transpiration rate ($mmol\ H_2O\ m^{-2}\ s^{-1}$)	Water Use ($\mu mol\ CO_2$ /$mmol\ H_2O\ m^{-2}\ s^{-1}$)	Substomatal CO2 ($\mu mol\ CO_2\ mol^{-1}$)	Stomatal Conduct. ($mol\ CO_2\ m^{-2}\ s^{-1}$)	Stomatal Resistance ($m^2\ s\ mol^{-1}\ CO_2$)
0h	Mock-inoc. immat. leaves	1.54 ± 0.25	1.18 ± 0.26	1.39 ± 0.31	331 ± 16	0.07 ± 0.02	17.4 ± 4.33
	Ea-inoc. immat. leaves	4.01 ± 1.93	0.64 ± 0.26	9.92 ± 6.01	200 ± 73	0.04 ± 0.01	28.4 ± 5.60
	Mock-inoc. mat. leaves	5.33 ± 2.29	1.32 ± 0.28	4.27 ± 1.70	264 ± 45	0.07 ± 0.01	15.3 ± 3.45
	Ea-inoc. mat. leaves	2.41 ± 1.61	1.69 ± 0.27	1.48 ± 0.98	333 ± 28	0.10 ± 0.02	10.7 ± 1.95
24h	Mock-inoc. immat. leaves	-0.11 ± 1.13	1.22 ± 0.64	-3.41 ± 3.26	539 ± 28	0.16 ± 0.03	7.14 ± 1.79
	Ea-inoc. immat. leaves	0.66 ± 0.19	2.14 ± 0.15	0.30 ± 0.07	510 ± 11	0.31 ± 0.07	3.68 ± 1.01
	Mock-inoc. mat. leaves	0.13 ± 0.44	1.79 ± 0.70	0.29 ± 0.31	479 ± 26	0.17 ± 0.04	6.24 ± 1.17
	Ea-inoc. mat. leaves	-1.30 ± 0.44	2.19 ± 0.99	-1.21 ± 0.77	**587 ± 21**	0.62 ± 0.37	7.61 ± 6.21
48h	Mock-inoc. immat. leaves	3.49 ± 2.70	2.80 ± 0.25	1.11 ± 0.80	454 ± 27	0.21 ± 0.04	4.89 ± 0.33
	Ea-inoc. immat. leaves	5.68 ± 0.88	2.27 ± 0.76	3.33 ± 1.27	401 ± 40	0.19 ± 0.08	7.21 ± 2.59
	Mock-inoc. mat. leaves	2.40 ± 1.28	3.14 ± 0.35	0.69 ± 0.37	443 ± 16	0.25 ± 0.01	4.33 ± 0.85
	Ea-inoc. mat. leaves	1.27 ± 0.94	1.97 ± 0.41	0.76 ± 0.47	**515 ± 16**	0.14 ± 0.02	7.52 ± 0.96
72h	Mock-inoc. immat. leaves	6.23 ± 0.93	1.70 ± 0.21	3.70 ± 0.53	370 ± 37	0.18 ± 0.02	5.75 ± 0.70
	Ea-inoc. immat. leaves	4.87 ± 1.20	0.97 ± 0.21	6.03 ± 2.29	383 ± 41	**0.10 ± 0.01**	10.8 ± 1.78
	Mock-inoc. mat. leaves	3.58 ± 0.70	1.46 ± 0.22	2.42 ± 0.17	411 ± 13	0.16 ± 0.04	7.21 ± 2.22
	Ea-inoc. mat. leaves	1.71 ± 0.25	0.35 ± 0.34	0.62 ± 2.22	464 ± 16	0.10 ± 0.05	22.0 ± 14.1

5. Discussion

This study showed that fundamental differences existed between immature and mature leaves concerning the behaviour of the plant against fire blight. *Ea*-inoculated immature leaves expressed disease symptoms much faster than the *Ea*-inoculated mature leaves as shown by our disease progression percentages and TH3 values.

A 3,3'-diaminobenzidine staining (Thordal-Christensen *et al.*, 1997) showed the presence of ROS near the wound where inoculation took place, both for mock-inoculated and *Ea*-inoculated leaves and independent of leaf age. However, in the *Ea*-inoculated leaves, ROS presence was not only limited to the inoculation zone, but was also present in the regions close to the wound, especially in the small veins and the intracellular regions near the artificial lesion.

This increase in ROS, previously already shown by Venisse et al. (2001), does not lead to univocal differences in the expression of some stress related genes. However, large significant differences in expression values existed between immature and mature leaves. In that way, *FSD1*, *FSD2*, *CAT1* and *CAT3* showed a significant higher transcription, whereas *APX4* and *CSD2* had a reduced transcription in the mature leaves compared to the immature leaves. It is clear that ageing not only influences the concentration of other metabolites such as dimeric and trimeric procyanidins in pear (Andreotti et al., 2006) but that it also has an effect on the transcription levels of some genes. For *CAT1* and *CAT3*, the effect of ageing can even be noticed during the experiment, as relative expression values of immature leaves increased independent of the treatment, reaching the highest values 72h after inoculation. The higher levels of transcripts for *FSD1*, *FSD2*, *CAT1* and *CAT3* genes in the mature leaves could partially explain the different infection rates that exist between immature and mature leaves as shown in table 3.2 and 3.3. As the infection caused by the necrogenic pathogen *E. amylovora* makes progress in the cell tissue, the production of two bacterial effectors HrpN and DspA is stimulated (Venisse *et al.*, 2003) and the amount of ROS will further increase. However, too high concentrations of ROS will induce cell death and will paradoxically improve further infection and will optimize the environment for *E. amylovora*, as shown

by Venisse *et al.* (2001). High natural amounts of antioxidative enzymes in the not necrotic tissue of mature leaves produced by *FSD1* and *FSD2* (mainly present in the plastids) and *CAT1* and *CAT3* (mainly present in peroxisomes and mitochondria) could maybe lower these toxic concentrations during the first hours after infection, resulting in a lower susceptibility to fire blight and a reduced expression of visible disease symptoms. The fact that only these four genes were higher up-regulated in mature leaves whereas *APX4* and *CSD2* – both present in the stroma and the chloroplasts- activities were down-regulated could be explained by a strict selection of the plant in energy investment due to the ageing of the plant and/or an inverse regulation of these genes by microRNA's. For instance, it is known that *CSD2* and *FSD1* both are antagonistically regulated in certain circumstances (Gielen *et al.*, 2012).

The similar age-related difference in the stress-related genes was demonstrated here for some genes of the phenylpropanoid-flavonoid pathway in the same leaf samples. The average level of some gene transcripts and metabolites points out clear developmental patterns in all leaves analysed, indicating a coordinated developmental regulation of the pathway to produce specific pools of end products at a certain leaf age. *FLS* for instance, was down-regulated in the mature leaves compared to the immature leaves for all time points. This difference was confirmed by HPLC as flavonols accumulated at higher levels in the immature leaves compared to the mature leaves. Simple phenolics exhibited the same difference between the developmental stages, just like chlorogenic acid and cis-ferulic acid. This developmental pattern with subsequent shifts in concentration of phenols, flavonoids and other secondary metabolites is consistent with results found in strawberry (Carbone *et al.*, 2009; Guidarelli *et al.*, 2011) and pear (Andreotti *et al.*, 2006). Carbone *et al.* (2009) even demonstrate that developmental cues regarding the flavonoid metabolism are predominant over genotype and environmental factors.
Moreover, our results not only emphasize these developmental differences, but also show that some compounds of the phenylpropanoid-flavonoid pathway are stimulated *in planta* after inoculation with *E. amylovora* and support the idea that these compounds could play a role in protecting the pear cultivar Conférence against fire blight.

Our microscopic analysis of both safranin-astra blue and NA-stained leaf sections taken close to the artificial lesion, showed the deposition of phenolic compounds in close proximity to the inoculation site and near the small veins neighbouring this wound. It has to be taken aware that this effect is not exclusively the result of wounding the leaf tissue with scissors, but also by the occurrence of *E. amylovora* in the tissue, as these inoculated samples often showed a more dense and pronounced staining.

The results of these microscopic analysis are confirmed both by our RT-qPCR and by HPLC analyses. For RT-qPCR, the relative expression values of *PAL*, *CHS*, *FHT*, *DFR*, *LAR1*, *ANS* and *ANR* were all significantly up-regulated in the *Ea*-inoculated mature leaves for almost all measured time points, a result which is consistent with work performed in poplar inoculated with *Melampsora medusae* (Miranda *et al.*, 2007), but the most striking effect was noticed 48h after inoculation. At this time point, a 7-fold difference for *CHS* and *ANR* was measured between the *Ea*-inoculated and untreated mature leaves.

The rise in *CHS* is in agreement with the work of Baldo *et al.* (2010), who used a cDNA-AFLP analysis combined with quantitative reverse transcription PCR to demonstrate a sudden rise of *CHS* in the fire blight susceptible apple rootstock M.26 after infection with *E. amylovora*. It is known that CHS functions as an important core enzyme and gatekeeper responsible for the production of further defence related secondary metabolites during infection of different pathogens (Dao *et al.*, 2011).

ANR instead is a central enzyme for the production of epicatechin out of cyanidin. Merely one day after the rapid amplification of *ANR*, epicatechin occurred in larger quantities in the Ea-inoculated mature leaf tissue compared to the other treatments. HPLC results coincided well with the quantitative reverse transcription PCR data of *ANR*. The transcription of the gene that codes for ANR started quite early in comparison with the production of epicatechin, which clearly results from a *de novo* synthesis as the induction of the *ANR*-gene is needed first in order to produce the ANR-enzyme and the metabolite in later stages. When comparing Ea-inoculated mature leaves and mock-inoculated mature leaves, it has to be taken into account that the concentration of epicatechin was only slightly higher in Ea-inoculated mature leaves. Nevertheless, these results could indicate that epicatechin has a probable

function in both wound healing and protection against fire blight in the mature leaves. It is known that flavonoids, including flavan-3-ols such as epicatechin, are able to act as important direct antioxidants or as modulators of cell signalling, by inhibiting pro-oxidant enzymes, such as NADPH oxidases and lipoxygenases, by altering phosphorylation state of target molecules or by chelating transition metals that mask pro-oxidant actions of reactive nitrogen and oxygen species, both in plants (Skadhauge *et al.*, 1997; Treutter, 2005) and in human and mammalian tissue (Fraga and Oteiza, 2011; Williams *et al.*, 2004). Flavan-3-ols have also been shown to contain better antioxidative and radical-scavenging activities than those of vitamins, ascorbic acid, α-tocopherol and other phenolics (Feucht *et al.*, 1996). As mentioned before, the production of two bacterial effectors HrpN and DspA is stimulated when the necrogenic pathogen *E. amylovora* moves further into the cell tissue (Venisse *et al.*, 2003), triggering a significant amplification of ROS (Venisse *et al.*, 2001). High induced levels of epicatechin could have the same function as some antioxidative related enzymes and could lower these elevated levels of ROS during infection and this could confirm the results of Venisse *et al.* (2002).

Second, epicatechin and flavonoids in general could also be involved in structural defence, as research in other plant-pathogenic interactions reveals ultrastructural modifications of infected cells and shows that flavonoids accumulate and are incorporated into cell walls, middle lamellae or callose-rich papillae in order to obstruct further progress of the pathogen (Dai *et al.*, 1996; Loureiro *et al.*, 2012; Soylu, 2006).

Besides a role in antioxidative capability and structural defence, epicatechin could also fulfil a function in chemical defence for this specific plant-pathogen interaction. Many flavonoids show an antibacterial, antitoxin, antiviral and/or antifungal activity (Friedman, 2007; Treutter, 2005; Yamaji and Ichihara, 2012) and it has been shown that apple epicatechin has the ability to attenuate the *in vitro* growth of the fungus *Venturia inaequalis* (Golba *et al.*, 2011). Unpublished results by our lab confirm the fact that epicatechin could also affect the bacterial growth of *E. amylovora* in vitro. The fact that the bacterium even possesses an efflux pump AcrAB, which has the ability to protect the bacteria against harmful phytoalexins and some secondary metabolites in apple, supports the idea that

the phenylpropanoid-flavonoid pathway is crucial in this plant-pathogen interaction in mature leaves (Burse *et al.*, 2004).
Flavonols, produced via *FLS*, do not seem to be involved neither in protection against fire blight nor in wound healing, as no differences were found independent of the leaf ontogenesis. These results are consistent with the work of Pontais *et al.* (2008) in apple. *F7GT* also remained more or less constant between the treatments, which assumes that flavonones in both mature and immature leaves are not involved as well.
In immature leaves, the control of the synthesis of epicatechin and its function are clearly different compared to the mature leaves. There was hardly any up-regulation of the *ANR*-gene as shown by quantitative reverse transcription PCR and there was no significant increase in the concentration of epicatechin as shown by HPLC. Moreover, bearing in mind that chlorogenic acid, cis-ferulic acid, flavonols and simple phenolics are present in much greater concentrations in the immature tissues compared to the mature leaves and although Pontais *et al.* (2008) perceive a minor rise of HCAs in the susceptible apple rootstock MM106 after vacuum infiltration with *E. amylovora*, it seems unlikely that these metabolites fulfil a function as preformed defence molecules in this specific interaction between *E. amylovora* and *Pyrus*. A rather quick induction of the phenylpropanoid-flavonoid pathway leading to an increased production of epicatechin (and maybe other metabolites) and the generation of a time-dose dependent relationship seems to be more crucial in this part of the defence mechanism and in a possible survival method of the plant, a phenomenon that seems to be lacking in immature leaves.

Although respiration measurements provided no unambiguous results, it is clear that photosynthesis is affected in both mature and immature leaves by the presence of the bacteria and the increased production of ROS, as PEA parameters indicated a lowered photosynthetic efficiency and an increased chlorophyll fluorescence before the appearance of necrotic symptoms. Photosynthesis-based differences in susceptibility to *E. amylovora* could not be detected between mature and immature leaves.

In conclusion, ontogenesis seems to influence fire blight manifestation. It could be that the natural presence of certain stress-related genes and the quick induction of the phenylpropanoid-flavonoid pathway and especially epicatechin results in a lower susceptibility of mature leaves against *E. amylovora* in comparison with immature leaves. These secondary metabolites could then act as an antioxidant, as a defence barrier strategy or as toxic compound against the bacteria. However, the phenylpropanoid-flavonoid pathway is a complex system and surely more processes, enzymes and metabolites are involved in this system. Furthermore, the induction of some components of the phenylpropanoid-flavonoid pathway and the natural presence of certain stress-related genes is possibly not the only defence mechanism involved, as a plant has a wide range of defence mechanisms available (Nicaise *et al.*, 2009), varying from the activity of certain phytohormones to other metabolites (Robert-Seilaniantz *et al.*, 2007). Huvenne *et al.* (2009) even demonstrated that the flow of sugars *in planta* is important in a *Brenneria*-willow pathosystem, which indicates that plant pathology is more complicated than it seems and that defence mechanisms are not the only factor involved.

Chapter 4:

Comparison

Conférence and Doyenné

1. Introduction

Plant defence mechanisms as a response to the fire blight pathogen *E. amylovora* not only differ between apple and pear, but also between cultivars. In our experiments, we used two distinct pear cultivars which are both cultivated in Belgium.
The first cultivar is the most common cultivated pear cultivar in Belgium, namely Conférence. Conférence produces slender fruit with a distinctive long conical shape and a green to bronze colour which will turn yellow when ripened. Regarding shoot infections, Conférence has a moderate susceptibility to fire blight according to a susceptibility list published by the Walloon Agricultural Research Centre of Gembloux, Belgium (cra.wallonie.be). The second one is Doyenné Du Comice, a pear cultivar that produces large fruit with a short stalk and a yellow-green colour with a brown-red bloom. Doyenné du Comice is extremely susceptible to fire blight.

In this chapter, transcriptional changes, HPLC and PEA measurements are analysed in an attempt to characterise essential differences between the behaviour of Conférence and Doyenné after shoot inoculation with *E. amylovora*. However, transcriptional changes and analysis of secondary metabolites are only a small part of a plant's responses to a pathogen, as most biological functions in a cell are executed by a wide amount of proteins rather than by mRNA. It is known that specific proteins are transiently phosphorylated minutes after elicitation of PAMPs *in planta* (Peck, 2003; Stulemeijer and Joosten, 2008). Transcript profiling however does not provide vital information about protein activation and turnover in a specific plant-pathogen interaction. A good way to overcome this, is using proteomics.
Proteomics, or the comprehensive analysis of the presence, localisation, modification or interactions of proteins expressed by a genome, provides experimental continuity between genome sequence information and the protein profile in a specific tissue, cell or cellular compartment during standard growth or different treatment conditions. Moreover, by using proteomic approaches, differences in the abundance of proteins actually present at the time of sampling can be distinguished and different forms of the same protein can be resolved

(Barbier-Brygoo and Joyard, 2004; Kaufmann *et al.*, 2011; Quirino *et al.*, 2010; Van Wijk, 2001). Two main complementary proteomic approaches have been developed, namely a gel-based approach and a gel-free approach. Gel-free approaches use a bottom-up strategy which digest proteins with a proteolytic enzyme and the obtained complex peptide mixture is separated in a next phase, whereas the gel-based approach relies on the powerful technique of two-dimensional electrophoresis that sorts proteins according to two independent characteristics in two discrete steps. The first dimension step is the isoelectric focusing (IEF), at which proteins are separated according to their isoelectric point (pI) on immobilised pH gradient strips. The second dimension step is sodium dodecyl sulphate – polyacrylamide gel electrophoresis (SDS-PAGE), at which proteins are separated according to their molecular weight. Proteins on gels are then visualised by Coomassie staining, by silver staining or by using fluorescent dyes. Thousands of different proteins can be separated this way, providing extra information of their pI and the molecular weight. Gel spots that are differentially expressed based on statistical analysis, are excised and in-gel digested. In this process, the protein -still in the gel matrix- is digested with an enzyme that cleaves at specific points. Trypsin, for instance, cleaves the peptide chain at the carboxyl side of lysine and arginine, except when these are followed by proline (Carpentier *et al.*, 2008b; Quirino *et al.*, 2010; Van Wijk, 2001).

The study of proteomes from organisms has been performed extensively by exploring this high resolution of two-dimensional electrophoresis coupled with mass-spectrometry (MS). The methodology of mass-spectrometry employs chemical fragmentation of the trypsin-cleaved protein into charged particles and measurements of charge and mass of these resulting particles. Ionisation of these molecules is generally obtained by using electrospray (ESI) or matrix-assisted laser desorption/ionization (MALDI) techniques. Ionised molecules, which gain or lose their charge by protonation, deprotonation or electron ejection, are electrostatically propelled inside the instrument and detected according to their mass to charge ratio. Usually, MALDI and ESI techniques are combined with tandem mass spectrometry MS/MS. In MS/MS, a particular ion is selected with a mass filter/analyser and then the selected ion is further fragmented and analysed. Fragmentation can be induced by introducing the ion into a chamber with a collision gas such as argon or nitrogen. Next, these data

obtained by mass spectrometry are processed through a series of sequence-identifying algorithms, which are then compared to protein sequence databases in order to identify the proteins or peptides present in the sample (Barbier-Brygoo and Joyard, 2004; Carpentier *et al.*, 2008b; Kaufmann *et al.*, 2011; Quirino *et al.*, 2010; Van Wijk, 2001).

Over the years, proteomics have drastically evolved in the pursuit of a large-scale functional assignment of candidate proteins and, by using this approach, several defence, photosynthesis and antioxidant related proteins that were differentially expressed during different phytopathogenic interactions in many crops including tomato and rice have been identified, providing a full picture and in-depth understanding of these mechanisms (Afroz *et al.*, 2011; Kaufmann *et al.*, 2011; Mehta *et al.*, 2008; Quirino *et al.*, 2010; Rampitsch and Bykova, 2012; Zimaro *et al.*, 2011). Nevertheless, some proteins, including regulatory proteins and rare membrane proteins, remain out of the scope of most proteomic techniques because of their low abundancy. Wilkins *et al.* (1998) estimated that 2D cannot visualise or produce analytical quantities of proteins present at less than 1000 copies per cell.

The use of model systems such as *Arabidopsis* has significant benefits compared to non-model plants such as pear. One of the most important advantages is the short growth cycle and the availability of the complete genome which increases the likelihood of obtaining a correct return during the homology based matching of databases. Thus, from a technical point of view, *Arabidopsis* is one of the most optimal organisms to work with when conducting a proteomics study. However, *Arabidopsis* is far from an agricultural crop species or tree, limiting the knowledge transfer of *Arabidopsis* to other crops. Non-model plants therefore have to rely on the availability of expressed sequence tags (EST) databases and homology-based searching (Carpentier *et al.*, 2008a; Carpentier *et al.*, 2008b; Van Wijk, 2001).

Unfortunately, the genome of *Pyrus communis* is still not sequenced (although it was expected to be published in 2009-2010) and EST databases of *Pyrus* are not well spread, making proteomic research of pear very hard.

2. Objective

Because Conférence and Doyenné du Comice differ in their susceptibility to fire blight, we wanted to determine if the phenylpropanoid-flavonoid pathway could be the reason for these cultivar dependent differences regarding their response to the fire blight pathogen *Erwinia amylovora*.

Therefore, shoots of two-year-old pear trees (*Pyrus communis* cv. Conférence and Doyenné du Comice) were inoculated with *E. amylovora* strain SGB 225/12 or were mock inoculated. From a more practical point of view, i.e to increase the amount of trees in our experimental design and to have a better clue about the effect of inoculating, we excluded the untreated leaves in the experimental design of this chapter. Leaf samples were taken at specific time points after inoculation and the expression patterns of phenylpropanoid-flavonoid pathway related genes of not necrotic tissue close to the infection site were analysed with RT-qPCR. Soluble phenolics were studied by HPLC methodology.

Furthermore, we also investigated the transcription profiles of the first leaf above and the first leaf below the *Ea*-inoculated or mock-inoculated immature leaf (= leaf 4). In that way, we are able to generate a more complete overall picture of the phenylpropanoid-flavonoid pathway in the adjacent leaves and are able to check whether or not these leaves follow the same profile pattern as the inoculated leaf.

In addition, chlorophyll fluorescence measurements were executed using PEA equipment to visualise the effect of the bacteria on the global photosynthesis in the plant and to detect possible differences in susceptibility between the two cultivars based on photosynthesis.

Last but not least, a proteomic approach was performed in order to receive vital information about the involvement of other proteins that are related to defence mechanisms in both cultivars Conférence and Doyenné after inoculation with *E. amylovora*. The time point "72hours after inoculation" was favoured to do proteomics on, as HPLC, microscopy and RT-qPCR in the previous chapter indicated the largest effects around this specific time point.

In this chapter, we merely focussed on the immature leaves for different reasons. First to be sure a successful infection is guaranteed. Secondly, because of the relatively low amount of significant real-time qPCR data for the immature

leaves in the previous chapter, it seemed more opportunistic to increase the number of replicates and the number of sampling time points in order to be sure that the phenylpropanoid-flavonoid pathway is not that pronounced as a possible defence mechanism in immature leaves. Thirdly, using immature leaves has a higher rate of success compared to the mature leaves when extracting the proteins for 2DE-electrophoresis.

3. Material and Methods

3.1 Experimental design

Two-year-old trees (*Pyrus communis*) of the moderately susceptible cultivar Conférence and the highly susceptible cultivar Doyenné du Comice, both on Quince C rootstock were grown in containers of 20l in a quarantine protected greenhouse (pcfruit, Kerkom, Belgium) in a controlled environment to maintain a temperature of 22°C, a relative humidity of 60% and a minimal light intensity of 150 µmol $m^{-2}s^{-1}$. Trees were grown until they contained enough active growing shoots with an average length of 25cm and a minimum of eight leaves on each shoot. Next, each tree with corresponding shoots was subjected to only one of the following treatments: (a) Mock-inoculated Conférence leaves, (b) *Ea*-inoculated Conférence leaves, (c) Mock-inoculated Doyenné leaves and (d) *Ea*-inoculated Doyenné leaves (figure 4.1).

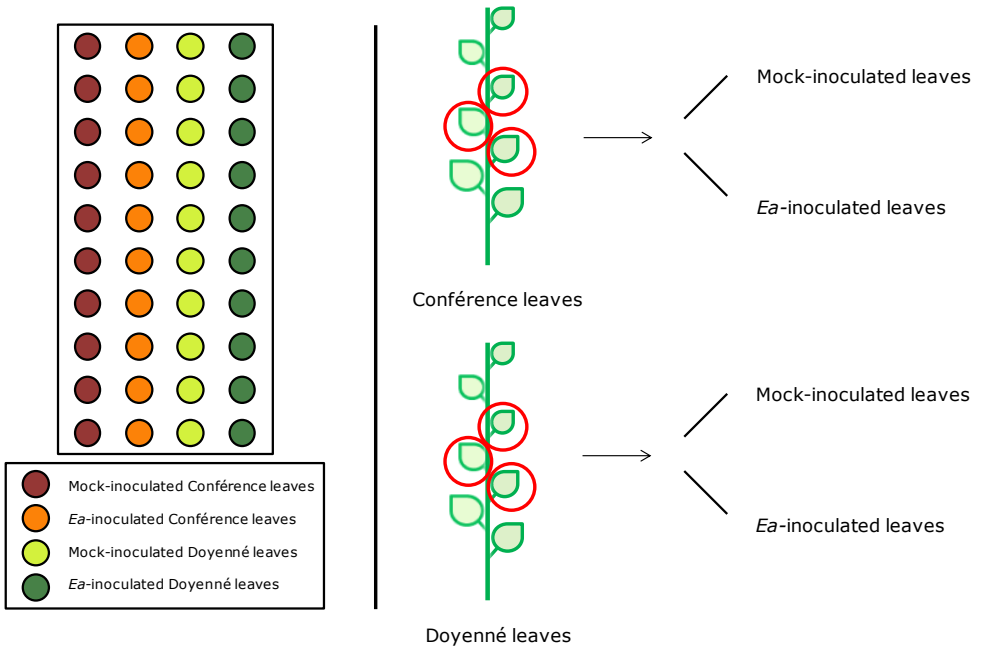

Figure 4.1: Experimental design with the different treatments (left) and the sampling of the 3rd , 4th and 5th leaf in Conférence and Doyenné (right)

A highly aggressive *E. amylovora* strain (BG16, isolated from *Malus sylvestris* (Bulgaria) with collection number SGB 225/12) was cultivated at a temperature of 25°C on YPGA growth medium. After 24 hours, a suspension liquid of these

bacteria was prepared in PBS at a density of 10^8 CFU ml^{-1} and used for inoculations.

For inoculation, only the fourth immature leaf starting from the apex was cut perpendicular to the main vein with scissors dipped in the bacterial suspension liquid. For mock-inoculated leaves, scissors were dipped in PBS. Ten biological repetitions were applied, as ten leaves (trees) were used per variant and sampling date.

Mock- and *Ea*-inoculated leaf samples (4^{th} leaf), but also samples of the leaf above (3^{rd} leaf) and below (5^{th} leaf) the mock- and *Ea*-inoculated leaf were taken 3h, 24h, 48h, 72h, 4days and 6days after inoculation (figure 4.1). Total leaf samples were stored at -80°C for further analysis with RT-qPCR, HPLC and proteomics. The progression of the shoot infection was measured 7, 9 and 13 days after inoculation according to the formulae of chapter 3.

3.2 RT- qPCR

RT-qPCR techniques were performed in the same manner as mentioned in chapter 3. The primers were the same as in table 3.1. Both the mock- and *Ea*-inoculated leaf, but also the first leaf above and the first leaf below these leaves were analysed. Reference genes coding for an elongation factor *ef4-a* (Malus_v4_Contig5101 derived from source file AY347787.1) and glyceraldehyde-3-phosphate dehydrogenase *gapc2* (JQ302967.1 derived from source file CN906865.1; left primer: CAAGCATCTTTGACGCCAAG; right primer: CACGATCAAGTCAACCACACG) were used to normalise the data. Ten biological independent replicates were used per treatment.

3.3 HPLC

HPLC techniques for mock-inoculated and *Ea*-inoculated leaves were performed in the same manner as mentioned in chapter 3. Four biological independent replicates were used per treatment. To eliminate seasonal effects, proanthocyanidins were normalised against a constant which was calculated by comparing the total concentration of unknown proanthocyanidins of this chapter and the previous chapter. Hydroxycinnamic acids were normalised against the total concentration of unknown hydroxycinnamic acids.

3.4 Proteomics

3.4.1 Total extraction procedure

The extraction procedure was executed according to the protocol of Carpentier *et al.* (2005). Fresh plant material taken 72hours after inoculation was grinded in a mortar, together with some liquid nitrogen and resuspended in ice-cold extractionbuffer (5ml/g sample; 50mM Tris-HCl pH 8.5, 5mM EDTA, 100mM KCl, 1% w/v DTT, 30% w/v sucrose, 0.4% PMSF and 5% PVPP) and vortexed for 30s. One ml of each sample was transferred to a 2ml eppendorf tube. Next, one ml of ice-cold Tris saturated phenol (pH 8.0) was added to the sample and vortexed during 15min at 4°C. After centrifugation (3min at 6000g), the phenolic phase (= upper layer) was collected with a glass pipette, re-extracted with an equal amount of extraction buffer and vortexed for 30s. After centrifugation (3min at 6000g; 4°C), the phenol phase was collected and precipitated overnight with five volumes of 100mM ammonium acetate in methanol at -20°C. After centrifugation at 16000g for 30min at 4°C, the supernatant was removed and the pellet was rinsed twice in ice-cold acetone/0.2% DTT. Between the two rinsing steps, the sample was incubated for 60min at -20°C. The pellet was air-dried, resuspended in about 100µl lysis buffer (7M urea, 2M thiourea and 4% CHAPS) and vortexed for 1h at room temperature. Afterwards, the resuspended samples were centrifugated at high speed (30min, 70000g) to remove nucleic acids.

3.4.2 Protein clean-up and quantification

To overcome poor 2-D results caused by a high conductivity, by high levels of interfering substances or by low protein concentrations, the protein sample was precipitated using the 2-D Clean-Up Kit (GE Healtcare) according to the manufacturer's instructions. The protein concentration was determined using the 2-D Quant kit from Amersham Biosciences.

3.4.3 Iso-electric focusing

The protein sample was diluted with lysis buffer with 0.005% bromophenol blue, 60mM DTT and 2% IPG-Ampholyte Mix (SERVA) to 60µg sample per 140 µl in the presence of IPG-buffer and was applied to an IPGphor unit (Amersham Biosciences) via anodic cuploading. The strips of 24cm and pH 3-10 (IPG

BlueStrips, SERVA) were rehydrated in IPG-enriched (5µl/ml) Destreak (GE Healtcare) for at least 8h and then put into the IPGphor. Protein samples were separated on the IPGphor using the following settings: 1h 250V (step), 7h 1000V (gradient), 3h 8000V (step), 3h45 8000V (gradient) for a total of 49.2 kVh (50µA/strip, 20°C).

3.4.4 2-D gel electrophoresis

After separation in the first dimension, strips were equilibrated 2x 15minutes in equilibration buffer using the SERVA buffer kit according to the manufacturer's protocol. For 2-D gel electrophoresis, the HPE-FlatTop Tower (SERVA) was used according to the manufacturer's instructions (figure 4.2). The unit consists of four horizontal electrophoresis chambers which are built as drawers into a metal housing. The instrument is run with an external power supply and thermostatic circulator (cooling unit). The plastic-backed gels (2DGel flatbed NF 10-15% gradient gels) are run directly on an aluminium oxide ceramic cooling plate. The following running conditions were used: 30min at 100V with 7mA/gel and 1W/gel (step1), 30min at 200V with 13mA/gel and 3W/gel (step2); 10min at 300V with 20mA/gel and 5W/gel (step3), 4h50min at 1500V with 40mA/gel and 30W/gel (step4) and last 50min at 1500V with 45mA/gel and 40W/gel (step5).

Figure 4.2: The HPE-FlatTop Tower (SERVA).

3.4.5 Silver staining

Gels were silver stained using the Protein Silver Staining kit (SERVA) according to manufacturer's protocol.

3.4.6 Spotpicking and protein digestion

Spots were analysed with the Imagemaster Platinum Program. Four gels were analysed per treatment. For spot picking (Ettan SpotPicker, GE Healthcare) reference stickers were applied on the glass plate containing spacers before pouring the gel, thereby ensuring the accuracy of robotic protein excision. In-gel digestion using trypsin (Promega) was performed manually as described by Shevchenko *et al.* (1996).

3.4.7 Mass spectrometric analysis and protein identification

The mass spectrometer was calibrated and tuned as described in the LCQ 'Operator's Manual' Revision B July 1996. Instrumental ion optics were further optimized for analysis of doubly charged peptide ions by direct infusion (1 ml/minute) of synthetic peptide 'IFGKGTTLSVSSNIQ' at 10 pmol/ml in 0.1M acetic acid ($[M+2H]^{2+}$ = 776.42). Tryptic digests were dried in vacuo, solubilised in 20ml 0.1M acetic acid in water containing cortisol (4pg/ml) as an internal standard and analyzed in data-dependent mode by nanoflow HPLC/ESI(+)-MS/MS (Dumont *et al.*, 2004). Stability of the chromatographic process and ESI efficiency were monitored using cortisol base peak m/z 361.2. Bovine serum albumin (10fmole BSA on-column) was used for analytical system control.

LCQ Xcalibur v2.0 SR2 raw files and spectra were selected from within Proteome Discoverer 1.0.0.43 (Thermo Electron) with following settings: minimal peak count, 50; total intensity threshold, 4000; and S/N, 6. Peak lists were searched with Sequest v1.0.43 and Mascot v2.2.0.2 against the Viridiplantae database (NCBI) or a self-constructed green plants database based on Phytozome databases (www.phytozome.org) with respectively 793311 and 9125 entries) with following settings: fragment tolerance, 1.00Da (monoisotopic); parent tolerance, 3.0Da (monoisotopic); fixed modifications, carbamidomethylation of cystein; variable modifications, oxidation of methionin; max missed cleavages, 1. Outcome of both search engines was validated with Scaffold v.3.00.03 (Proteome Software) with minimum peptide and protein probability set to 95% and 99.9% respectively. The protein identifications thus returned by Scaffold for each gel spot were manually validated considering spectral quality.

3.5 Chlorophyll fluorescence

Chlorophyll fluorescence measurements with the PEA were performed in the same manner as mentioned in chapter 3. The photosynthetic efficiency was analysed on mock-inoculated and *Ea*-inoculated leaves of Conférence and Doyenné du Comice. Furthermore, the first leaf positioned beneath the infected leaf was measured as well. Due to the small size of the Doyenné leaves, it was not possible to measure the first leaf above the mock- or *Ea*-inoculated leaf. Per treatment, five trees were measured with the PEA as described in chapter 3. Trees were measured before inoculation and 24h, 48h, 72h, 6 days and 8 days after inoculation.

3.6 Statistics

For RT-qPCR data and HPLC, the different treatment means were respectively subjected to a 1-way ANOVA and a 2-way ANOVA with Tukey's pairwise comparisons. All data were tested for their equality of variances using a Levene's test and for their normal distribution using a Shapiro-Wilk test.

PEA data were subjected to a pairwise comparison for their different parameters.

Proteomic data were statistically analysed through to the ImageMaster Platinum Software.

Outliers were excluded based on a maximum normed residual test for all data. All statistical analyses were performed using the SAS 9.2 software.

4. Results

4.1 Symptom development

The development of infection in mock-inoculated and *Ea*-inoculated Conférence and Doyenné du Comice trees was measured 7, 9 and 13 days after inoculation. The mock-inoculated leaves of both cultivars showed no visual signs of infection. *Ea*-inoculated leaves however did show disease symptoms after seven days in both Conférence and Doyenné. Thirtheen days after inoculation, disease was a little bit more pronounced in the *Ea*-inoculated Doyenné leaves compared to the *Ea*-inoculated Conférence leaves (table 4.1). Shoot infections were less severe than in the previous experiment (chapter 3). It was interesting to notice that in Doyenné shoots, infection symptoms still were not visible after nine days, but suddenly appeared after thirteen days, whereas in Conférence, symptoms developed slowly but steadily in the tissue. Furthermore, these shoot infections in Doyenné were then more severe than in the shoots of Conférence (table 4.2).

Table 4.1: Shoot infection values expressed as TH3 values, measured 7, 9 and 13 days after inoculation, p<0.001 (Tukey)

TH3 value	7DAI	9DAI	13DAI
Mock inoculation Conférence leaf	0.00 a[1]	0.00 a	0.00 a
Mock inoculation Doyenné leaf	0.00 a	0.00 a	0.00 a
Ea-inoculation of a Conférence leaf	33.33 b	35.67 b	40.35 b
Ea-inoculation of a Doyenné leaf	33.33 b	33.33 b	45.09 b

[1]Means in a column followed by the same letter do not differ significantly

Table 4.2: Percentage of the necrosis in the shoot, measured 9 and 13 days after inoculation, p<0.001 (Tukey)

% of necrosis in the shoot	9DAI		13DAI	
Mock inoculation Conférence leaf	0.00	a[1]	0.00	a
Mock inoculation Doyenné leaf	0.00	a	0.00	a
Ea-inoculation of a Conférence leaf	1.40	a	6.11	ab
Ea-inoculation of a Doyenné leaf	0.00	a	17.60	b

[1]Means in a column followed by the same letter do not differ significantly

4.2 Conférence and Doyenné appear to have different transcription profiles regarding the phenylpropanoid-flavonoid pathway

To visualise the large amount of data, a heat map was chosen as representation manner for the mock- and *Ea*-inoculated leaf (4th leaf; table 4.4), but also for the leaf above (3rd leaf; table 4.3) and below (5th leaf; table 4.5) these leaves. Due to fluctuations, a very low amount of coherent data was noticed in these tables, forming a serious contrast with the data represented in chapter three (table 3.4) and raising the suspicion that the phenylpropanoid-flavonoid pathway probably has a minor function during a fire blight infection in immature leaves. Despite this lack in coherence, both Conférence and Doyenné appeared to have a different profile for the analysed genes in leaf 4 (table 4.4).

In Conférence, *PAL*, *FHT*, *DFR*, *ANS* and *ANR* displayed a fluctuating pattern, reaching significant differences between the treatments at different time points. For instance, *PAL*, *FHT*, *DFR*, *ANS* and *ANR* were significantly down-regulated in *Ea*-inoculated tissue 48h after inoculation, whereas 72h after inoculation, *FHT* was still significantly down-regulated but both *ANS* and *ANR* were significantly up-regulated in *Ea*-inoculated leaves. *CHS* has high values throughout the experiment for both treatments. *FLS*, *F7GT* and *LAR1* were all down-regulated in *Ea*-inoculated leaves, reaching very low relative expression values 4days and 6days after inoculation for both *FLS* and *F7GT*.

In Doyenné, all genes were generally down-regulated in leaf 4 starting from 24h after inoculation, ending in very low relative expression values 4 and 6 days after inoculation and in most cases with a clear distinction between mock-inoculated and *Ea*-inoculated samples.

For all time points except 6 days after inoculation, the expression pattern of the analysed genes in leaf 3 and especially leaf 5 followed the pattern of leaf 4 to some extent, both in Conférence and Doyenné. No clear induced transcription patterns could be detected in leaf 3 and leaf 5.

Table 4.3, 4.4 and 4.5: Heat map representation of the relative expression values for all investigated genes for the different treatments, x hours after inoculation for both Conférence (Conf) and Doyenné (Doy). Each cell represents a relative expression value according to the colour scale at the bottom. Values in the cell are mean ± SE of 10 biological independent replicates. Gene expression data were expressed relatively to the reference genes and to the values of mock-inoculated immature leaves 3hours after inoculation (= relative expression value of 1) following the $2^{-\Delta Ct}$ method divided by the geometric mean of the reference genes. Bold numbers indicate a significant difference (α=0.05) compared to the corresponding mock-inoculated leaves. Table 4.3 corresponds to leaf 3, table 4.4 corresponds to leaf 4 (= inoculated leaf) and table 4.5 corresponds to leaf 5. For enzyme abbreviations, see text.

Table 4.3

Treatment\gene		*PAL*	*CHS*	*FHT*	*FLS*	*F7GT*	*DFR*	*LAR1*	*ANS*	*ANR*
3h	Mock-inoc. Conf. leaves	1.00 ± 0.11	1.00 ± 0.20	1.00 ± 0.15	1.00 ± 0.08	1.00 ± 0.07	1.00 ± 0.17	1.00 ± 0.11	1.00 ± 0.14	1.00 ± 0.19
	Ea-inoc. Conf. leaves	1.23 ± 0.17	**2.01 ± 0.23**	1.19 ± 0.08	1.14 ± 0.06	0.97 ± 0.05	1.03 ± 0.14	0.93 ± 0.09	1.11 ± 0.09	1.04 ± 0.10
24h	Mock-inoc. Conf. leaves	1.21 ± 0.17	1.92 ± 0.13	1.26 ± 0.12	0.66 ± 0.07	1.00 ± 0.07	0.82 ± 0.06	0.82 ± 0.05	1.26 ± 0.08	1.26 ± 0.15
	Ea-inoc. Conf. leaves	0.97 ± 0.15	1.82 ± 0.16	**0.90 ± 0.08**	0.65 ± 0.11	**0.70 ± 0.06**	0.64 ± 0.10	0.68 ± 0.12	**0.94 ± 0.07**	**0.87 ± 0.07**
48h	Mock-inoc. Conf. leaves	2.07 ± 0.14	3.43 ± 0.36	1.69 ± 0.09	0.89 ± 0.10	1.40 ± 0.19	1.16 ± 0.08	1.00 ± 0.06	1.13 ± 0.07	1.53 ± 0.10
	Ea-inoc. Conf. leaves	**1.25 ± 0.15**	**1.69 ± 0.30**	**1.14 ± 0.12**	0.70 ± 0.08	**0.83 ± 0.05**	**0.58 ± 0.06**	**0.82 ± 0.03**	**0.78 ± 0.07**	**1.06 ± 0.15**
72h	Mock-inoc. Conf. leaves	2.00 ± 0.17	1.94 ± 0.35	1.14 ± 0.10	0.78 ± 0.11	1.62 ± 0.21	0.53 ± 0.05	0.74 ± 0.03	0.64 ± 0.07	0.83 ± 0.10
	Ea-inoc. Conf. leaves	**1.29 ± 0.11**	**3.63 ± 0.54**	1.29 ± 0.19	**0.44 ± 0.09**	1.35 ± 0.16	0.85 ± 0.13	0.72 ± 0.17	**1.17 ± 0.12**	**1.44 ± 0.32**
4d	Mock-inoc. Conf. leaves	2.22 ± 0.22	0.97 ± 0.18	0.61 ± 0.06	0.89 ± 0.12	0.84 ± 0.04	1.29 ± 0.12	1.30 ± 0.17	1.28 ± 0.15	0.50 ± 0.06
	Ea-inoc. Conf. leaves	1.93 ± 0.27	0.97 ± 0.17	0.48 ± 0.05	1.04 ± 0.22	**1.12 ± 0.09**	1.03 ± 0.12	1.05 ± 0.18	1.12 ± 0.12	0.42 ± 0.06
6d	Mock-inoc. Conf. leaves	2.08 ± 0.23	1.63 ± 0.24	1.19 ± 0.12	1.19 ± 0.20	1.30 ± 0.06	1.05 ± 0.10	1.36 ± 0.14	1.89 ± 0.21	0.88 ± 0.12
	Ea-inoc. Conf. leaves	3.23 ± 0.53	**3.75 ± 0.51**	1.79 ± 0.25	1.33 ± 0.32	1.29 ± 0.18	1.44 ± 0.23	1.45 ± 0.30	**2.78 ± 0.33**	1.43 ± 0.25
3h	Mock-inoc. Doy. leaves	1.00 ± 0.17	1.00 ± 0.09	1.00 ± 0.12	1.00 ± 0.11	1.00 ± 0.11	1.00 ± 0.13	1.00 ± 0.23	1.00 ± 0.11	1.00 ± 0.15
	Ea-inoc. Doy. leaves	1.04 ± 0.16	1.43 ± 0.30	1.18 ± 0.18	**1.54 ± 0.17**	1.02 ± 0.17	1.19 ± 0.18	0.98 ± 0.13	1.06 ± 0.19	1.44 ± 0.35
24h	Mock-inoc. Doy. leaves	0.87 ± 0.14	0.93 ± 0.12	0.98 ± 0.07	1.13 ± 0.08	0.98 ± 0.09	0.93 ± 0.14	0.86 ± 0.16	0.73 ± 0.09	1.08 ± 0.19
	Ea-inoc. Doy. leaves	**0.45 ± 0.05**	**0.37 ± 0.03**	**0.43 ± 0.05**	0.94 ± 0.11	**0.73 ± 0.07**	**0.56 ± 0.06**	0.69 ± 0.07	**0.38 ± 0.02**	**0.41 ± 0.06**
48h	Mock-inoc. Doy. leaves	0.38 ± 0.03	0.30 ± 0.04	0.42 ± 0.04	0.90 ± 0.15	0.89 ± 0.08	0.41 ± 0.04	0.53 ± 0.04	0.24 ± 0.03	0.39 ± 0.03
	Ea-inoc. Doy. leaves	**0.76 ± 0.10**	**1.26 ± 0.10**	**1.06 ± 0.16**	0.95 ± 0.29	0.61 ± 0.10	0.62 ± 0.15	0.49 ± 0.11	**0.77 ± 0.09**	**1.38 ± 0.35**
72h	Mock-inoc. Doy. leaves	0.95 ± 0.08	0.27 ± 0.03	0.71 ± 0.06	1.47 ± 0.28	1.86 ± 0.33	0.87 ± 0.10	2.19 ± 0.44	0.32 ± 0.03	0.70 ± 0.10
	Ea-inoc. Doy. leaves	**1.66 ± 0.22**	**1.31 ± 0.20**	**1.04 ± 0.11**	1.58 ± 0.34	**1.10 ± 0.14**	1.68 ± 0.40	1.56 ± 0.37	**0.89 ± 0.08**	**2.06 ± 0.36**
4d	Mock-inoc. Doy. leaves	0.31 ± 0.04	0.10 ± 0.02	0.38 ± 0.05	0.36 ± 0.06	0.73 ± 0.06	0.42 ± 0.06	0.46 ± 0.08	0.32 ± 0.05	0.46 ± 0.10
	Ea-inoc. Doy. leaves	0.23 ± 0.03	0.16 ± 0.04	0.36 ± 0.04	0.67 ± 0.13	0.62 ± 0.08	0.38 ± 0.07	0.53 ± 0.10	0.30 ± 0.05	0.37 ± 0.08
6d	Mock-inoc. Doy. leaves	1.09 ± 0.15	0.77 ± 0.18	1.17 ± 0.15	0.72 ± 0.14	0.79 ± 0.12	0.75 ± 0.13	0.47 ± 0.06	0.69 ± 0.09	1.86 ± 0.25
	Ea-inoc. Doy. leaves	0.79 ± 0.07	**0.31 ± 0.06**	**0.82 ± 0.08**	0.91 ± 0.12	**1.91 ± 0.22**	0.59 ± 0.06	**1.41 ± 0.11**	**0.46 ± 0.04**	**1.17 ± 0.15**

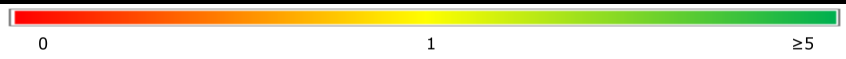

Table 4.4

Treatment\gene		*PAL*	*CHS*	*FHT*	*FLS*	*F7GT*	*DFR*	*LAR1*	*ANS*	*ANR*
3h	Mock-inoc. Conf. leaves	1.00 ± 0.10	1.00 ± 0.15	1.00 ± 0.10	1.00 ± 0.10	1.00 ± 0.10	1.00 ± 0.10	1.00 ± 0.12	1.00 ± 0.12	1.00 ± 0.15
	Ea-inoc. Conf. leaves	1.08 ± 0.06	**2.30 ± 0.31**	1.07 ± 0.06	1.22 ± 0.09	**0.70 ± 0.03**	1.08 ± 0.12	0.83 ± 0.06	0.98 ± 0.09	0.95 ± 0.11
24h	Mock-inoc. Conf. leaves	0.84 ± 0.07	2.46 ± 0.17	1.14 ± 0.06	0.47 ± 0.05	0.59 ± 0.05	1.32 ± 0.11	0.84 ± 0.07	1.30 ± 0.07	1.45 ± 0.14
	Ea-inoc. Conf. leaves	1.01 ± 0.07	2.79 ± 0.32	0.99 ± 0.11	0.63 ± 0.08	0.61 ± 0.06	1.10 ± 0.15	0.76 ± 0.03	**0.94 ± 0.08**	1.16 ± 0.11
48h	Mock-inoc. Conf. leaves	1.69 ± 0.17	4.68 ± 0.63	1.56 ± 0.25	1.08 ± 0.17	1.01 ± 0.10	1.12 ± 0.13	1.03 ± 0.21	1.27 ± 0.14	1.62 ± 0.24
	Ea-inoc. Conf. leaves	**0.55 ± 0.11**	**2.15 ± 0.38**	**0.71 ± 0.12**	**0.42 ± 0.14**	**0.52 ± 0.10**	**0.49 ± 0.08**	**0.46 ± 0.13**	**0.62 ± 0.06**	**0.71 ± 0.14**
72h	Mock-inoc. Conf. leaves	2.18 ± 0.46	3.65 ± 0.90	0.44 ± 0.07	1.04 ± 0.27	0.82 ± 0.19	1.32 ± 0.33	0.51 ± 0.14	1.87 ± 0.18	0.68 ± 0.10
	Ea-inoc. Conf. leaves	1.85 ± 0.35	3.14 ± 0.17	**0.75 ± 0.10**	0.55 ± 0.13	0.67 ± 0.16	2.20 ± 0.41	0.75 ± 0.19	**2.39 ± 0.38**	**1.38 ± 0.23**
4d	Mock-inoc. Conf. leaves	1.29 ± 0.25	1.22 ± 0.20	0.35 ± 0.06	0.57 ± 0.14	0.57 ± 0.09	1.22 ± 0.27	0.83 ± 0.22	1.04 ± 0.17	0.41 ± 0.07
	Ea-inoc. Conf. leaves	0.83 ± 0.17	2.01 ± 0.68	0.73 ± 0.30	**0.18 ± 0.08**	**0.14 ± 0.03**	1.03 ± 0.24	0.47 ± 0.13	0.56 ± 0.14	0.74 ± 0.17
6d	Mock-inoc. Conf. leaves	1.33 ± 0.23	3.26 ± 0.47	0.98 ± 0.16	0.64 ± 0.14	0.78 ± 0.14	1.01 ± 0.19	0.58 ± 0.12	2.09 ± 0.27	0.91 ± 0.20
	Ea-inoc. Conf. leaves	0.86 ± 0.23	6.12 ± 1.73	1.68 ± 0.41	**0.05 ± 0.01**	**0.19 ± 0.02**	1.41 ± 0.35	0.41 ± 0.10	**1.01 ± 0.28**	1.65 ± 0.48
3h	Mock-inoc. Doy. leaves	1.00 ± 0.12	1.00 ± 0.15	1.00 ± 0.10	1.00 ± 0.13	1.00 ± 0.11	1.00 ± 0.13	1.00 ± 0.12	1.00 ± 0.14	1.00 ± 0.14
	Ea-inoc. Doy. leaves	1.08 ± 0.16	1.59 ± 0.30	1.11 ± 0.16	1.30 ± 0.15	0.82 ± 0.08	1.11 ± 0.18	1.07 ± 0.14	0.97 ± 0.13	1.20 ± 0.25
24h	Mock-inoc. Doy. leaves	0.89 ± 0.09	1.27 ± 0.22	1.08 ± 0.11	0.79 ± 0.09	0.90 ± 0.09	1.12 ± 0.12	0.82 ± 0.08	0.88 ± 0.14	1.53 ± 0.22
	Ea-inoc. Doy. leaves	**0.59 ± 0.05**	**0.75 ± 0.08**	**0.64 ± 0.05**	0.72 ± 0.07	0.81 ± 0.09	**0.77 ± 0.07**	0.65 ± 0.07	**0.65 ± 0.05**	**0.96 ± 0.10**
48h	Mock-inoc. Doy. leaves	0.35 ± 0.05	0.74 ± 0.19	0.40 ± 0.06	0.60 ± 0.33	0.45 ± 0.07	0.38 ± 0.13	0.17 ± 0.05	0.31 ± 0.03	0.42 ± 0.04
	Ea-inoc. Doy. leaves	**0.85 ± 0.05**	1.15 ± 0.18	**0.97 ± 0.07**	0.85 ± 0.26	**1.03 ± 0.14**	**1.10 ± 0.19**	**0.73 ± 0.16**	**0.79 ± 0.11**	**1.47 ± 0.27**
72h	Mock-inoc. Doy. leaves	0.41 ± 0.04	0.25 ± 0.03	0.41 ± 0.05	0.85 ± 0.20	1.33 ± 0.22	0.90 ± 0.14	1.04 ± 0.19	0.35 ± 0.04	0.63 ± 0.09
	Ea-inoc. Doy. leaves	**0.80 ± 0.15**	**0.66 ± 0.12**	**0.90 ± 0.15**	1.48 ± 0.29	1.28 ± 0.18	**2.38 ± 0.51**	1.71 ± 0.34	**0.71 ± 0.10**	**2.35 ± 0.38**
4d	Mock-inoc. Doy. leaves	0.20 ± 0.03	0.09 ± 0.01	0.26 ± 0.03	0.32 ± 0.06	0.51 ± 0.04	0.34 ± 0.05	0.32 ± 0.06	0.23 ± 0.03	0.27 ± 0.06
	Ea-inoc. Doy. leaves	0.24 ± 0.03	**0.29 ± 0.07**	**0.42 ± 0.06**	0.35 ± 0.12	0.40 ± 0.05	0.44 ± 0.09	0.33 ± 0.09	0.33 ± 0.04	**0.66 ± 0.12**
6d	Mock-inoc. Doy. leaves	0.87 ± 0.13	0.37 ± 0.06	0.81 ± 0.14	0.25 ± 0.04	1.75 ± 0.16	0.76 ± 0.12	1.01 ± 0.11	0.37 ± 0.05	1.30 ± 0.31
	Ea-inoc. Doy. leaves	**0.24 ± 0.04**	**0.12 ± 0.03**	**0.39 ± 0.06**	0.30 ± 0.07	**0.82 ± 0.07**	**0.29 ± 0.05**	**0.45 ± 0.08**	**0.17 ± 0.04**	**0.54 ± 0.12**

Table 4.5

Treatment\gene		*PAL*	*CHS*	*FHT*	*FLS*	*F7GT*	*DFR*	*LAR1*	*ANS*	*ANR*
3h	Mock-inoc. Conf. leaves	1.00 ± 0.10	1.00 ± 0.17	1.00 ± 0.13	1.00 ± 0.09	1.00 ± 0.11	1.00 ± 0.21	1.00 ± 0.13	1.00 ± 0.19	1.00 ± 0.13
	Ea-inoc. Conf. leaves	0.85 ± 0.08	**1.87 ± 0.22**	1.03 ± 0.11	1.06 ± 0.13	**0.69 ± 0.06**	0.78 ± 0.10	**0.60 ± 0.07**	0.97 ± 0.11	1.25 ± 0.15
24h	Mock-inoc. Conf. leaves	0.91 ± 0.05	1.59 ± 0.12	1.18 ± 0.07	0.52 ± 0.04	0.62 ± 0.05	0.85 ± 0.08	0.65 ± 0.06	0.76 ± 0 .04	1.26 ± 0.11
	Ea-inoc. Conf. leaves	0.87 ± 0.10	1.88 ± 0.20	1.06 ± 0.09	**0.79 ± 0.10**	0.68 ± 0.04	0.76 ± 0.08	0.58 ± 0.06	0.74 ± 0.07	1.17 ± 0.12
48h	Mock-inoc. Conf. leaves	1.01 ± 0.18	2.19 ± 0.36	0.93 ± 0.13	0.42 ± 0.11	0.62 ± 0.08	0.55 ± 0.11	0.34 ± 0.09	0.69 ± 0.10	1.10 ± 0.17
	Ea-inoc. Conf. leaves	0.58 ± 0.16	2.06 ± 0.77	0.76 ± 0.26	0.32 ± 0.09	**0.31 ± 0.04**	0.43 ± 0.11	0.29 ± 0.09	0.56 ± 0.14	1.37 ± 0.62
72h	Mock-inoc. Conf. leaves	2.18 ± 0.29	2.16 ± 0.40	0.56 ± 0.08	0.76 ± 0.09	0.73 ± 0.08	1.41 ± 0.21	0.58 ± 0.12	1.49 ± 0.16	1.00 ± 0.17
	Ea-inoc. Conf. leaves	2.89 ± 0.50	2.12 ± 0.53	**0.93 ± 0.12**	**1.18 ± 0.18**	0.89 ± 0.07	2.14 ± 0.37	**1.20 ± 0.16**	2.02 ± 0.34	1.78 ± 0.37
4d	Mock-inoc. Conf. leaves	1.47 ± 0.27	0.96 ± 0.17	**0.49 ± 0.07**	0.72 ± 0.19	0.47 ± 0.09	0.86 ± 0.12	0.59 ± 0.17	0.87 ± 0.12	0.69 ± 0.09
	Ea-inoc. Conf. leaves	1.38 ± 0.24	1.33 ± 0.31	**0.83 ± 0.11**	0.79 ± 0.05	0.64 ± 0.02	1.67 ± 0.53	0.88 ± 0.17	1.32 ± 0.25	1.30 ± 0.37
6d	Mock-inoc. Conf. leaves	1.48 ± 0.28	2.55 ± 0.41	1.19 ± 0.15	0.81 ± 0.18	0.57 ± 0.05	1.10 ± 0.13	0.52 ± 0.11	1.80 ± 0.14	1.64 ± 0.33
	Ea-inoc. Conf. leaves	1.47 ± 0.24	4.84 ± 0.94	1.20 ± 0.20	0.64 ± 0.15	0.49 ± 0.08	0.87 ± 0.14	0.40 ± 0.12	1.75 ± 0.19	1.71 ± 0.39
3h	Mock-inoc. Doy. leaves	1.00 ± 0.02	1.00 ± 0.21	1.00 ± 0.07	1.00 ± 0.16	1.00 ± 0.08	1.00 ± 0.14	1.00 ± 0.13	1.00 ± 0.12	1.00 ± 0.18
	Ea-inoc. Doy. leaves	1.31 ± 0.23	1.77 ± 0.38	1.16 ± 0.18	1.21 ± 0.11	1.25 ± 0.16	1.35 ± 0.22	1.01 ± 0.13	1.27 ± 0.21	1.51 ± 0.35
24h	Mock-inoc. Doy. leaves	0.38 ± 0.05	0.69 ± 0.09	0.51 ± 0.06	0.46 ± 0.07	0.53 ± 0.07	0.59 ± 0.06	0.41 ± 0.05	0.41 ± 0.05	0.55 ± 0.08
	Ea-inoc. Doy. leaves	**0.18 ± 0.03**	**0.26 ± 0.02**	**0.26 ± 0.04**	0.40 ± 0.07	0.47 ± 0.06	**0.33 ± 0.05**	0.28 ± 0.04	**0.25 ± 0.03**	0.40 ± 0.12
48h	Mock-inoc. Doy. leaves	0.80 ± 0.11	0.93 ± 0.30	1.12 ± 0.18	1.06 ± 0.17	1.22 ± 0.14	1.28 ± 0.16	1.21 ± 0.15	0.69 ± 0.11	1.62 ± 0.38
	Ea-inoc. Doy. leaves	1.08 ± 0.12	1.66 ± 0.21	**1.65 ± 0.14**	1.31 ± 0.31	1.12 ± 0.12	1.60 ± 0.23	1.16 ± 0.19	**1.15 ± 0.12**	**2.52 ± 0.55**
72h	Mock-inoc. Doy. leaves	0.35 ± 0.04	0.26 ± 0.04	0.39 ± 0.05	0.34 ± 0.06	0.69 ± 0.09	1.04 ± 0.21	0.81 ± 0.11	0.31 ± 0.04	0.79 ± 0.15
	Ea-inoc. Doy. leaves	0.51 ± 0.09	**0.89 ± 0.11**	**0.83 ± 0.09**	0.88 ± 0.23	0.66 ± 0.07	1.53 ± 0.31	0.73 ± 0.10	**0.80 ± 0.11**	**2.34 ± 0.39**
4d	Mock-inoc. Doy. leaves	0.22 ± 0.04	0.21 ± 0.06	0.38 ± 0.06	0.30 ± 0.06	0.49 ± 0.07	0.51 ± 0.09	0.29 ± 0.06	0.38 ± 0.07	0.70 ± 0.17
	Ea-inoc. Doy. leaves	0.16 ± 0.02	0.26 ± 0.06	0.31 ± 0.03	0.22 ± 0.06	0.40 ± 0.06	0.30 ± 0.08	**0.16 ± 0.05**	0.33 ± 0.04	0.44 ± 0.05
6d	Mock-inoc. Doy. leaves	0.93 ± 0.07	0.71 ± 0.11	1.17 ± 0.07	0.19 ± 0.06	1.30 ± 0.15	0.67 ± 0.07	1.05 ± 0.04	0.56 ± 0.05	2.32 ± 0.27
	Ea-inoc. Doy. leaves	**0.63 ± 0.06**	0.68 ± 0.11	1.14 ± 0.10	**0.47 ± 0.07**	1.20 ± 0.11	0.92 ± 0.10	0.93 ± 0.08	0.65 ± 0.09	2.43 ± 0.33

4.3 HPLC profiling mainly shows differences between between the cultivars but not between treatments

Phenolic profiling with HPLC was performed on samples 72h and 4 days after the onset of all treatments (mock-inoculated and *Ea*-inoculated).

When considering the total concentration of flavonols and simple phenolics in the leaves, values of around 4 mg g^{-1} dry weight (DW) and 10 mg g^{-1} dry weight were respectively present in Conférence 72h and 4 days after inoculation both for the mock-inoculated and *Ea*-inoculated tissue (figure 4.3 A), whereas Doyenné reached concentrations of approximately 10 mg g^{-1} dry weight flavonols and 16 mg g^{-1} dry weight simple phenolics (figure 4.3 B). No differences between the treatments were present.

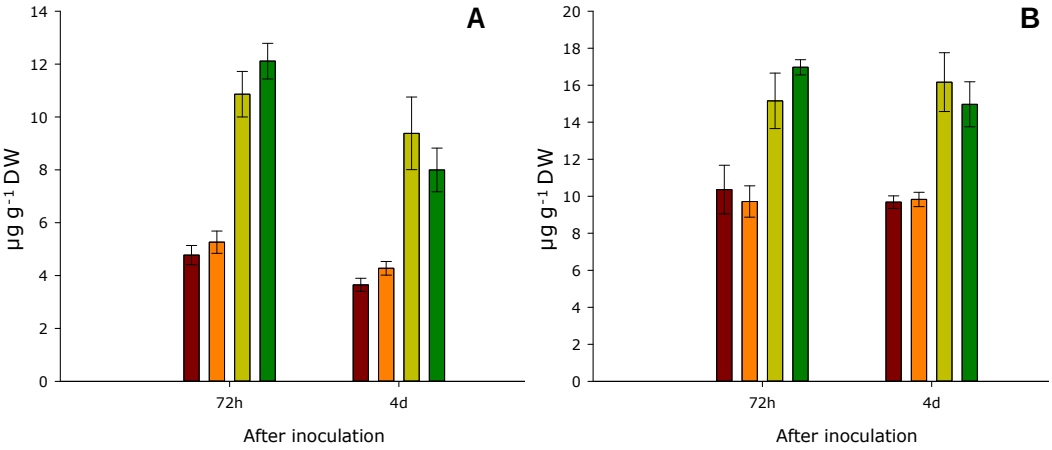

Figure 4.3: Total concentration (mg g^{-1} DW) of flavonols (A) and simple phenolics (B) for the different treatments (mock-inoculated Conférence leaves ( ), *Ea*-inoculated Conférence leaves ( ), mock-inoculated Doyenné leaves ( ) and *Ea*-inoculated Doyenné leaves ( )), 72hours and 4days after inoculation. Values are mean ± SE of 4 biological independent replicates.

Concerning the hydroxycinnamic acids, cis- and trans-neochlorogenic acid (figure 4.4 A and 4.4 B) were both higher in Conférence than in Doyenné. (values respectively around 100-150 µg g^{-1} DW and 1000 µg g^{-1} DW compared to 25 µg g^{-1} DW and 400-600 µg g^{-1} DW in Doyenné). Chlorogenic acid (figure 4.4 C) was the same in both cultivars. The concentration of cis-ferulic acid (figure 4.4 D) was slightly higher in Doyenné 4 days after inoculation. Few significant differences between treatments were found, as the amount of cis-neochlorogenic acid was a little bit higher in *Ea*-inoculated Conférence tissue 4

days after inoculation and the concentration of cis-ferulic acid in Doyenné was slightly higher in *Ea*-inoculated leaves 72h after inoculation.

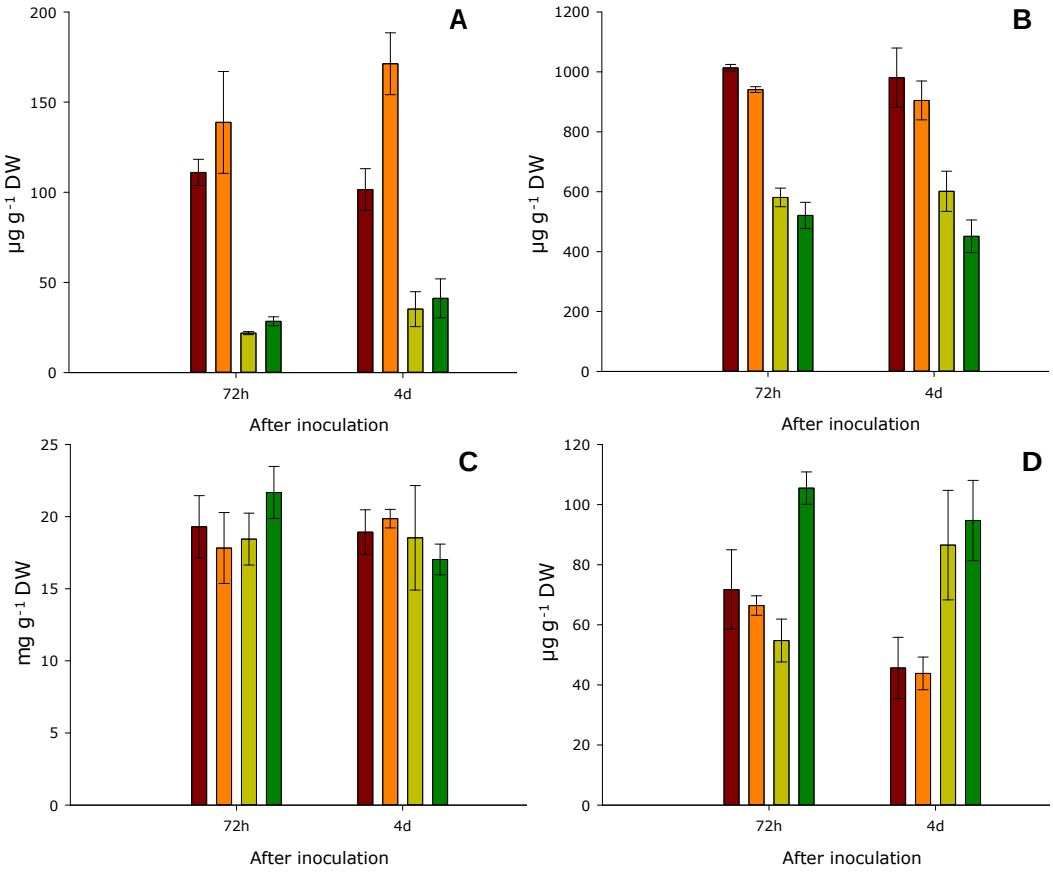

Figure 4.4: Total concentration of the hydroxycinnamic acids cis-neochlorogenic acid (A; µg g^{-1} DW), trans-neochlorogenic acid (B; µg g^{-1} DW), chlorogenic acid (C; mg g^{-1} DW) and cis-ferulic acid (D; µg g^{-1} DW) for the different treatments (mock-inoculated Conférence leaves (■), *Ea*-inoculated Conférence leaves (■), mock-inoculated Doyenné leaves (■) and *Ea*-inoculated Doyenné leaves (■)), 72hours and 4days after inoculation. Values are mean ± SE of 4 biological independent replicates.

The flavan-3-ols, consisting of procyanidin B2, procyanidin B5, catechin and epicatechin were all present in higher concentration in Doyenné compared to Conférence (figure 4.5 A, B, C and D). Between the treatments, no differences were visible. Procyanidin E-B5 was present in too low concentrations or not detectable at all and therefore, no clear conclusions could be made. All

measured metabolites in Conférence conserved more or less the same concentrations as observed in the previous chapter.

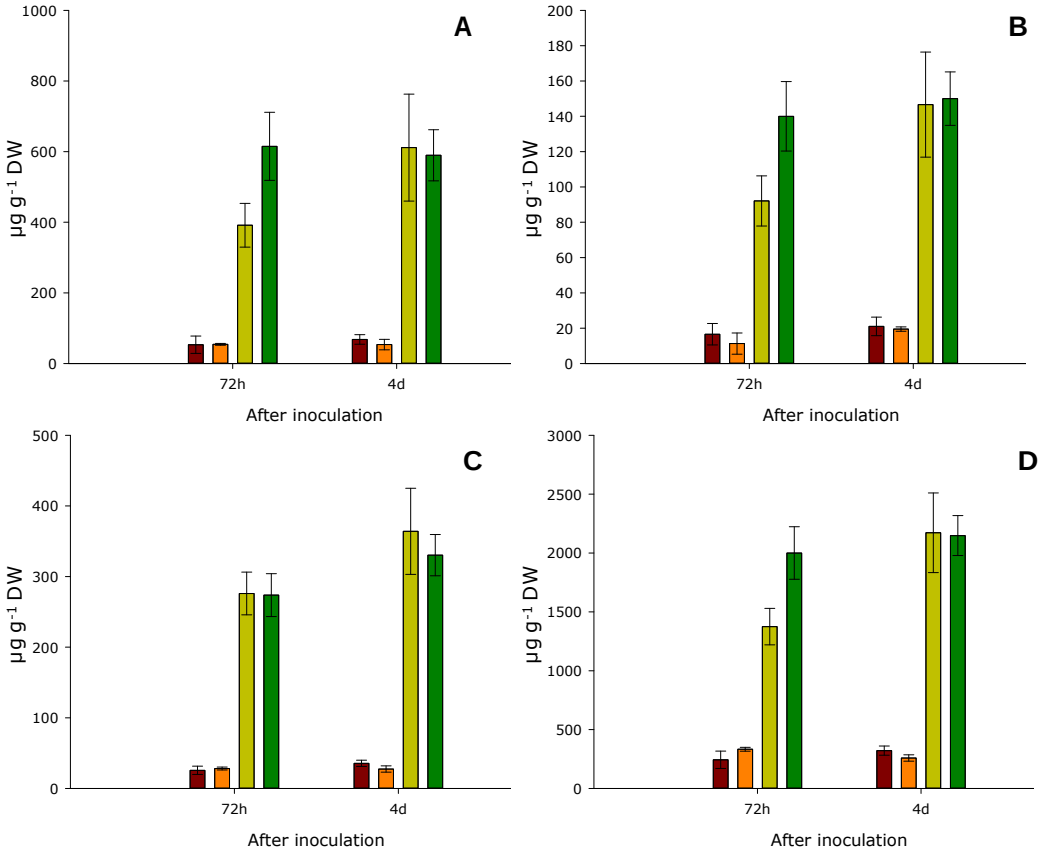

Figure 4.5: Total concentration (µg g^{-1} DW) of the flavan-3-ols procyanidin B2 (A), procyanidin B5 (B), catechin (C) and epicatechin (D) for the different treatments (mock-inoculated Conférence leaves ( ), *Ea*-inoculated Conférence leaves ( ), mock-inoculated Doyenné leaves ( ) and *Ea*-inoculated Doyenné leaves ( )), 72hours and 4days after inoculation. Values are mean ± SE of 4 biological independent replicates.

4.4 Chlorophyll fluorescence in both cultivars indicates the presence of stress as a response to fire blight

Chlorophyll fluorescence measurements with the PEA were performed on mock-inoculated and *Ea*-inoculated leaves of Conférence and Doyenné du Comice (indicated as leaf 4). In order to know if not *Ea*-inoculated leaves positioned beneath the *Ea*-inoculated leaf also responded to the infection, these leaves were measured as well (indicated as leaf 5).

Because most of the described PEA parameters of table 3.5 utilise specific time points of the OJIP transient curve in their formulae and to decrease the large amount of data, only these OJIP transient and FvF curves together with the trapping probability $\Phi_{P0}= TR_0/ABS=(1-(F_0/F_M)$ were mentioned here.

In contrast with the previous chapter, a rise in fluorescence during the first three days after inoculation was not observed, which could be due to the lower severity of the shoot infections compared to the previous chapter. However, in Conférence, the OJIP transient of the *Ea*-inoculated leaf 4 started to change after four days of inoculation, which was still before the appearance of any visual blight symptoms (figure 4.6). At this time point, both $F_5=F_{30ms}$ and F_M were lowered in comparison with the other treatments. At F_5, the fluorescence reached a level of 2329,6mV in the infected leaf 4 compared to 2500-2600mV for the other treatments, whereas the maximal fluorescence F_M attenuated to a value of 2869,8mV compared to 3100mV in the other treatments. These differences intensified 8 days after inoculation, as the maximal fluorescence in the *Ea*-inoculated leaf 4 widely stayed under 2500mV. The transient FvF depicts the same OJIP transient curve, with the big difference that the data have been normalised at 50µs (F_1) and F_M in order to be able to visualise the variable fluorescence at point I and point J and the effects on F_0 (figure 4.7). Eight days after inoculation, a slight increase of the FvF curve for the *Ea*-inoculated leaf 4 could be noticed between point J = 2ms and point I= 30ms, indicating more closed reaction centers in PS II, a reduced electron transport and an accumulation of reduced plastoquinone, finally resulting in a lowered efficiency of photosynthesis.

Doyenné only had a slightly lowered F_M four and eight days after inoculation, compared to the F_M in the other treatments (figure 4.8). The FVF curve of the *Ea*-inoculated leaf 4 of Doyenné however was situated significantly higher four and eight days after inoculation, demonstrating a reduced photosynthetic efficiency in the plant tissue (figure 4.9).

Both the Conférence trees as the Doyenné trees maintained a value of about 0.80 for the quantum yield efficiency parameter Φ_{P0}, independent of the treatment or the time of measurement. Eight days after inoculation however, only Φ_{P0} of the *Ea*-inoculated leaf 4 in Conférence decreased to 0.75, as cells collapsed and necrosis visibly started to occur in these leaf tissues (figure 4.10).

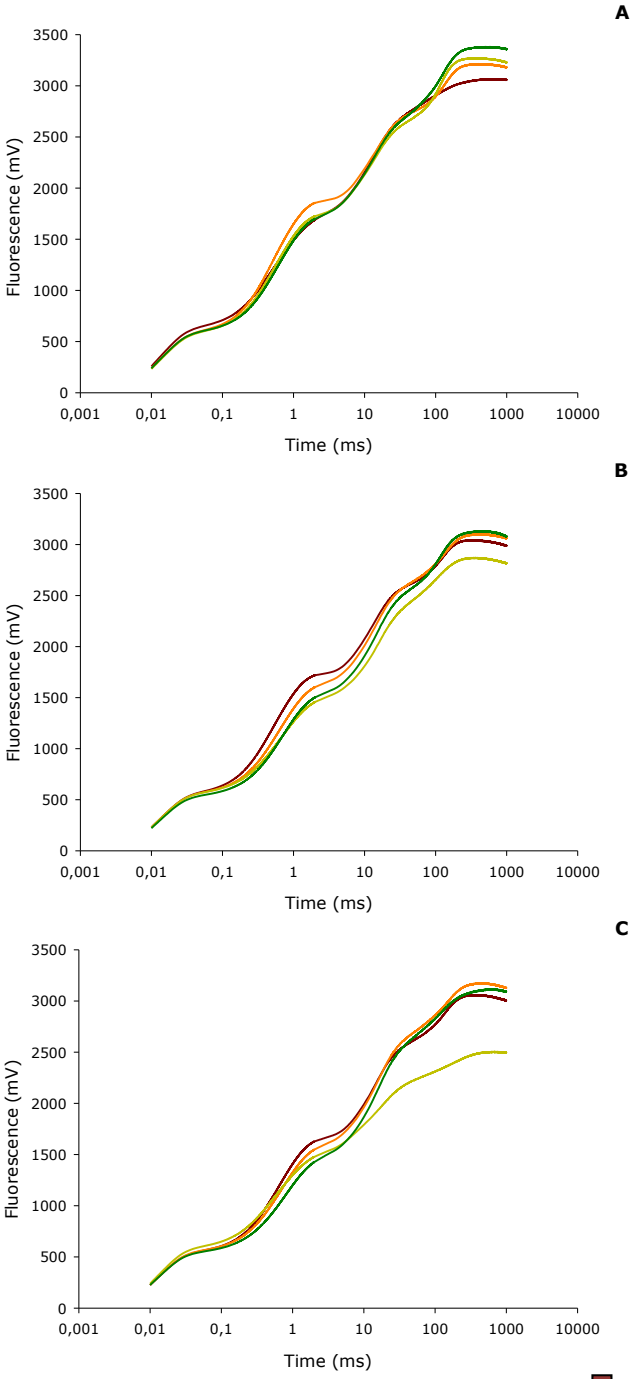

Figure 4.6: OJIP transient curves of leaf 4 (mock-inoculated) (■), leaf 5 (with mock-inoculated leaf 4) (■), leaf 4 (*Ea*-inoculated) (■) and leaf 5 (with *Ea*-inoculated leaf 4) (■) in Conférence, before inoculation (A), 4days after inoculation (B) and 8days after inoculation (C).

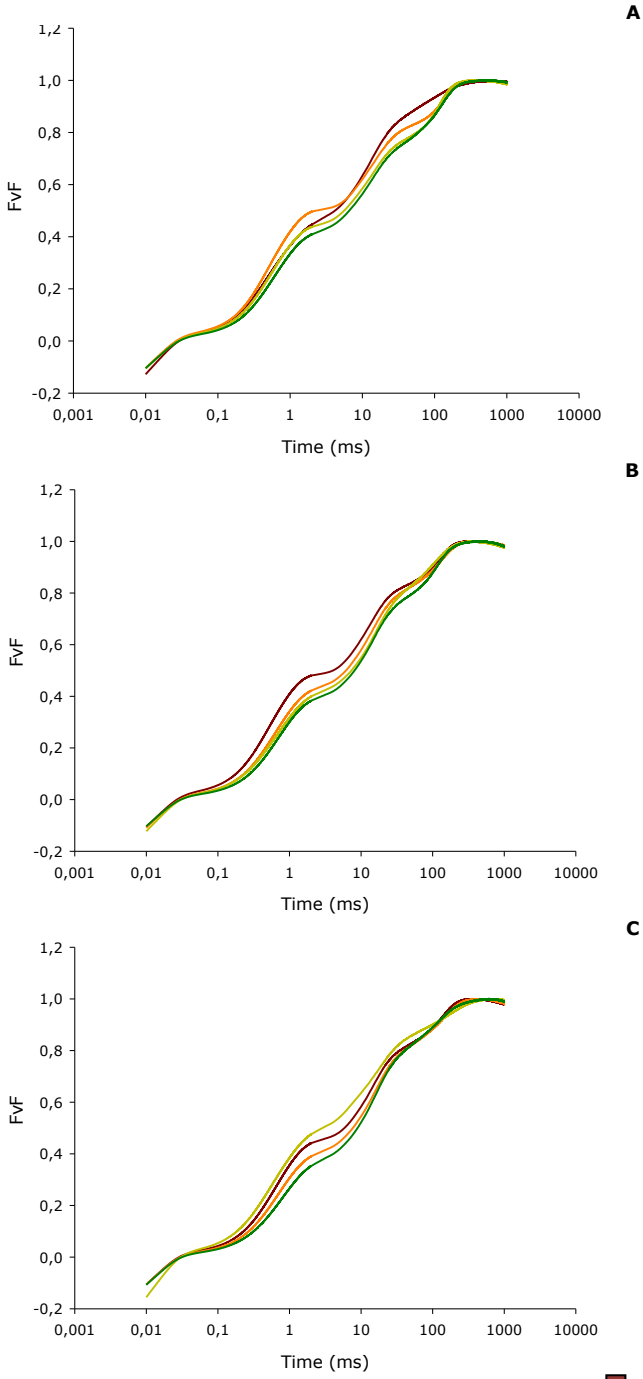

Figure 4.7: Normalised FvF curves of leaf 4 (mock-inoculated) (■), leaf 5 (with mock-inoculated leaf 4) (■), leaf 4 (*Ea*-inoculated) (■) and leaf 5 (with *Ea*-inoculated leaf 4) (■) in Conférence, before inoculation (A), 4days after inoculation (B) and 8days after inoculation (C).

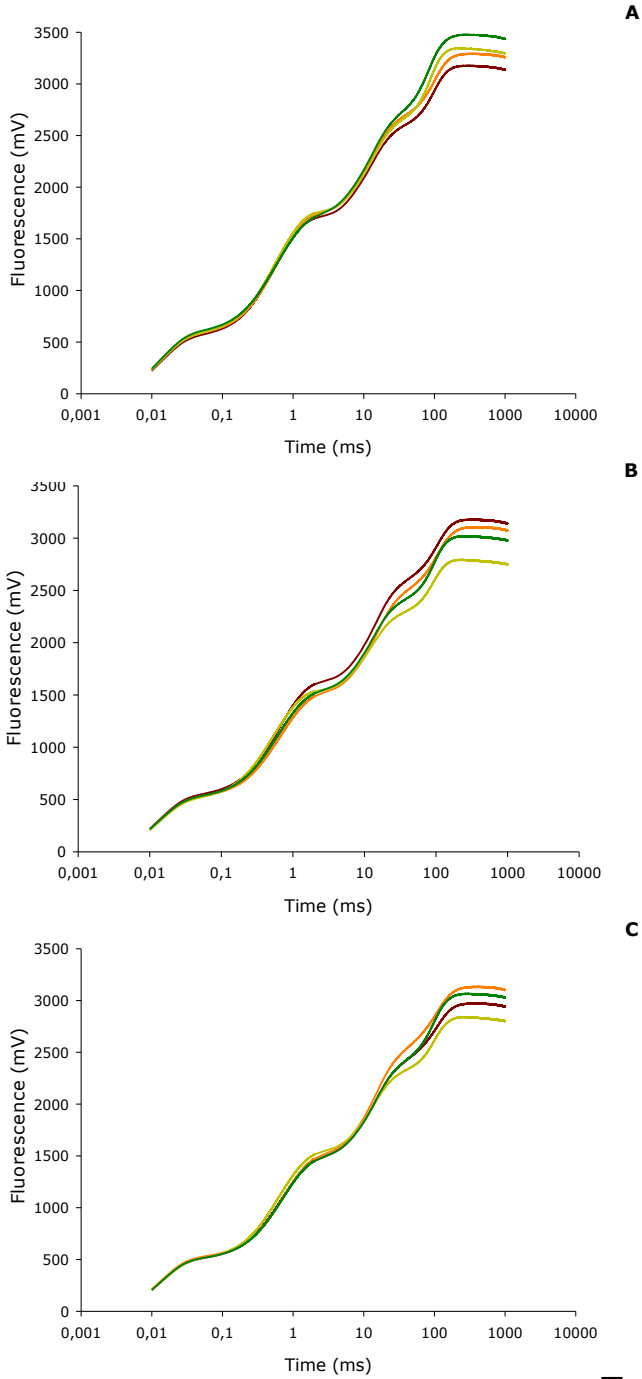

Figure 4.8: OJIP transient curves of leaf 4 (mock-inoculated) (■), leaf 5 (with mock-inoculated leaf 4) (■), leaf 4 (*Ea*-inoculated) (■) and leaf 5 (with *Ea*-inoculated leaf 4) (■) in Doyenné, before inoculation (A), 4days after inoculation (B) and 8days after inoculation (C).

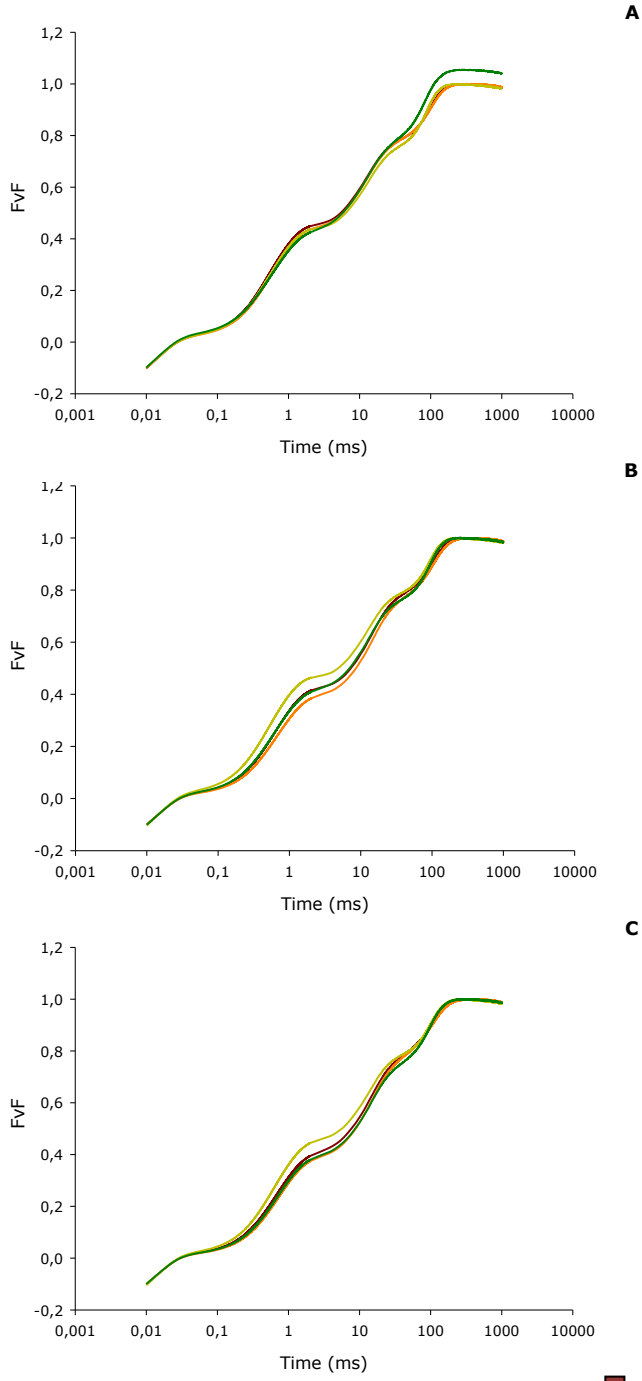

Figure 4.9: Normalised FvF curves of leaf 4 (mock-inoculated) (■), leaf 5 (with mock-inoculated leaf 4) (■), leaf 4 (*Ea*-inoculated) (■) and leaf 5 (with *Ea*-inoculated leaf 4) (■) in Doyenné, before inoculation (A), 4days after inoculation (B) and 8days after inoculation (C).

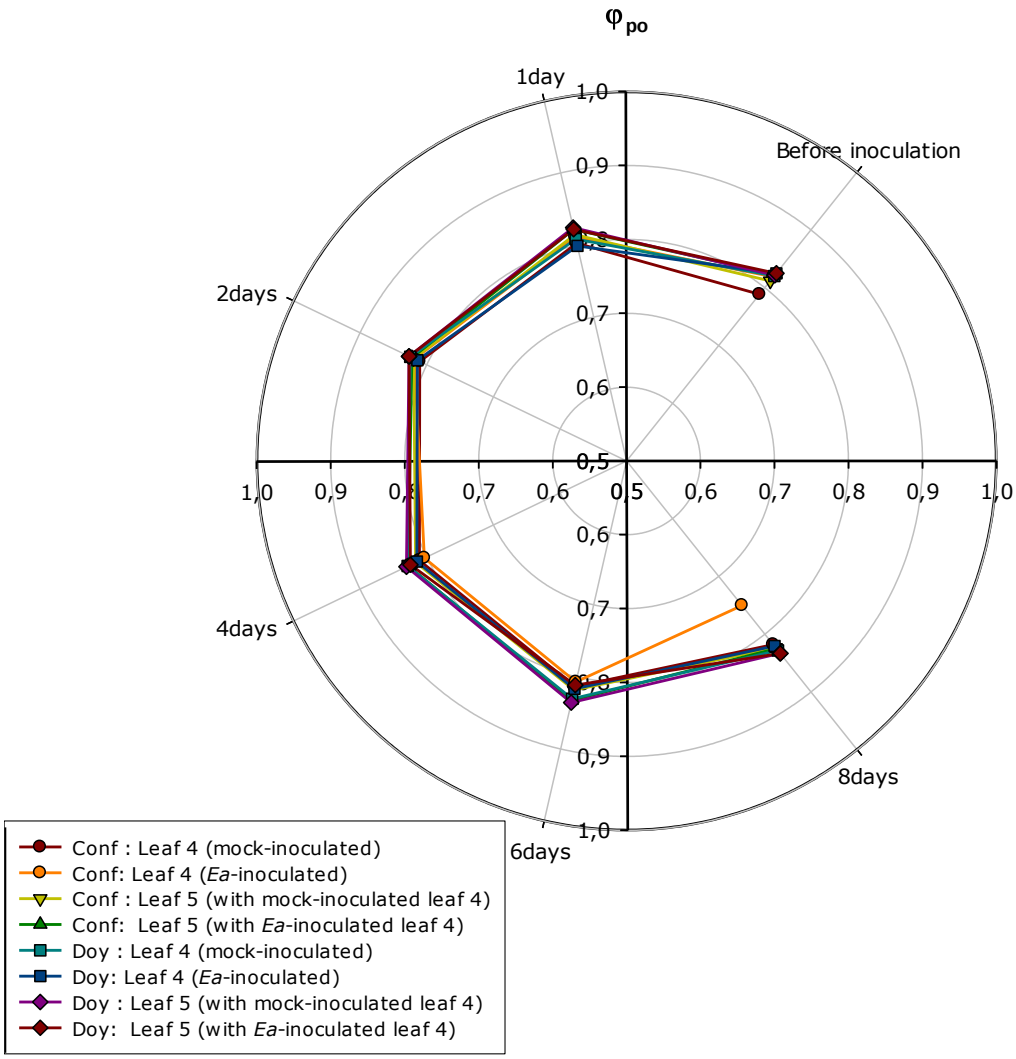

Figure 4.10: Spider plot of the trapping probability Φ_{P0} of leaf 4 (mock-inoculated), leaf 5 (with mock-inoculated leaf 4), leaf 4 (*Ea*-inoculated) and leaf 5 (with *Ea*-inoculated leaf 4) in Conférence and Doyenné, before inoculation and x days after inoculation.

4.5 Proteomics demonstrates differentially expressed spots in both Conférence and Doyenné after *Ea*-inoculation

Because most of the changes in mature tissue appeared around 72hours after inoculation (chapter 3), leaf samples of immature tissue were taken at the same time point, were extracted and a 2D-gelectrophoresis was performed, both for Conférence and Doyenné.

In Conférence, 55 spots of about 2000 spots were differently expressed when comparing mock-inoculated and *Ea*-inoculated immature plant tissue within this cultivar. Thirty of these spots were significantly (p-value<0.05) up-regulated in *Ea*-inoculated tissue, whereas 25 were significantly down-regulated (table 4.6). All these differently expressed spots were excised in an attempt to identify them. The majority of the down-regulated proteins was related to general metabolism pathways, such as photosynthesis (transketolase, large subunit of rubisco), glycolysis (triose phosphate isomerase) and energy production (ATPase and ATP synthase β and γ). The up-regulated proteins were involved in defence mechanisms (lipoxygenase, major allergen genes), energy (ATP synthase ε) and photosynthesis (chlorophyll a/b binding proteins, psbP protein and ferredoxin-$NADP^+$ reductase). For ferredoxin-$NADP^+$ reductase, a 25 times increase in spot abundance was observed (figure 4.11).

In Doyenné, 69 spots of about 2000 spots were differently expressed when comparing mock-inoculated and *Ea*-inoculated immature plant tissue within this cultivar. Thirty-one of these spots were significantly (p-value<0.05) up-regulated in *Ea*-inoculated tissue, whereas 38 were significantly down-regulated (table 4.7). Of the identified spots, the proteins spots which were up-regulated had photosynthetic (Rubisco small subunit and activase) and energetic (ATPase) properties, whereas the down-regulated proteins mainly had functions in general metabolisms (catalase, transferase, aldolase,...), photosynthesis (chlorophyll a/b binding proteins) and glycolysis (glyceraldehyde-3-phosphate dehydrogenase, phosphoglycerate kinase). An isopentenyl-diphosphate Δ-isomerase (secondary metabolism) and an allergen gene (defence) were down-regulated as well (figure 4.11).

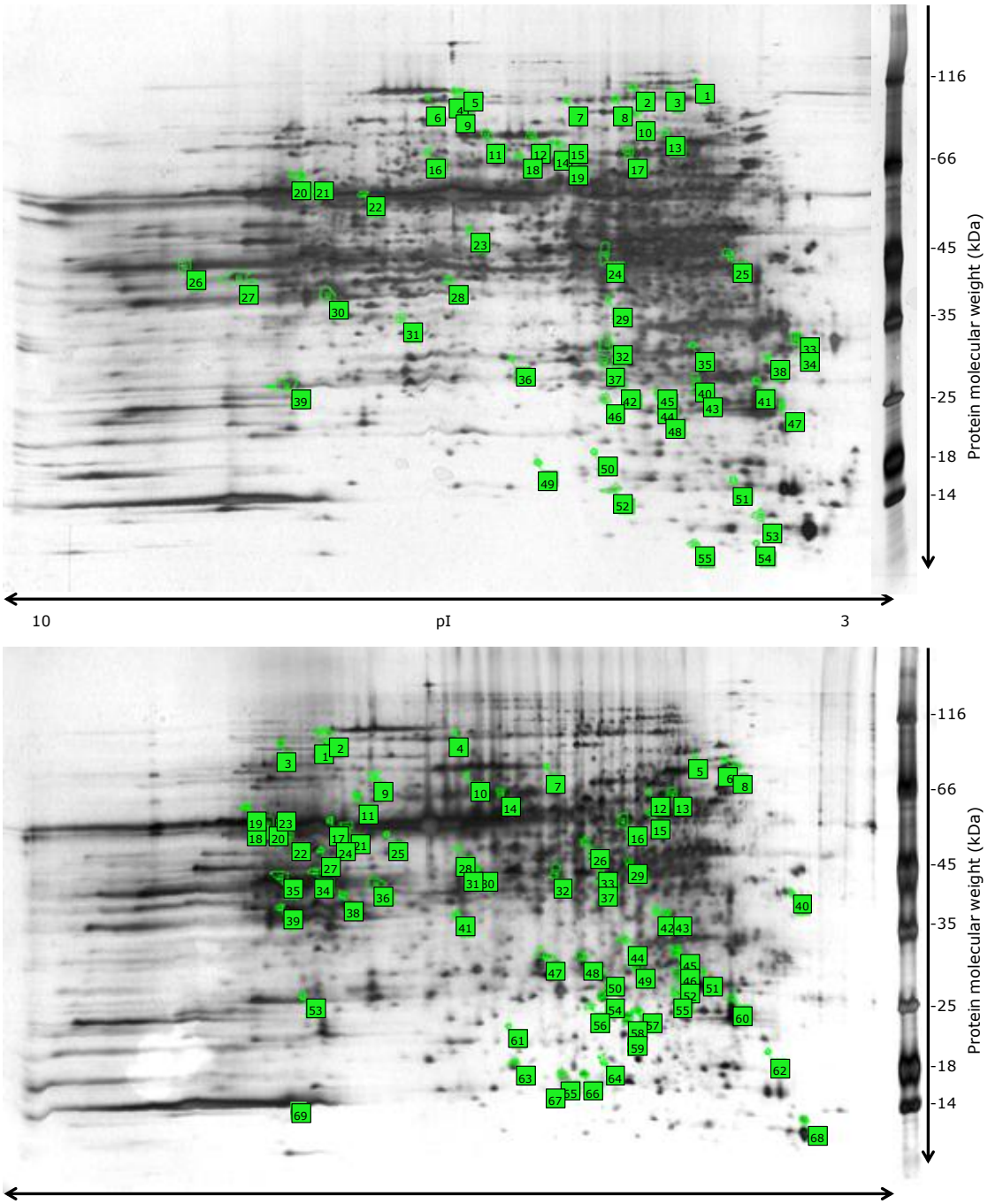

Figure 4.11: Comparison between mock-inoculated and Ea-inoculated leaves leads to 55 differently expressed spots in Conférence (top) and 69 differently expressed spots in Doyenne (bottom), 72h after inoculation.

Table 4.6: Differentially expressed proteins in Conférence, 72h after inoculation.

Spot number	Protein name + accession number	Function	MW (Da)	Fold change
1	Not identified	-	-	-1.29
2	Not identified	-	-	-0.50
3	Not identified	-	-	Only present in mock
4	Not identified	-	-	1.72
5	Not identified	-	-	2.33
6	Not identified	-	-	-0.83
7	Not identified	-	-	Only present in mock
8	Lipoxygenase [*Camellia sinensis*]; gi|213876486	Defence, precursor of metabolic regulators	102378.20	1.76
9	Not identified	-	-	1.70
10	Not identified	-	-	3.12
11	Transketolase 1 [*Capsicum annuum*]; gi|3559814	Pentose phosphate pathway; Photosynthesis	80282.40	-0.64
12	Transketolase 1 [*Capsicum annuum*]; gi|3559814	Pentose phosphate pathway; Photosynthesis	80107.6	-0.72
13	Not identified	-	-	-0.60
14	Not identified	-	-	2.60
15	Not identified	-	-	2.89
16	Not identified	-	-	3.52
17	Not identified	-	-	-0.63
18	Not identified	-	-	-0.33
19	Not identified	-	-	0.64
20	Not identified	-	-	1.82
21	Not identified	-	-	-0.65
22	Ribulose-1,5-bisphosphate carboxylase/oxygenase large subunit [*Cansjera leptostachya*]; gi|112408786	Photosynthesis	51563.60	-0.52
23	Not identified	-	-	Only present in mock
24	Not identified	-	-	-0.53
25	Not identified	-	-	-0.63
26	Not identified	-	-	-0.54
27	Not identified	-	-	-0.64
28	ATP synthase subunit γ, chloroplastic [*Vigna unguiculata*]; gi|110278823	Energy-related processes	41227.00	-0.30
29	Not identified	-	-	1.48

30	Hypothetical protein (Predicted: ferredoxin-NADP$^+$ reductase) [*Vitis vinifera*]; gi|225457947	Photosynthesis	40270.30	25.6
31	Putative ATP synthase β subunit [*Ricinus communis*]; 29923.m000793	Energy-related processes	26829.10	-0.65
32	Not identified	-	-	-0.72
33	Not identified	-	-	-0.57
34	Not identified	-	-	-0.62
35	Not identified	-	-	-0.63
36	Triose phosphate isomerase [*Ficus popenoei*]; gi|161610432	Glycolysis	4259.40	-0.06
37	Not identified	-	-	-0.46
38	Not identified	-	-	-0.58
39	Hypothetical protein POPTRDRAFT_818640-photosystem II reaction center psbP protein [*Populus trichocarpa*]; gi|224085421	Photosynthesis	28140.00	1.60
40	V-ATPase catalytic subunit A [*Prunus persica*]; gi|15982954	Energy-related processes	68573.80	-0.18
41	Not identified	-	-	-0.48
42	Chlorophyll a/b binding protein 8, chloroplastic [*Solanum lycopersicum*]; gi|115813	Photosynthesis	29364.30	2.11
43	Chloroplast chlorophyll a/b binding protein 8 [*Oryza sativa Indica* Group] ; gi|149392115	Photosynthesis	20902.90	3.60
44	Not identified	-	-	2.69
45	Not identified	-	-	3.30
46	Hypothetical protein ARALYDRAFT_483511 [*Arabidopsis lyrata* subsp. *lyrata*]; gi|297828115	Unknown	32167.60	5.93
47	Not identified	-	-	1.72
48	Chloroplast chlorophyll a/b binding protein [*Oenothera elata* subsp. hookeri]; gi|169261102	Photosynthesis	26418.20	1.82
49	Major allergen Pyr c 1 [*Pyrus communis*]; gi|14423877	Pathogenesis-related protein, plant defence	17581.90	2.05
50	Major allergen Mal d 1 [*Malus* x *domestica*]; gi|1313966	Pathogenesis-related protein, plant defence	17579.20	6.83
51	Not identified	-	-	5.00
52	ATP synthase CF1 ε subunit [*Prunus persica*]; gi|313183828	Energy-related processes	14616.00	2.38
53	Not identified	-	-	3.88
54	Not identified	-	-	4.17
55	Not identified	-	-	3.86

Table 4.7: Differentially expressed proteins in Doyenné, 72h after inoculation.

Spot number	Protein name + accession number	Function	MW (Da)	Fold change
1	Not identified	-	-	1.64
2	Not identified	-	-	2.00
3	Not identified	-	-	-0.62
4	Not identified	-	-	2.00
5	Not identified	-	-	4.55
6	Not identified	-	-	1.76
7	Not identified	-	-	7.33
8	Not identified	-	-	2.21
9	Not identified	-	-	3.17
10	Not identified	-	-	2.50
11	Not identified	-	-	-0.44
12	Not identified	-	-	3.17
13	Not identified	-	-	1.38
14	Not identified	-	-	3.69
15	Not identified	-	-	1.48
16	H^+-transporting two-sector ATPase [*Medicago truncatula*]; Medtr3g043810.1	Energy-related processes	67116.80	1.51
17	Glyceraldehyde-3-phosphate dehydrogenase ($NADP^+$) [*Vitis vinifera*]; GSVIVT01013403001	Glycolysis	48119.70	-0.70
18	Not identified	-	-	-0.54
19	Not identified	-	-	-0.21
20	Catalase [*Malus* x *domestica*]; MDP0000147628	General metabolism, stress defence	78209.10	-0.60
21	Serine hydroxymethyltransferase [*Malus* x *domestica*]; MDP0000332596	General metabolism	56850.6	-0.66
22	Not identified	-	-	2.41
23	Not identified	-	-	2.85
24	Not identified	-	-	2.53
25	Not identified	-	-	4.09
26	Phosphoglycerate kinase [*Malus* x *domestica*]; MDP0000174843	Glycolysis	50310.5	-0.61
27	Not identified	-	-	1.90
28	Not identified	-	-	2.64
29	Ribulose-1,5-bisphosphate carboxylase/oxygenase activase [*Cucumis sativus*]; Cucsa.136160.1	Photosynthesis	51737.5	1.92
30	Not identified	-	-	1.60

31	Not identified	-	-	-0.37
32	Not identified	-	-	-0.59
33	Not identified	-	-	-0.52
34	Not identified	-	-	-0.66
35	Not identified	-	-	-0.79
36	Not identified	-	-	-0.58
37	Not identified	-	-	-0.41
38	Not identified	-	-	-0.35
39	Not identified	-	-	3.00
40	Not identified	-	-	2.26
41	Phosphoglycerate kinase [*Malus* x *domestica*]; MDP0000325406	Glycolysis	50310.50	1.62
42	Not identified	-	-	5.7
43	Not identified	-	-	-0.59
44	Not identified	-	-	-0.30
45	Not identified	-	-	-0.57
46	Not identified	-	-	-0.65
47	Not identified	-	-	-0.51
48	Not identified	-	-	-0.75
49	NAD(P)-binding Rossmann-fold superfamily protein [*Citrus clementina*]; clementine0.9_015406m	General metabolism	36008.50	-0.57
50	Isopentenyl-diphosphate Δ-isomerase [*Malus* x *domestica*]; MDP0000198327	Secondary metabolism	57416.90	-0.63
51	Not identified	-	-	-0.20
52	Aldolase-type TIM barrel [*Malus* x *domestica*]; MDP0000134805	General metabolism	31969.90	-0.61
53	Not identified	-	-	2.41
54	Chlorophyll a/b binding protein 8, chloroplastic [*Solanum lycopersicum*]; gi|115813	Photosynthesis	29364.30	-0.66
55	V-ATPase catalytic subunit A [*Prunus persica*]; gi|15982954	Energy-related processes	68573.80	-0.61
56	chloroplast chlorophyll a/b binding protein [*Oenothera elata* subsp. hookeri]; gi|169261102	Photosynthesis	26418.20	-0.44
57	Not identified	-	-	-0.38
58	Not identified	-	-	-0.47
59	Not identified	-	-	-0.64
60	Not identified	-	-	1.39
61	Not identified	-	-	4.00
62	Not identified	-	-	Only present in mock

63	Mal d I type allergen [*Malus* x *domestica*] ; MDP0000942516	Pathogenesis-related protein, plant defence	17539.60	-0.34
64	Not identified	-	-	-0.27
65	Not identified	-	-	-0.86
66	Not identified	-	-	-0.79
67	Not identified	-	-	-0.71
68	Ribulose-1,5-bisphosphate carboxylase small subunit [*Malus* x *domestica*]; MDP0000252890	Photosynthesis	20559.00	2.58
69	Not identified	-	-	-0.62

5. Discussion

Because Conférence and Doyenné du Comice differ in their susceptibility to fire blight, the involvement of the phenylpropanoid-flavonoid pathway for these cultivar dependent differences was examined during an inoculation with the fire blight pathogen *Erwinia amylovora*.
Shoots of two year old pear trees *Pyrus communis* cv. Conférence and Doyenné du Comice were inoculated with *E. amylovora* strain SGB 225/12 or were mock inoculated.
As expected, disease was more pronounced in the *Ea*-inoculated leaves of the more susceptible cultivar Doyenné du Comice, thirteen days after inoculation. However, these symptoms were not visible after nine days and literally bursted out afterwards, making them more severe as in Conférence, where symptoms gradually appeared in the tissue and became visible around the 5th day after inoculation.

To pursue the phenylpropanoid-flavonoid pathway in greater depth and to achieve a better image of the transcription activity in the surrounding leaves, not only mock- and *Ea*-inoculated immature leaf samples (=leaf 4) were taken at specific time points after inoculation, but the transcription profiles of the first leaf above (= leaf 3) the mock- or *Ea*-inoculated leaf and the first leaf below (= leaf 5) the mock- or *Ea*-inoculated leaf were investigated as well. Although the heat maps showed great fluxes within a cultivar, some general conclusions could be established.
First, both Conférence and Doyenné were characterised by a different transcriptional profile when focusing on the phenylpropanoid-flavonoid pathway. In broad senses, transcription profiles were rather down-regulated in Doyenné, whereas Conférence showed more fluctuations during the treatments. Secondly, the relative expression values of the 3rd and 5th leaf seem to coincide with the respectively mock-inoculated or *Ea*-inoculated leaf 4, both in Doyenné as in Conférence. Therefore, the chance that this down-regulation in Doyenné and the fluctuations in Conférence were caused by infection seems to be very unlikely, as the phenylpropanoid-flavonoid related genes in the mock-inoculated leaves more or less followed the same pattern. A systemic reaction as a result of the

wounding of the tissue could be a possible explanation. However, for a systemic acquired resistance (SAR) microbursts of SA via PAL are needed within a few hours after the perception of a biotic or abiotic stress (Dempsey and Klessig, 2012; Dixon *et al.*, 2002; Durrant and Dong, 2004). Felton *et al.* (1999) already demonstrated that silencing of PAL, reduces a SAR, whereas overexpression of PAL results in an enhancement of SAR. *PAL* was down-regulated in our *Ea*-inoculated leaves both for Conférence and Doyenné, making a SA-dependent SAR in the *Ea*-inoculated tissue not plausible. In the mock-inoculated Conférence leaf tissue however, a significant rise in *PAL* can be observed 48h after inoculation, which could indicate that a SAR is being established as a result of the wounding of the tissue.

Another explanation for this transcriptional behaviour is the effect of diurnal, seasonal and environmental influences in both Conférence and Doyenné. Hence, already small differences in light perception, humidity and temperature could affect the circadian rhythms inside the plant and recoordinate the metabolism and the physiology (Izawa, 2012; Mas and Yanovsky, 2009; McClung, 2008; Stitt and Zeeman, 2012).

Last but not least, it seems that infection took its toll. Both *FLS* and *F7GT* reached very low expression values in the *Ea*-inoculated leaf 4 of Conférence after six days, whereas on the other hand the transcription levels of nearly all investigated genes in the *Ea*-inoculated leaf 4 of Doyenné were reduced to the same minimum levels at six days after inoculation. This difference could be explained by the higher susceptibility of Doyenné to fire blight, causing cell death to occur faster and therefore transcripts in the whole pathway to reach very basal levels more quickly. These very low expression values were not reached in leaf 3 and leaf 5, suggesting infection did not reached these leaves yet.

Looking at the results of the HPLC analysis, a clear distinction between Conférence and Doyenné could be made, as flavonols, simple phenolics, cis-ferulic acid and all proanthocyanidins had substantial higher concentrations in Doyenné. The fact that the transcription levels of most phenylpropanoid-flavonoid related genes in Doyenné decreased during the experiment, could indicate that these high levels of secondary metabolites were already present as preformed molecules before the experiment took place. No clear differences

between the treatments could be observed, assuming that the effect of the phenylpropanoid-flavonoid pathway in a defence-related framework is minor in the immature leaves of both Conférence and Doyenné. The higher concentrations of epicatechin in the very susceptible cultivar Doyenné (4-6 times higher) compared to moderately susceptible cultivar Conférence makes us assume that a natural high level of epicatechin (and maybe other polyphenols) as preformed defence molecules do not automatically guarantee a high level of protection against *E. amylovora* in *Pyrus*, but that the generation of a time-dose dependent relationship seems to be more important in this part of the defence mechanism as demonstrated in figure 4.12. An equal type of correlation has already been demonstrated by Davey *et al.* (2007) who found that the susceptibility of fruits of different apple genotypes to postharvest infection with Botrytis cinerea decreases with increasing harvest date and that susceptibility is correlated with fruit vitamin C levels. Hence, epicatechin has to be present at the site of inoculation in order to act as an antioxidative quencher, as an ultrastructural defence molecule or as a direct toxin in the leaves.

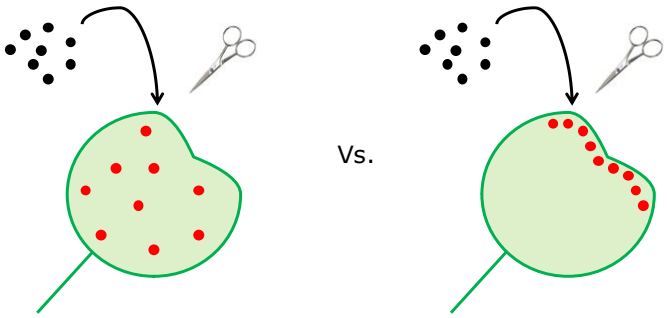

Figure 4.12: The hypothetical distribution of epicatechin (red) after inoculation with *E. amylovora* by scissors (black). It could be that epicatechin is more effective against fire blight when these molecules are present at the site of inoculation (right figure).

The fact that immature leaves probably not rely on the activity of the phenylpropanoid-flavonoid pathway does not necessarily mean that those leaves are not able to adapt their metabolism to a pathogen nor that they have defence mechanisms lacking. Therefore, a proteomic approach was conducted to receive vital information about protein expression in samples 72hours after inoculation for this specific plant-pathogen interaction in both Conférence and Doyenné.

First of all, it is very difficult to make extensive conclusions, as in Conférence only 29% of the spots was identified and in Doyenné no more than 22%. The

reason for these low percentages is mentioned in the introduction, namely the still unsequenced genome and the rare EST databases of *Pyrus*.

In Conférence, 55 spots were differently expressed when comparing mock-inoculated and *Ea*-inoculated immature plant tissue. In general, both energy production and photosynthesis seem to be affected by the fire blight infection.

ATPase A, ATP synthase β and ATP synthase γ were of a lower abundance, whereas ATP synthase ε occurred in a much higher level. ATPases are multimeric enzymes that catalyse the hydrolysis of ATP and are the primary pumps responsible for the establishment of membrane potential *in planta* (Cipriano *et al.*, 2008). Oppositely, ATP synthase generates the synthesis of ATP. Elmore and Coaker (2011) suggest that ATPases -due to their importance in regulating basic aspects of plant cell function, stomatal closure and nutrient transport- are dynamically regulated during plant immune responses, especially those that are located in the plasma membrane. In that way, the effect of the fire blight pathogen on ATPases and ATP synthases could indicate a serious rearrangement of the energy production and nutrient distribution inside the plant.

The fact that photosynthesis was affected by infection is shown by PEA measurements, indicating a lowered photosynthetic capacity starting four days after inoculation. Seventy-two hours after inoculation, transketolases and the large subunit of Rubisco were down-regulated, whereas chlorophyll a/b binding proteins, a psbP protein and Fd-$NADP^+$ reductase were all up-regulated. Particularly the Fd-$NADP^+$ reductase is of great interest, as it was 25 times more present in the *Ea*-inoculated leaf tissues. Ferredoxin–$NADP^+$ reductase mediates the final step of photosynthetic electron flow by transferring electrons from ferredoxin to $NADP^+$ with the concomitant generation of reducing power (NADPH). This NADPH is then used for carbon fixation, nitrogen metabolism, lipid and chlorophyll biosynthesis, as well as for stromal redox regulation. The rise of ferredoxin–$NADP^+$ reductase is in agreement with the work of Jones *et al.* (2006), who investigated defence mechanisms in *Arabidopsis* after inoculation with *Pseudomonas syringae*, and with the work of Dahal *et al.* (2010), who studied the tomato-*Ralstonia solanacearum* pathosystem. The enormous increase could suggest a last remedy to account for the loss in photosynthesis near PS II, as already transketolases and Rubisco are affected by infection.

Besides these general metabolisms of photosynthesis and energy housekeeping, major allergen genes and lipoxygenases were significantly up-regulated in *Ea*-inoculated leaves. Both protein families are related to defence. Major allergen genes are intracellular proteins belonging to family 10 of the pathogenesis-related proteins (Van Loon and Van Strien, 1999), which are up-regulated upon stress and pathogen attack. This increase is in agreement with studies conducted by Mayer *et al.* (2011) and Heyens *et al.* (2006), who both noticed an increase of Mal d1 in *Ea*-inoculated apple seedlings. Lipoxygenases (LOX) are non-heme containing dioxygenases that catalyse the conversion of polyunsaturated fatty acids with a (Z,Z)-1,4-pentadiene structure into conjugated unsaturated hydroperoxy fatty acids, which in turn are further metabolized via seven different pathways into multiple biologically active oxylipins including jasmonic acid (JA), green leaf volatiles and divinyl ethers (Andreou and Feussner, 2009). Several studies have suggested a role in cellular defense for 9-LOX and 13-LOX in particular by positively affecting the jasmonic acid pathway or by producing antimicrobial compounds (Howe and Schilmiller, 2002), which could also be true for a fire blight infection in pear.
In Doyenné, 69 spots were differently expressed when comparing mock-inoculated and *Ea*-inoculated immature plant tissue. Just like in Conférence, ATPase A was down-regulated. Besides a suppression of the small subunit of Rubisco and Rubisco activase, chlorophyll a/b binding proteins –in contrast to Conférence- decreased as well, indicating that photosynthesis is being tackled. PEA measurements confirmed these photosynthetic imbalances. Furthermore, glycolysis, which is responsible for the production of pyruvate out of glucose thereby releasing free energy, seemed to be disturbed as glyceraldehyde-3-phosphate dehydrogenase was decreased and phosphoglycerate kinases showed opposite reactions. Surprisingly, an isopentenyl-diphosphate delta-isomerase, a catalase and a Mal d1 allergen gene, which are all proteins that could take part in defence-related mechanisms were down-regulated as well. It could be that the decrease in these proteins could partly explain the higher susceptibility of Doyenné for fire blight.

In conclusion, Conférence and Doyenné reacted in different ways to an inoculation of the immature leaves with fire blight. Although the

phenylpropanoid-flavonoid pathway seemed to have a minor effect in immature leaves of both cultivars, a clear difference in polyphenolic activity between cultivars was noticed, as transcripts were immediately down-regulated in Doyenné, whereas transcripts in Conférence appeared to fluctuate more during the experiment. No induction of the investigated transcripts was noticed in the leaf above and below the *Ea*-inoculated leaf.

The high natural concentrations of epicatechin in the very susceptible cultivar Doyenné compared to moderately susceptible cultivar Conférence could put forward that a natural high level of epicatechin (and maybe other polyphenols) as preformed defence molecules do not automatically guarantee a high level of protection against *E. amylovora* in *Pyrus*, but the generation of a time-dose dependent relationship seems to be more important in this part of the defence mechanism. These induced metabolites can then act as an antioxidant, as a defence barrier strategy or as toxic compound against the bacteria. However, more evidence and further research are needed to test this hypothesis.

When digging deeper into the proteome and although not all spots were identified, both cultivars seem to adapt their energy-related metabolic and photosynthetic processes. However, in Conférence, the increased amount of defence related major allergen genes and lipoxygenases could suggest a better dealing of the built-up stress caused by *E. amylovora* compared to Doyenné and could partially explain the higher susceptibility of Doyenné to fire blight.

Chapter 5:

Influence of a heat shock on defence mechanisms against *E. amylovora* in *Pyrus*

1. Introduction

Plant defence mechanisms can be triggered by a wide variety of commercial products. For fire blight, these products are limited to the use of benzothiadiazole (Actigard®, Bion®, Blockade® or Boost®), prohexadione-Ca (Apogee® or Regalis®), phosetyl-Al (Aliette®), Laminarin (Vacciplant®) and harpin protein (Employ® or Harp-N-Tek®). However, it is also possible to increase the defence of a plant by using alternative methods, such as a short-time application of UV radiation, which alters the resistance against certain insects and fungi (Kunz *et al.*, 2008; Schreiner *et al.*, 2012; Stratmann, 2003).

The method that is investigated here, is the application of a short-period heat shock. In fruit and wine culture often trailed heated air cannons are used to protect developing blossoms against possible frost damage or to improve fruit set during periods of low day temperatures. Hot air of about 80°C-100°C is blown out of an outlet into the trees in a certain time interval, thereby covering up a distance of a few meters at each side of the machine. If heat treatments proof to be beneficial in triggering possible defence mechanisms, fruit growers could apply this strategy against *Erwinia amylovora* (and other pathogens).
After all, temperature is a very important factor in plant growth, as plants are highly sensitive to temperature differences and are able to distinguish even the slightest differences of as little as 1°C (Lee *et al.*, 2012). Temperature is sensed by an alteration in membrane fluidity, in specific the proportion of saturated and unsaturated fatty acids, suggesting that sensory devices are located in certain microdomains of membranes, capable of detecting physical phase transition and eventually leading to conformational changes and/or phosphorylation and dephosphorylation events. In a following step, phospolipase D and a phosphatidylinositolphosphate kinase are activated, resulting in the generation of a Ca^{2+} cascade and the opening of Ca^{2+} channels. These increased Ca^{2+} levels are then sensed by specific calcium-dependent effectors, such as calmodulin and calmodulin-like proteins, calcineurin B-like proteins and calcium-dependent protein kinases. The sensing and signalling of Ca^{2+} is connected and cannot be dissociated as the sensing event immediately implies the transmission of the

perceived signal and the signalling event implies that a signal was sensed (Conde *et al.*, 2011; Lee *et al.*, 2012; Saidi *et al.*, 2011).

In a next phase, heat stress transcription factors are the crucial regulators of the signal transduction pathways mediating the activation of heat shock-induced transcripts and heat shock proteins, which are proposed to act as molecular chaperones in protein quality control and which will accumulate within days and therefore weaken adverse effects from heat stress. The general purpose of these sophisticated and efficient mechanisms is to attenuate the amount of misfolded or unfolded proteins, to detoxify the cell, to accumulate compatible solutes and osmoprotectants, to rearrange solute transport and compartmentation and finally to re-establish and maintain ion and cellular homeostasis (Conde *et al.*, 2011).

Together with these transcriptional changes, plants will respond to acute heat stress by the modulation of plant hormones, primary and secondary metabolites (Wahid *et al.*, 2007), by producing reactive oxygen species (Locato *et al.*, 2008) and by closing stomata to prevent any transpirational water loss (Mahajan and Tuteja, 2005). This process of stomatal closure is referred to as hydropassive closure when the closure results from direct evaporation of water from the guard cells with no metabolic involvement, and is referred to as hydroactive closure when the closure is metabolically dependent and requires the regulation by hormones, in particular abscisic acid (ABA). This stomatal closure also results in a decline in the rate of photosynthesis and probably affects the general photosynthetic machinery during a heat shock.

Little is known how plant immunity and heat resistance are interconnected, but although the responsible Ca^{2+} channel still needs to be discovered, it is known that just like in heat perception, Ca^{2+} plays a distinct role in plant defence, as both PAMPs and pathogens are able to affect Ca^{2+} influx. Generally, it is believed that the combination of biotic stress and higher temperatures both work in an antagonistic manner. For instance, it was reported that high temperatures cause higher susceptibility to *Pseudomonas syringae* in both *Arabidopsis thaliana* and *Nicotiana benthamiana* (Wang *et al.*, 2009b) and to Tobacco Mosaic Virus, *Oidium neolycopersici*, root-knot nematodes and *Cladosporium fulvum* in tomato (de Jong *et al.*, 2002; Hwang *et al.*, 2000; Prokopova *et al.*, 2010; Whitham *et al.*, 1996). But whether the application of heat shocks really improves or

counteracts a plant's defence mechanism, still remains an open question in many other pathosystems.

2. Objective

Because temperature perception is very important in plants, the effect of the application of a heat shock in pear leaves of the moderately susceptible cultivar Conférence was investigated. The goal is to know if the phenylpropanoid-flavonoid pathway is stimulated in the heat shock-treated plants and if this has a positive, a negative or no effect at all on the plant's response to the fire blight pathogen *Erwinia amylovora*. If heat shocks prove to be valuable against *E. amylovora*, fruit growers could use trailed heated air cannons as an extra alternative method to fight fire blight infections.

Therefore, two-year-old pear trees *Pyrus communis* cv. Conférence were put in a climate chamber at 60°C for 15min, as heat shocks above 40°C are needed to induce changes such as the activation of heat shock proteins (Wang *et al.*, 2004). The day after, they were inoculated with *E. amylovora* strain SGB 225/12 or were mock inoculated.

Leaf samples were taken at specific time points after inoculation and the expression pattern of phenylpropanoid-flavonoid pathway related genes of not necrotic tissue close to the inoculation site was analysed with RT-qPCR.

In addition, chlorophyll fluorescence measurements were executed using PEA equipment to visualise the effect of the bacteria on the global photosynthesis in the plant and to detect possible differences in susceptibility between the heat shock treated and untreated plants based on photosynthesis.

Last but not least, a proteomic approach was performed to receive vital information about the effect of a heat shock on other proteins in this specific plant-pathogen interaction. The time point "72hours after inoculation" was again favoured to do proteomics on.

3. Material & methods

3.1 Experimental design

Two-year-old trees (*Pyrus communis*) of the moderately susceptible cultivar Conférence on Quince C rootstock were grown in containers of 20l in a greenhouse (pcfruit, Kerkom, Belgium) in a controlled environment to maintain a temperature of 22°C, a relative humidity of 60% and a minimal light intensity of 150 µmol $m^{-2}s^{-1}$. When still in the active growing phase, trees were put in a climate chamber with a temperature of 22°C during 15min (= no heat shock) or were put in a climate chamber with a temperature of 60°C during 15min (= heat shock). Afterwards, they were set back to a quarantine protected greenhouse.

During the heat shock, it was noticed that several leaves started to wilt, indicating that the heat shock had an effect, but these symptoms disappeared the day after. A highly aggressive *E. amylovora* strain (BG16, isolated from *Malus sylvestris* (Bulgaria) with collection number SGB 225/12) was cultivated at a temperature of 25°C on YPGA growth medium. After 24 hours, a suspension liquid of these bacteria was prepared in a PBS buffer at a density of 10^8 CFU ml^{-1} and used for inoculations.

For inoculation with *E. amylovora*, only the fourth leaf was cut perpendicular to the main vein with scissors dipped in the bacterial suspension liquid. For mock-inoculated leaves, scissors were dipped in PBS. To recover from the heat shock , trees were inoculated one day after the application of the heat shock. Only active growing shoots containing a minimum of eight leaves were inoculated when they reached an average length of 25cm.

The following experimental design was applied: (a) Mock-inoculated leaves without heat shock, (b) Mock-inoculated leaves with heat shock, (c) *Ea*-inoculated leaves without heat shock and (d) *Ea*-inoculated leaves with heat shock (figure 5.1).

Total leaf samples were taken 3h, 24h, 48h and 72h after inoculation. Leaf samples were stored at -80°C for further analysis with RT-qPCR and proteomics.

The progression of the shoot infection was measured 7 and 9 days after inoculation according to the formulae of chapter 3.

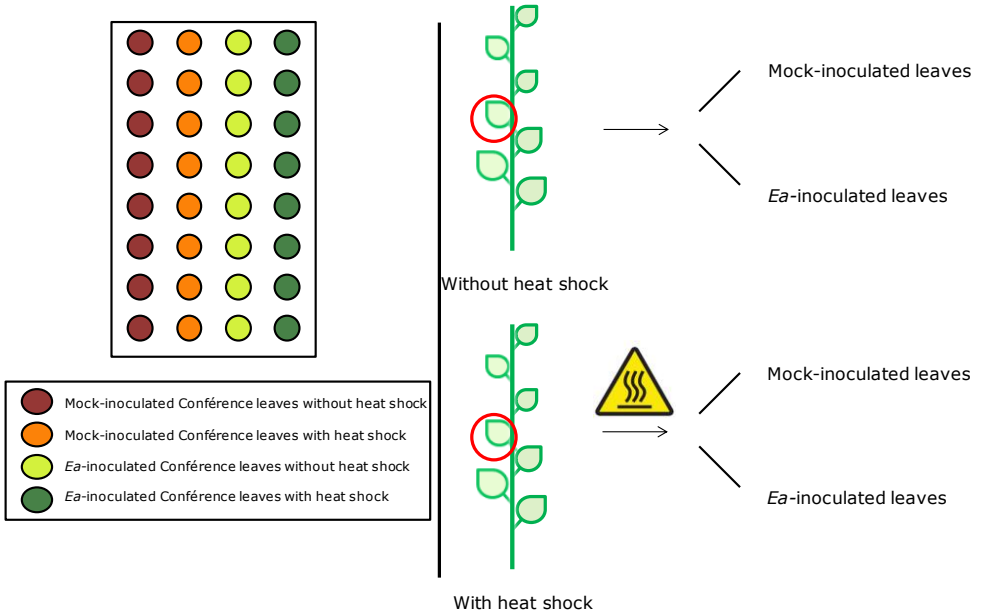

Figure 5.1: Experimental design with the different treatments (left) and the sampling of the heat shock in Conférence (right)

3.2 RT-qPCR

RT-qPCR techniques were performed in the same manner as mentioned in chapter 3. The primers were the same as in table 3.1. Reference genes coding for an elongation factor *ef1-a* (CN941921 derived from source file DQ341381.1) and an elongation factor *ef4-a* (Malus_v4_Contig5101 derived from source file AY347787.1) were used to normalise the data. Eight biological replicates were used per treatment.

3.3 Proteomics

The extraction procedure, the protein clean-up and quantification, the iso-electric focusing, the 2-D gel electrophoresis, the silver staining, the spotpicking and protein digestion, the mass spectrometric analysis and protein identification were all performed as written in the previous chapter. Three gels were analysed per treatment.

3.4 Chlorophyll fluorescence

Chlorophyll fluorescence measurements with the PEA were performed in the same manner as mentioned in chapter 3. The photosynthetic efficiency was analysed on mock-inoculated and *Ea*-inoculated leaves of Conférence, both with or without heat shock. Per treatment, six leaves were measured with the PEA. After thirty minutes dark adaptation, chlorophyll fluorescence induction curves were measured using a PEA as described in chapter three.

Trees were measured before inoculation (= the day after the heat shock application) and 3h, 24h, 48h, 72h and 7 days after inoculation.

3.5 Statistics

For RT-qPCR data, the different treatment means were respectively subjected to a 2-way ANOVA with Tukey's pairwise comparisons. All data were tested for their equality of variances using a Levene's test and for their normal distribution using a Shapiro-Wilk test.

PEA data were subjected to a pairwise comparison for their different parameters.

Proteomic data were statistically analysed through to the ImageMaster Platinum Software.

Outliers were excluded based on a maximum normed residual test for all data. All statistical analyses were performed using the SAS 9.2 software.

4. Results

4.1 Symtom development

The development of the shoot infection in mock-inoculated and *Ea*-inoculated Conférence trees was measured 7 and 9 days after inoculation. The mock-inoculated leaves and shoots showed no visual signs of infection. *Ea*-inoculated leaves however did show disease symptoms. The TH3 values were higher nine DAI when the inoculation was performed without an heat shock (table 5.1). However, when focusing only on the total percentage of necrosis in the shoots, the *Ea*-inoculated leaves with and without heat shock were in the same close range, both seven and nine days after inoculation (table 5.2).

Table 5.1: Shoot infection values expressed as TH3 values, measured 7 and 9 days after inoculation, p<0.001 (Tukey)

TH3 value	7DAI		9DAI	
Mock inoculation without heat shock	0.00	a[1]	0.00	a
Mock inoculation with 15min heat shock	0.00	a	0.00	a
Ea-inoculated leaves without heat shock	47.83	b	91.30	c
Ea-inoculated leaves with 15 min heat shock	40.35	b	64.91	b

[1]Means in a column followed by the same letter do not differ significantly

Table 5.2: Percentage of necrosis in the shoot, measured 7 and 9 days after inoculation, p<0.001 (Tukey)

% of necrosis in the shoot	7DAI		9DAI	
Mock inoculation without heat shock	0.00	a[1]	0.00	a
Mock inoculation with 15min heat shock	0.00	a	0.00	a
Ea-inoculated leaves without heat shock	2.87	a	48.26	b
Ea-inoculated leaves with 15 min heat shock	3.58	a	39.22	b

[1]Means in a column followed by the same letter do not differ significantly

4.2 RT-qPCR indicates a down-regulation of some phenylpropanoid-flavonoid related genes in heat shock treated plants

To present the data, a heat map was chosen as representation manner for the mock- and *Ea*-inoculated leaf. With the heat map representation, some genes analysed with quantitative reverse transcription PCR showed different expression patterns, especially when a heat shock was applied (table 5.3).

For *CHS*, *FHT*, *ANS* and *ANR*, both the heat shock treated mock-inoculated and *Ea*-inoculated leaves showed decreased relative expression values 3h and 24h after inoculation. Forty-eight and 72h after inoculation, the activity for all treatments rose again to a value of about 1.00 and higher, but was generally lower in the heat shock treated trees than the trees that did not received a heat shock.

The same lowered values were observed for *DFR* and *LAR1,* but in contrast with the transcripts of *CHS*, *FHT*, *ANS* and *ANR*, these values remained more or less below 1.00, both 48h and 72hours after inoculation. The activity of both genes 48h after inoculation was significantly lower when a heat shock was applied. The relative expression values of *FLS* instead were low in the heat shock treated *Ea*-inoculated leaves compared to the other treatments, both 3h, 24h and 48h after inoculation. Seventy-two hours after inoculation, the *FLS* transcripts in both *Ea*-inoculated treatments were lower than the mock-inoculated treatments. Finally, the transcription activities of *F7GT* and *PAL* more or less stayed constant during the experiment.

Table 5.3: Heat map representation of the relative expression values for all investigated genes for the different treatments in Conférence (s h.s. = sine heat shock, c h.s. = cum heat shock), x hours after inoculation. Each cell represents a relative expression value according to the colour scale at the bottom. Values in the cell are mean ± SE of 8 biological independent replicates. Gene expression data were expressed relatively to the reference genes and to the values of mock-inoculated leaves without a heat shock, 3hours after inoculation (= relative expression value of 1) following the $2^{-\Delta Ct}$ method divided by the geometric mean of the reference genes. Mean values are followed by a letter. If values have the same letter, they do not differ significantly. Statistics are performed by a 2-way anova. For enzyme abbreviations, see text.

Treatment\gene		*PAL*	*CHS*	*FHT*	*FLS*	*F7GT*	*DFR*	*LAR1*	*ANS*	*ANR*
3h	Mock-inoc. leaves s h.s.	1.00 ±0.14 **a**	1.00 ±0.42 **a**	1.00 ±0.30 **a**	1.00 ±0.31 **ab**	1.00 ±0.10 **a**	1.00 ±0.42 **ab**	1.00 ±0.06 **a**	1.00 ±0.40 **a**	1.00 ±0.24 **a**
	Ea-inoc. leaves s h.s.	1.82 ±0.31 **a**	0.74 ±0.09 **a**	1.92 ±0.54 **a**	1.22 ±0.06 **b**	1.05 ±0.15 **a**	1.31 ±0.26 **b**	0.91 ±0.08 **a**	2.10 ±0.82 **a**	1.30 ±0.17 **a**
	Mock-inoc. leaves c h.s.	1.12 ±0.25 **a**	0.30 ±0.08 **a**	0.52 ±0.10 **a**	0.91 ±0.08 **ab**	1.15 ±0.20 **a**	0.17 ±0.06 **a**	0.52 ±0.27 **a**	0.20 ±0.07 **a**	0.70 ±0.32 **a**
	Ea-inoc. leaves c h.s.	0.99 ±0.24 **a**	0.17 ±0.08 **a**	0.62 ±0.19 **a**	0.56 ±0.11 **a**	1.22 ±0.15 **a**	0.12 ±0.03 **a**	0.47 ±0.12 **a**	0.20 ±0.04 **a**	0.38 ±0.04 **a**
24h	Mock-inoc. leaves s h.s.	1.87 ±0.14 **a**	1.08 ±0.23 **a**	1.13 ±0.17 **a**	2.59 ±0.30 **a**	1.52 ±0.19 **a**	1.10 ±0.34 **b**	0.83 ±0.18 **a**	0.92 ±0.26 **a**	1.77 ±0.43 **a**
	Ea-inoc. leaves s h.s.	2.50 ±0.56 **a**	1.13 ±0.18 **a**	1.40 ±0.36 **a**	2.55 ±0.61 **a**	0.98 ±0.07 **a**	0.80 ±0.19 **ab**	0.51 ±0.05 **a**	1.66 ±0.64 **a**	2.25 ±0.83 **a**
	Mock-inoc. leaves c h.s.	1.63 ±0.61 **a**	0.78 ±0.40 **a**	0.78 ±0.28 **a**	1.77 ±0.64 **a**	1.15 ±0.32 **a**	0.45 ±0.24 **ab**	0.80 ±0.40 **a**	0.29 ±0.22 **a**	1.14 ±0.54 **a**
	Ea-inoc. leaves c h.s.	0.74 ±0.11 **a**	0.29 ±0.10 **a**	0.46 ±0.06 **a**	0.94 ±0.25 **a**	0.74 ±0.15 **a**	0.18 ±0.06 **a**	0.26 ±0.06 **a**	0.42 ±0.20 **a**	0.54 ±0.14 **a**
48h	Mock-inoc. leaves s h.s.	2.39 ±0.21 **ab**	1.93 ±0.50 **ab**	1.84 ±0.20 **ab**	2.49 ±0.19 **b**	2.00 ±0.35 **a**	2.40 ±0.51 **bc**	1.39 ±0.08 **b**	3.95 ±0.66 **ab**	3.50 ±0.62 **ab**
	Ea-inoc. leaves s h.s.	4.03 ±1.18 **b**	2.85 ±0.25 **b**	2.71 ±0.24 **b**	1.63 ±0.40 **ab**	1.49 ±0.34 **a**	3.73 ±0.36 **c**	1.50 ±0.20 **b**	5.91 ±1.22 **b**	6.65 ±0.65 **b**
	Mock-inoc. leaves c h.s.	1.17 ±0.34 **a**	1.02 ±0.46 **a**	1.02 ±0.26 **a**	1.16 ±0.24 **a**	1.49 ±0.16 **a**	0.42 ±0.10 **a**	0.36 ±0.12 **a**	0.99 ±0.44 **a**	1.20 ±0.30 **a**
	Ea-inoc. leaves c h.s.	1.73 ±0.53 **ab**	1.16 ±0.37 **a**	1.24 ±0.31 **a**	0.68 ±0.15 **a**	0.93 ±0.16 **a**	1.09 ±0.45 **b**	0.66 ±0.15 **a**	2.10 ±0.95 **a**	2.52 ±0.80 **a**
72h	Mock-inoc. leaves s h.s.	2.59 ±0.39 **a**	2.27 ±0.69 **a**	1.50 ±0.13 **ab**	1.89 ±0.42 **b**	1.85 ±0.20 **b**	2.44 ±0.74 **a**	1.77 ±0.45 **a**	3.96 ±1.34 **a**	2.49 ±0.20 **a**
	Ea-inoc. leaves s h.s.	3.94 ±1.80 **a**	3.57 ±5.45 **a**	2.77 ±0.85 **b**	0.68 ±0.03 **ab**	2.22 ±0.79 **b**	2.57 ±2.01 **a**	1.29 ±0.99 **a**	7.25 ±5.57 **a**	7.56 ±8.94 **a**
	Mock-inoc. leaves c h.s.	2.14 ±0.22 **a**	1.57 ±0.28 **a**	1.25 ±0.18 **a**	1.47 ±0.04 **ab**	1.43 ±0.07 **ab**	1.02 ±0.28 **a**	0.85 ±0.09 **a**	1.25 ±0.37 **a**	1.84 ±0.19 **a**
	Ea-inoc. leaves c h.s.	1.67 ±0.42 **a**	0.78 ±0.24 **a**	0.95 ±0.27 **a**	0.49 ±0.13 **a**	0.82 ±0.19 **a**	0.57 ±0.17 **a**	0.73 ±0.18 **a**	1.44 ±0.70 **a**	1.92 ±0.37 **a**

4.3 Chlorophyll fluorescence measurements indicate a negligible effect on photosynthesis after the heat shock

Chlorophyll fluorescence measurements with the PEA were performed on mock-inoculated leaves without a heat shock, on mock-inoculated leaves with a heat shock, on *Ea*-inoculated leaves without a heat shock and on *Ea*-inoculated leaves with a heat shock.

Because most of the described PEA parameters in table 3.5 (chapter 3) utilise the specific time points of the OJIP transient curve in their formulae and to decrease the large amount of data, there was opted to mention only these OJIP transient curves together with their normalised Fvf curves.

Before inoculation, fluorescence reached levels between 2500 and 3000mV. Seventy-two hours after inoculation, the fluorescence levels of the mock-inoculated trees were significantly higher than those in the *Ea*-inoculated leaves, independent of the heat shock. At that time point, it seemed that the effect of a heat shock was negligible in these trees, as the mock-inoculated and the *Ea*-inoculated leaves each followed their own pattern (figure 5.2). The normalised transient FvF showed no real differences 72h after infections, and therefore not leaving behind any indications concerning a reduced electron capacity e.d. (figure 5.3).

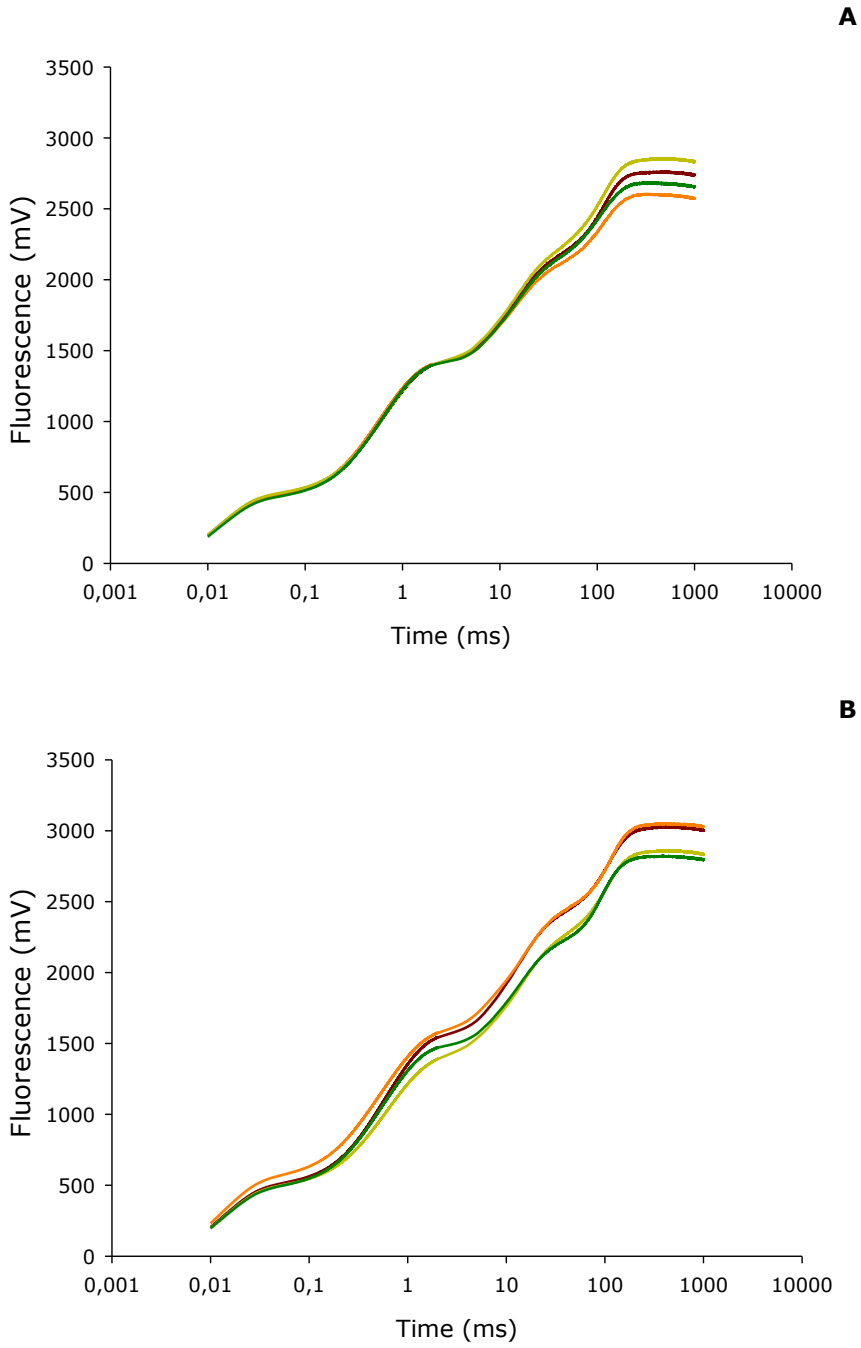

Figure 5.2: OJIP transient curves of mock-inoculated leaves without heat shock (■), mock-inoculated leaves with 15min heat shock (■), *Ea*-inoculated leaves without heat shock (■) and *Ea*-inoculated leaves with 15min heat shock (■), before inoculation (A) and 72h after inoculation (B).

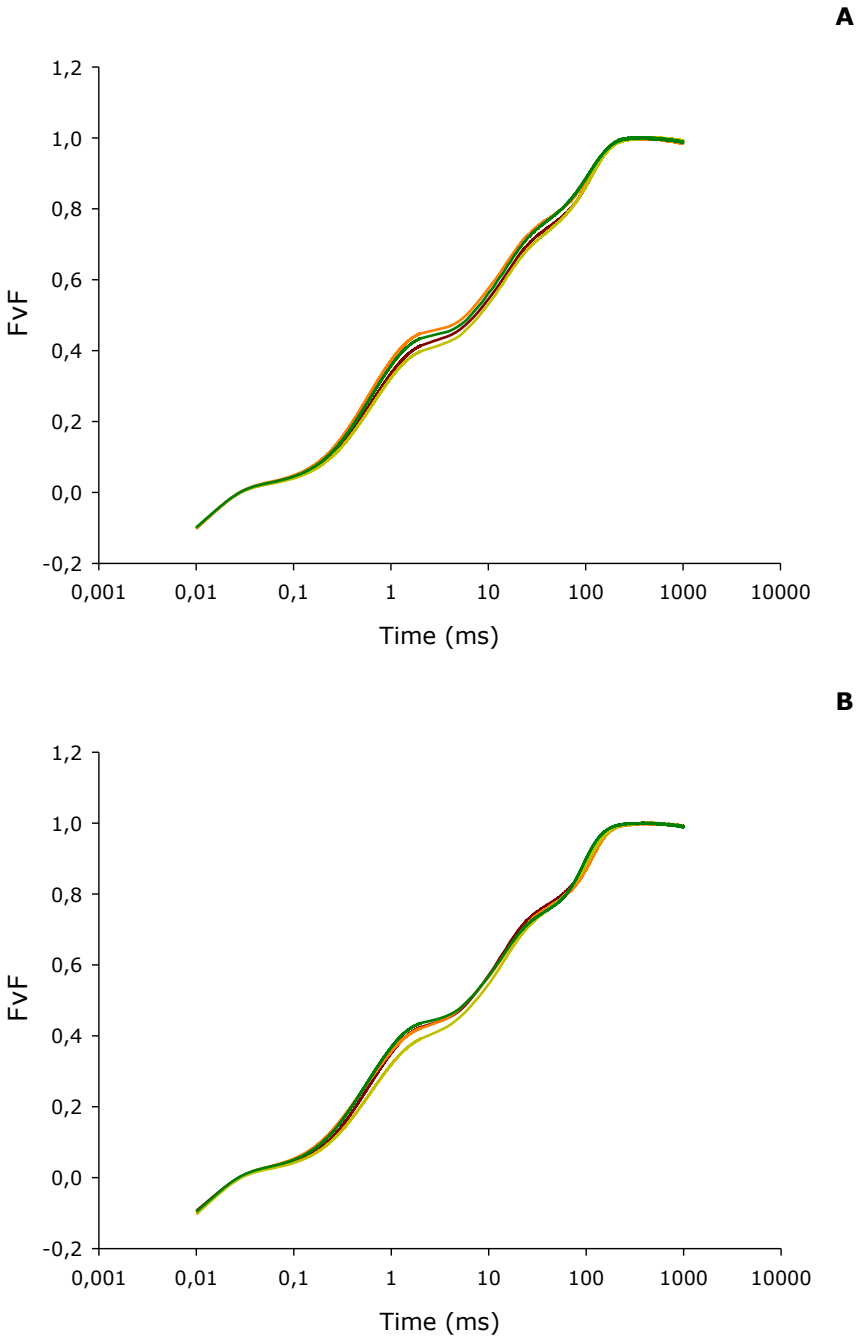

Figure 5.3: Normalised FvF curves of mock-inoculated leaves without heat shock (■), mock-inoculated leaves with 15min heat shock (■), *Ea*-inoculated leaves without heat shock (■) and *Ea*-inoculated leaves with 15min heat shock (■),, before inoculation (A) and 72h after inoculation (B).

4.4 Proteomics demonstrates differentially expressed spots after a heat shock and inoculation with *E. amylovora*

Because most of the changes in mature tissue appeared around 72hours after inoculation (chapter 3), leaf samples of immature tissue were taken at this time point, were extracted and a 2D-gelelectrophoresis was performed.

In Conférence, 70 spots of about 2000 spots were differently expressed when comparing mock-inoculated and *Ea*-inoculated immature plant tissue without a heat shock (figure 5.4). Twenty of these spots were significantly (p-value<0.05) up-regulated in *Ea*-inoculated tissue, whereas 50 spots were significantly down-regulated (table 5.4). All these differently expressed spots were excised in an attempt to identify these spots. Of the spots that could be identified, the majority of the down-regulated proteins were related to photosynthesis and PS II in particular (Magnesium chelatase, Fd-$NADP^+$ reductase, PS II oxygen-evolving enhancer protein 1 and 2, predicted PS II reaction center PSB28 and a 31kDa ribonucleoprotein). Furthermore, the expression of proteins belonging to general metabolic pathways decreased for haloacid dehydrogenase, hydrolase protein, serine endopeptidase, alanine-2-oxoglutarate aminotransferase, etc. An isopentenyl-diphosphate Δ-isomerase, involved in secondary metabolism and a monodehydroascorbate reductase, involved in glycolysis, were attenuated as well. Although a bet v I allergen was down-regulated in *Ea*-inoculated tissue, some of the up-regulated proteins were clearly involved in defence-related mechanisms (thaumatin-like protein, germin-like protein and quinone reductase). Furthermore, some photosynthesis-related proteins (Rubisco small chain protein, carbonic anhydrase and Rieske iron-sulphur protein) increased, just like a glutathione synthesis-related protein (Lactoylglutathione lyase) and cell wall synthesising proteins (3R-hydroxymyristoyl ACP dehydrase and xyloglucan:xyloglucosyl transferase).

When applying a heat shock of 60°C during 15min, 97 spots of about 2000 spots were differently expressed 72h after inoculation when comparing mock-inoculated and *Ea*-inoculated immature plant tissue (figure 5.4). Twenty-six of these spots were significantly (p-value<0.05) up-regulated in *Ea*-inoculated tissue, whereas 71 were significantly down-regulated (table 5.5). Of the identified spots, the proteins spots which increased in expression had

photosynthetic (Rubisco large subunit, chlorophyll a/b binding protein, a chloroplast precursor and the Rieske iron-sulphur protein) and energetic (ATPase subunit b and d) properties. Besides these functions, proteins involved in general metabolisms such as cyclophilin, disulfide reductase,... and plant defence (Pyr c 1 allergen) were up-regulated as well.

On the other hand, several proteins involved in photosynthesis (plastocyanin, PS II oxygen-evolving enhancer protein, phosphoribulokinase, fructose bisphophate, ...), energy related processes (ATPase and ATP synthases) and different members of the family of kinases (nucleoside-diphosphate kinase, phosphoglycerate kinase, pyrophosphate-dependent phosphofructokinase, ...) were down-regulated. When comparing both treatments (with or without a heat shock), both the Rieske iron-sulphur protein together with some Rubisco fragments increased, whereas Fd-$NADP^+$ reductase and the PS II oxygen-evolving enhancer protein both decreased.

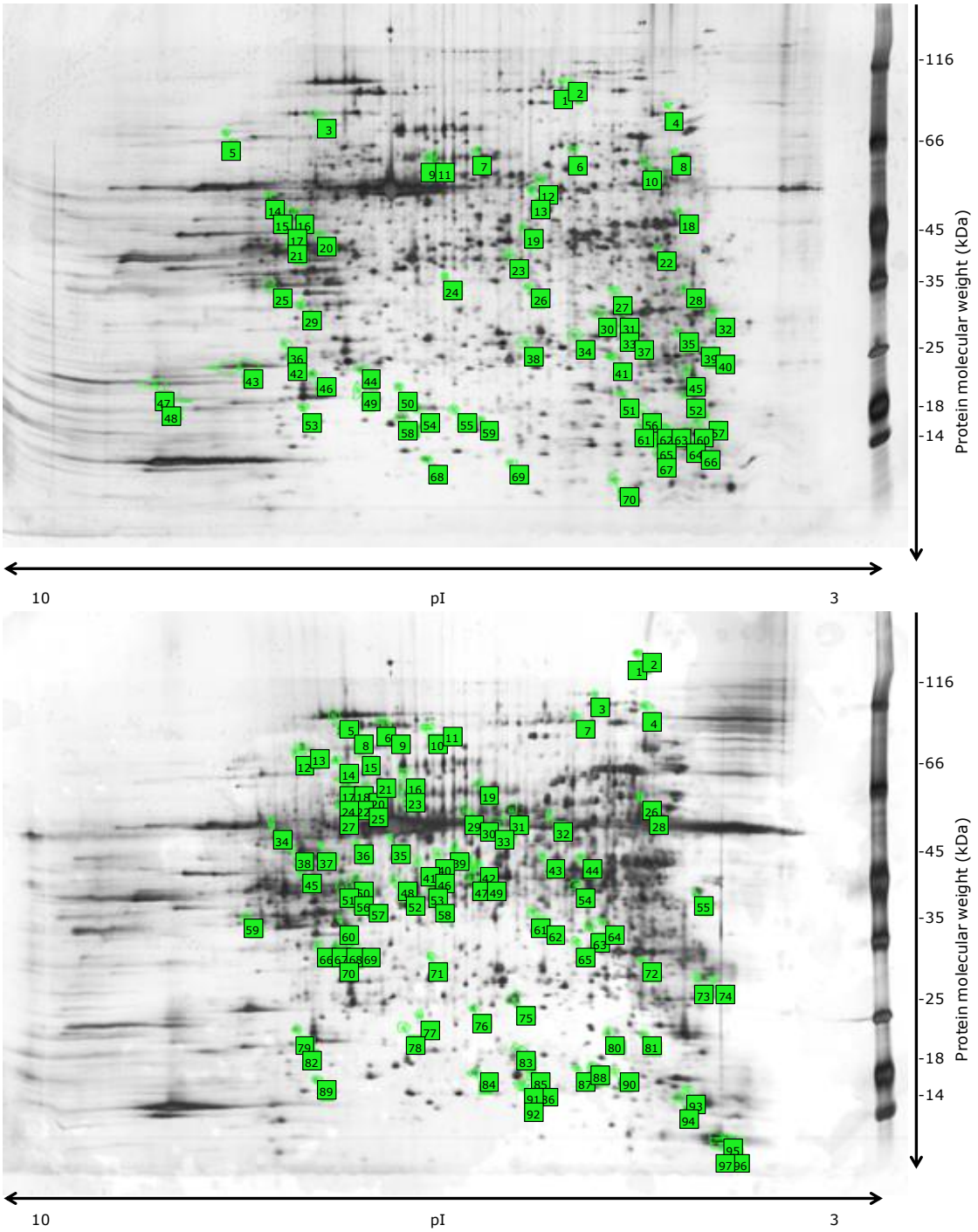

Figure 5.4: Differently expressed spots in Conférence without a heat shock (top; 70 spots) and with a heat shock (bottom; 97 spots), 72h after inoculation.

Table 5.4: Differentially expressed proteins in Conférence leaves without heat shock, 72h after inoculation.

Spot number	Protein name + accession number	Function	MW (Da)	Fold change
1	Not identified	-	-	-0.50
2	Not identified	-	-	-0.20
3	Not identified	-	-	-0.48
4	Not identified	-	-	-0.18
5	Sorting and Assembly Machinery (SAM50) protein [*Malus* x *domestica*]; MDP0000672481	Protein sorting	88705.80	1.62
6	Not identified	-	-	1.27
7	Not identified	-	-	-0.42
8	Not identified	-	-	-0.16
9	Not identified	-	-	1.29
10	Not identified	-	-	-0.43
11	Not identified	-	-	-0.75
12	Not identified	-	-	-0.52
13	Ribulose-bisphosphate carboxylase small chain [*Malus* x *domestica*]; MDP0000185022	Photosynthesis	20420.40	1.71
14	Not identified	-	-	1.92
15	Not identified	-	-	2.00
16	Not identified	-	-	2.31
17	3R-hydroxymyristoyl ACP dehydrase [*Malus* x *domestica*]; MDP0000157497	Fatty acid biosynthesis	24443.70	1.61
18	Not identified	-	-	-0.58
19	Not identified	-	-	-0.57
20	Not identified	-	-	2.08
21	Glyceraldehyde 3-phosphate dehydrogenase, putative [*Ricinus communis*]; 30131.m006931	Glycolysis	42490.10	1.35
22	Magnesium chelatase subunit I [*Malus* x *domestica*]; MDP0000639265	Photosynthesis	45986.60	-0.61
23	Not identified	-	-	-0.58
24	Not identified	-	-	1.22
25	Ferredoxin-$NADP^+$ reductase [*Malus* x *domestica*]; MDP0000198078	Photosynthesis	40478.40	-0.76
26	Not identified	-	-	-0.70
27	Not identified	-	-	-0.57
28	Not identified	-	-	-0.56
29	Xyloglucan:xyloglucosyl transferase [*Malus* x *domestica*]; MDP0000269483	Cell wall synthesis	33765.60	1.95

30	Lactoylglutathione lyase, putative [*Ricinus communis*]; 29912.m005471	Glutathione synthesis	40666.70	2.27
31	Photosystem II oxygen-evolving enhancer protein 1 [*Malus* x *domestica*]; MDP0000248920	Photosynthesis	35082.50	-0.70
32	Thaumatin pathogenesis related protein [*Malus* x *domestica*]; MDP0000122958	Pathogenesis-related protein, plant defence	18603.9	1.64
33	HaloAcid Dehydrogenase (HAD)-like domain protein[*Malus* x *domestica*]; MDP0000018462	General metabolism	34414.20	-0.44
34	α/β-Hydrolases superfamily protein [*Malus* x *domestica*]; MDP0000254363	General metabolism	26278.10	-0.64
35	Not identified	-	-	-0.52
36	Carbonic anhydrase [*Malus* x *domestica*]; MDP0000156226	Photosynthesis	47628.10	3.07
37	Isopentenyl-diphosphate Δ-isomerase [*Malus* x *domestica*]; MDP0000198327	Secondary metabolism	57416.90	-0.74
38	Not identified	-	-	-0.27
39	Serine-type endopeptidase [*Malus* x *domestica*]; MDP0000242270	General metabolism	23862.30	-0.55
40	31 kDa ribonucleoprotein, chloroplastic-like [*Prunus persica*]; ppa009295m	Photosynthesis	32014.50	-0.34
41	Not identified	-	-	0.70
42	Not identified	-	-	1.81
43	Photosystem II oxygen-evolving enhancer protein 2 [*Malus* x *domestica*]; MDP0000361338	Photosynthesis	32454.50	-0.69
44	Not identified	-	-	-0.44
45	Conserved hypothetical protein [*Ricinus communis*]; 29907.m000629	Unknown	22866.20	-0.48
46	Predicted quinone reductase protein [*Malus* x *domestica*]; MDP0000509613	General metabolism, plant defence	21461.00	2.03
47	Not identified	-	-	-0.56
48	Not identified	-	-	-0.51
49	Alanine-2-oxoglutarate aminotransferase 1 [*Arabidopsis thaliana*]; AT1G23310.1	General metabolism	53302.60	-0.37
50	Not identified	-	-	-0.41
51	Not identified	-	-	-0.72
52	Germin-like protein[*Malus* x *domestica*]; MDP0000521048	Plant defence	22193.20	1.73
53	Not identified	-	-	-0.63
54	Not identified	-	-	-0.76
55	Monodehydroascorbate reductase (NADH) [*Malus* x *domestica*]; MDP0000261821	Glutathione-ascorbate cycle	47000.4	-0.24
56	Not identified	-	-	-0.28

57	Not identified	-	-	-0.33
58	Cofilin [*Malus* x *domestica*]; MDP0000245712	Actin disassembly	35089.90	-0.50
59	Not identified	-	-	-0.69
60	Not identified	-	-	-0.37
61	Hypothetical protein [*Malus* x *domestica*];MDP0000217142	Unknown	22056.9	-0.37
62	Not identified	-	-	-0.65
63	Not identified	-	-	Only present in mock
64	Bet v i allergen family protein [*Malus* x *domestica*];MDP0000427722	Pathogenesis-related protein, plant defence	16916.30	-0.71
65	4-methyl-5(b-hydroxyethyl)-thiazole monophosphate biosynthesis [*Malus* x *domestica*]; MDP0000132914	General metabolism	43955.20	-0.41
66	Rieske iron-sulphur protein [*Cucumis sativus*]; Cucsa.148060.1	Photosynthesis, mitochondrial permeability transition	12230.60	2.89
67	Not identified	-	-	-0.61
68	Not identified	-	-	-0.74
69	Not identified	-	-	-0.62
70	Predicted photosystem II reaction center PSB28 protein [*Cucumis sativus*]; Cucsa.348850.1	Photosynthesis	20072.50	-0.40

Table 5.5: Differentially expressed proteins in Conférence leaves with 15min heat shock, 72h after inoculation.

Spot number	Protein name + accession number	Function	MW (Da)	Fold change
1	Not identified	-	-	-0.18
2	Not identified	-	-	-0.20
3	Not identified	-	-	-0.32
4	Not identified	-	-	Only present in mock
5	Predicted glycine dehydrogenase [*Malus* x *domestica*]; MDP0000588069	General metabolism	114048.10	-0.66
6	Not identified	-	-	-0.29
7	Not identified	-	-	-0.45
8	Not identified	-	-	-0.62
9	Not identified	-	-	-0.51
10	Not identified	-	-	-0.23
11	Not identified	-	-	-0.31
12	Not identified	-	-	-0.26

13	5-methyltetrahydropteroyltriglutamate--homocysteine methyltransferase [*Malus* x *domestica*]; MDP0000153762	General metabolism	84602.40	-0.68
14	Not identified	-	-	-0.29
15	5-methyltetrahydropteroyltriglutamate--homocysteine methyltransferase [*Malus* x *domestica*]; MDP0000153762	General metabolism	84679.60	-0.42
16	Not identified	-	-	-0.45
17	Cysteine-rich protein [*Arabidopsis lyrata*]; 488005	General metabolism	64611.90	-0.36
18	Predicted thioredoxin superfamily protein [*Arabidopsis lyrata*];488005	General metabolism	64083.60	-0.43
19	Succinate dehydrogenase (ubiquinone) flavoprotein subunit [*Malus* x *domestica*]; MDP0000188391	Photosynthesis	66769.40	-0.53
20	Not identified	-	-	-0.24
21	Not identified	-	-	-0.34
22	Not identified	-	-	-0.36
23	Not identified	-	-	-0.06
24	Pyrophosphate-dependent phosphofructokinase [*Malus* x *domestica*]; MDP0000293776	Glycolysis	9638.70	-0.32
25	Not identified	-	-	-0.50
26	Not identified	-	-	2.44
27	Not identified	-	-	-0.33
28	Not identified	-	-	3.41
29	Putative chloroplast precursor [*Ricinus communis*]; 29646.m001077	General metabolism	63813.90	1.85
30	Not identified	-	-	-0.61
31	Not identified	-	-	1.42
32	Not identified	-	-	1.76
33	Not identified	-	-	-0.49
34	Not identified	-	-	2.09
35	Putative ATP synthase β subunit [*Ricinus communis*];29923.m000793	Energy related processes	26829.10	-0.18
36	Not identified	-	-	-0.33
37	Not identified	-	-	-0.39
38	Protein-disulfide reductase [*Manihot esculenta*]; cassava4.1_009452m	General metabolism	44001.90	0.46
39	Not identified	-	-	-0.37
40	Not identified	-	-	-0.36
41	Not identified	-	-	-0.38
42	Not identified	-	-	-0.27
43	Not identified	-	-	2.44

44	Not identified	-	-	1.81
45	Not identified	-	-	1.75
46	Not identified	-	-	-0.45
47	Phosphoglycerate kinase [*Malus* x *domestica*];MDP0000174843	Energy related processes	55562.10	-0.21
48	Not identified	-	-	-0.65
49	Phosphoglycerate kinase [*Malus* x *domestica*];MDP0000174843	Energy related processes	50310.50	-0.46
50	Not identified	-	-	-0.54
51	Fructose-bisphosphate cytoplasmic isozyme 1-like protein [*Prunus persica*]; ppa007744m	Photosynthesis	38396.60	-0.60
52	Not identified	-	-	-0.37
53	Not identified	-	-	-0.53
54	Phosphoribulokinase [*Malus* x *domestica*]; MDP0000148186	Photosynthesis	44745.20	-0.53
55	Cyclophilin 38 [*Arabidopsis lyrata*]; 477375	General metabolism, signal transduction	47982.60	2.02
56	Phosphoglycerate kinase [*Malus* x *domestica*]; MDP0000456708	Energy related processes	42680.60	-0.34
57	ATPase like protein [*Malus* x *domestica*]; MDP0000944409	Energy related processes	51737.50	-0.47
58	Hypothetical protein [*Linum usitatissimum*]; Lus10023701	Unknown	37914.50	-0.46
59	Ribulose bisphosphate carboxylase, large chain [*Medicago truncatula*]; Medtr6g059160.1	Photosynthesis	52675.50	1.58
60	Ferredoxin-NADP$^+$ reductase [*Malus* x *domestica*]; MDP0000811918	Photosynthesis	40381.70	-0.45
61	Not identified	-	-	-0.34
62	Not identified	-	-	-0.52
63	Not identified	-	-	-0.66
64	Not identified	-	-	-0.64
65	Not identified	-	-	2.02
66	Pirin like protein [*Malus* x *domestica*]; MDP0000748916	General metabolism	18026.00	-0.38
67	Ribulose bisphosphate carboxylase, large chain [*Medicago truncatula*]; Medtr6g059160.1	Photosynthesis	52675.50	-0.35
68	Putative ATP synthase β subunit [*Ricinus communis*]; 29923.m000793	Energy related processes	26829.10	-0.30
69	Not identified	-	-	-0.31
70	Not identified	-	-	-0.24
71	Not identified	-	-	-0.29

72	Unspecific monooxygenase [*Carica papaya*]; evm.model.supercontig_33.70	General metabolism	54641.10	-0.44
73	Small nuclear ribonucleoprotein [*Mimulus guttatus*]; mgv1a000548m	General metabolism	121513.30	2.78
74	RNA recognition motif domain [*Malus* x *domestica*]; MDP0000224531	General metabolism	41631.40	8.00
75	Predicted oxygen-evolving enhancer protein 2, chloroplastic-like [*Populus trichocarpa*]; Potri.005G206700.2	Photosynthesis	28140.00	-0.75
76	Chlorophyll a/b binding protein [*Malus* x *domestica*]; MDP0000269859	Photosynthesis	29606.40	1.44
77	Not identified	-	-	-0.61
78	Not identified	-	-	-0.03
79	Pectinesterase [*Linum usitatissimum*]; Lus10007111	Cell wall modification	21709.80	-0.36
80	Hypothetical protein ARALYDRAFT_483511 [*Arabidopsis lyrata* subsp. *lyrata*]; gi|297828115	Unknown	32167.60	2.37
81	F-type H^+-transporting ATPase subunit d [*Malus* x *domestica*]; MDP0000734166	Energy related processes	19782.10	1.99
82	Not identified	-	-	-0.41
83	Phototropic-responsive NPH3 family protein [*Arabidopsis thaliana*]; AT3G26490.1	General metabolism	66349.20	-0.37
84	Major allergen Pyr c 1 [*Pyrus communis*]; gi|14423877	Pathogenesis-related protein, plant defence	17581.90	2.80
85	Not identified	-	-	5.29
86	Not identified	-	-	5.91
87	Not identified	-	-	6.90
88	Not identified	-	-	Only present in mock
89	Nucleoside-diphosphate kinase [*Malus* x *domestica*]; MDP0000259403	General metabolism	28865.90	-0.22
90	Not identified	-	-	2.68
91	Not identified	-	-	-0.75
92	Small subunit ribosomal protein S12e [*Malus* x *domestica*]; MDP0000006123	General metabolism	35022.90	1.48
93	Rieske iron-sulphur protein [*Cucumis sativus*]; Cucsa.148060.1	Photosynthesis	12230.60	5.29
94	F-type H^+-transporting ATPase subunit b [*Malus* x *domestica*]; MDP0000291815	Energy related processes	46971.80	2.36
95	Plastocyanin [*Malus* x *domestica*]; MDP0000740648	Photosynthesis	16770.60	-0.52
96	Not identified	-	-	-0.55
97	Not identified	-	-	-0.51

5. Discussion

In the present chapter, the effect of a heat shock in immature pear leaves (= leaf 4) of the moderately susceptible cultivar Conférence was investigated. We examined if the phenylpropanoid-flavonoid pathway was stimulated in the heat shock-treated plants and if this had a positive effect on the plant's response to the fire blight pathogen *Erwinia amylovora*. If heat shocks prove to be valuable against *E. amylovora*, fruit growers could use trailed heated air cannons as an extra alternative method to fight fire blight infections.

Two-year-old pear trees (*Pyrus communis*) cv. Conférence were put in a climate chamber at 60°C for 15min (= heat shock) or not (= no heat shock). The day after, they were inoculated with *E. amylovora* strain SGB 225/12 or were mock inoculated.
The spread of disease was not more pronounced in heat shock treated plants, as the amount of necrotic tissue more or less stayed the same. However, when focusing on the phenylpropanoid-flavonoid pathway, there was a tendency of a general down-regulation in the investigated transcripts when applying a heat shock, especially 3h and 24h after inoculation. The fact that *CHS*, *FHT*, *ANS*, *ANR*, *DFR* and *LAR1* retained very low relative expression values could be a strategy of the plant in not investing in the production of very high energy-consuming secondary metabolites (Kliebenstein and Rowe, 2008), but in other direct energy-related strategies that help recover the plant from the applied heat shock. Seventy-two hours after inoculation, the *FLS* transcripts in both *Ea*-inoculated treatments were lower than in the mock-inoculated treatments, which could indicate that necrosis has started to occur.

A proteomic approach was conducted in order to try to find some essential differences between heat shock treated and non-heat shock treated plants after the inoculation with *E. amylovora*. Just like in the previous chapter (chapter 4), it is not possible to provide an all-embracing and conclusive anwer about specific pathways that are triggered, as in the experiment without a heat shock merely 41% of the spots was identified, compared to about 39% in the trees where a 15min heat shock was applied.

Although the proteomic results of the previous chapter and this chapter (only the plants without heat shock!) in theory should be the same, new differentially expressed spots were identified. Just like in the previous chapter, the importance of the photosynthetic actors again came to the front, both in heat shock and non-heat shock treated trees. Heat shocks are believed to affect photosynthesis and to increase fluorescence, especially the first hours after application (Oukarroum *et al.*, 2012; Vanloven *et al.*, 1993). PEA measurements indicated a neglectable effect of heat shocks on fluorescence levels 24h and 72h after inoculation, suggesting that fluorescence already has faded away after one day.

In contrast with the previous chapter, Fd-$NADP^+$ reductase did not increase. An interesting molecule however is the Rieske Fe-S protein, which was more present in the *Ea*-inoculated samples, both in the heat shock treated and non-heat shock treated plants. Jones *et al.* (2006) propose a role for the Rieske Fe-S protein in programmed cell death of *Arabidopsis* when infected by *Pseudomonas syringae*. After all, a critical step in programmed cell death is mitochondrial permeability transition, which is regulated by the Rieske protein. So it could be that the Rieske protein in our pathosystem acts in the same manner or is forced by the bacteria to do so.

Furthermore, in trees without a heat shock a bet v I allergen was down-regulated in *Ea*-inoculated tissue, but the loss in this particular defence mechanism was compensated by an increase of a defence-related thaumatin-like protein, a germin-like protein and a quinone reductase. Thaumatin-like proteins belong to family 5 of the pathogenesis-related proteins (Van Loon and Van Strien, 1999), whereas germin-like proteins have different enzymatic functions that include two hydrogen peroxide-generating enzymes, oxalate oxidase and superoxide dismutase (Dunwell *et al.*, 2008). Quinone reductase instead catalyses the reduction of quinone substrates to hydroquinone and protects plant cells from oxidative stress by scavenging lipid peroxide-derived α and β unsaturated aldehydes (Mano *et al.*, 2002). The increase of the glutathione synthesis-related protein lactoylglutathione lyase could also suggest a role of glutathione in detoxifying the excess of ROS (Noctor and Foyer, 1998). The higher activity of 3R-hydroxymyristoyl ACP dehydrase and xyloglucan:xyloglucosyl transferase could confirm our results of the previous

chapters and imply a possible role in cell wall defence against fire blight (Afroz *et al.*, 2011).

With the exception of an allergen gene and a cyclophilin, which it assumed to have a distinct function in signal transduction and plant protection (Heyens *et al.*, 2006; Romano *et al.*, 2004) and which is upregulated in *Arabidopsis* after inoculation with *Pseudomonas syringae* and in *Brassica napus* after inoculation with *Leptosphaeria maculans* (Jones *et al.*, 2006; Marra *et al.*, 2010), a lot of proteins that have a role in some general metabolisms were down-regulated when heat shock was applied before the inoculation. Whether this could be caused by the heat shock and the thereby related favour of the plant for recovery against the applied heat shock instead of a proper defence against the pathogen is not certain, as a lot of the spots remained unidentified. To our surprise, no heat shock proteins were detected/identified at all.

In conclusion, it seems that applying a heat shock as some sort of added value to fight fire blight has a rather negative impact when only concenring the phenylpropanoid-flavonoid pathway, as the relative expression values of some phenylpropanoid-flavonoid pathway related genes decreased. Furthermore, infection was not slowed down but remained more or less the same without the heat shock. Last, although not all spots were identified, less defence-related mechanisms were found after the heat shock, suggesting that the plant favors recovery against the applied heat shock instead of plant defence.

Chapter 6:

General Conclusion

and

Future Perspectives

Fire blight, caused by the gram-negative bacterium *Erwinia amylovora*, is characterised by a rapid dissemination and a systemic distribution in *Rosaceaous* plants, of which both apple and pear are economic important species. Due to the destructive character of the bacterium, the lack of effective control methods and the low adaptability grade of both apple and pear against environmental traits (Chloupek and Hrstkova, 2005), sustaining a considerable fruit yield has become a major challenge in many parts of the world, especially in extensive cultivation regions such as the Hesbaye region in Belgium.
Every year, sudden outbreaks are able to diminish orchards planted with moderately resistant to highly sensitive apple and pear cultivars in a short amount of time. In Europe, fire blight is considered as a growing problem as higher temperatures, breeding of cultivars on susceptible rootstocks such as M9 and the introduction of susceptible cultivars such as Kanzi will probably enlarge the risk of infection in the near future (Deckers and Schoofs, 2008).

Much research has been performed concerning specific pathways and stages in this plant pathogen interaction, for instance on the level of ROS (paragraph 2.2.1), plant growth hormones (paragraph 2.2.3), pathogenesis-related proteins (2.2.4), phytoalexins (paragraph 2.2.5) and photosynthesis (paragraph 2.2.6). Recent reviews about these subjects are written by Malnoy *et al.* (2012) and Vrancken *et al.* (2012) (paper accepted with minor revisions).

Another important pathway is the phenylpropanoid-flavonoid pathway, which is responsible for the production of a vast array of polyphenols based on the few intermediates of the shikimate pathway as core units and each with their own functions. The phenylpropanoid-flavonoid pathway is characterised by an enormous complexity, caused by a large amount of branches and branchpoints and a lot of endproducts resulting from the pathway. The amino acid L-phenylalanine, the last step of the plant shikimate pathway, is the entry to the biosynthesis of these polyphenols.
Polyphenols not only contribute to fruit colour and photoprotection, they also may provide antimicrobial and structural components during interaction with micro-organisms. However, in the interaction between *E. amylovora* and

Rosaceae, different results were reported throughout the literature regarding the phenylpropanoid-flavonoid pathway (paragraph 2.2.2).

The use of a multidisciplinary approach gives us the opportunity to clear the role of the phenylpropanoid-flavonoid pathway and to reveal other defence mechanisms involved in the pathosystem between *Erwinia amylovora* and *Pyrus communis*.

In chapter 3, ontogenesis-related differences in both mature and immature leaves of two-year-old pear trees *Pyrus communis* cv. Conférence on Quince C rootstock after an inoculation with *Erwinia amylovora* strain SGB 225/12 were investigated.
We showed that fundamental differences were present between immature and mature leaf tissue, as inoculation of immature leaves expressed disease symptoms much faster than the mature leaves and transcripts of both antioxidative and phenylpropanoid-related genes differed in mature and immature leaves. The higher levels of certain antioxidative related transcripts and their respectively antioxidative endproducts in the older leaves could have a function in decreasing too high amounts of ROS during the first hours after infection and could partially explain the different infection rates that existed between these two types of leaves. Clear differences in antioxidative related transcripts as a result of an inoculation were not found.
Nevertheless, transcription patterns of two key genes anthocyanidin reductase (*ANR*) and chalcone synthase (*CHS*) related to the phenylpropanoid-flavonoid pathway showed differences between control, mock-inoculated and *Ea*-inoculated mature leaves, with the strongest reaction 48h after inoculation for the *Ea*-inoculated mature leaves. The impact of *E. amylovora* was also visualised in histological sections, and confirmed by HPLC, as epicatechin –which is produced via ANR- slightly augmented in *Ea*-inoculated leaf tissue 72h after inoculation. These results could indicate that a rather quick induction of the phenylpropanoid-flavonoid pathway and maybe epicatechin in particular could have a distinct function in protecting mature leaves against fire blight, as these metabolites can act as an antioxidant, as a defence barrier strategy or as toxic compound against the bacteria. Compared to the mature leaves, the role of the

phenylpropanoid-flavonoid pathway seemed to be attenuated in the immature leaves.

In chapter 4, we investigated possible cultivar dependent variations in immature pear leaves (=leaf 4) of the cultivar Conférence and the cultivar Doyenné du Comice regarding their response to the fire blight pathogen *Erwinia amylovora* with a special emphasis on the phenylpropanoid-flavonoid pathway.
Conférence and Doyenné reacted in different ways to an inoculation of the immature leaves with fire blight. Although the phenylpropanoid-flavonoid pathway seemed to have a minor effect in immature leaves of both cultivars, a difference between cultivars was noticed, as transcripts were immediately down-regulated in Doyenné, whereas transcripts in Conférence appeared to fluctuate more during the experiment. No induction of the investigated transcripts was noticed in the leaf above and below the *Ea*-inoculated leaf.
The higher concentrations of epicatechin in the very susceptible cultivar Doyenné compared to moderately susceptible cultivar Conférence makes us assume that a natural high level of epicatechin (and maybe other polyphenols) that could act as preformed defence molecules do not automatically guarantee a high level of protection against *E. amylovora* in *Pyrus*, but the generation of a time-dose dependent relationship seems to be more important in this part of the defence mechanism. An equal type of relationship has already been demonstrated by Davey *et al.* (2007) who found that the susceptibility of fruits of different apple genotypes to postharvest infection with *Botrytis cinerea* decreases with increasing harvest date and that susceptibility is correlated with fruit vitamin C levels. Hence, epicatechin has to be present at the site of inoculation in order to act as at an antioxidative quencher, as an ultrastructural defence molecule or as a direct toxin in the leaves. Nevertheless, more research is needed to confirm this.
When digging deeper into the proteome and although not all spots were identified, both cultivars seem to adapt their energy-related metabolic and photosynthetic processes. However, in Conférence, the increased amount of defence related major allergen genes and lipoxygenases could suggest a better dealing of the built-up stress caused by *E. amylovora* compared to Doyenné.

In chapter 5, we investigated the possible effect of the application of a heat shock in immature pear leaves (= leaf 4) of the cultivar Conférence regarding its response to the fire blight pathogen *Erwinia amylovora*. The goal was to known if application of heat shocks really improves or counteracts the plant's defence mechanism against fire blight. If heat shocks prove to be valuable against *E. amylovora*, fruit growers could use trailed heated air cannons as an extra alternative method to fight fire blight infections. However, it seems that applying a heat shock as an added value to fight fire blight has a rather negative impact, as the relative expression values of some phenylpropanoid-flavonoid pathway related genes decreased. Furthermore, infection was not slowed down but remained more or less the same without the heat shock. Last, although not all spots were identified, less defence-related mechanisms were found after the heat shock, suggesting that the plant favors recovery from the heat shock instead of plant defence.
Although this set-up for the non-heatshock treated was exactly the same set-up as in chapter 4, different results were obtained, clearly indicating that biological differences exist between different trees and that conditions such as small temperature fluctions, differences in sugar transport, radiation differences, etc. could affect the proteomic result.

An overview of all chapters is given in table 6.1.

The phenylpropanoid-flavonoid pathway seems to be a very important pathway in fruits, not only regarding their taste and colour, but also as an important factor in defence related mechanisms, which is definitely worth investigating further. Our results indicate that large differences occur between the behaviour of immature and mature leaves. Scientist studying phytopathological phenomena really should keep this in mind, as inoculations of leaves of different age could result in different outcomes.
Next, it would be also worth examining other applications such as UV treatment or the use of Prohexadione-Ca in order to know the effect of these treatments on the phenylpropanoid-flavonoid pathway.
The induction of some components of the phenylpropanoid-flavonoid pathway and the natural presence of certain stress-related genes is not the only defence

mechanism involved, as a plant has a wide range of defence mechanisms available (Robert-Seilaniantz *et al.*, 2007). Despite the extensive research in this pathosystem, some niches remain largely underexplored (Allen *et al.*, 2009).

Regarding *E. amylovora*, little is known about end-stage disease, latent infections, survival away from the host, interactions between other microbic organisms and secondary bloom infections. Furthermore, regarding the infection process, the function and presence of avirulence genes, the amount of pathogenicity factors and the mechanism of the T3SS system remains poorly understood. The recent publishing of the complete genome of *Erwinia amylovora* CFBP1430 by Smits *et al.* (2010) is a welcome tool in revealing novel insights into the genome, which will warrant more insight in the virulence, host range and ecological behaviour of this pathogen on its host plants in the near future.

However, knowing the bacteria is not enough. It is essential to study the plant as well. In *Pyrus communis*, many defence responses and signalling events are undetected or hardly understood. The availability of molecular markers and genetic mapping of pear would allow us to identify major genes and disease specific loci, permitting us to improve the resistance against *E. amylovora* and other pathogens, but also certain breeding characteristics such as plant growth and fruit yield in the near future (Le Roux *et al.*, 2012b).

Based on our proteomic data, PR proteins, cyclophilin, the Rieske iron-sulfur protein and the ferredoxin–$NADP^+$ reductase seem to be important proteins in a possible defence mechanism of pear and deserve more attention in further research. Especially the Rieske iron-sulfur protein is of great interest, as it forms an essential molecule between PS I and PS II and it is reported that plants that are inoculated with *E. amylovora* and that are put in the dark afterwards, are more susceptible to fire blight infection (personal communication Ir. Deckers, pcfruit). This could indicate that interfering with the photosynthesis of the host plant is one of the strategies of fire blight. Also PR proteins are worth investigating in the near future, as they were constantly upregulated during our proteomics data and still little is known about these molecules.

However, many spots remained unidentified as the genome of *Pyrus communis* remains unsequenced (although it was expected to be published in 2009-2010) and EST databases of *Pyrus* are not well spread, making proteomic research of pear very difficult and hard to interpret.

In conclusion, due to the rapid spread and aggressiveness of *E. amylovora* and the importance of fire blight in fruit cultivation, a continuous high grade scientific research is essential in developing resistant cultivars, in gaining insight in infection strategies and plant signalling and finally in discovering new management techniques and chemical compounds, which hopefully could result in a fire blight free environment.

Table 6.1: Summary table with the major trends of the conducted research.

	Ontogenesis	Comparison Conférence and Doyenné	Heat Shock
Shoot necrosis	Higher rates of necrosis & TH3 levels in immat. leaves compared to the mat. leaves	Slightly higher rate of necrosis & a similar TH3 level in Doyenné compared to Conférence	Similar rates of necrosis & a slightly lower TH3 level in heat shock treated Conf. compared to the untreated Conf.
Antioxidative transcripts	• High levels of *FSD1*, *FSD2*, *CAT1* & *CAT3* in mat. leaves • No clear differences between treatments	/	/
Transcripts of the phenylpropanoid-flavonoid pathway	• Steady-state expression values in immat. leaves • Upregulation of most genes (*ANR*, *CHS*,...) in *Ea*-inoculated mat. leaves, 48h after inoculation • Ontogenesis related differences	• Fluctuating pattern in Conférence • More downregulation in Doyenné • No clear differences between the treatments	Possible negative effect of the heat shock based on the transcripts of the phenylpropanoid-flavonoid pathway
Secondary metabolites	• High levels of flavonols, simple phenolics, chlorogenic acid and cis-ferulic acid in immat. leaves compared to the mat. leaves • Small upregulation of epicatechin in Ea-inoc. mat. leaves 72h after inoc.	• Higher levels of flavonols, simple phenolics, cis-ferulic acid, B2, B5, catechin and epicatechin in Doyenné • No clear differences between the treatments	/
Fluorescence imaging	Changes in chlorophyll fluorescence in both mat. & immat. leaves after inoculation	Changes in chlorophyll fluorescence in both Conférence and Doyenné after inoculation	Changes in chlorophyll fluorescence as a result of the heat shock are negligible
Proteomics	/	Proteomics indicate an effect on photosynthesis, energy-related processes and defence-related mechanisms, both in Conférence and Doyenné	Proteomics indicate an effect on photosynthesis, energy-related processes and defence-related mechanisms, both in heat shock treated and untreated Conf.

References

Abramovitch, R. B. and Martin, G. B. (2004). Strategies used by bacterial pathogens to suppress plant defenses. *Current Opinion in Plant Biology* **7:** 356-364.

Afroz, A., Ali, G. M., Mir, A. and Komatsu, S. (2011). Application of proteomics to investigate stress-induced proteins for improvement in crop protection. *Plant Cell Reports* **30:** 745-763.

Agati, G. and Tattini, M. (2010). Multiple functional roles of flavonoids in photoprotection. *New Phytologist* **186:** 786-793.

Ahuja, I., Kissen, R. and Bones, A. M. (2012). Phytoalexins in defense against pathogens. *Trends in Plant Science* **17:** 73-90.

Al-Karablieh, N., Weingart, H. and Ullrich, M. S. (2009). The outer membrane protein TolC is required for phytoalexin resistance and virulence of the fire blight pathogen *Erwinia amylovora*. *Microbial Biotechnology* **2:** 465-475.

Alfano, J. R. and Collmer, A. (2004). Type III secretion system effector proteins: Double agents in bacterial disease and plant defense. *Annual Review of Phytopathology* **42:** 385-414.

Allen, C., Bent, A. and Charkowski, A. (2009). Underexplored niches in research on plant pathogenic bacteria. *Plant Physiology* **150:** 1631-1637.

Allen, J. F. (2004). Cytochrome b(6)f: structure for signalling and vectorial metabolism. *Trends in Plant Science* **9:** 130-137.

Alscher, R. G., Donahue, J. L. and Cramer, C. L. (1997). Reactive oxygen species and antioxidants: Relationships in green cells. *Physiologia Plantarum* **100:** 224-233.

Alves, A. A., Guimaraes, L. M. D., Chaves, A. R. D., DaMatta, F. M. and Alfenas, A. C. (2011). Leaf gas exchange and chlorophyll a fluorescence of *Eucalyptus urophylla* in response to *Puccinia psidii* infection. *Acta Physiologiae Plantarum* **33:** 1831-1839.

Andreotti, C., Costa, G. and Treutter, D. (2006). Composition of phenolic compounds in pear leaves as affected by genetics, ontogenesis and the environment. *Scientia Horticulturae* **109:** 130-137.

Andreou, A. and Feussner, I. (2009). Lipoxygenases - Structure and reaction mechanism. *Phytochemistry* **70:** 1504-1510.

Apel, K. and Hirt, H. (2004). Reactive oxygen species: Metabolism, oxidative stress, and signal transduction. *Annual Review of Plant Biology* **55:** 373-399.

Ardi, R., Kobiler, I., Jacoby, B., Keen, N. T. and Prusky, D. (1998). Involvement of epicatechin biosynthesis in the activation of the mechanism of resistance of

avocado fruits to *Colletotrichum gloeosporioides*. *Physiological and Molecular Plant Pathology* **53:** 269-285.

Arora, A., Sairam, R. K. and Srivastava, G. C. (2002). Oxidative stress and antioxidative system in plants. *Current Science* **82:** 1227-1238.

Asai, T., Tena, G., Plotnikova, J., Willmann, M. R., Chiu, W. L., Gomez-Gomez, L. *et al.* (2002). MAP kinase signalling cascade in *Arabidopsis* innate immunity. *Nature* **415:** 977-983.

Aziz, A., Poinssot, B., Daire, X., Adrian, M., Bezier, A., Lambert, B. *et al.* (2003). Laminarin elicits defense responses in grapevine and induces protection against *Botrytis cinerea* and *Plasmopara viticola*. *Molecular Plant-Microbe Interactions* **16:** 1118-1128.

Baker, C. J. and Orlandi, E. W. (1995). Active oxygen in plant pathogenesis. *Annual Review of Phytopathology* **33:** 299-321.

Baker, C. J., Orlandi, E. W. and Mock, N. M. (1993). Harpin, an elicitor of the hypersensitive response in Tobacco caused by *Erwinia amylovora*, elicits active oxygen production in suspension Cells. *Plant Physiology* **102:** 1341-1344.

Baldo, A., Norelli, J. L., Farrell, R. E., Bassett, C. L., Aldwinckle, H. S. and Malnoy, M. (2010). Identification of genes differentially expressed during interaction of resistant and susceptible apple cultivars (*Malus* x *domestica*) with *Erwinia amylovora*. *Bmc Plant Biology* **10**.

Baniulis, D., Yamashita, E., Zhang, H., Hasan, S. S. and Cramer, W. A. (2008). Structure-Function of the Cytochrome b(6)f Complex. *Photochemistry and Photobiology* **84:** 1349-1358.

Barber, J. (2002). Photosystem II: a multisubunit membrane protein that oxidises water. *Current Opinion in Structural Biology* **12:** 523-530.

Barbier-Brygoo, H. and Joyard, J. (2004). Focus on plant proteomics. *Plant Physiology and Biochemistry* **42:** 913-917.

Barnard, A. M. L. and Salmond, G. P. C. (2007). Quorum sensing in *Erwinia* species. *Analytical and Bioanalytical Chemistry* **387:** 415-423.

Bassanezi, R. B., Amorim, L., Bergamin, A. and Berger, R. D. (2002). Gas exchange and emission of chlorophyll fluorescence during the monocycle of rust, angular leaf spot and anthracnose on bean leaves as a function of their trophic characteristics. *Journal of Phytopathology-Phytopathologische Zeitschrift* **150:** 37-47.

Bauriegel, E., Giebel, A. and Herppich, W. B. (2010). Rapid *Fusarium* head blight detection on winter wheat ears using chlorophyll fluorescence imaging. *Journal of Applied Botany and Food Quality-Angewandte Botanik* **83:** 196-203.

Bechtold, U., Karpinski, S. and Mullineaux, P. M. (2005). The influence of the light environment and photosynthesis on oxidative signalling responses in plant-biotrophic pathogen interactions. *Plant Cell and Environment* **28:** 1046-1055.

Becker, W. M., Kleinsmith, L. J. and Hardin, J. (2000). The world of the cell. Benjamin-Cummings Publishing Company.

Belkhadir, Y., Subramaniam, R. and Dangl, J. L. (2004). Plant disease resistance protein signaling: NBS-LRR proteins and their partners. *Current Opinion in Plant Biology* **7:** 391-399.

Bellemann, P. and Geider, K. (1992). Localization of transposon insertions in pathogenicity mutants of *Erwinia amylovora* and their biochemical-characterization. *Journal of General Microbiology* **138:** 931-940.

Bent, A. F. and Mackey, D. (2007). Elicitors, effectors, and R genes: The new paradigm and a lifetime supply of questions. *Annual Review of Phytopathology* **45:** 399-436.

Berg, J. M., Tymoczko, J. L. and Stryer, L. (2002). Biochemistry Fifth Edition. W. H. Freeman

Berger, S., Benediktyova, Z., Matous, K., Bonfig, K., Mueller, M. J., Nedbal, L. *et al.* (2007). Visualization of dynamics of plant-pathogen interaction by novel combination of chlorophyll fluorescence imaging and statistical analysis: differential effects of virulent and avirulent strains of *P. syringae* and of oxylipins on *A. thaliana*. *Journal of Experimental Botany* **58:** 797-806.

Billing, E. (1974). Effect of temperature on growth of the fireblight pathogen, *Erwinia amylovora*. *Journal of Applied Bacteriology* **37:** 643-648.

Billing, E. (2007). Challenges in adaptation of plant disease warning systems to new locations: re-appraisal of Billing's integrated system for predicting fire blight in a warm dry environment. *Phytopathology* **97:** 1036-1039.

Block, A., Li, G. Y., Fu, Z. Q. and Alfano, J. R. (2008). Phytopathogen type III effector weaponry and their plant targets. *Current Opinion in Plant Biology* **11:** 396-403.

Blokhina, O., Virolainen, E. and Fagerstedt, K. V. (2003). Antioxidants, oxidative damage and oxygen deprivation stress: a review. *Annals of Botany* **91:** 179-194.

Bocsanczy, A. M., Nissinen, R. M., Oh, C. S. and Beer, S. V. (2008). HrpN of *Erwinia amylovora* functions in the translocation of DspA/E into plant cells. *Molecular Plant Pathology* **9:** 425-434.

Bogs, J., Bruchmuller, I., Erbar, C. and Geider, K. (1998). Colonization of host plants by the fire blight pathogen *Erwinia amylovora* marked with genes for bioluminescence and fluorescence. *Phytopathology* **88:** 416-421.

Bolwell, G. P. and Wojtaszek, P. (1997). Mechanisms for the generation of reactive oxygen species in plant defence - a broad perspective. *Physiological and Molecular Plant Pathology* **51:** 347-366.

Bonasera, J. M., Kim, J. F. and Beer, S. V. (2006a). PR genes of apple: identification and expression in response to elicitors and inoculation with *Erwinia amylovora*. *Bmc Plant Biology* **6**.

Bonasera, J. M., Meng, X., Beer, S. V., Owens, T. and Kim, W. S. (2006b). Interaction of DspE/A, a pathogenicity/avirulence protein of *Erwinia amylovora*, with pre-ferredoxin from apple and its relationship to photosynthetic efficiency. *Acta Horticulturae* **704:** 473-477.

Bonfig, K. B., Schreiber, U., Gabler, A., Roitsch, T. and Berger, S. (2006). Infection with virulent and avirulent *P. syringae* strains differentially affects photosynthesis and sink metabolism in *Arabidopsis* leaves. *Planta* **225:** 1-12.

Boureau, T., ElMaarouf-Bouteau, H., Garnier, A., Brisset, M. N., Perino, C., Pucheu, I. *et al.* (2006). DspA/E, a type III effector essential for *Erwinia amylovora* pathogenicity and growth in planta, induces cell death in host apple and nonhost tobacco plants. *Molecular Plant-Microbe Interactions* **19:** 16-24.

Brettel, K. (1997). Electron transfer and arrangement of the redox cofactors in photosystem I. *Biochimica et Biophysica Acta-Bioenergetics* **1318:** 322-373.

Broggini, G. A. L., Duffy, B., Holliger, E., Scharer, H. J., Gessler, C. and Patocchi, A. (2005). Detection of the fire blight biocontrol agent *Bacillus subtilis* BD170 (Biopro ®) in a Swiss apple orchard. *European Journal of Plant Pathology* **111:** 93-100.

Bubab, T., Foldes, L., Kormany, A., Hauptmann, S., Stammler, G. and Rademacher, W. (2003). Prohexadione-Ca in apple trees: Control of shoot growth and reduction of fire blight incidence in blossoms and shoots. *Journal of Applied Botany-Angewandte Botanik* **77:** 95-102.

Buchanan, B. B. and Balmer, Y. (2005). Redox regulation: A broadening horizon. *Annual Review of Plant Biology* **56:** 187-220.

Bugert, P. and Geider, K. (1997). Characterization of the amsI gene product as a low molecular weight acid phosphatase controlling exopolysaccharide synthesis of *Erwinia amylovora*. *Febs Letters* **400:** 252-256.

Burr, T. J., Norelli, J. L., Reid, C. L., Capron, L. K., Nelson, L. S., Aldwinckle, H. S. *et al.* (1993). Streptomycin-resistant bacteria associated with fire blight infections. *Plant Disease* **77:** 63-66.

Burse, A., Weingart, H. and Ullrich, M. S. (2004). The phytoalexin-inducible multidrug efflux pump AcrAB contributes to virulence in the fire blight pathogen, *Erwinia amylovora*. *Molecular Plant-Microbe Interactions* **17:** 43-54.

Buttner, D. and Bonas, U. (2003). Common infection strategies of plant and animal pathogenic bacteria. *Current Opinion in Plant Biology* **6:** 312-319.

Buttner, D. and Bonas, U. (2006). Who comes first? How plant pathogenic bacteria orchestrate type III secretion. *Current Opinion in Microbiology* **9:** 193-200.

Buttner, D. and He, S. Y. (2009). Type III protein secretion in plant pathogenic bacteria. *Plant Physiology* **150:** 1656-1664.

Cabrefiga, J., Bonaterra, A. and Montesinos, E. (2007). Mechanisms of antagonism of *Pseudomonas fluorescens* EPS62e against *Erwinia amylovora*, the causal agent of fire blight. *International Microbiology* **10:** 123-132.

Carbone, F., Preuss, A., De Vos, R. C. H., D'Amico, E., Perrotta, G., Bovy, A. G. *et al.* (2009). Developmental, genetic and environmental factors affect the expression of flavonoid genes, enzymes and metabolites in strawberry fruits. *Plant Cell and Environment* **32:** 1117-1131.

Carpentier, S. C., Coemans, B., Podevin, N., Laukens, K., Witters, E., Matsumura, H. *et al.* (2008a). Functional genomics in a non-model crop: transcriptomics or proteomics? *Physiologia Plantarum* **133:** 117-130.

Carpentier, S. C., Panis, B., Vertommen, A., Swennen, R., Sergeant, K., Renaut, J. *et al.* (2008b). Proteome analysis of non-model plants: A challenging but powerful approach. *Mass Spectrometry Reviews* **27:** 354-377.

Carpentier, S. C., Witters, E., Laukens, K., Deckers, P., Swennen, R. and Panis, B. (2005). Preparation of protein extracts from recalcitrant plant tissues: An evaluation of different methods for two-dimensional gel electrophoresis analysis. *Proteomics* **5:** 2497-2507.

Carretero, R., Bancal, M. O. and Miralles, D. J. (2011). Effect of leaf rust (*Puccinia triticina*) on photosynthesis and related processes of leaves in wheat crops grown at two contrasting sites and with different nitrogen levels. *European Journal of Agronomy* **35:** 237-246.

Cavalcanti, F. R., Resende, M. L. V., Lima, J. P. M. S., Silveira, J. A. G. and Oliveira, J. T. A. (2006). Activities of antioxidant enzymes and photosynthetic responses in tomato pre-treated by plant activators and inoculated by *Xanthomonas vesicatoria*. *Physiological and Molecular Plant Pathology* **68:** 198-208.

Chaerle, L., Hagenbeek, D., De Bruyne, E., Valcke, R. and Van der Straeten, D. (2004). Thermal and chlorophyll-fluorescence imaging distinguish plant-pathogen interactions at an early stage. *Plant and Cell Physiology* **45:** 887-896.

Chaerle, L., Lenk, S., Hagenbeek, D., Buschmann, C. and Van der Straeten, D. (2007). Multicolor fluorescence imaging for early detection of the hypersensitive reaction to tobacco mosaic virus. *Journal of Plant Physiology* **164:** 253-262.

Chamnongpol, S., Willekens, H., Moeder, W., Langebartels, C., Sandermann, H., Van Montagu, A. *et al.* (1998). Defense activation and enhanced pathogen tolerance induced by H_2O_2 in transgenic tobacco. *Proceedings of the National Academy of Sciences of the United States of America* **95:** 5818-5823.

Chang, X. L. and Nick, P. (2012). Defence signalling triggered by flg22 and harpin is integrated into a different stilbene output in *Vitis* cells. *Plos One* **7**.

Chen, X. H., Scholz, R., Borriss, M., Junge, H., Mogel, G., Kunz, S. *et al.* (2009). Difficidin and bacilysin produced by plant-associated *Bacillus amyloliquefaciens* are efficient in controlling fire blight disease. *Journal of Biotechnology* **140:** 38-44.

Chisholm, S. T., Coaker, G., Day, B. and Staskawicz, B. J. (2006). Host-microbe interactions: Shaping the evolution of the plant immune response. *Cell* **124:** 803-814.

Chizzali, C. and Beerhues, L. (2012). Phytoalexins of the *Pyrinae*: Biphenyls and dibenzofurans. *Beilstein Journal of Organic Chemistry* **8:** 613-620.

Chizzali, C., Gaid, M. M., Belkheir, A. K., Hansch, R., Richter, K., Flachowsky, H. *et al.* (2012a). Differential expression of biphenyl synthase gene family members in fire blight-infected Apple 'Holsteiner Cox'. *Plant Physiology* **158:** 864-875.

Chizzali, C., Khalil, M. N. A., Beuerle, T., Schuehly, W., Richter, K., Flachowsky, H. *et al.* (2012b). Formation of biphenyl and dibenzofuran phytoalexins in the transition zones of fire blight-infected stems of *Malus x domestica* cv. 'Holsteiner Cox' and *Pyrus communis* cv. 'Conference'. *Phytochemistry* **77:** 179-185.

Chloupek, O. and Hrstkova, P. (2005). Adaptation of crops to environment. *Theoretical and Applied Genetics* **111:** 1316-1321.

Cipriano, D. J., Wang, Y., Bond, S., Hinton, A., Jefferies, K. C., Qi, J. *et al.* (2008). Structure and regulation of the vacuolar ATPases. *Biochimica et Biophysica Acta-Bioenergetics* **1777:** 599-604.

Ciscato, M., Vangronsveld, J. and Valcke, R. (1999). Effects of heavy metals on the fast chlorophyll fluorescence induction kinetics of photosystem II: a comparative study. *Zeitschrift fur Naturforschung C-A Journal of Biosciences* **54:** 735-739.

Conde, A., Chaves, M. M. and Geros, H. (2011). Membrane transport, sensing and signaling in plant adaptation to environmental stress. *Plant and Cell Physiology* **52:** 1583-1602.

Cornelis, G. R. and Van Gijsegem, F. (2000). Assembly and function of type III secretory systems. *Annual Review of Microbiology* **54:** 735-774.

Cortleven, A. and Valcke, R. (2012). Evaluation of the photosynthetic activity in transgenic tobacco plants with altered endogenous cytokinin content: lessons from cytokinin. *Physiologia Plantarum* **144:** 394-408.

Costa, G., Andreotti, C., Bucchi, F., Sabatini, E., Bazzi, C., Malaguti, S. *et al.* (2001). Prohexadione-Ca (Apogee®): Growth regulation and reduced fire blight incidence in pear. *Hortscience* **36:** 931-933.

Dahal, D., Pich, A., Braun, H. P. and Wydra, K. (2010). Analysis of cell wall proteins regulated in stem of susceptible and resistant tomato species after inoculation with *Ralstonia solanacearum*: a proteomic approach. *Plant Molecular Biology* **73:** 643-658.

Dai, G. H., Nicole, M., Andary, C., Martinez, C., Bresson, E., Boher, B. *et al.* (1996). Flavonoids accumulate in cell walls, middle lamellae and callose-rich papillae during an incompatible interaction between *Xanthomonas campestris* pv *malvacearum* and cotton. *Physiological and Molecular Plant Pathology* **49:** 285-306.

Damour, G., Simonneau, T., Cochard, H. and Urban, L. (2010). An overview of models of stomatal conductance at the leaf level. *Plant Cell and Environment* **33:** 1419-1438.

Dao, T. T. H., Linthorst, H. J. M. and Verpoorte, R. (2011). Chalcone synthase and its functions in plant resistance. *Phytochemistry Reviews* **10:** 397-412.

Dat, J., Vandenabeele, S., Vranova, E., Van Montagu, M., Inze, D. and Van Breusegem, F. (2000). Dual action of the active oxygen species during plant stress responses. *Cellular and Molecular Life Sciences* **57:** 779-795.

Davey, M. E. and O'toole, G. A. (2000). Microbial biofilms: from ecology to molecular genetics. *Microbiology and Molecular Biology Reviews* **64:** 847-867.

Davey, M. W., Auwerkerken, A. and Keulemans, J. (2007) Relationship of apple vitamin C and antioxidant contents to harvest date and postharvest pathogen infection. *Journal of the Science of Food and Agriculture* **87:** 802-813.

de Bernonville, T. D., Gaucher, M., Flors, V., Gaillard, S., Paulin, J. P., Dat, J. F. *et al.* (2012). T3SS-dependent differential modulations of the jasmonic acid pathway in susceptible and resistant genotypes of *Malus* spp. challenged with *Erwinia amylovora*. *Plant Science* **188:** 1-9.

de Bernonville, T. D., Gaucher, M., Guyot, S., Durel, C. E., Dat, J. F. and Brisset, M. N. (2011). The constitutive phenolic composition of two *Malus* x *domestica* genotypes is not responsible for their contrasted susceptibilities to fire blight. *Environmental and Experimental Botany* **74:** 65-73.

de Jong, C. F., Takken, F. L. W., Cai, X. H., De Wit, P. J. G. M. and Joosten, M. H. A. J. (2002). Attenuation of Cf-mediated defense responses at elevated

temperatures correlates with a decrease in elicitor-binding sites. *Molecular Plant-Microbe Interactions* **15:** 1040-1049.

Deckers, T. (1996). Fire blight: the present state of its occurence in Belgium and phytosanitary measures to control the problem. *Parasitica* **52[3]:** 127-131.

Deckers, T. and Schoofs, H. (2008). Status of the Pear Production in Europe. *Acta Horticulturae* **800:** 95-105.

Dekker, J. P. and Boekema, E. J. (2005). Supramolecular organization of thylakoid membrane proteins in green plants. *Biochimica et Biophysica Acta-Bioenergetics* **1706:** 12-39.

Delalieux, S., Auwerkerken, A., Verstraeten, W. W., Somers, B., Valcke, R., Lhermitte, S. *et al.* (2009). Hyperspectral reflectance and fluorescence imaging to detect scab induced stress in apple leaves. *Remote Sensing* **1:** 858-874.

Dellagi, A., Brisset, M. N., Paulin, J. P. and Expert, D. (1998). Dual role of desferrioxamine in *Erwinia amylovora* pathogenicity. *Molecular Plant-Microbe Interactions* **11:** 734-742.

Dempsey, D. A. and Klessig, D. F. (2012). SOS - too many signals for systemic acquired resistance? *Trends in Plant Science* **17:** 538-545.

Denny, T. P. (1995). Involvement of bacterial polysaccharides in plant pathogenesis. *Annual Review of Phytopathology* **33:** 173-197.

Desikan, R., Reynolds, A., Hancock, J. T. and Neill, S. J. (1998). Harpin and hydrogen peroxide both initiate programmed cell death but have differential effects on defence gene expression in *Arabidopsis* suspension cultures. *Biochemical Journal* **330:** 115-120.

Develey-Riviere, M. P. and Galiana, E. (2007). Resistance to pathogens and host developmental stage: a multifaceted relationship within the plant kingdom. *New Phytologist* **175:** 405-416.

Dewdney, M. M., Biggs, A. R. and Turechek, W. W. (2007). A statistical comparison of the blossom blight forecasts of MARYBLYT and cougarblight with receiver operating characteristic curve analysis. *Phytopathology* **97:** 1164-1176.

Dinis, L. T., Peixoto, F., Zhang, C. H., Martins, L., Costa, R. and Gomes-Laranjo, J. (2011). Physiological and biochemical changes in resistant and sensitive chestnut (*Castanea*) plantlets after inoculation with *Phytophthora cinnamomi*. *Physiological and Molecular Plant Pathology* **75:** 146-156.

Dixon, R. A., Achnine, L., Kota, P., Liu, C. J., Reddy, M. S. S. and Wang, L. J. (2002). The phenylpropanoid pathway and plant defence - a genomics perspective. *Molecular Plant Pathology* **3:** 371-390.

Dixon, R. A., Xie, D. Y. and Sharma, S. B. (2005). Proanthocyanidins - a final frontier in flavonoid research? *New Phytologist* **165:** 9-28.

Dow, M., Newman, M. A. and von Roepenak, E. (2000). The induction and modulation of plant defense responses by bacterial lipopolysaccharides. *Annual Review of Phytopathology* **38:** 241-261.

Dumont, D., Noben, J. P., Raus, J., Stinissen, P. and Robben, J. (2004). Proteomic analysis of cerebrospinal fluid from multiple sclerosis patients. *Proteomics* **4:** 2117-2124.

Dunwell, J. M., Gibbings, J. G., Mahmood, T. and Naqvi, S. M. S. (2008). Germin and germin-like proteins: Evolution, structure, and function. *Critical Reviews in Plant Sciences* **27:** 342-375.

Durrant, W. E. and Dong, X. (2004). Systemic acquired resistance. *Annual Review of Phytopathology* **42:** 185-209.

Eastgate, J. A. (2000). *Erwinia amylovora*: the molecular basis of fireblight disease. *Molecular Plant Pathology* **1:** 325-329.

Elmore, J. M. and Coaker, G. (2011). The role of the plasma membrane H^+-ATPase in plant-microbe interactions. *Molecular Plant* **4:** 416-427.

Expert, D. (1999). Withholding and exchanging iron: Interactions between *Erwinia* spp. and their plant hosts. *Annual Review of Phytopathology* **37:** 307-334.

Eyles, A., Bonello, P., Ganley, R. and Mohammed, C. (2010). Induced resistance to pests and pathogens in trees. *New Phytologist* **185:** 893-908.

Faize, M., Brisset, M. N., Paulin, J. P. and Tharaud, M. (1999). Secretion and regulation Hrp mutants of *Erwinia amylovora* trigger different responses in apple. *Fems Microbiology Letters* **171:** 173-178.

Felix, G., Duran, J. D., Volko, S. and Boller, T. (1999). Plants have a sensitive perception system for the most conserved domain of bacterial flagellin. *Plant Journal* **18:** 265-276.

Felton, G. W., Korth, K. L., Bi, J. L., Wesley, S. V., Huhman, D. V., Mathews, M. C. *et al.* (1999). Inverse relationship between systemic resistance of plants to microorganisms and to insect herbivory. *Current Biology* **9:** 317-320.

Feucht, W., Treutter, D., Santosbuelga, C. and Christ, E. (1996). Catechin as a radical scavenger in paraquat-treated *Prunus avium*. *Journal of Applied Botany-Angewandte Botanik* **70:** 119-123.

Fischer, T. C., Gosch, C., Pfeiffer, J., Halbwirth, H., Halle, C., Stich, K. *et al.* (2007). Flavonoid genes of pear (*Pyrus communis*). *Trees-Structure and Function* **21:** 521-529.

Flachowsky, H., Halbwirth, H., Treutter, D., Richter, K., Hanke, M. V., Szankowski, I. *et al.* (2012). Silencing of flavanone-3-hydroxylase in apple (*Malus* x *domestica* Borkh.) leads to accumulation of flavanones, but not to reduced fire blight susceptibility. *Plant Physiology and Biochemistry* **51:** 18-25.

Flachowsky, H., Hanke, M. V., Peil, A., Strauss, S. H. and Fladung, M. (2009). A review on transgenic approaches to accelerate breeding of woody plants. *Plant Breeding* **128:** 217-226.

Flachowsky, H., Szankowski, I., Fischer, T. C., Richter, K., Peil, A., Hofer, M. *et al.* (2010). Transgenic apple plants overexpressing the Lc gene of maize show an altered growth habit and increased resistance to apple scab and fire blight. *Planta* **231:** 623-635.

Foyer, C. H. and Noctor, G. (2005a). Oxidant and antioxidant signalling in plants: a re-evaluation of the concept of oxidative stress in a physiological context. *Plant Cell and Environment* **28:** 1056-1071.

Foyer, C. H. and Noctor, G. (2005b). Redox homeostasis and antioxidant signaling: A metabolic interface between stress perception and physiological responses. *Plant Cell* **17:** 1866-1875.

Fraga, C. G. and Oteiza, P. I. (2011). Dietary flavonoids: Role of (-)-epicatechin and related procyanidins in cell signaling. *Free Radical Biology and Medicine* **51:** 813-823.

Friedman, M. (2007). Overview of antibacterial, antitoxin, antiviral, and antifungal activities of tea flavonoids and teas. *Molecular Nutrition & Food Research* **51:** 116-134.

Fromme, P., Jordan, P. and Krauss, N. (2001). Structure of photosystem I. *Biochimica et Biophysica Acta-Bioenergetics* **1507:** 5-31.

Galan, J. E. and Wolf-Watz, H. (2006). Protein delivery into eukaryotic cells by type III secretion machines. *Nature* **444:** 567-573.

Gander, S. and Gilbert, P. (1997). The development of a small-scale biofilm model suitable for studying the effects of antibiotics on biofilms of Gram-negative bacteria. *Journal of Antimicrobial Chemotherapy* **40:** 329-334.

Gasic, K., Hernandez, A. and Korban, S. (2004). RNA extraction from different apple tissues rich in polyphenols and polysaccharides for cDNA library construction. *Plant Molecular Biology Reporter* **22:** 437-438.

Gaudriault, S., Paulin, J. P., and Barny, M. A. (2002). The DspB/F protein of *Erwinia amylovora* is a type III secretion chaperone ensuring efficient

intrabacterial production of the Hrp-secreted DspA/E pathogenicity factor. *Molecular Plant Pathology* **3:** 313-320.

Gayler, S., Leser, C., Priesack, E. and Treutter, D. (2004). Modelling the effect of environmental factors on the "trade-off" between growth and defensive compounds in young apple trees. *Trees-Structure and Function* **18:** 363-371.

Geider, K. (1999). Interference of copper sulphate in growth of *Erwinia amylovora*. *Journal of Phytopathology-Phytopathologische Zeitschrift* **147:** 521-526.

Geier, G. and Geider, K. (1993). Characterization and influence on virulence of the levansucrase gene from the fireblight pathogen *Erwinia amylovora*. *Physiological and Molecular Plant Pathology* **42:** 387-404.

Gerber, I. B., Zeidler, D., Durner, J. and Dubery, I. A. (2004). Early perception responses of *Nicotiana tabacum* cells in response to lipopolysaccharides from *Burkholderia cepacia*. *Planta* **218:** 647-657.

Giddens, S. R., Houliston, G. J. and Mahanty, H. K. (2003). The influence of antibiotic production and pre-emptive colonization on the population dynamics of *Pantoea agglomerans* (*Erwinia herbicola*) Eh1087 and *Erwinia amylovora* in planta. *Environmental Microbiology* **5:** 1016-1021.

Gielen, B., Vandermeiren, K., Horemans, N., D'Haese, D., Serneels, R. and Valcke, R. (2006). Chlorophyll a fluorescence imaging of ozone-stressed *Brassica napus* L. plants differing in glucosinolate concentrations. *Plant Biology* **8:** 698-705.

Gielen, H., Remans, T., Vangronsveld, J. and Cuypers, A. (2002). MicroRNA's in metal stress: specific roles on secondary compounds. *International Journal of Molecular Sciences* **13:** 15826-15847.

Gill, J. J., Svircev, A. M., Smith, R. and Castle, A. J. (2003). Bacteriophages of *Erwinia amylovora*. *Applied and Environmental Microbiology* **69:** 2133-2138.

Golba, B., Treutter, D. and Kollar, A. (2011). Effects of apple (*Malus x domestica* Borkh.) phenolic compounds on proteins and cell wall-degrading enzymes of *Venturia inaequalis*. *Trees - Structure and Function* 1-9.

Goltsev, V., Zaharieva, I., Chernev, P. and Strasser, R. J. (2009). Delayed fluorescence in photosynthesis. *Photosynthesis Research* **101:** 217-232.

Gorbe, E. and Calatayud, A. (2012). Applications of chlorophyll fluorescence imaging technique in horticultural research: A review. *Scientia Horticulturae* **138:** 24-35.

Gosch, C., Puhl, I., Halbwirth, H., Schlangen, K., Roemmelt, S., Andreotti, C. *et al.* (2003). Effect of prohexadione-Ca on various fruit crops: Flavonoid

composition and substrate specificity of their dihydroflavonol 4-reductases. *European Journal of Horticultural Science* **68:** 144-151.

Gould, K. S. (2004). Nature's Swiss army knife: The diverse protective roles of anthocyanins in leaves. *Journal of Biomedicine and Biotechnology* 314-320.

Grant, S. R., Fisher, E. J., Chang, J. H., Mole, B. M. and Dangl, J. L. (2006). Subterfuge and manipulation: Type III effector proteins of phytopathogenic bacteria. *Annual Review of Microbiology* **60:** 425-449.

Guidarelli, M., Carbone, F., Mourgues, F., Perrotta, G., Rosati, C., Bertolini, P. *et al.* (2011). *Colletotrichum acutatum* interactions with unripe and ripe strawberry fruits and differential responses at histological and transcriptional levels. *Plant Pathology* **60:** 685-697.

Gunen, Y., Misirli, A. and Gulcan, R. (2005). Leaf phenolic content of pear cultivars resistant or susceptible to fire blight. *Scientia Horticulturae* **105:** 213-221.

Guo, Y. and Tan, J. G. (2011). Modeling and simulation of the initial phases of chlorophyll fluorescence from Photosystem II. *Biosystems* **103:** 152-157.

Gutha, L. R., Casassa, L. F., Harbertson, J. F. and Naidu, R. A. (2010). Modulation of flavonoid biosynthetic pathway genes and anthocyanins due to virus infection in grapevine (*Vitis vinifera* L.) leaves. *Bmc Plant Biology* **10**.

Halbwirth, H., Fischer, T. C., Roemmelt, S., Spinelli, F., Schlangen, K., Peterek, S. *et al.* (2003). Induction of antimicrobial 3-deoxyflavonoids in pome fruit trees controls fire blight. *Zeitschrift fur Naturforschung C-A Journal of Biosciences* **58:** 765-770.

Hauben, L., Moore, E. R. B., Vauterin, L., Steenackers, M., Mergaert, J., Verdonck, L. *et al.* (1998). Phylogenetic position of phytopathogens within the *Enterobacteriaceae*. *Systematic and Applied Microbiology* **21:** 384-397.

He, P., Shan, L. and Sheen, J. (2007). Elicitation and suppression of microbe-associated molecular pattern-triggered immunity in plant-microbe interactions. *Cellular Microbiology* **9:** 1385-1396.

He, S. Y., Nomura, K. and Whittam, T. S. (2004). Type III protein secretion mechanism in mammalian and plant pathogens. *Biochimica et Biophysica Acta-Molecular Cell Research* **1694:** 181-206.

Hernandez, I., Alegre, L., Van Breusegem, F. and Munne-Bosch, S. (2009). How relevant are flavonoids as antioxidants in plants? *Trends in Plant Science* **14:** 125-132.

Heyens, K. and Valcke, R. (2006). Fluorescence imaging of the infection pattern of apple leaves with *Erwinia amylovora*. *Acta Horticulturae* **704:** 69-74.

Heyens, K., Valcke, R., Dumont, D., Robben, J., and Noben, J. P. (2006). Differential expression of proteins in apple following inoculation with *Erwinia amylovoria*. *Acta Horticulturae* **704:** 489-494.

Hildebrand, M., Aldridge, P. and Geider, K. (2006). Characterization of hns genes from *Erwinia amylovora*. *Molecular Genetics and Genomics* **275:** 310-319.

Horton, P., Johnson, M. P., Perez-Bueno, M. L., Kiss, A. Z. and Ruban, A. V. (2008). Photosynthetic acclimation: Does the dynamic structure and macro-organisation of photosystem II in higher plant grana membranes regulate light harvesting states? *Febs Journal* **275:** 1069-1079.

Howe, G. A. and Schilmiller, A. L. (2002). Oxylipin metabolism in response to stress. *Current Opinion in Plant Biology* **5:** 230-236.

Hueck, C. J. (1998). Type III protein secretion systems in bacterial pathogens of animals and plants. *Microbiology and Molecular Biology Reviews* **62:** 379-433.

Huttner, C., Beuerle, T., Scharnhop, H., Ernst, L. and Beerhues, L. (2010). Differential effect of elicitors on biphenyl and dibenzofuran formation in *Sorbus aucuparia* cell cultures. *Journal of Agricultural and Food Chemistry* **58:** 11977-11984.

Huvenne, H., Messens, E. and Maes, M. (2009). Willow wood sap promotes the density-dependent pathogenesis of *Brenneria salicis*. *Environmental Microbiology* **11:** 1463-1472.

Hwang, C. F., Bhakta, A. V., Truesdell, G. M., Pudlo, W. M. and Williamson, V. M. (2000). Evidence for a role of the N terminus and leucine-rich repeat region of the Mi gene product in regulation of localized cell death. *Plant Cell* **12:** 1319-1329.

Iwata, S. and Barber, J. (2004). Structure of photosystem II and molecular architecture of the oxygen-evolving centre. *Current Opinion in Structural Biology* **14:** 447-453.

Izawa, T. (2012). Physiological significance of the plant circadian clock in natural field conditions. *Plant Cell and Environment* **35:** 1729-1741.

Jensen, P. E., Bassi, R., Boekema, E. J., Dekker, J. P., Jansson, S., Leister, D. *et al.* (2007). Structure, function and regulation of plant photosystem I. *Biochimica et Biophysica Acta-Bioenergetics* **1767:** 335-352.

Jensen, P. E., Haldrup, A., Rosgaard, L. and Scheller, H. V. (2003). Molecular dissection of photosystem I in higher plants: topology, structure and function. *Physiologia Plantarum* **119:** 313-321.

Jensen, P. J., Halbrendt, N., Fazio, G., Makalowska, I., Altman, N., Praul, C. *et al.* (2012). Rootstock-regulated gene expression patterns associated with fire blight resistance in apple. *Bmc Genomics* **13**.

Jin, Q. L., Hu, W. Q., Brown, I., McGhee, G., Hart, P., Jones, A. L. *et al.* (2001). Visualization of secreted Hrp and Avr proteins along the Hrp pilus during type III secretion in *Erwinia amylovora* and *Pseudomonas syringae*. *Molecular Microbiology* **40:** 1129-1139.

Johnson, K. B., Stockwell, V. O., Sawyer, T. L. and Sugar, D. (2000). Assessment of environmental factors influencing growth and spread of *Pantoea agglomerans* on and among blossoms of pear and apple. *Phytopathology* **90:** 1285-1294.

Jones, A. L. (1992). Evaluation of the computer-model Maryblyt for predicting fire blight blossom infection on apple in Michigan. *Plant Disease* **76:** 344-347.

Jones, A. M. E., Thomas, V., Bennett, M. H., Mansfield, J. and Grant, M. (2006). Modifications to the *Arabidopsis* defense proteome occur prior to significant transcriptional change in response to inoculation with *Pseudomonas syringae*. *Plant Physiology* **142:** 1603-1620.

Jones, J. D. G. and Dangl, J. L. (2006). The plant immune system. *Nature* **444:** 323-329.

Karpinski, S., Gabrys, H., Mateo, A., Karpinska, B. and Mullineaux, P. M. (2003). Light perception in plant disease defence signalling. *Current Opinion in Plant Biology* **6:** 390-396.

Kaufmann, K., Smaczniak, C., de Vries, S., Angenent, G. C. and Karlova, R. (2011). Proteomics insights into plant signaling and development. *Proteomics* **11:** 744-755.

Khanna-Chopra, R. (2012). Leaf senescence and abiotic stresses share reactive oxygen species-mediated chloroplast degradation. *Protoplasma* **249:** 469-481.

Kim, I. Y., Pusey, P. L., Zhao, Y. F., Korban, S. S., Choi, H., and Kim, K. K. (2012). Controlled release of *Pantoea agglomerans* E325 for biocontrol of fire blight disease of apple. *Journal of Controlled Release* **161:** 109-115.

Kim, J. F. and Beer, S. V. (1998). HrpW of *Erwinia amylovora*, a new harpin that contains a domain homologous to pectate lyases of a distinct class. *Journal of Bacteriology* **180:** 5203-5210.

Kim, W. S., Salm, H., and Geider, K. (2004). Expression of bacteriophage phi Ea1h lysozyme in *Escherichia coli* and its activity in growth inhibition of *Erwinia amylovora*. *Microbiology-Sgm* **150:** 2707-2714.

Klarzynski, O., Plesse, B., Joubert, J. M., Yvin, J. C., Kopp, M., Kloareg, B. *et al.* (2000). Linear beta-1,3 glucans are elicitors of defense responses in tobacco. *Plant Physiology* **124:** 1027-1037.

Kliebenstein, D. J. and Rowe, H. C. (2008). Ecological costs of biotrophic versus necrotrophic pathogen resistance, the hypersensitive response and signal transduction. *Plant Science* **174:** 551-556.

Koczan, J. M., Lenneman, B. R., McGrath, M. J. and Sundin, G. W. (2011). Cell surface attachment structures contribute to biofilm formation and xylem colonization by *Erwinia amylovora*. *Applied and Environmental Microbiology* **77:** 7031-7039.

Koczan, J. M., McGrath, M. J., Zhao, Y. F. and Sundin, G. W. (2009). Contribution of *Erwinia amylovora* exopolysaccharides amylovoran and levan to biofilm formation: Implications in pathogenicity. *Phytopathology* **99:** 1237-1244.

Krieger-Liszkay, A. (2005). Singlet oxygen production in photosynthesis. *Journal of Experimental Botany* **56:** 337-346.

Kuckenberg, J., Tartachnyk, I. and Noga, G. (2009). Temporal and spatial changes of chlorophyll fluorescence as a basis for early and precise detection of leaf rust and powdery mildew infections in wheat leaves. *Precision Agriculture* **10:** 34-44.

Kunkel, B. N., Bent, A. F., Dahlbeck, D., Innes, R. W. and Staskawicz, B. J. (1993). Rps2, an *Arabidopsis* disease resistance locus specifying recognition of *Pseudomonas syringae* strains expressing the avirulence gene Avrrpt2. *Plant Cell* **5:** 865-875.

Kunz, B. A., Dando, P. K., Grice, D. M., Mohr, P. G., Schenk, P. M. and Cahill, D. M. (2008). UV-induced DNA damage promotes resistance to the biotrophic pathogen *Hyaloperonospora parasitica* in *Arabidopsis*. *Plant Physiology* **148:** 1021-1031.

Kus, J. V., Zaton, K., Sarkar, R. and Cameron, R. K. (2002). Age-related resistance in *Arabidopsis* is a developmentally regulated defense response to *Pseudomonas syringae*. *Plant Cell* **14:** 479-490.

Kyselakova, H., Prokopova, J., Naus, J., Novak, O., Navratil, M., Safarova, D. *et al.* (2011). Photosynthetic alterations of pea leaves infected systemically by pea enation mosaic virus: A coordinated decrease in efficiencies of CO_2 assimilation and photosystem II photochemistry. *Plant Physiology and Biochemistry* **49:** 1279-1289.

Lagonenko, A. L., Komardina, V. S., Nikolaichik, Y. A. and Evtushenkov, A. N. (2008). First report of *Erwinia amylovora* fire blight in Belarus. *Journal of Phytopathology* **156:** 638-640.

Lahaye, T. and Bonas, U. (2001). Molecular secrets of bacterial type III effector proteins. *Trends in Plant Science* **6:** 479-485.

Langlotz, C., Schollmeyer, M., Coplin, D. L., Nimtz, M. and Geider, K. (2011). Biosynthesis of the repeating units of the exopolysaccharides amylovoran from

Erwinia amylovora and stewartan from *Pantoea stewartii*. *Physiological and Molecular Plant Pathology* **75:** 163-169.

Lazar, D. and Jablonsky, J. (2009). On the approaches applied in formulation of a kinetic model of photosystem II: Different approaches lead to different simulations of the chlorophyll a fluorescence transients. *Journal of Theoretical Biology* **257:** 260-269.

Le Roux, P. M., Flachowsky, H., Hanke, M. V., Gessler, C. and Patocchi, A. (2012a). Use of a transgenic early flowering approach in apple (*Malus* x *domestica* Borkh.) to introgress fire blight resistance from cultivar Evereste. *Molecular Breeding* **30:** 857-874.

Le Roux, P. M. F., Christen, D., Duffy, B., Tartarini, S., Dondini, L., Yamamoto, T. *et al.* (2012b). Redefinition of the map position and validation of a major quantitative trait locus for fire blight resistance of the pear cultivar 'Harrow Sweet' (*Pyrus communis* L.). *Plant Breeding* **131:** 656-664.

Lecomte, P., Paulin, J. P. and Billing, E. (1998). Fire blight risk assessment during bloom in an experimental orchard using BIS (Billing's Integrated System). *European Journal of Plant Pathology* **104:** 667-675.

Lee, J. H., Yun, H. S. and Kwon, C. (2012). Molecular communications between plant heat shock responses and disease resistance. *Molecules and Cells* **34:** 109-116.

Li, B. and Xu, X. (2002). Infection and development of apple scab (*Venturia inaequalis*) on old leaves. *Journal of Phytopathology-Phytopathologische Zeitschrift* **150:** 687-691.

Livaja, M., Zeidler, D., von Rad, U. and Durner, J. (2008). Transcriptional responses of *Arabidopsis thaliana* to the bacteria-derived PAMPs harpin and lipopolysaccharide. *Immunobiology* **213:** 161-171.

Llop, P., Barbe, S. and Lopez, M. M. (2012). Functions and origin of plasmids in *Erwinia* species that are pathogenic to or epiphytically associated with pome fruit trees. *Trees-Structure and Function* **26:** 31-46.

Llop, P., Cabrefiga, J., Smits, T. H. M., Dreo, T., Barbe, S., Pulawska, J. *et al.* (2011). *Erwinia amylovora* novel plasmid pEI70: Complete sequence, biogeography, and role in aggressiveness in the fire blight phytopathogen. *Plos One* **6**.

Locato, V., Gadaleta, C., De Gara, L. and De Pinto, M. C. (2008). Production of reactive species and modulation of antioxidant network in response to heat shock: a critical balance for cell fate. *Plant Cell and Environment* **31:** 1606-1619.

Loncaric, I., Donat, C., Antlinger, B., Oberlerchner, J. T., Heissenberger, B. and Moosbeckhofer, R. (2008). Strain-specific detection of two *Aureobasidium*

pullulans strains, fungal biocontrol agents of fire blight by new, developed multiplex-PCR. *Journal of Applied Microbiology* **104:** 1433-1441.

Loper, J. E., Henkels, M. D., Roberts, R. G., Grove, G. G., Willett, M. J. and Smith, T. J. (1991). Evaluation of streptomycin, oxytetracycline, and copper resistance of *Erwinia amylovora* isolated from pear orchards in Washington State. *Plant Disease* **75:** 287-290.

Loquet, A., Sgourakis, N. G., Gupta, R., Giller, K., Riedel, D., Goosmann, C. *et al.* (2012). Atomic model of the type III secretion system needle. *Nature* **486:** 276-279.

Lotze, E., Huybrechts, C., Sadie, A., Theron, K. I. and Valcke, R. M. (2006). Fluorescence imaging as a non-destructive method for pre-harvest detection of bitter pit in apple fruit (*Malus* x *domestica* Borkh.). *Postharvest Biology and Technology* **40:** 287-294.

Loureiro, A., Nicole, M. R., Varzea, V., Moncada, P., Bertrand, B. and Silva, M. C. (2012). Coffee resistance to *Colletotrichum kahawae* is associated with lignification, accumulation of phenols and cell death at infection sites. *Physiological and Molecular Plant Pathology* **77:** 23-32.

Maes, M., Orye, K., Bobev, S., Devreese, B., Van Beeumen, J., De Bruyn, A. *et al.* (2001). Influence of amylovoran production on virulence of *Erwinia amylovora* and a different amylovoran structure in *E. amylovora* isolates from *Rubus*. *European Journal of Plant Pathology* **107:** 839-844.

Mahajan, S. and Tuteja, N. (2005). Cold, salinity and drought stresses: An overview. *Archives of Biochemistry and Biophysics* **444:** 139-158.

Malnoy, M., Jin, Q., Borejsza-Wysocka, E. E., He, S. Y. and Aldwinckle, H. S. (2007). Overexpression of the apple MpNPR1 gene confers increased disease resistance in *Malus* x *domestica*. *Molecular Plant-Microbe Interactions* **20:** 1568-1580.

Malnoy, M., Martens, S., Norelli, J. L., Barny, M. A., Sundin, G. W., Smits, T. H. M. *et al.* (2012). Fire Blight: applied genomic insights of the pathogen and host. *Annual Review of Phytopathology* **50:** 475-494.

Malnoy, M., Venisse, J. S. and Chevreau, E. (2005). Expression of a bacterial effector, harpin N, causes increased resistance to fire blight in *Pyrus communis*. *Tree Genetics & Genomes* **1:** 41-49.

Manetas, Y. (2006). Why some leaves are anthocyanic and why most anthocyanic leaves are red? *Flora* **201:** 163-177.

Mano, J., Torii, Y., Hayashi, S., Takimoto, K., Matsui, K., Nakamura, K. *et al.* (2002). The NADPH : quinone oxidoreductase P1-zeta-crystallin in *Arabidopsis* catalyzes the alpha,beta-hydrogenation of 2-alkenals: Detoxication of the lipid peroxide-derived reactive aldehydes. *Plant and Cell Physiology* **43:** 1445-1455.

Mansfield, J. W. (2009). From bacterial avirulence genes to effector functions via the hrp delivery system: an overview of 25 years of progress in our understanding of plant innate immunity. *Molecular Plant Pathology* **10:** 721-734.

Marra, R., Li, H., Barbetti, M. J., Sivasithamparam, K., Vinale, F., Cavallo, P. *et al.* (2010). Proteomic analysis of the interaction between *Brassica napus* Cv. Surpass 400 and virulent or avirulent isolates of *Leptosphaeria maculans*. *Journal of Plant Pathology* **92:** 89-101.

Martin, G. B., Bogdanove, A. J. and Sessa, G. (2003). Understanding the functions of plant disease resistance proteins. *Annual Review of Plant Biology* **54:** 23-61.

Mas, P. and Yanovsky, M. J. (2009). Time for circadian rhythms: plants get synchronized. *Current Opinion in Plant Biology* **12:** 574-579.

Matous, K., Benediktyova, Z., Berger, S., Roitsch, T. and Nedbal, L. (2006). Case study of combinatorial imaging: What protocol and what chlorophyll fluorescence image to use when visualizing infection of *Arabidopsis thaliana* by *Pseudomonas syringae*? *Photosynthesis Research* **90:** 243-253.

Maxson-Stein, K., He, S. Y., Hammerschmidt, R. and Jones, A. L. (2002). Effect of treating apple trees with acibenzolar-S-methyl on fire blight and expression of pathogenesis-related protein genes. *Plant Disease* **86:** 785-790.

Maxwell, K. and Johnson, G. N. (2000). Chlorophyll fluorescence - a practical guide. *Journal of Experimental Botany* **51:** 659-668.

Mayer, M., Oberhuber, C., Loncaric, I., Heissenberger, B., Keck, M., Scheiner, O. *et al.* (2011). Fireblight (*Erwinia amylovora*) affects Mal d 1-related allergenicity in apple. *European Journal of Plant Pathology* **131:** 1-7.

Mayr, U., Michalek, S., Treutter, D. and Feucht, W. (1997). Phenolic compounds of apple and their relationship to scab resistance. *Journal of Phytopathology-Phytopathologische Zeitschrift* **145:** 69-75.

Mayr, U., Treutter, D., Santosbuelga, C., Bauer, H. and Feucht, W. (1995). Developmental changes in the phenol concentrations of Golden Delicious apple fruits and leaves. *Phytochemistry* **38:** 1151-1155.

Mccann, H. C. and Guttman, D. S. (2008). Evolution of the type III secretion system and its effectors in plant-microbe interactions. *New Phytologist* **177:** 33-47.

McClung, C. R. (2008). Comes a time. *Current Opinion in Plant Biology* **11:** 514-520.

McDowell, J. M. and Simon, S. A. (2006). Recent insights into R gene evolution. *Molecular Plant Pathology* **7:** 437-448.

McDowell, J. M. and Simon, S. A. (2008). Molecular diversity at the plant-pathogen interface. *Developmental and Comparative Immunology* **32:** 736-744.

Mcghee, G. C. and Jones, A. L. (2000). Complete nucleotide sequence of ubiquitous plasmid pEA29 from *Erwinia amylovora* strain Ea88: Gene organization and intraspecies variation. *Applied and Environmental Microbiology* **66:** 4897-4907.

McManus, P. S., Stockwell, V. O., Sundin, G. W. and Jones, A. L. (2002). Antibiotic use in plant agriculture. *Annual Review of Phytopathology* **40:** 443-465.

Mcnally, R. R., Toth, I. K., Cock, P. J. A., Pritchard, L., Hedley, P. E., Morris, J. A. *et al.* (2012). Genetic characterization of the HrpL regulon of the fire blight pathogen *Erwinia amylovora* reveals novel virulence factors. *Molecular Plant Pathology* **13:** 160-173.

Mehta, A., Brasileiro, A. C. M., Souza, D. S. L., Romano, E., Campos, M. A., Grossi-De-Sa, M. F. *et al.* (2008). Plant-pathogen interactions: what is proteomics telling us? *Febs Journal* **275:** 3731-3746.

Meng, X. D., Bonasera, J. M., Kim, J. F., Nissinen, R. M. and Beer, S. V. (2006). Apple proteins that interact with DspA/E, a pathogenicity effector of *Erwinia amylovora*, the fire blight pathogen. *Molecular Plant-Microbe Interactions* **19:** 53-61.

Meyer, A., Puhler, A. and Niehaus, K. (2001a). The lipopolysaccharides of the phytopathogen *Xanthomonas campestris* pv. *campestris* induce an oxidative burst reaction in cell cultures of *Nicotiana tabacum*. *Planta* **213:** 214-222.

Meyer, S., Saccardy-Adji, K., Rizza, F. and Genty, B. (2001b). Inhibition of photosynthesis by *Colletotrichum lindemuthianum* in bean leaves determined by chlorophyll fluorescence imaging. *Plant Cell and Environment* **24:** 947-955.

Milcevicova, R., Gosch, C., Halbwirth, H., Stich, K., Hanke, M. V., Peil, A. *et al.* (2010). *Erwinia amylovora*-induced defense mechanisms of two apple species that differ in susceptibility to fire blight. *Plant Science* **179:** 60-67.

Miller, T. D. and Schroth, M. N. (1972). Monitoring epiphytic population of *Erwinia amylovora* on pear with a selective medium. *Phytopathology* **62:** 1175-1182.

Miranda, M., Ralph, S. G., Mellway, R., White, R., Heath, M. C., Bohlmann, J. *et al.* (2007). The transcriptional response of hybrid poplar (*Populus trichocarpa* x *P-deltoides*) to infection by *Melampsora medusae* leaf rust involves induction of flavonoid pathway genes leading to the accumulation of proanthocyanidins. *Molecular Plant-Microbe Interactions* **20:** 816-831.

Mittler, R., Vanderauwera, S., Gollery, M. and Van Breusegem, F. (2004) Reactive oxygen gene network of plants. *Trends in Plant Science* **9:** 490-498.

Mittler, R., Vanderauwera, S., Suzuki, N., Miller, G., Tognetti, V. B., Vandepoele, K. *et al.* (2011). ROS signaling: the new wave? *Trends in Plant Science* **16:** 300-309.

Mohammadi, M. (2010). Enhanced colonization and pathogenicity of *Erwinia amylovora* strains transformed with the near-ubiquitous pEA29 plasmid on pear and apple. *Plant Pathology* **59:** 252-261.

Molina, L., Rezzonico, F., Defago, G. and Duffy, B. (2005). Autoinduction in *Erwinia amylovora*: Evidence of an acyl-homoserine lactone signal in the fire blight pathogen. *Journal of Bacteriology* **187:** 3206-3213.

Mudgett, M. B. (2005). New insights to the function of phytopathogenic bacterial type III effectors in plants. *Annual Review of Plant Biology* **56:** 509-531.

Muller, P., Li, X. P. and Niyogi, K. K. (2001). Non-photochemical quenching. A response to excess light energy. *Plant Physiology* **125:** 1558-1566.

Nagy, J. K., Kiraly, L. and Ildiko, S. (2012). Phage therapy for plant disease control with a focus on fire blight. *Central European Journal of Biology* **7:** 1-12.

Navrot, N., Rouhier, N., Gelhaye, E. and Jacquot, J. P. (2007). Reactive oxygen species generation and antioxidant systems in plant mitochondria. *Physiologia Plantarum* **129:** 185-195.

Nelson, N. and Ben-Shem, A. (2005). The structure of photosystem I and evolution of photosynthesis. *Bioessays* **27:** 914-922.

Newman, M. A., von Roepenack-Lahaye, E., Parr, A., Daniels, M. J. and Dow, J. M. (2002). Prior exposure to lipopolysaccharide potentiates expression of plant defenses in response to bacteria. *Plant Journal* **29:** 487-495.

Nicaise, V., Roux, M. and Zipfel, C. (2009). Recent advances in PAMP-triggered immunity against bacteria: pattern recognition receptors watch over and raise the alarm. *Plant Physiology* **150:** 1638-1647.

Nimtz, M., Mort, A., Domke, T., Wray, V., Zhang, Y. X., Qiu, F. *et al.* (1996). Structure of amylovoran, the capsular exopolysaccharide from the fire blight pathogen *Erwinia amylovora*. *Carbohydrate Research* **287:** 59-76.

Nissinen, R. M., Ytterberg, A. J., Bogdanove, A. J., Van Wijk, K. J. and Beer, S. V. (2007). Analyses of the secretomes of *Erwinia amylovora* and selected hrp mutants reveal novel type III secreted proteins and an effect of HrpJ on extracellular harpin levels. *Molecular Plant Pathology* **8:** 55-67.

Noctor, G. and Foyer, C. H. (1998). Ascorbate and glutathione: Keeping active oxygen under control. *Annual Review of Plant Physiology and Plant Molecular Biology* **49:** 249-279.

Norelli, J. L., Jones, A. L. and Aldwinckle, H. S. (2003). Fire blight management in the twenty-first century - Using new technologies that enhance host resistance in apple. *Plant Disease* **87:** 756-765.

Norelli, J. L. and Miller, S. S. (2004). Effect of prohexadione-calcium dose level on shoot growth and fire blight in young apple trees. *Plant Disease* **88:** 1099-1106.

Nurnberger, T., Brunner, F., Kemmerling, B. and Piater, L. (2004). Innate immunity in plants and animals: striking similarities and obvious differences. *Immunological Reviews* **198:** 249-266.

Oh, C. S. and Beer, S. V. (2005). Molecular genetics of *Erwinia amylovora* involved in the development of fire blight. *Fems Microbiology Letters* **253:** 185-192.

Oh, C. S., Carpenter, C. D., Hayes, M. L. and Beer, S. V. (2010). Secretion and translocation signals and DspB/F-binding domains in the type III effector DspA/E of *Erwinia amylovora*. *Microbiology-Sgm* **156:** 1211-1220.

Oh, C. S., Kim, J. F. and Beer, S. V. (2005). The Hrp pathogenicity island of *Erwinia amylovora* and identification of three novel genes required for systemic infection. *Molecular Plant Pathology* **6:** 125-138.

Oh, C. S., Martin, G. B. and Beer, S. V. (2007). DspA/E, a type III effector of *Erwinia amylovora*, is required for early rapid growth in *Nicotiana benthamiana* and causes NbSGT1-dependent cell death. *Molecular Plant Pathology* **8:** 255-265.

Ordax, M., Marco-Noales, E., Lopez, M. M. and Biosca, E. G. (2006). Survival strategy of *Erwinia amylovora* against copper: Induction of the viable-but-nonculturable state. *Applied and Environmental Microbiology* **72:** 3482-3488.

Ordax, M., Marco-Noales, E., Lopez, M. M. and Biosca, E. G. (2010). Exopolysaccharides favor the survival of *Erwinia amylovora* under copper stress through different strategies. *Research in Microbiology* **161:** 549-555.

Oukarroum, A., El Madidi, S. and Strasser, R. J. (2012). Exogenous glycine betaine and proline play a protective role in heat-stressed barley leaves (*Hordeum vulgare* L.): A chlorophyll a fluorescence study. *Plant Biosystems* **146:** 1037-1043.

Ozaktan, H. and Bora, T. (2004). Biological control of fire blight in pear orchards with a formulation of *Pantoea agglomerans* strain Eh 24. *Brazilian Journal of Microbiology* **35:** 224-229.

Papageorgiou, G. C. and Govindjee (2011). Photosystem II fluorescence: Slow changes - Scaling from the past. *Journal of Photochemistry and Photobiology B-Biology* **104:** 258-270.

Papageorgiou, G. C., Tsimilli-Michael, M. and Stamatakis, K. (2007). The fast and slow kinetics of chlorophyll a fluorescence induction in plants, algae and cyanobacteria: a viewpoint. *Photosynthesis Research* **94:** 275-290.

Paternoster, T., Defago, G., Duffy, B., Gessler, C. and Pertot, I. (2010). Selection of a biocontrol agent based on a potential mechanism of action: degradation of nicotinic acid, a growth factor essential for *Erwinia amylovora*. *International Microbiology* **13:** 195-206.

Paulin J. P. (2000). *Erwinia amylovora*: General characteristics, biochemistry and serology. In: Fire Blight. The disease and its causative agent, *Erwinia amylovora*. Vanneste J. L. (ed), CABI Publishing, Oxon, 87-115

Peck, S. C. (2003). Early phosphorylation events in biotic stress. *Current Opinion in Plant Biology* **6:** 334-338.

Peil, A., Garcia-Libreros, T., Richter, K., Trognitz, F. C., Trognitz, B., Hanke, M. V. *et al.* (2007). Strong evidence for a fire blight resistance gene of *Malus robusta* located on linkage group 3. *Plant Breeding* **126:** 470-475.

Perez-Bueno, M. L., Ciscato, M., vandeVen, M., Garcia-Luque, I., Valcke, R. and Baron, M. (2006). Imaging viral infection: studies on *Nicotiana benthamiana* plants infected with the Pepper Mild Mottle Tobamovirus. *Photosynthesis Research* **90:** 111-123.

Pester, D., Milcevicova, R., Schaffer, J., Wilhelm, E. and Blumel, S. (2012). *Erwinia amylovora* expresses fast and simultaneously hrp/dsp virulence genes during flower infection on apple trees. *Plos One* **7**.

Pfeiffer, J., Kuhnel, C., Brandt, J., Duy, D., Punyasiri, P. A. N., Forkmann, G. *et al.* (2006). Biosynthesis of flavan-3-ols by leucoanthocyanidin-4-reductases and anthocyanidin reductases in leaves of grape (*Vitis vinifera* L.), apple (*Malus* x *domestica* Borkh.) and other crops. *Plant Physiology and Biochemistry* **44:** 323-334.

Pina, A. and Errea, P. (2008). Differential induction of phenylalanine ammonia-lyase gene expression in response to in vitro callus unions of *Prunus* spp. *Journal of Plant Physiology* **165:** 705-714.

Pontais, I., Treutter, D., Paulin, J. P. and Brisset, M. N. (2008). *Erwinia amylovora* modifies phenolic profiles of susceptible and resistant apple through its type III secretion system. *Physiologia Plantarum* **132:** 262-271.

Prokopova, J., Mieslerova, B., Hlavackova, V., Hlavinka, J., Lebeda, A., Naus, J. *et al.* (2010). Changes in photosynthesis of *Lycopersicon* spp. plants induced by tomato powdery mildew infection in combination with heat shock pre-treatment. *Physiological and Molecular Plant Pathology* **74:** 205-213.

Pujol, M., Badosa, E., Manceau, C., and Montesinos, E. (2006). Assessment of the environmental fate of the biological control agent of fire blight, *Pseudomonas*

fluorescens EPS62e, on apple by culture and real-time PCR methods. *Applied and Environmental Microbiology* **72:** 2421-2427.

Pusey, P. L. (1999). Effect of nectar on microbial antagonists evaluated for use in control of fire blight of pome fruits. *Phytopathology* **89:** 39-46.

Pusey, P. L. (2002). Biological control agents for fire blight of apple compared under conditions limiting natural dispersal. *Plant Disease* **86:** 639-644.

Pusey, P. L. and Curry, E. A. (2004). Temperature and pomaceous flower age related to colonization by *Erwinia amylovora* and antagonists. *Phytopathology* **94:** 901-911.

Pusey, P. L., Stockwell, V. O., Reardon, C. L., Smits, T. H. M. and Duffy, B. (2011). Antibiosis activity of *Pantoea agglomerans* biocontrol strain E325 against *Erwinia amylovora* on apple flower stigmas. *Phytopathology* **101:** 1234-1241.

Quirino, B. F., Candido, E. S., Campos, P. F., Franco, O. L. and Kruger, R. H. (2010). Proteomic approaches to study plant-pathogen interactions. *Phytochemistry* **71:** 351-362.

Ramey, B. E., Koutsoudis, M., von Bodman, S. B. and Fuqua, C. (2004). Biofilm formation in plant-microbe associations. *Current Opinion in Microbiology* **7:** 602-609.

Rampitsch, C. and Bykova, N. V. (2012). Proteomics and plant disease: Advances in combating a major threat to the global food supply. *Proteomics* **12:** 673-690.

Reboutier, D., Frankart, C., Briand, J., Biligui, B., Laroche, S., Rona, J. P. *et al.* (2007). The HrpN(ea) harpin from *Erwinia amylovora* triggers differential responses on the non-host *Arabidopsis thaliana* cells and on the host apple cells. *Molecular Plant-Microbe Interactions* **20:** 94-100.

Renard, C. M. G. C., Dupont, N. and Guillermin, P. (2007). Concentrations and characteristics of procyanidins and other phenolics in apples during fruit growth. *Phytochemistry* **68:** 1128-1138.

Rezzonico, F. and Duffy, B. (2008). Lack of genomic evidence of AI-2 receptors suggests a non-quorum sensing role for luxS in most bacteria. *Bmc Microbiology* **8**.

Robert-Seilaniantz, A., Navarro, L., Bari, R. and Jones, J. D. (2007). Pathological hormone imbalances. *Current Opinion in Plant Biology* **10:** 372-379.

Rodriguez-Moreno, L., Pineda, M., Soukupova, J., Macho, A. P., Beuzon, C. R., Baron, M. *et al.* (2008). Early detection of bean infection by *Pseudomonas syringae* in asymptomatic leaf areas using chlorophyll fluorescence imaging. *Photosynthesis Research* **96:** 27-35.

Roemmelt, S., Fischer, T. C., Halbwirth, H., Peterek, S., Schlangen, K., Speakman, J. B. *et al.* (2003a). Effect of dioxygenase inhibitors on the resistance-related flavonoid metabolism of apple and pears: Chemical, biochemical and molecular biological aspects. *European Journal of Horticultural Science* **68:** 129-136.

Roemmelt, S., Zimmermann, N., Rademacher, W. and Treutter, D. (2003b). Formation of novel flavonoids in apple (*Malus* x *domestica*) treated with the 2-oxoglutarate-dependent dioxygenase inhibitor prohexadione-Ca. *Phytochemistry* **64:** 709-716.

Rohacek, K. and Bartak, M. (1999). Technique of the modulated chlorophyll fluorescence: basic concepts, useful parameters, and some applications. *Photosynthetica* **37:** 339-363.

Rolfe, S. A. and Scholes, J. D. (2010). Chlorophyll fluorescence imaging of plant-pathogen interactions. *Protoplasma* **247:** 163-175.

Romano, P. G. N., Horton, P. and Gray, J. E. (2004). The *Arabidopsis* cyclophilin gene family. *Plant Physiology* **134:** 1268-1282.

Ronald, P. C., Salmeron, J. M., Carland, F. M. and Staskawicz, B. J. (1992). The cloned avirulence gene Avrpto induces disease resistance in tomato cultivars containing the Pto resistance gene. *Journal of Bacteriology* **174:** 1604-1611.

Saidi, Y., Finka, A. and Goloubinoff, P. (2011). Heat perception and signalling in plants: a tortuous path to thermotolerance. *New Phytologist* **190:** 556-565.

Sarowar, S., Zhao, Y. F., Soria-Guerra, R. E., Ali, S., Zheng, D. M., Wang, D. P. *et al.* (2011). Expression profiles of differentially regulated genes during the early stages of apple flower infection with *Erwinia amylovora*. *Journal of Experimental Botany* **62:** 4851-4861.

Sauer, K., Camper, A. K., Ehrlich, G. D., Costerton, J. W. and Davies, D. G. (2002). *Pseudomonas aeruginosa* displays multiple phenotypes during development as a biofilm. *Journal of Bacteriology* **184:** 1140-1154.

Schansker, G., Toth, S. Z., Kovacs, L., Holzwarth, A. R. and Garab, G. (2011). Evidence for a fluorescence yield change driven by a light-induced conformational change within photosystem II during the fast chlorophyll a fluorescence rise. *Biochimica et Biophysica Acta-Bioenergetics* **1807:** 1032-1043.

Schansker, G., Toth, S. Z. and Strasser, R. J. (2006). Dark recovery of the Chl a fluorescence transient (OJIP) after light adaptation: The qT-component of non-photochemical quenching is related to an activated photosystem I acceptor side. *Biochimica et Biophysica Acta-Bioenergetics* **1757:** 787-797.

Schollmeyer, M., Langlotz, C., Huber, A., Coplin, D. L. and Geider, K. (2012). Variations in the molecular masses of the capsular exopolysaccharides

amylovoran, pyrifolan and stewartan. *International Journal of Biological Macromolecules* **50:** 518-522.

Schraidt, O. and Marlovits, T. C. (2011). Three-Dimensional Model of Salmonella's Needle Complex at Subnanometer Resolution. *Science* **331:** 1192-1195.

Schreiner, M., Mewis, I., Huyskens-Keil, S., Jansen, M. A. K., Zrenner, R., Winkler, J. B. *et al.* (2012). UV-B-induced secondary plant metabolites - potential benefits for plant and human health. *Critical Reviews in Plant Sciences* **31:** 229-240.

Schroth, M. N., Thomson, S. V. and Moller, W. J. (1979). Streptomycin resistance in *Erwinia amylovora*. *Phytopathology* **69:** 565-568.

Schutzendubel, A., Stadler, M., Wallner, D. and von Tiedemann, A. (2008). A hypothesis on physiological alterations during plant ontogenesis governing susceptibility of winter barley to *Ramularia* leaf spot. *Plant Pathology* **57:** 518-526.

Seemuller, E. A. and Beer, S. V. (1976). Absence of cell-wall polysaccharide degradation by *Erwinia amylovora*. *Phytopathology* **66:** 433-436.

Segonzac, C. and Zipfel, C. (2011). Activation of plant pattern-recognition receptors by bacteria. *Current Opinion in Microbiology* **14:** 54-61.

Sels, J., Mathys, J., De Coninck, B. M. A., Cammue, B. P. A. and De Bolle, M. F. C. (2008). Plant pathogenesis-related (PR) proteins: A focus on PR peptides. *Plant Physiology and Biochemistry* **46:** 941-950.

Shaner, G., Stromberg, E. L., Lacy, G. H., Barker, K. R. and Pirone, T. P. (1992). Nomenclature and concepts of pathogenicity and virulence. *Annual Review of Phytopathology* **30:** 47-66.

Shetty, N. P., Jorgensen, H. J. L., Jensen, J. D., Collinge, D. B. and Shetty, H. S. (2008). Roles of reactive oxygen species in interactions between plants and pathogens. *European Journal of Plant Pathology* **121:** 267-280.

Shevchenko, A., Wilm, M., Vorm, O. and Mann, M. (1996). Mass spectrometric sequencing of proteins from silver stained polyacrylamide gels. *Analytical Chemistry* **68:** 850-858.

Shi, L. X. and Schroder, W. P. (2004). The low molecular mass subunits of the photosynthetic supracomplex, photosystem II. *Biochimica et Biophysica Acta-Bioenergetics* **1608:** 75-96.

Shtienberg, D. (1992). Effects of foliar diseases on gas-exchange processes - A comparative study. *Phytopathology* **82:** 760-765.

Singh, D. K., Maximova, S. N., Jensen, P. J., Lehman, B. L., Ngugi, H. K. and McNellis, T. W. (2010). FIBRILLIN4 is required for plastoglobule development and stress resistance in apple and *Arabidopsis*. *Plant Physiology* **154:** 1281-1293.

Sinn, J. P., Oh, C. S., Jensen, P. J., Carpenter, S. C. D., Beer, S. V. and McNellis, T. W. (2008). The C-terminal half of the HrpN virulence protein of the fire blight pathogen *Erwinia amylovora* is essential for its secretion and for its virulence and avirulence activities. *Molecular Plant-Microbe Interactions* **21:** 1387-1397.

Skadhauge, B., Thomsen, K. K. and von Wettstein, D. (1997). The role of the barley testa layer and its flavonoid content in resistance to *Fusarium* infections. *Hereditas* **126:** 147-160.

Sklodowska, M., Gajewska, E., Kuzniak, E., Wielanek, M., Mikicinski, A. and Sobiczewski, P. (2011). Antioxidant profile and polyphenol oxidase activities in apple leaves after *Erwinia amylovora* infection and pretreatment with a Benzothiadiazole-type resistance inducer (BTH). *Journal of Phytopathology* **159:** 495-504.

Smits, T. H. M. and Duffy, B. (2011). Genomics of iron acquisition in the plant pathogen *Erwinia amylovora*: insights in the biosynthetic pathway of the siderophore desferrioxamine E. *Archives of Microbiology* **193:** 693-699.

Smits, T. H. M., Rezzonico, F., Kamber, T., Blom, J., Goesmann, A., Frey, J. E. *et al.* (2010). Complete genome sequence of the fire blight pathogen *Erwinia amylovora* CFBP 1430 and comparison to other *Erwinia* spp. *Molecular Plant-Microbe Interactions* **23:** 384-393.

Soylu, S. (2006). Accumulation of cell-wall bound phenolic compounds and phytoalexin in *Arabidopsis thaliana* leaves following inoculation with pathovars of *Pseudomonas syringae*. *Plant Science* **170:** 942-952.

Sparla, F., Rotino, L., Valgimigli, M. C., Pupillo, P. and Trost, P. (2004). Systemic resistance induced by benzothiadiazole in pear inoculated with the agent of fire blight (*Erwinia amylovora*). *Scientia Horticulturae* **101:** 269-279.

Spinelli, F., Ciampolini, F., Cresti, M., Geider, K. and Costa, G. (2005a). Influence of stigmatic morphology on flower colonization by *Erwinia amylovora* and *Pantoea agglomerans*. *European Journal of Plant Pathology* **113:** 395-405.

Spinelli, F., Speakman, J. B., Rademacher, W., Halbwirth, H., Stich, K. and Costa, G. (2005b). Luteoforol, a flavan 4-ol, is induced in pome fruits by prohexadione-calcium and shows phytoalexin-like properties against *Erwinia amylovora* and other plant pathogens. *European Journal of Plant Pathology* **112:** 133-142.

Spinelli, F., Costa, G., Rondelli, E., Busi, S., Vanneste J. L., Rodriguez, E. M. T. *et al*. (2011).; Emission of volatiles during the pathogenic interaction between *Erwinia amylovora* and *Malus domestica*. *Acta Horticulturae* **896:** 55-63

Starr, M. P. and Mandel, M. (1950). The nutrition of phytopathogenic bacteria. IV. Minimal nutritive requirements of the genus *Erwinia*. *Journal of Bacteriology* **60:** 669-672

Stirbet, A. and Govindjee (2011). On the relation between the Kautsky effect (chlorophyll a fluorescence induction) and Photosystem II: Basics and applications of the OJIP fluorescence transient. *Journal of Photochemistry and Photobiology B-Biology* **104:** 236-257.

Stitt, M. and Zeeman, S. C. (2012). Starch turnover: pathways, regulation and role in growth. *Current Opinion in Plant Biology* **15:** 282-292.

Stockwell, V. O., Johnson, K. B., Sugar, D. and Loper, J. E. (2002). Antibiosis contributes to biological control of fire blight by *Pantoea agglomerans* strain Eh252 in orchards. *Phytopathology* **92:** 1202-1209.

Stockwell, V. O., Johnson, K. B., Sugar, D., and Loper, J. E. (2011). Mechanistically compatible mixtures of bacterial antagonists improve biological control of fire blight of pear. *Phytopathology* **101:** 113-123.

Strasser, R. J., Srivastava, A. and Govindjee (1995). Polyphasic chlorophyll α fluorescence transient in plants and *Cyanobacteria*. *Photochemistry and Photobiology* **61:** 32-42.

Stratmann, J. (2003). Ultraviolet-B radiation co-opts defense signaling pathways. *Trends in Plant Science* **8:** 526-533.

Stulemeijer, I. J. E. and Joosten, M. H. A. J. (2008). Post-translational modification of host proteins in pathogen-triggered defence signalling in plants. *Molecular Plant Pathology* **9:** 545-560.

Suhayda, C. G. and Goodman, R. N. (1981). Infection courts and systemic movement of P32-labeled *Erwinia amylovora* in apple petioles and stems. *Phytopathology* **71:** 656-660.

Swarbrick, P. J., Schulze-Lefert, P. and Scholes, J. D. (2006). Metabolic consequences of susceptibility and resistance (race-specific and broad-spectrum) in barley leaves challenged with powdery mildew. *Plant Cell and Environment* **29:** 1061-1076.

Tai, T. H., Dahlbeck, D., Clark, E. T., Gajiwala, P., Pasion, R., Whalen, M. C. *et al.* (1999). Expression of the Bs2 pepper gene confers resistance to bacterial spot disease in tomato. *Proceedings of the National Academy of Sciences of the United States of America* **96:** 14153-14158.

Takeuchi, K., Taguchi, F., Inagaki, Y., Toyoda, K., Shiraishi, T. and Ichinose, Y. (2003). Flagellin glycosylation island in *Pseudomonas syringae* pv. *glycinea* and its role in host specificity. *Journal of Bacteriology* **185:** 6658-6665.

Thomson, S. V. and Gouk, S. C. (2003). Influence of age of apple flowers on growth of *Erwinia amylovora* and biological control agents. *Plant Disease* **87:** 502-509.

Thomson, S. V., Schroth, M. N., Moller, W. J. and Reil, W. O. (1975). Occurrence of fire blight of pears in relation to weather and epiphytic populations of *Erwinia amylovora*. *Phytopathology* **65:** 353-358.

Thordal-Christensen, H., Zhang, Z. G., Wei, Y. D. and Collinge, D. B. (1997). Subcellular localization of H_2O_2 in plants. H_2O_2 accumulation in papillae and hypersensitive response during the barley-powdery mildew interaction. *Plant Journal* **11:** 1187-1194.

Torres, M. A., Jones, J. D. G. and Dangl, J. L. (2006). Reactive oxygen species signaling in response to pathogens. *Plant Physiology* **141:** 373-378.

Treutter, D. (2001). Biosynthesis of phenolic compounds and its regulation in apple. *Plant Growth Regulation* **34:** 71-89.

Treutter, D. (2005). Significance of flavonoids in plant resistance and enhancement of their biosynthesis. *Plant Biology* **7:** 581-591.

Treutter, D. (2010). Managing phenol contents in crop plants by phytochemical farming and breeding-Visions and constraints. *International Journal of Molecular Sciences* **11:** 807-857.

Treutter, D., Santosbuelga, C., Gutmann, M. and Kolodziej, H. (1994). Identification of flavan-3-Ols and procyanidins by High Performance Liquid-Chromatography and chemical reaction detection. *Journal of Chromatography A* **667:** 290-297.

Triplett, L. R., Melotto, M. and Sundin, G. W. (2009). Functional analysis of the N Terminus of the *Erwinia amylovora* secreted effector DspA/E reveals features required for secretion, translocation, and binding to the chaperone DspB/F. *Molecular Plant-Microbe Interactions* **22:** 1282-1292.

Triplett, L. R., Wedemeyer, W. J. and Sundin, G. W. (2010). Homology-based modeling of the *Erwinia amylovora* type III secretion chaperone DspF used to identify amino acids required for virulence and interaction with the effector DspE. *Research in Microbiology* **161:** 613-618.

Tsiamis, G., Mansfield, J. W., Hockenhull, R., Jackson, R. W., Sesma, A., Athanassopoulos, E. *et al.* (2000). Cultivar-specific avirulence and virulence functions assigned to avrPphF in *Pseudomonas syringae* pv. *phaseolicola*, the cause of bean halo-blight disease. *Embo Journal* **19:** 3204-3214.

Tsiantos, J., Psallidas, P. and Chatzaki, A. (2003). Efficacy of alternatives to antibiotic chemicals for the control of fire blight of pears. *Annals of Applied Biology* **143:** 319-323.

Van Breusegem, F., Bailey-Serres, J. and Mittler, R. (2008). Unraveling the tapestry of networks involving Reactive Oxygen Species in plants. *Plant Physiology* **147:** 978-984.

Van Loon, L. C. and Van Strien, E. A. (1999). The families of pathogenesis-related proteins, their activities, and comparative analysis of PR-1 type proteins. *Physiological and Molecular Plant Pathology* **55:** 85-97.

Van Wijk, K. J. (2001). Challenges and prospects of plant proteomics. *Plant Physiology* **126:** 501-508.

Van der Zwet, T., Biggs, A. R., Heflebower, R. and Lightner, G. W. (1994). Evaluation of the Maryblyt computer model for predicting blossom blight on apple in West Virginia and Maryland. *Plant Disease* **78:** 225-230.

Van der Zwet, T. and Keil H. L. (1979). Fire Blight. A bacterial disease of Rosaceous Plants. Washington D.C.

Van der Zwet, T., Orolaza-Halbrendt, N. and Zeller, W. (2012). Fire Blight. History, Biology and Management. APS Press.

Vandesompele, J., De Preter, K., Pattyn, F., Poppe, B., Van Roy, N., De Paepe, A. *et al.* (2002). Accurate normalization of real-time quantitative RT-PCR data by geometric averaging of multiple internal control genes. *Genome Biology* **3**.

Vanloven, K., Beinsberger, S. E. I., Valcke, R. L. M., Vanonckelen, H. A. and Clijsters, H. M. M. (1993). Morphometric analysis of the growth of Phsp70-Ipt transgenic tobacco plants. *Journal of Experimental Botany* **44:** 1671-1678.

Venisse, J. S., Barny, M. A., Paulin, J. P. and Brisset, M. N. (2003). Involvement of three pathogenicity factors of *Erwinia amylovora* in the oxidative stress associated with compatible interaction in pear. *Febs Letters* **537:** 198-202.

Venisse, J. S., Gullner, G. and Brisset, M. N. (2001). Evidence for the involvement of an oxidative stress in the initiation of infection of pear by *Erwinia amylovora*. *Plant Physiology* **125:** 2164-2172.

Venisse, J. S., Malnoy, M., Faize, M., Paulin, J. P. and Brisset, M. N. (2002). Modulation of defense responses of *Malus* spp. during compatible and incompatible interactions with *Erwinia amylovora*. *Molecular Plant-Microbe Interactions* **15:** 1204-1212.

Viljevac, M., Dugalic, K., Stolfa, I., Dermic, E., Cvjetkovic, B., Sudar, R. *et al.* (2009). Biochemical basis of apple leaf resistance to *Erwinia amylovora* infection. *Food Technology and Biotechnology* **47:** 281-287.

Vogt, T. (2010). Phenylpropanoid Biosynthesis. *Molecular Plant* **3:** 2-20.

Wahid, A., Gelani, S., Ashraf, M. and Foolad, M. R. (2007). Heat tolerance in plants: An overview. *Environmental and Experimental Botany* **61:** 199-223.

Wang, D. P., Korban, S. S. and Zhao, Y. F. (2009a). The Rcs phosphorelay system is essential for pathogenicity in *Erwinia amylovora*. *Molecular Plant Pathology* **10:** 277-290.

Wang, W. X., Vinocur, B., Shoseyov, O. and Altman, A. (2004). Role of plant heat-shock proteins and molecular chaperones in the abiotic stress response. *Trends in Plant Science* **9:** 244-252.

Wang, Y., Bao, Z. L., Zhu, Y. and Hua, J. (2009b). Analysis of temperature modulation of plant defense against biotrophic microbes. *Molecular Plant-Microbe Interactions* **22:** 498-506.

Wei, Z. M., Laby, R. J., Zumoff, C. H., Bauer, D. W., He, S. Y., Collmer, A. *et al.* (1992). Harpin, elicitor of the hypersensitive response produced by the plant pathogen *Erwinia amylovora*. *Science* **257:** 85-88.

Whalen, M. C. (2005). Host defence in a developmental context. *Molecular Plant Pathology* **6:** 347-360.

White, F. F., Yang, B. and Johnson, L. B. (2000). Prospects for understanding avirulence gene function. *Current Opinion in Plant Biology* **3:** 291-298.

Whitham, S., McCormick, S. and Baker, B. (1996). The N gene of tobacco confers resistance to Tobacco Mosaic Virus in transgenic tomato. *Proceedings of the National Academy of Sciences of the United States of America* **93:** 8776-8781.

Wilkins, M. R., Gasteiger, E., Sanchez, J. C., Bairoch, A. and Hochstrasser, D. F. (1998). Two-dimensional gel electrophoresis for proteome projects: The effects of protein hydrophobicity and copy number. *ELECTROPHORESIS* **19:** 1501-1505.

Williams, R. J., Spencer, J. P. E. and Rice-Evans, C. (2004). Flavonoids: Antioxidants or signalling molecules? *Free Radical Biology and Medicine* **36:** 838-849.

Wilson, M. and Lindow, S. E. (1993). Interactions between the biological control agent *Pseudomonas fluorescens* A506 and *Erwinia amylovora* in pear blossoms. *Phytopathology* **83:** 117-123.

Winkel-Shirley, B. (2001). Flavonoid biosynthesis. A colorful model for genetics, biochemistry, cell biology, and biotechnology. *Plant Physiology* **126:** 485-493.

Winslow, C. E. A., Broadhurst, J., Buchanan, R. E., Krumwiede, C., Rogers, L. A. and Smith, G. H. (1920). The families and genera of the bacteria: *Erwinieae*. *Journal of Bacteriology* **5:** 209.

Wright, S. A. I., Zumoff, C. H., Schneider, L. and Beer, S. V. (2001). *Pantoea agglomerans* strain EH318 produces two antibiotics that inhibit *Erwinia amylovora* in vitro. *Applied and Environmental Microbiology* **67:** 284-292.

Yamaji, K. and Ichihara, Y. (2012). The role of catechin and epicatechin in chemical defense against damping-off fungi of current-year *Fagus crenata* seedlings in natural forest. *Forest Pathology* **42:** 1-7.

Zhang, Y. X., Bak, D. D., Heid, H. and Geider, K. (1999). Molecular characterization of a protease secreted by *Erwinia amylovora*. *Journal of Molecular Biology* **289:** 1239-1251.

Zhao, Y. F., Wang, D. P., Nakka, S., Sundin, G. W. and Korban, S. S. (2009). Systems level analysis of two-component signal transduction systems in *Erwinia amylovora*: Role in virulence, regulation of amylovoran biosynthesis and swarming motility. *Bmc Genomics* **10**.

Zimaro, T., Gottig, N., Garavaglia, B. S., Gehring, C. and Ottado, J. (2011). Unraveling plant responses to bacterial pathogens through proteomics. *Journal of Biomedicine and Biotechnology*.

Zipfel, C. and Felix, G. (2005). Plants and animals: a different taste for microbes? *Current Opinion in Plant Biology* **8:** 353-360.

List of Publications and Presentations

Publications

- Vrancken, K., Schoofs, H., Deckers, T. and Valcke, R. (2011). The analysis of the transcription levels of diverse SOD, APX and CAT isoforms in *Pyrus communis* cv. Conférence after infection with *Erwinia amylovora*. *Acta Horticulturae* **896:** 253-258 – Proceedings of the XIIth International Workshop on Fire Blight.

- Vrancken, K., Schoofs, H., Deckers, T. and Valcke, R. (2012). Real time qPCR expression analysis of some stress related genes in leaf tissue of *Pyrus communis* cv. Conférence after infection with *Erwinia amylovora*. *Trees* **26:** 67-73

- Vrancken, K., Holtappels, M., Schoofs, H., Deckers, T. and Valcke, R. (2012). *Erwinia amylovora* affects the phenylpropanoid-flavonoid pathway in mature leaves of *Pyrus communis* cv. Conférence.
  Accepted with revisions at Plant Physiology and Biochemistry

- Vrancken, K., Holtappels, M., Schoofs, H., Deckers, T. and Valcke, R. (2012). Pathogenicity and infection strategies of the fire blight pathogen *Erwinia amylovora* in *Rosaceae*: State of the Art.
  Accepted with revisions at Microbiology-SGM

Presentations

- 2012: XXVIth International Conference on Polyphenols, Florence, Italy
  Title: *Erwinia amylovora* affects the phenylpropanoid-flavonoid pathway in mature leaves of *Pyrus communis* cv. Conférence.

- 2011: Final Cost Meeting 864, Combining traditional and advanced strategies for plant protection in pome fruit growing, Diepenbeek, Belgium
  Title: Plant - *Erwinia amylovora* interactions: State of the Art.

- 2010: XIIth International Workshop on Fire blight, Warsawa, Poland
  Title: The analysis of the transcription levels of diverse SOD, APX and CAT isoforms in *Pyrus communis* cv. Conférence after infection with *Erwinia amylovora*.

- 2009: Plant-Microbe Interactions: from disease to symbiosis, Göteborg, Sweden
  Title: The involvement of the phenylpropanoid pathway in *Pyrus communis* cv. Conférence after infection with *Erwinia amylovora*.

- 2009: Cost Meeting 864, Combining traditional and advanced strategies for plant protection in pome fruit growing, Valencia, Spain
  Title: The involvement of the phenylpropanoid pathway in *Pyrus communis* cv. Conférence after infection with *Erwinia amylovora*.

Posters

- 2010: XIIth International Workshop on Fire blight, Warsawa, Poland
  Title: Chlorophyll Fluorescence analysis of leaves of *Pyrus communis* cv. Conférence after infection with *Erwinia amylovora*.

Other contributions

- 2010 (18-4-2012 tot 22-4-2010): Short Term Scientific Mission, COST action 864 Combining traditional and advanced strategies for plant protection in pome fruit growing: HPLC analysis of secondary metabolites in pear leaves.
  Host: Prof. Dieter Treutter, Centre of Life and Food Science Weihenstephan, Technische Universität München, Dürnast 2 D 85354 Freising (Germany)

- 2010: Joint meeting COST action Plant Proteomics in Europe, Systems biology and Omic approaches, Namur, Belgium

- 2007: XIIth Eucarpia Symposium on fruit breeding and genetics, Zaragoza, Spain